CHARLES UNIVERSITY IN PRAGUE

FACULTY OF PHARMACY IN HRADEC KRÁLOVÉ

Department of Biochemical Sciences

Interaction of proteins with low-molecular substances *in vitro*. Effect of glycation, substances of plant origin, and combination of these factors on function and spectral properties of selected proteins.

Doctoral thesis

Supervisor: Prof. MUDr. Jaroslav Dršata, CSc.

Supervisor specialist: PharmDr. Iva Boušová, Ph.D.

Hradec Králové

2012

Ing. Lucie Trnková

PROHLÁŠENÍ

Prohlašuji, že tato práce je mým původním autorským dílem, které jsem vypracovala samostatně. Veškerá literatura a další zdroje, z nichž jsem při zpracování čerpala, jsou uvedeny v seznamu použité literatury a v práci řádně citovány.

……

Ing. Lucie Trnková

ACKNOWLEDGEMENTS

Firstly, I would like to express my deepest gratitude to my supervisor, prof. MUDr. Jaroslav Dršata, CSc., for his encouragement to start this work and for the opportunity to realize it. His support, valuable advice and constructive criticism have been much appreciated. I thank also PharmDr. Iva Boušová, Ph.D. for her continuous support and useful advice during the whole course of my doctoral study. I would like to give a special thank prof. Fabio Altieri from Department of Biochemical Sciences „A. Rossi Fanelli“ of Sapienza University of Rome for possibility to spend a constructive time in his research team and to gain valuable experience and new skills.

Finally, I thank the staff and doctoral students at Department of Biochemical Sciences of Faculty of Pharmacy of Charles University and at Department Biochemical Sciences „A. Rossi Fanelli“ of Sapienza University of Rome for their help and the provision a friendly working environment. Naturally, I appreciate unfailing support of other important people in my life.

Financial support

The presented doctoral thesis and related papers were realizable due to the financial support from the following grants and research projects:

Development project of Czech Ministry of Education No. 141/2008.

Specific Research of UHK No. 2114/2008.

Development program of Czech Ministry of Education No. 14/87/2009.

Czech Science Foundantion, grant No. 524/09/P121.

Specific Research of UHK No. 2109/2009.

Grant No. SVV-2010-557 261-003.

Grant No. SVV-2011-557 263-004.

Grant No. SVV-2012-557 265-004.

List of abbreviations

AA	Acrylamide
ACE	Affinity capillary electrophoresis
AGE	Advanced glycation end products
APS	Ammonium persulfate
AST	Aspartate aminotransferase
bis-AA	Bis-Acrylamide
BPB	Bromophenol blue
BSA	Bovine serum albumin
C	(-)-Catechin
CA	Caffeic acid
CD	Circular dichroism
CE	Capillary electrophoresis
CEL	*N*-*ε*-carboxyethyllysine
Cg	(-)-Catechin gallate
CHA	Chlorogenic acid
CML	*N*-*ε*-carboxymethyllysine
DAD	Diode array detector
Di-E-GSSG	Dieosin glutathione disulfide
DM	Diabetes mellitus
DTT	*D,L*-Dithiothreitol
EC	(-)-Epicatechin
ECg	(-)-Epicatechin gallate
EDTA	Ethylene diamine tetraacetic acid
EGC	(-)-Epigallocatechin
EGCg	(-)-Epigallocatechin gallate
ERp57	Endoplasmic reticulum protein 57
FA	Ferulic acid
FLD	Fluorescent detector
FRET	Fluorescence resonance energy transfer
FTIR	Fourier transform infrared spectroscopy
Gal	Galactose
GC	(-)-Gallocatechin
GCg	(-)-Gallocatechin gallate
Glc	Glucose
GOLD	Glyoxal-lysine dimer
GSH	Glutathione reduced
GSSG	Glutathione disulfide / Glutathione oxidized
GST	Glutathione S-transferase
GTC	Green tea catechin
HbA_{1C}	Hemoglobin

HCA	Hydroxycinnamic acid
HPLC	High performance liquid chromatography
HSA	Human serum albumin
IDDM	Insulin-dependent diabetes mellitus
MA	*m*-Coumaric acid
MALDI-TOF MS	Matrix-assisted laser desorption/ionization time-of-flight mass spectrometry
MGO	Methylglyoxal
MHC	Major histocompatibility complex
MOLD	Methylglyoxal-lysine dimer
MS	Mass spectrometry
NEM	*N*-ethylmaleimide
Neo	Neohesperidose
NIDDM	Non-insulin-dependent diabetes mellitus
NMR	Nuclear magnetic resonance
OA	*o*-Coumaric acid
PA	*p*-Coumaric acid
PAGE	Polyacrylamide gel electrophoresis
PBS	Phosphate-buffered saline
PDI	Protein disulfide isomerase
RA	Rosmarinic acid
Rha	Rhamnose
RONS	Reactive oxygen and nitrogen species
ROS	Reactive oxygen species
Rut	Rutinose
SA	Sinapic acid
SPR	Surface plasmon resonance
Stat3	Signal transducer and activator of transcription 3
TBS	Tris buffer saline
TBST	Tris buffer saline-Tween-20 buffer
TEMED	*N,N,N´,N´*-tetramethylethylendiamine
Tris	Tris(hydroxymethyl)aminomethane
T2DM	Type 2 diabetes mellitus
UV-Vis	Ultraviolet-visible
λ_{ex}	Excitation wavelength
λ_{em}	Emission wavelength

CONTENT

1 INTRODUCTION

This doctoral thesis has been elaborated at the Department of Biochemical Sciences of the Faculty of Pharmacy in Hradec Králové, Charles University, in the research team of professor Dršata. The team has been engaged in the non-enzymatic glycation of enzymes in various *in vitro* models [Beránek et al. 2001, Dršata et al. 2002] and also in the possibilities to slow down this process by naturally occurring substances [Boušová et al. 2005a, Boušová et al. 2009] for many years.

Dietary plant polyphenols are naturally occurring substances with various biological and pharmacological activities in living organism. However, many mechanisms of their actions have not been fully elucidated yet. It seems that the interaction between polyphenols and biological macromolecules may play a role during these actions. A great significance possesses the interactions of plant polyphenols with serum albumin which acts as a carrier of various endogenous and exogenous low molecular compounds in blood stream. One of the main goals of this thesis was to study structure-binding affinity relationships between serum albumin and two selected groups of polyphenolic compounds such as hydroxycinnamic acids and catechins (flavanols) in the *in vitro* models using spectroscopic (UV-Vis absorption and fluorescence spectroscopy) and electrophoretic (native and SDS PAGE) methods. Green tea catechins were selected as representatives of the most outstanding plant polyphenols with a broad spectrum of beneficial biological and pharmacological properties. Their potential inhibitory effects on methylglyoxal-mediated non-enzymatic glycation of serum albumin in the *in vitro* models have been investigated by fluorescence methods and their structure-activity relationships are discussed.

Moreover, effects of methylglyoxal as a very potent glycating agent on structural and catalytic properties of recombinant cytosolic glutathion S-transferase from *Schistosoma japonicum* in the *in vitro* model have been investigated by spectroscopic (UV-Vis absorption and fluorescence spectroscopy) and electrophoretic (native PAGE, SDS PAGE/western blotting) methods.

A part of the results of this thesis has been obtained at the Department of Biochemical Sciences „A. Rossi Fanelli“ of Sapienza University of Rome in the research team of professor Altieri in the frame of Lifelong Learning programme - Erasmus.

Effects of green tea catechins on catalytic and structural properties of ERp57 enzyme have been investigated and their structure-activity relationships are discussed.

2 GENERAL INTRODUCTION

2.1 PROTEIN STRUCTURE AS A PREREQUISITE FOR THEIR PROPER FUNCTION

Proteins are the most abundant and functionally diverse biological macromolecules in living organisms. Most proteins spontaneously fold to a unique three dimensional "native" conformation, which is a prerequisite for their proper function (e.g. transport, enzymatic activity). Failure to assume this structure has often various catastrophic consequences for the cell metabolism (e.g. Creutzfeldt-Jakob disease [Herges et al. 2002]). Moreover, this native conformation can be reversibly or irreversibly changed or disrupted by various processes such as non-covalent or covalent modifications, denaturation, peptide bond cleavage [Berg et al. 2002]. Particular examples can be non-covalent or covalent protein modifications during their interaction with plant polyphenols or covalent process of non-enzymatic protein glycation due to reducing sugars or reactive α-dicarbonyl compounds.

2.2 PROTEIN OXIDATION AS AN IMPORTANT FACTOR OF THEIR DAMAGE

2.2.1 Pro-oxidants and oxidative stress

Living organisms are constantly exposed to many different systems (**Figure 1**), which generate **reactive oxygen and nitrogen species** (RONS) as very effective pro-oxidants. These systems include environmental factors, such as irradiation (e.g. X-rays, γ-rays, UV light) and pollutants in the atmosphere (e.g. ozone, NO_2, cigarette smoke) [Kelly 2004, Schröder and Krutmann 2005], and many of them are by-products of normal metabolic processes such as autoxidation of reduced forms of electron carriers (e.g. NAD(P)H, reduced flavins, cytochrome P450s), inflammatory reactions, nitric oxide synthesis, oxidase-catalyzed reactions, lipid peroxidation, glycation/glycoxidation reactions, or metal-catalyzed reactions [Halliwell and Gutteridge 1998, Stadtman and Levine 2000].

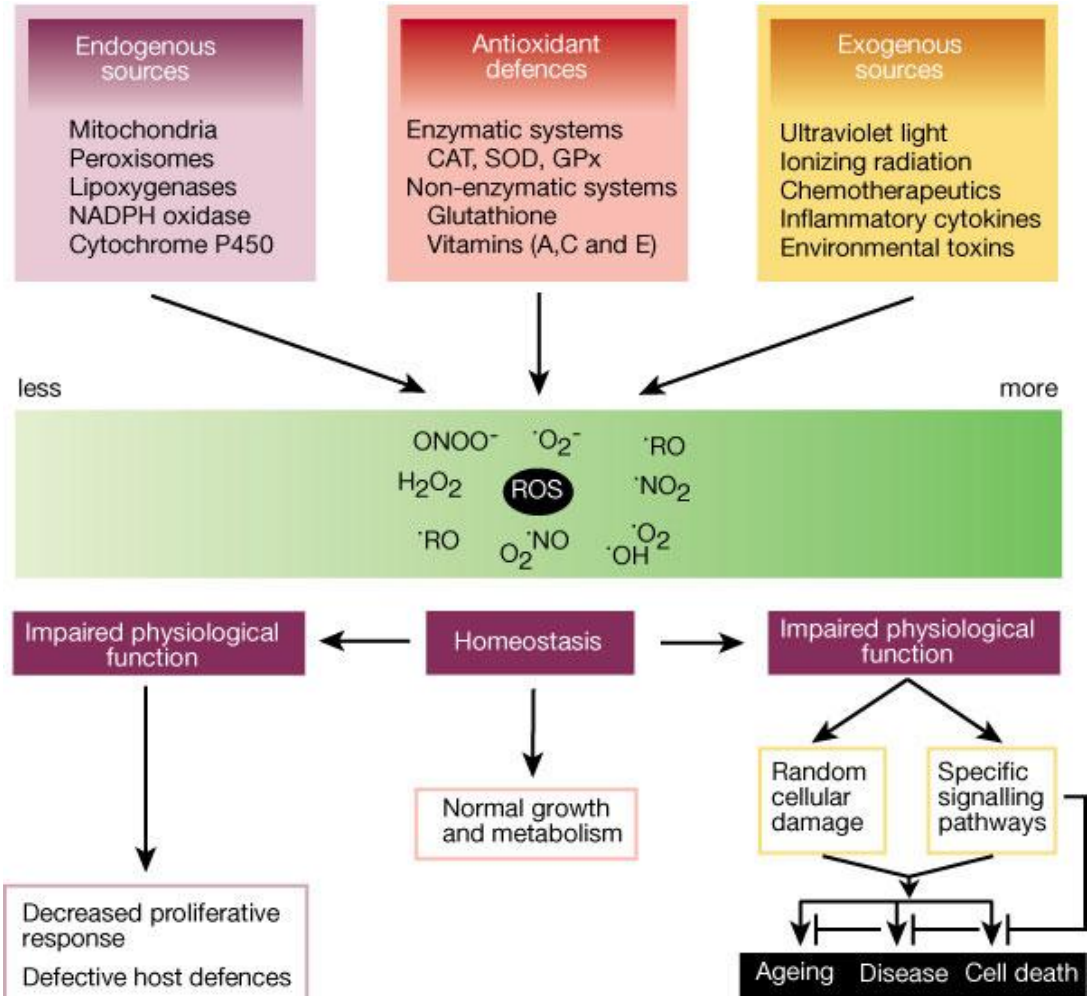

Figure 1: **The sources and cellular responses to reactive oxygen and nitrogen species** [Finkel and Holbrook 2000].

Free radicals are molecules or molecular fragments containing one or more unpaired electrons in their outer valance shell. **Reactive oxygen and nitrogen species** is a general term for both free radicals (e.g. O_2^{-}•, HO•, or NO•) and their reactive non-radical metabolites without unpaired electron(s) (e.g. H_2O_2, $ONOO^{-}$) [Halliwell and Gutteridge 1998]. The examples of RONS with their biological life-times are stated in Table 1. RONS and their metabolites are usually very unstable and reactive particles. They are able to promptly react with various biological structures such as fatty acids and lipids, amino acids and proteins, mono- and polynucleotides (nucleic acids), low-molecular metabolites, coenzymes, and many others [Avery 2011].

Table 1: **Reactive oxygen and nitrogen species with their biological life-times**. Modified according to Štípek et al. [2000].

REACTIVE OXYGEN SPECIES (ROS)	
Free radicals	***Non-radicals***
superoxide anion, O_2^{-}• (2-4 μs)	hydrogen peroxide, H_2O_2 (1 ms)
hydroxyl radical, OH^{-}• (1-10 ns)	hypochlorous acid, HClO
peroxyl radical, ROO• (7 s)	ozone, O_3
alkoxyl radical, RO• (1 ns)	singlet oxygen, $^1O_2$
hydroperoxyl radical, HO_2• (> 1 s)	
REACTIVE NITROGEN SPECIES (RNS)	
Free radicals	***Non-radicals***
nitric oxide, NO• (1-10 s)	nitrosyl, NO^+
nitrogen dioxide, NO_2•	nitrous acid, HNO_2
	peroxonitrite, $OONO^-$ (1s)

The **transition metals** are able due to their variable oxidation number to catalyze both redox reactions necessary for physiological functions and undesirable free radical reactions *in vivo* [Halliwell and Gutteridge 1998]. Generally, hydrogen peroxide and alkyl peroxides are the most common end products of most pro-oxidant systems. These peroxides themselves are relatively un-reactive compounds. However, in the presence of the transition metals such as Fe(II) or Cu(I), they are converted to the highly reactive hydroxyl (HO•) or alkoxyl (RO•) radicals, which immediately attack important biomolecules.

RONS and their reactive metabolites can play a double role in the organism, a positive and a negative one. Under certain circumstances they are required for the proper physiological functions of some systems (e.g. important inter-mediators of energy transfer, immunity defense factors, and signal molecules of cell regulation), but on the other hand, if they are produced in large quantities, they can become harmful to the organism and are able to damage or even kill organism [Dröge 2002, Ďuráčková 2010, Pan et al. 2009]. Generally, in healthy organism there exists a balance between the production and manifestation of RONS and other reactive metabolites, and a biological system's ability to readily detoxify the reactive intermediates or to repair the resulting oxidative damage. The condition when this fragile balance is disrupted is called **oxidative stress** [Halliwell and Gutteridge 1998]. This imbalance can be caused by an excessive generation of RONS, an insufficient activity of the antioxidant

protection systems, or a failure to repair oxidative damage. The **oxidative stress** is a very complicated and complex process and its impact on the organism depends on the type of pro-oxidant, on the site and intensity of its production, on the composition and activities of various antioxidants, and on the ability of repair systems. It can lead either to cellular adaption (i.e. up-regulation of the defense systems), to issue injury (e.g. serious oxidation damage of important biomolecules, loss of physiological function, pathological accumulation of oxidized products in cells), or to cell death caused by apoptosis or necrosis [Halliwell and Gutteridge 1998, Stadtman 2004]. At present, the opinion that oxidative stress is not always harmful has been accepted. However, it is not exactly known where a border between their physiological and pathological effect is, what that effect depends on, and how a shift to one or to the other side can be influenced [Ďuráčková 2010].

The **oxidative stress** has been implicated in the pathological development of many human age-related disorders and diseases. It is well known that it is not always the main cause of the disease but usually occurs as a consequence of previous tissue damage (e.g. infection, toxins, trauma). Among diseases which significantly contribute to oxidative impairment range atherosclerosis and cardiovascular diseases [Elahi et al. 2009, Kondo et al. 2009], neurodegenerative diseases such as Parkinson's and Alzheimer's diseases [Gella and Durany 2009, Jomova et al. 2010], diabetes and metabolic syndrome [Cohen and Tong 2010, Whaley-Connell et al. 2011], chronic inflammatory diseases [Ferguson 2010], carcinogenesis [Klaunig et al. 2010, Pan et al. 2009] and many others. Oxidative stress plays an important role also in the physiological process of aging [Drew and Leeuwenburgh 2002, Romano et al. 2010, Stadtman 2004].

To fight excessive production of RONS and their reactive metabolites, the organism has evolved **protective systems and mechanisms** against their toxic effects. Protection of the organism is organized at three levels. First of them includes **systems preventing RONS formation**, such as inhibitors of enzymes catalyzing RONS formation (e.g. allopurinol inhibits xanthine oxidase producing superoxide), or trapping of transition metal ions by chelating agents and thus elimination of their catalytic activity during production of RONS. When these primary protective systems are insufficient and RONS have already been formed, **scavengers and trappers of RONS** come into

action and eliminate the high reactivity of RONS by turning them into inactive and non-toxic metabolites. These compounds are called antioxidants, which prevent oxidation of biologically important molecules by RONS. If protection of the organism fails at this level, then **repair systems** recognize impaired molecules and decompose them, as it is in case of proteinases at oxidatively modified proteins, lipases at oxidatively damaged lipids, or DNA repair systems at modified DNA bases [Halliwell and Gutteridge 1998, Štípek et al. 2000].

It is well known that some high and low molecular weight endogenous and exogenous compounds act as antioxidants. **High molecular weight antioxidants** include the enzymes (e.g. superoxide dismutase, glutathione peroxidase, glutathione transferase, catalase) and non-enzymatic antioxidants involve proteins, which are able to bind transition metals (e.g. transferrin, lactoferrin, ceruloplasmin, albumin) and thus suppress their possibility to catalyze unwanted free radical reactions. Recently, a large attention has been focused also on the function of so-called chaperones whose synthesis is induced by oxidative stress. They are probably able to recognize the oxidized proteins, bind them and accelerate their elimination in proteosomes. They participate also in protein conformation reparation (e.g. ERp57). **Low molecular weight antioxidants** comprise hydrophilic and lipophilic compounds produced either endogenously in the organism (e.g. uric acid, lipoic acid, glutathione, ubiquinol as reduced co-enzyme Q) or they are obtained from diet as exogenous antioxidants (e.g. vitamin C, vitamin E, plant polyphenolic compounds including hydroxycinnamic acids and flavonoids) [Ďuráčková 2010, Halliwell and Gutteridge 1998, Štípek 2000]. It is very important to note that antioxidants do not possess only beneficial effects. Under certain circumstances they can act as pro-oxidants and thus can participate in tissue impairments and consequently in development of diseases [Procházková 2011].

2.2.2 Protein oxidation

Protein oxidation is posttranslational process which is implicated in the physiological process of ageing [Romano et al. 2010] and the development of many pathological age-related diseases [Cohen and Tong 2010, Elahi et al. 2009, Lyons 1995, Martínez et al. 2010]. RONS and their metabolites can lead to oxidation of the protein backbone resulting in protein fragmentation, oxidation of amino acid residue side

chains, and formation of protein-protein cross-linkages [Stadtman and Levine 2003]. These oxidatively modified proteins are not mostly repaired and must be removed from organism by proteolytic degradation. Decrease in the efficiency of proteolysis will cause their accumulation in the cellular content which can lead to disruption of cellular functions either by loss of catalytic and structural integrity or by interruption of regulatory pathways [Stadtman and Levine 2000]. Extent of oxidative modified proteins in cells reflects the balance between the pro-oxidant and antioxidant activities of the organism and is dictated by prevailing environmental, genetic, and dietary factors [Stadtman 2004]. Oxidation also takes place during non-enzymatic protein glycation that is described in the following chapter.

2.2.3 Non-enzymatic glycation as a complex process of protein damage

Non-enzymatic glycation, also known as Maillard reaction, was first described in 1912 by Louis Camille Maillard and it had been extensively studied by food chemists [Monnier 1989]. Much later, around 1980s, it was recognized that also proteins in human body are modified by non-enzymatic glycation leading to the onset and progression of many human diseases, such as diabetes mellitus and its related complications, atherosclerosis, Alzheimer´s disease, and a process of aging [Nursten 2005]. Plenty of *in vitro* and *in vivo* studies have been devoted to non-enzymatic glycation process with respect to investigation of protein structural and functional changes [Seidler and Kowalewski 2003, Zhao et al. 2000, Zeng et al. 2006] and to finding suitable therapeutic intervention to the glycation process [Martini et al. 2010, Stuchbury and Münch 2005].

2.2.3.1 Term and individual steps of glycation process

Non-enzymatic protein glycation is a covalent modification involving several steps. Firstly, free amino groups of proteins react slowly with the carbonyl groups of reducing sugars (e.g. glucose, fructose, galactose) or certain related compounds (e.g. α-oxoaldehydes, ascorbic acid) to yield acid-labile Shiff base intermediates (early glycated products) that undergo rearrangement to produce relatively stable derivatives known as Amadori or Heyns products (intermediate glycated products) in

the case of aldose (e.g. glucose) or ketose (e.g. fructose), respectively (Figure 2) [Janebová et al. 1999, Schalkwijk et al. 2004].

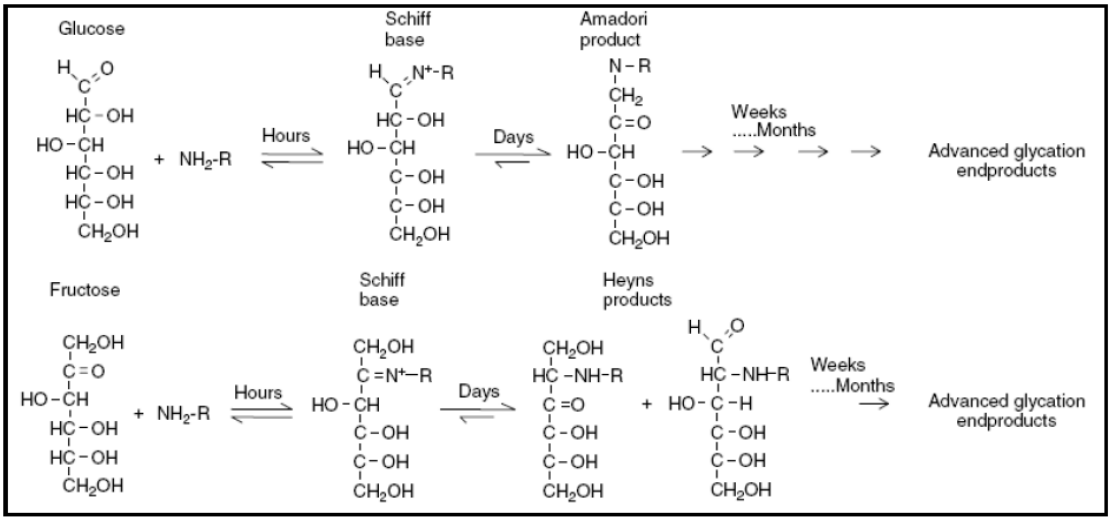

Figure 2: **Non-enzymatic glycation between protein free amino groups and glucose or fructose** [Schalkwijk et al. 2004].

The intermediate glycated products are either directly converted into irreversible advanced glycation end products (AGEs) or more often together with Schiff bases degraded into compounds known as α-dicarbonyls or α-oxoaldehydes (e.g. glyoxal, methylglyoxal, 3-deoxyglucosone) (**Figure 3**) that are more reactive than the parent sugars [Yim et al. 2001]. In addition, carbonyl compounds can be generated during metal-catalyzed autoxidation of glucose. During this process, hydrogen peroxide and free radicals are also formed and they are able to initiate other oxidative steps. The glycation process accompanied by oxidation steps is termed **glycoxidation** [Baynes et al. 1991, Hunt et al. 1988, West 2000, Wolff and Dean 1987]. Possibilities of AGEs formation pathways are displayed in **Figure 4**.

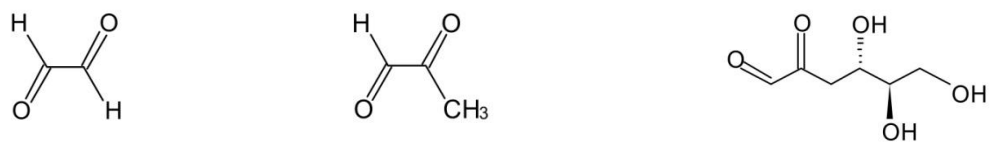

glyoxal (GO) methylglyoxal (MGO) 3-deoxyglucosone (3-DG)

Figure 3: **Some α-dicarbonyl derivatives formed during non-enzymatic glycation.**

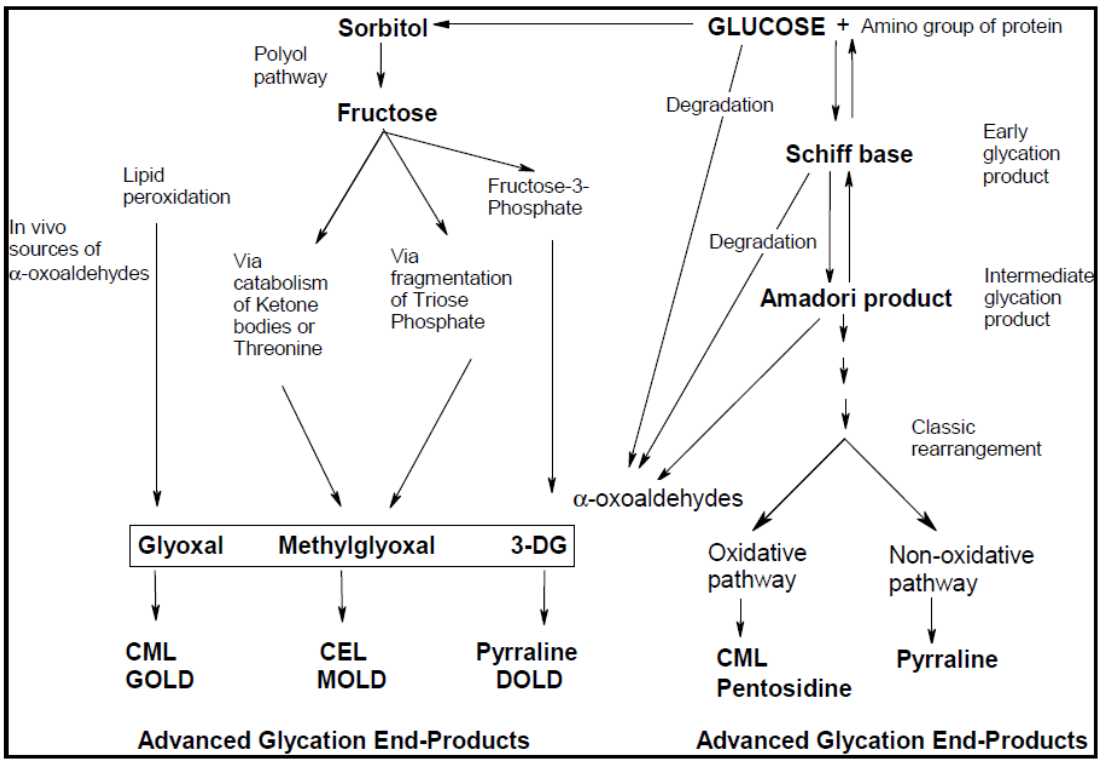

Figure 4: **Glucose and AGEs formation pathways including the polyol pathway and AGE formation by the α-oxoaldehydes** [Singh et al. 2001].

Non-enzymatic glycation has been decribed in long-lived proteins such as lens crystallins, collagen, elastin, and myelin [Cervantes-Laurean et al. 2006, Winlove et al. 1996, Zhao et al. 1996] as well as short-lived proteins (e.g. serum albumin [Suarez et al. 1989, Vetter and Indurthi 2011, Westwood and Thornalley 1995], hemoglobin [Bae and Lee 2004, Lee et al. 2011], histones [Gugliucci et al. 2009], ovoalbumin [Zeng et al. 2006]) and enzymes (e.g. catalase [Yan and Harding 1997, Zhao et al. 2000], alanine aminotransferase [Beránek et al. 2001], aspartate aminotransferase [Boušová et al. 2005b, Seidler and Seibel 2000], glutathione reductase [Blankytny and Harding 1992], superoxide dismutase [Yan and Harding 1997, Zhao et al. 2000]).

2.2.3.2 Glycating agents

In general, reducing sugars (e.g. glucose, fructose, galactose, mannose, ribose), their metabolites (e.g. α-oxoaldehydes), and also certain other carbohydrate relatives (e.g. ascorbic acid) are reactive toward nucleophiles such as free amino groups of proteins, lipids, or nucleic acids. In fact, **glucose** is the least reactive among the common sugars, perhaps leading to its evolutionary selection as the principal sugar *in*

vivo [Bunn et al. 1978]. Due to its low reactivity towards proteins, AGEs have been thought to be formed only at long-lived extracellular proteins, such as collagen, crystallines, elastin, and myelin [Cervantes-Laurean et al. 2006, Winlove et al. 1996, Zhao et al. 1996]. However, also rapid intracellular AGE formation by various **intracellular sugars and their metabolites** (e.g. fructose, ribose, glyceraldehyde, glyceraldehyde-3-phosphate, glyoxal, methylglyoxal, 3-deoxyglucosone) *in vivo* has been described [Nursten 2005, Schalkwijk et al. 2004, Yan and Harding 1997, Zeng et al. 2006]. For example, the rate of glycation of fructose, glyceraldehyde-3-phosphate, and methylglyoxal is 7.5-fold, 200-fold, and 10,000-fold faster in comparison with equimolar amount of glucose, respectively [Beisswenger et al. 2003, Boušová et al. 2011, Schalkwijk et al. 2004].

Alpha-dicarbonyl compounds, formed *in vivo* during glycation or basal metabolism (e.g. β-oxidation of fatty acids), are very potent glycating agents. These compounds are thought to be principal agents in generation of inter- and intra-molecular cross-links which are responsible for irreversible changes in proteins and can induce oxidative stress and cell apoptosis [Nass et al. 2007, Yim et al. 2001]. Excessive generation of α-dicarbonyls can lead to their accumulation in human body and it is called **carbonyl stress** [Miyata et al. 1998].

2.2.3.3 Advanced glycation end products

The **advanced glycation end products** (AGEs) represent a heterogeneous group of compounds rising from different precursors. Their chemical structures have not been fully described yet. They are formed endogenously inside as well as outside of cells during the last stage of glycation process either by oxidative (e.g CML, pentosidine) or non-oxidative (e.g. pyrraline, imidazolone) pathways or by reaction between α-dicarbonyl compounds and protein free amino groups (e.g. CEL, CML, GOLD, MOLD, pyrraline) (**Figure 4**) [Singh et al. 2001, Ulrich and Cerami 2001]. **Proteins modified by non-enzymatic glycation** show significant changes in their physical-chemical properties such as a considerable increase in molecular weight, a yellow-brown pigmentation, a typical fluorescent spectra (e.g. excitation 370 nm and emission 440 nm), an ability of aggregation and cross-links formation, an increase in biological half-life, a change in solubility and protein charge, a decrease in isoelectric point, a resistance against

proteolytic degradation and denaturation, and an easy chemical hydrolysis [Janebová et al. 1999, Nass et al. 2007].

The **advanced glycation end products** formed under physiological conditions are often classified according to their fluorescent properties and to their ability to form cross-links (**Figure 5**). The first group includes fluorescent AGE cross-links, such as pentosidine, crossline, and various vesperlysines, which are probably responsible for a majority of the harmful effects of AGEs in diabetes and ageing. Fluorescence is a good qualitative indicator used to estimate of AGEs formation. However, also non-fluorescent AGE cross-links, such as glucosepan and imidazolium dilysines (e.g. GOLD, MOLD) are found *in vivo*. They account only for 1% of all cross-links and their isolation and identification is more complicated. The third group represents non-cross-linking protein bound AGEs, such as arpyrimidine, pyrraline, imidazolones, and carboxyalkyllysines (e.g. CML and CEL). They may possess deleterious effects as precursors of cross-links or as biological receptor ligands inducing a variety of adverse cellular and tissue changes [Ahmed 2005, Ulrich and Cerami 2001].

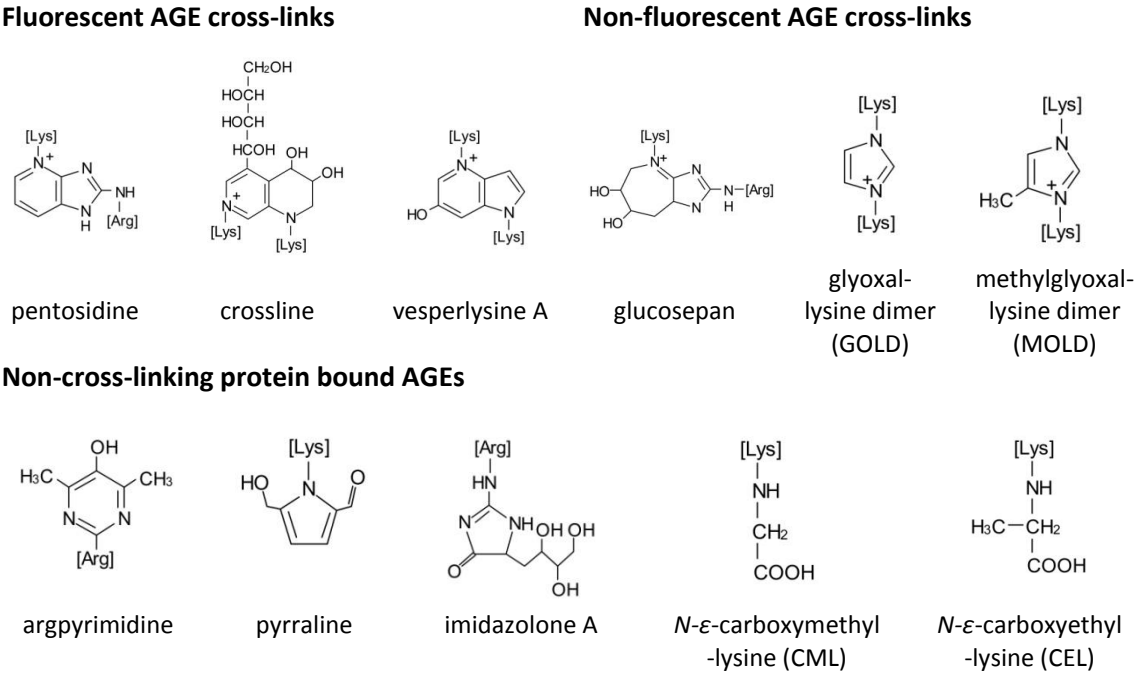

Figure 5: Classification and structures of AGEs formed under physiological conditions [Ulrich and Cerami 2001].

The AGEs can be degraded into AGE peptides by macrophages or T-lymphocytes through their specific **scavenger receptors** located on cell surfaces. These peptides are

subsequently released and excreted by kidney [Vlassara 1997]. Serum level of AGE peptides well correlates with renal function. If their level is decreased and they are not excreted by kidney, they covalently react with proteins and form so-called second generation of AGE proteins [Janebová et al. 1999]. However, the AGE modified proteins can induce oxidative stress by their binding to AGE specific cellular receptors. For example, a **receptor for AGE** (RAGE) is expressed by various cell systems such as smooth muscle cells, T lymphocytes, monocytes, macrophages, microglia, endothelial, and mesangial cells [Ahmed 2005]. Interaction of AGEs with RAGE on macrophages causes oxidative stress and activation of transcription nuclear factor NF-κB, which induces production of cytokines and tissue growth factors [Lapolla et al. 2005, Singh et al. 2001]. **AGE-R3**, also called galectin-3, expressed on macrophages represents another protein receptor with high affinity for AGE that promotes high molecular weight complexes formation after the binding of AGE. It is associated with development of several tumours [Mercer et al. 2004, Nass et al. 2007].

2.2.3.4 Consequences of glycation and importance in human pathology

The AGE modifications influence the structural as well as the functional properties of proteins. It has been shown that the presence of an AGE modification alters activity of several enzymes [Ahmed and Thornalley 2005, Boušová et al. 2011, Zeng and Davies 2005]. The excessive formation of AGEs and their accumulation in tissues possesses a wide range of harmful effects on human body such as direct structural damage, changes in physical properties and metabolism of extracellular matrix, or indirect induction of oxidative stress by their binding to AGE specific receptors on cell surfaces (e.g. RAGE) [Janebová et al. 1999, Nass et al. 2007, Sato et al. 2006a]. It consequently contributes to the onset and progression of many human diseases, such as diabetes mellitus and its related complications, atherosclerosis, neurodegenerative diseases (e.g. Alzheimer´s diseases), and a process of ageing [Ahmed 2005, Nass et al. 2007, Nursten 2005, Yegin et al. 1995]. The glycation process, also known as glycoxidation, is closely connected with oxidative stress. During the AGE formation, the reactive oxygen species (ROS) are abundantly generated and consequently significantly contribute to glycation. Glycoxidation reactions are usually catalyzed by transition metal ions [Baynes 1999, West 2000].

Diabetes mellitus (DM) is a metabolic disorder with high prevalence in human population which is characterized by increased level of glucose in blood (hyperglycaemia) and its excretion by urine. There are mainly two types of diabetes mellitus – Type 1 and Type 2. In Type 1 DM (insulin-dependent diabetes mellitus, IDDM), in the absence of pancreatic β-cells the insulin is not produced. Type 2 DM (non-insulin-dependent diabetes mellitus, NIDDM, T2DM) is characterized by a progressive impairment of insulin secretion by pancreatic β-cells and by a relative decreased in sensitivity of target tissues to the action of this hormone [Štípek et al. 2000]. This disease is always accompanied by oxidative stress [Giacco and Brownlee 2010]. Diabetes without proper treatment can caused many complications. Acute complications include for example hypoglycaemia, diabetic ketoacidosis, or non-ketonic hyperosmolar coma. Serious long-term complications involve cardiovascular diseases, chronic renal failure, and retinal damage. Thus adequate treatment of DM is important as well as blood pressure control, levels of glycated hemoglobin (HbA_{1c}) control, and lifestyle factors such as smoking cessation and maintaining a healthy body weight [Nass et al. 2007].

Hyperglycaemia is regarded as the primary cause of diabetic **microvascular complications** such as retinopathy, nephropathy, and neuropathy. Diabetic retinopathy affects blood vessel formation in the retina of the eye. It can lead to reduced vision or potentially blindness [Durham and Herman 2011, Glenn and Stitt 2009]. Diabetic nephropathy can lead to scarring changes in the kidney tissue, loss of small or progressively large amount of protein in the urine, and eventually chronic kidney diseases requiring dialysis [Nursten 2005, Yamagishi and Matsui 2010]. Diabetic neuropathy possesses the impact on the nervous system which most commonly causes numbness, tingling, and pain in the feet. Together with vascular disease in the legs, neuropathy contributes to the risk of diabetes related foot problems such as diabetic foot ulcers connected with necrosis and gangrene formation leading to amputation [Ahmed 2005, Pinzur 2011].

Hyperglycaemia is also a contributing factor to diabetic **macrovascular disease**. It significantly accelerates atherosclerosis of large arteries and leads to ischemic heart disease (angina pectoris and myocardial infarction), stroke and peripheral vascular disease [Giacco and Brownlee 2010, Katwal and Dokun 2011, Yegin et al. 1995].

Also in the course of physiological process of **ageing**, increasing amounts of AGEs can be detected in many tissues with a further increase in patients with diabetes [Nass et al. 2007]. AGEs accumulate without any diseases just by age. The age-related accumulation of AGEs was shown in human cartilage, skin collagen and pericardial fluid [Dyer et al. 1992, Simm et al. 2007, Verzijl et al. 2000]. Recent studies have also revealed that Type 2 diabetes mellitus, which progressively increases with age, is a risk factor for **neurodegenerative diseases**, especially those related to Alzheimer's disease [Ristow 2004, Sato et al. 2006b].

2.2.3.5 Therapeutic strategies targeting the AGEs

As the AGEs are believed to contribute to the development of major diseases, several strategies have been developed to avoid AGE formation or to break present AGE cross-links. The therapeutic intervention leading to decrease of AGE formation has followed three main approaches. First approach is inhibition of AGE formation by carbonyl-blocking agents or by antioxidants. Aminoguanidine (Pimagedine), a prototype therapeutic agent, is a low-molecular nucleophilic hydrazine compound, which is able to rapidly react with α-dicarbonyls to prevent formation of AGE cross-links [Abdel-Rahman and Bolton 2002]. However, its side effects in clinical treatment of diabetic nephropathy appeared [Bolton et al. 2004, Thornalley 2003]. Other nucleophilic compounds, which were designed to trap reactive carbonyl intermediates generated during AGE formation, are for example OPB-9195, metformin, or pyridoxamine [Booth et al. 1996, Sztanke and Pasternak 2003, Yamagishi et al. 2008]. Also compounds with antioxidant ability, such as scavengers of free radicals and chelators of transition metal ions, were tested. These antioxidants include e.g. α-lipoic acid, α-tocopherol, ascorbic acid, β-carotene, dipeptide carnosine, antioxidant enzymes (e.g. SOD, CAT), or flavonoids [Golbidi 2011, Nicolle et al. 2011, Rahimi et al. 2005]. The second approach represents reducing AGE deposition using cross-link breakers (e.g. phenyl thiazolium bromide (PTB), alagebrium chloride (ALT-711)) or by enhancing cellular uptake and degradation [Vasan et al. 1996, Willemsen et al. 2010, Yamagishi et al. 2008]. The last approach involves inhibition of RAGE by neutralizing antibodies or suppression of post-receptor signaling using antioxidants [Hudson et al. 2003, Stuchbury and Münch 2005].

2.2.3.6 Methods suitable for monitoring of glycation process

Due to the complexity of non-enzymatic glycation process, no universal method exists for its powerful monitoring and assessment. Various techniques and methods based on different methodological approaches can be used for this intention. Each of them provides different information and possesses its advantages as well as disadvantages. Choice of methods depends on the intended purposes of monitoring. Sometimes, their combinations have been used for better understanding of the non-enzymatic glycation process and thus finding of convenient strategy for its suppression [Gugliucci et al. 2009, Tsuji-Naito et al. 2009].

One of the possibilities for monitoring of glycation process is application of **methods** which **study changes in** structural and catalytic properties of **proteins**. They involve for example spectroscopic (UV-Vis absorption, fluorescence, circular dichroism, FTIR) or electrophoretic (native PAGE, SDS PAGE/western blotting) methods suitable for investigation of protein changes in their spectral characteristics, molecular weight, charge, or solubility [Ahmad et al. 2007, Gugliucci et al. 2009, Mikulíková et al. 2005, Peng et al. 2008, Schmitt et al. 2005, Wu et al. 2009]. Moreover, in the case of enzymes, study of the changes in their catalytic activity is applied as the most characteristic feature of enzyme molecules [Beránek et al. 2001, Boušová et al. 2009].

Powerful approach for monitoring of glycation process includes **identification and quantification of** arising **AGEs** mostly by immunochemical, spectrofluorimetric, or chromatographic methods. The immunochemical methods are based on antigenic properties of AGEs. The total amount of individual AGEs (e.g. pentosidine, CML, pyrraline) can be determined by enzyme-linked immunosorbent assay (ELISA) with specific polyclonal or monoclonal antibody marked by enzyme [Ghanem et al. 2011, Izuhara et al. 1999, Jono et al. 2004, Nagai et al. 2008, Taneda and Monnier 1994]. Several commercial enzyme immunoassay kits for rapid detection and quantification of AGE protein adducts in biological fluids have been developed. Some cross-linked and non-cross-linked AGEs possess characteristic fluorescence spectra (e.g. $\lambda_{ex}/\lambda_{em}$: 370/440 nm or 330/410 nm for total amount of AGEs, 335/385 nm for pentosidine, 320/380 nm for argpyrimidine), which can be applied as a good indicator for their detection and quantification [Tsuji-Naito et al. 2009, Wu and Yen 2005] primarily in the

combination with appropriate separation techniques such as high performance liquid chromatography (HPLC). In general, chromatographic methods, especially HPLC and gas chromatography (GC), with specific fluorescent (FLD) or mass spectrometric (MS) detection, are highly accurate and sensitive methods that are widely applied for separation, identification and quantification of metabolic intermediates (e.g. α-oxoaldehydes) and individual AGEs in biological samples. For instance, HPLC with photometric (diode array detection, DAD) or fluorescent (FLD) detection with or without appropriate derivatization can be applied for determination of glyoxal, methylglyoxal, or 3-deoxyglucosone [Dhar et al. 2009, Espinosa-Mansilla et al. 2007, Thornalley et al. 1999], and individual AGEs such as pyrraline [Portero-Otin et al. 1995], *N*-*ε*-carboxymethyllysine (CML) [Ghanem et al. 2011, Mikulíková et al. 2005], pentosidine [Ghanem et al. 2011, Mikulíková et al. 2008, Scheijen et al. 2009] or argpyrimidine [Wilker et al. 2001]. Pentosidine and CML are used as good biomarkers of glycoxidation and oxidative stress, respectively [Moreira et al. 2005, Sell et al. 1991]. High performance liquid chromatography with mass spectrometry (HPLC-MS, HPLC-MS/MS) represents highly powerful technique for quantification of individual AGEs, e.g. CEL, CML, argpyrimidine, or pentosidine [Mikulíková et al. 2007, Srey et al. 2010, Zhang et al. 2011, Zmatlíková et al. 2010]. Also gas chromatography with mass spectrometry (GC-MS) is employed for determination of glyoxal, methyglyoxal [Lapolla et al. 2003, Wu et al. 2008], or 3-deoxyglucosone [Niwa 1999, Wu et al. 2008], and individual AGEs such as CEL or CML [Cantero et al. 2007, Petrovic 2005]. In addition, other sophisticated tehniques can be also applied for these purposes such as capillary (zone) electrophoresis [Mikulíková et al. 2007, Zmatlíková et al. 2010] or matrix-assisted laser desorption/ionization time-of-flight mass spectrometry (MALDI-TOF MS) [Barnaby et al. 2011, Frost et al. 2011].

2.3 ROLE OF PLANT POLYPHENOLS IN PROTEIN PROTECTION FROM OXIDATIVE DAMAGE

As has been mentioned above, one of the possibilities of **protein protection** against oxidative damage including non-enzymatic glycation/glycoxidation is the intake of naturally occurring compounds with antioxidant activities such as plant polyphenols which can protect proteins using various mechanisms (e.g. trapping of ROS or reactive α-dicarbonyl species, chelating of transition metal ions) [Gugliucci et al. 2009, Sang et al. 2007]. On the other hand, these compounds can act also as pro-oxidants under certain conditions and thus can contribute to protein oxidation and protein non-enzymatic glycation [Lambert JD and Elias 2010, Procházková et al. 2011]. The exact action of plant polyphenols in human organism has not been fully elucidated. It seems to be more complex process and other investigations need to be carried out.

Plant polyphenols represent a heterogeneous group of natural compounds with one or more aromatic and/or heterocyclic rings bearing one or more hydroxyl and/or methoxyl substituents. These secondary plant metabolites formed by the shikimate pathway are widely distributed in higher plants as glycosides or aglycons. The most common bound sugars are glucose, galactose, rhamnose, arabinose, xylose, and rutinose. Polyphenols possess several important physiological roles in plants, such as defense against herbivores and pathogens, pigmentation, and attraction of pollinating insects [Dewick 2002, Pietta 2000]. They are a part of the human diet and a great interest in these substances has been motivated by the potential health benefits arising from their antioxidant activity [Galleano et al. 2010, Rice-Evans et al. 1996]. These substances are widely used in Chinese folk medicine due to their biological and pharmacological properties. However, several negative effects have been also described [Kaku and Nakagawa 2009, Lambert and Elias 2010]. The major groups of plant polyphenols include flavonoids, hydroxycinnamic acids, phenolic acids, lignans, and tannins.

2.3.1 Hydroxycinnamic acids

Hydroxycinnamic acids (HCAs) are widely distributed polyphenolic compounds in plant tissues (**Table 2**). Some of the most common naturally occurring HCAs are *p*-coumaric, caffeic, ferulic, and sinapic acids. These compounds can be found in a free

form but more often in various conjugated forms resulting from enzymatic hydroxylation, *O*-glycosylation, *O*-methylation or esterification [Harborne and Williams 2000, Rice-Evans et al. 1997]. Hydroxycinnamic acids have been reported to possess antimicrobial, antiallergic and anti-inflammatory activities, as well as antimutagenic and immunomodulatory effects [Natarajan et al. 1996, Pannala et al. 1998]. They have also significant antioxidant and anti-radical activities [Croft 1998, Graf 1992, Natella et al. 1999, Rice-Evans et al. 1996]. Moreover, anti-glycating effects of several HCAs (e.g. chlorogenic acid) on non-enzymatic glycation of serum albumin by glucose and methylglyoxal have been described [Gugliucci et al. 2009, Kim et al. 2011, Wang et al. 2009]. The biological effects of HCAs are strongly dependent on their structures, namely the presence of aromatic rings and number and position of hydroxyl groups [Rice-Evans et al. 1996]. Just these structural features suggest their possibility of binding with proteins and thus they can alter the biophysical and biochemical properties of protein [Kang et al. 2004, Min et al. 2004].

Table 2: **Structures of cinnamic acid and its hydroxyderivatives.**

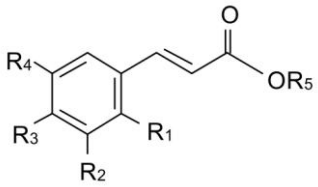

R_1	R_2	R_3	R_4	R_5	Compunds
H	H	H	H	H	Cinnamic acid
OH	H	H	H	H	*o*-Coumaric acid
H	OH	H	H	H	*m*-Coumaric acid
H	H	OH	H	H	*p*-Coumaric acid
H	OH	OH	H	H	Caffeic acid
H	OCH_3	OH	H	H	Ferulic acid
H	OCH_3	OH	OCH_3	H	Sinapic acid
H	OH	OH	H	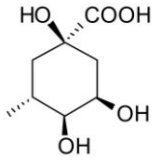	Chlorogenic acid
H	OH	OH	H	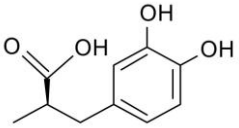	Rosmarinic acid

2.3.2 Flavonoids including green tea catechins

Flavonoids, a group of benzo-γ-pyron derivatives, are a major group of plant polyphenolic secondary metabolites widely distributed in the human diet occurring especially in fruits, vegetables, and some beverages (e.g. beer, wine, tea, coffee, fruit drinks) [Pietta 2000, Rice-Evans et al. 1996]. Over 9,000 individual compounds have been identified so far. Despite this huge diversity, all flavonoids can be recognized by their structural properties. Their structure is based on the flavonoid nucleus (flavan) (**Figure 6**) which consists of two aromatic rings (A and B rings) linked by an oxygen-containing heterocyclic ring (C ring). The major flavonoid subclasses comprise flavones, isoflavones, flavanones, flavonols, flavanols (catechins), and anthocyanidines. These subclasses differ in the level of oxidation and patern of substitution of the C ring, while individual compounds within a subclass vary in the pattern of substitution of the A and B rings. Substitutions include hydrogenation, hydroxylation, methylation, malonylation, sulfation, and glycosylation. Many flavonoids occur naturally as flavonoid glycosides including e.g. glucose, rhamnose, galactose, or rutinose as sugar component [Rice-Evans et al. 1997]. The subclasses of flavonoids with their best known representatives are given in **Table 3**.

Flavonoids exert a broad spectrum of multiple biological activities and important therapeutic applications including for example antioxidant, anti-inflammatory, antimicrobial, antiviral, antimutagenic, anticancer, cardioprotective, neuroprotective, antidiabetic, estrogenic/antiestrogenic, and antiallergic properties [Bastianetto et al. 2009, Cabrera et al. 2006, Clere et al. 2011, Croft 1998, Harbone and Williams 2000, Hwang 2012, Kawai et al. 2007, Nicole et al. 2011, Pietta 2000, Rathee et al. 2009, Yang et al. 2009]. However, several harmful effects of flavonoids involving for example pro-oxidant or cytotoxic activity have been already demostrated [Dickancaité et al. 1998, Lambert and Elias 2010, Procházková et al. 2011, Schmalhausen et al. 2007]. Many biologically active flavonoids appear to have effects on various proteins including enzymes such as xantine oxidase or glyceraldehyde-3-phosphate dehydrogenase [Harbone and Williams 2000, Schmalhausen et al. 2007]. The flavonoids possess suitable structural features, namely the aromatic rings and hydroxyl groups, which suggest their posibility of binding with molecules of proteins including enzymes.

Therefore, they are believed to affect the biophysical and biochemical properties of proteins.

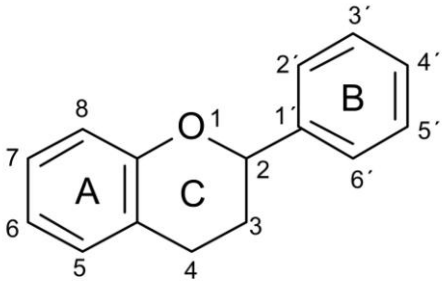

Figure 6: ***Generic structure of flavonoid (flavan).***

Table 3: **Overview of flavonoid subclasses with individual representatives.**

FLAVONES						
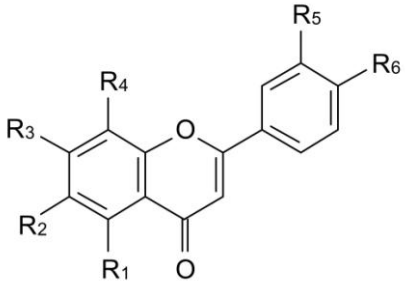						
R_1	**R_2**	**R_3**	**R_4**	**R_5**	**R_6**	**Flavone**
OH	H	OH	H	H	H	Chrysin
OH	OH	OH	H	H	H	Baicalein
OH	H	OH	H	H	OH	Apigenin
OH	H	OH	H	OH	OH	Luteolin
OH	H	OH	H	OH	OCH_3	Diosmetin
OH	H	OH	OCH_3	H	H	Wogonin
OH	OCH_3	OH	OCH_3	H	OCH_3	Nevadensin
OH	OH	OGlc	H	H	H	Baicalin
OH	H	ONeO	H	H	OH	Rhoifolin
OH	H	ORut	H	H	OH	Isorhoifolin
OH	H	ORut	H	OH	OCH_3	Diosmin

ISOFLAVONES					
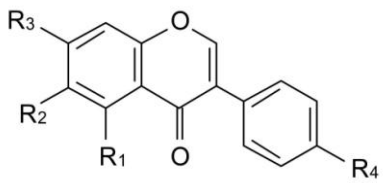					
R_1	**R_2**	**R_3**	**R_4**	**Isoflavone**	
H	H	OH	OH	Daidzein	
OH	H	OH	OH	Genistein	
OH	H	OH	OCH_3	Biochanin	
H	OCH_3	OH	OH	Glycitein	
H	H	OGlc	OH	Daidzin	
OH	H	OGlc	OH	Genistin	
H	OCH_3	OGlc	OH	Glycitin	

FLAVANONES

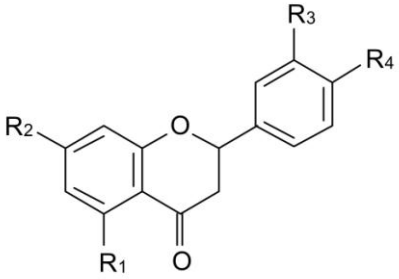

R_1	R_2	R_3	R_4	Flavanone
OH	OH	H	H	Pinocembrin
OH	OH	H	OH	Naringenin
OH	OH	OH	OH	Eridiktyol
OCH_3	OH	H	H	Alpinetin
OH	OH	OH	OCH_3	Hesperetin
OH	OGlc	H	OH	Pruning
OH	ORut	H	OH	Narirutin
OH	ORut	H	OCH_3	Didymin
OH	ORut	OH	OH	Eriocitrin
OH	ORut	OH	OCH_3	Hesperidin
OH	ONeo	H	OH	Naringin
OH	ONeo	H	OCH_3	Poncirin
OH	ONeo	OH	OH	Neoeriocitrin

FLAVONOLS

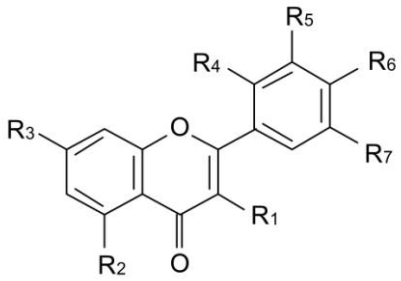

R_1	R_2	R_3	R_4	R_5	R_6	R_7	Flavanols
OH	H	OH	OH	H	OH	H	Morin
OH	OH	OH	H	H	OH	H	Kaempferol
OH	OH	OH	H	OH	OH	H	Quercetin
OH	OH	OH	H	OH	OH	OH	Myricetin
OH	OH	OH	H	H	OCH_3	H	Kemferid
OH	OH	OCH_3	H	OH	OH	H	Rhamnetin
OH	OH	OH	H	OCH_3	OH	H	Isorhamnetin
OGlc	OH	OH	H	H	OH	H	Astragalin
OGlc	OH	OH	H	OH	OH	H	Isoquercitrin
ORha	OH	OH	H	OH	OH	H	Quercitrin
OGal	OH	OH	H	OH	OH	H	Hyperosid
ORut	OH	OH	H	OH	OH	H	Rutin

ANTHOCYANIDINES

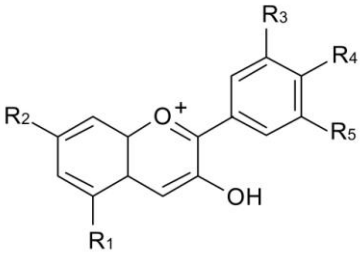

R_1	R_2	R_3	R_4	R_5	Anthocyanidine
OH	OH	H	OH	H	Pelargonidin
OH	OH	OH	OH	H	Kyanidin
OH	OH	OH	OH	OH	Delfinidin
OH	OH	OCH_3	OH	H	Peonidin
OH	OH	OCH_3	OH	OH	Petunidin
OH	OH	OCH_3	OH	OCH_3	Malvidin

<table>
<tr><th colspan="3">FLAVANOLS (CATECHINS)</th></tr>
<tr><td colspan="2"> 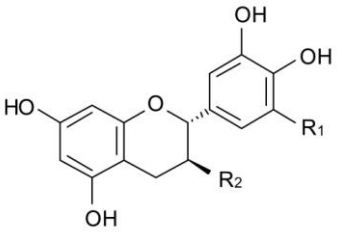 </td><td> 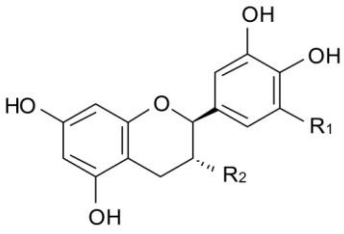 </td><td> 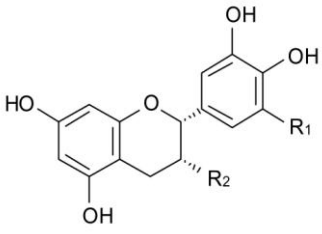 </td></tr>
<tr><td colspan="2">(+)-Catechin</td><td>(-)-Catechin</td><td>(-)-Epicatechin</td></tr>
<tr><th>R_1</th><th>R_2</th><th colspan="2">Flavanols</th></tr>
<tr><td>H</td><td>H</td><td colspan="2">(+)-Catechin, (-)-Catechin, (-)-Epicatechin</td></tr>
<tr><td>OH</td><td>H</td><td colspan="2">(+)-Gallocatechin, (-)-Gallocatechin, (-)-Epigallocatechin</td></tr>
<tr><td>H</td><td rowspan="2"> 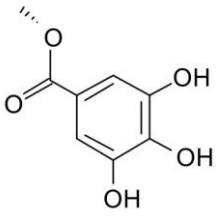 </td><td colspan="2">(-)-Catechin gallate, (-)-Epicatechin gallate</td></tr>
<tr><td>OH</td><td colspan="2">(-)-Gallocatechin gallate, (-)-Epigallocatechin gallate</td></tr>
</table>

Gal (galactose), Glc (glucose), Neo (neohesperidose), Rha (rhamnose), Rut (rutinose)

2.3.2.1 Green tea catechins

Green tea (*Camellia sinensis, Theaceae*), one of the most consumed beverages in the world, is rich source of polyphenols, mainly catechins (flavan-3-ols) so-called green tea catechins (GTCs). The major GTCs, which account for 30-40% of its dry weight, are epicatechin (6.4%), epicatechin gallate (13.6%), epigallocatechin (19.0%), and the most important epigallocatechin gallate (59.0%) [Singh et al. 2010]. They possess a broad spectrum of promoting biological activities such as antioxidant, anti-inflamantory, antimicrobial, and antiviral properties [Cabrera et al. 2006, Friedman 2007, Lambert and Elias 2010, Pastore and Fratellone 2006, Rice-Evans et al. 1997, Song and Seong 2007, Yang et al. 2009] and significantly contribute to the beneficial health effects of green tea in the prevention and treatment of various diseases such as cancer, heart diseases, diabetes, neurodegenerative disease, and metabolic syndrome [Cabrera et al. 2006, Crespy and Williamson 2004, Hodgson and Croft 2011, Khan and Mukhtar 2007, Lambert and Elias 2010, Sharangi 2009, Stote and Baer 2008, Thielecke and Boschmann 2009, Velayutham et al. 2008]. On the other hand, several negative activities of catechins such as pro-oxidative, cyto- and phytotoxic properties have been already described [Kaku and Nakagawa 2009, Lambert and Elias 2010, Lu et al. 2011].

Green tea and green tea catechins, mainly epigallocatechin gallate, have attracted a great interest among researches for several decades. Even though various *in vitro* and *in vivo* studies have been carried out, there are still many questions and unclearness.

In general, catechins comprise diphenyl propane skeleton (flavone backbone) where a polyphenolic ring (A) is condensed with six-membered oxygen containing heterocyclic ring (C) that carries another phenolic ring (B) at the 2 position (**Table 3**). Green tea catechins differ in number of hydroxyl groups and the presence or absence of the galloyl moiety at the 3 position. Their structures as well as structures of other low-molecular weight drugs suggest the possibilities of binding affinity to proteins (e.g. serum albumin [Maiti et al. 2006]), enzymes (e.g. glyceraldehyde-3-phosphate dehydrogenase [Ishii et al. 2008]), and other targets (e.g. lipids, [Sun et al. 2009], cell surface [Fujimura et al. 2008]), which can be realized by reversible non-covalent [Diniz et al. 2008, Frazier et al. 2006, Maiti et al. 2006, Nozaki et al. 2009, Papadopoulou et al. 2005, Soares et al. 2007] or irreversible covalent interactions [Ishii et al. 2008, Tanaka et al. 2011] depending on environmental conditions (e.g. presence of oxygen, pH, hydrophobicity), type of target, and structure and disposition of drugs. The studies dealing with interaction of catechins with serum albumin [Ishii e al. 2010a, Maiti et al. 2006], lipids bilayers [Hashimoto et al. 1999, Sun et al. 2009], or cell surface [Fujimura et al. 2008] showed that their binding affinity depends on structural features of individual catechins, mainly on the presence of the galloyl moiety, number of hydroxyl groups and the spatial arrangement of molecule. Moreover, anti-glycating effect of some catechins and green tea resulting apparently from their trapping activity of reactive oxygen and reactive carbonyl species has been already noticed [Lunceford and Gugliucci 2005, Jang et al. 2009, Wu and Yen 2005].

2.3.3 Polyphenol-protein interactions

In last two decades, a considerable attention has been focused on the study of interaction between low-molecular ligands (drugs) and biological macromolecules (e.g. proteins), especially discussing the thermodynamic quality, binding force quality, and mechanism of interactions. The drug-protein interactions can have the both positive and negative impacts on living organisms. For instance, it is well known that reversible binding of drugs to serum albumin is a key factor for their deposition, transportation,

metabolism, and thus efficacy in body [Carter and Ho 1994, Peters 1996]. In contrast, drugs can cause various irreversible changes in protein/enzyme conformation influencing its physiological functions [Ishii et al. 2008]. Generally, these studies play a crucial role in promoting research on proteins because they can provide useful information for study of pharmacological and biological effects of drugs and conformational changes of proteins caused by drugs [Otagiri 2005].

Dietary polyphenolic compounds such as hydroxycinnamic acids and flavonoids have received much attention owing to their biological properties and are considered as nutraceuticals. Polyphenols react readily with various proteins and enzymes by mostly non-specific way to form non-covalent [Prigent et al. 2003] or covalent [Ishii et al. 2008] complexes in dependence on their chemical structures, concentration of protein and polyphenols, and ambient conditions (e.g. pH, presence of oxidizing agent, temperature). Moreover, polyphenols can be converted into reactive intermediates which can form irreversible covalent bonds with nucleophiles of proteins such as thiol groups. In general, the hydrophobicity, presence or absence of some functional groups, steric hindrance, and spatial arrangement seem to be the key factors in the affinity of natural occurring polyphenols towards proteins [Diniz et al. 2008, Ishii et al. 2010a].

Research dealing with interactions between plant polyphenols and plasma proteins as carriers of numerous endogenous and exogenous compounds (e.g. serum albumin, hemoglobin, α-acid glycoprotein, α-amylase) [Diniz et al. 2008, Soares et al. 2007] possesses a great importance in pharmacology, pharmacodynamics, and biochemistry. The binding affinity of polyphenols towards plasma proteins, especially serum albumin, is believed to modulate their bioavailability and to be closely related to their biological function [Kusuda et al. 2006, Otagiri 2005]. One of the most used model proteins is serum albumin and a wide range of the studies concerning with serum albumin-polyphenol interactions have been carried out. These interactions suggest that binding of polyphenols with serum albumin is stabilized by hydrophobic interactions, hydrogen-bonding forces, and electrostatic forces [Minoda et al. 2010]. Moreover, serum albumin possesses also antioxidant properties and thus can prevent oxidation of polyphenols [Ishii et al. 2011].

2.3.3.1 Techniques used for assessment of ligand-protein interactions

In general, a wide range of techniques and methods have been developed for the study of ligand-protein interactions. Each of them provides different information about the character of interactions and binding parameters. Based on the procedures of mixture separation of the bound and free ligand, equilibrium dialysis and ultrafiltration followed by the sophisticated techniques such as high performance liquid chromatography (HPLC) or capillary electrophoresis (CE) had been commonly used to determine unbound ligand concentrations both *in vitro* and *in vivo* samples [Li et al. 2002, Zargar and Rabbani 2002]. However, the potential problems are that relatively large quantities of ligand are required and that the equilibrium between bound and unbound ligand may shift during the experiment. Moreover, these methods require expensive instruments and skilled operators. Surface plasmon resonance (SPR) [Zhang et al. 2007], affinity capillary electrophoresis (ACE) [Zhang et al. 2007], and sodium dodecyl sulphate (SDS) or native polyacrylamide gel electrophoresis (PAGE) [Kusuda et al. 2006] are other techniques, which have been applied for the studies of ligand-protein interactions.

Spectroscopic techniques such as UV-Vis absorption spectroscopy [Kanakis et al. 2006, Zhang et al. 2009], fluorescence spectroscopy [Liu et al. 2010, Sentchouk and Bondaryuk 2007], circular dichroism spectroscopy (CD) [Nozaki e al. 2009, He et al. 2005], and attenuated total reflectance-Fourier transform infrared spectroscopy (FTIR) [Tian et al. 2005, Xie et al. 2006] can be used to investigation of ligand-protein interactions because of their sensitivity, rapidity and ease of implementation. One of the most important attributes of these techniques is that they are equilibrium methods, which do not need any previous separation procedures that may disturb the equilibrium state of the sample solutions. They are ideal tools to observe conformational changes in protein structure since allow non-destructive measurements of substances at low concentration under physiological conditions. The techniques used for the purposes of this thesis are briefly described below.

2.3.3.1.1 UV-Vis absorption spectroscopy

Generally, **UV-Vis absorption measurement** is a very simple but effective method to explore the structural changes and the complex formation. Proteins show characteristic UV spectrum with maximum wavelength about 280 nm due to the presence of aromatic amino acids, especially tryptophan and tyrosine. Several approaches dealing with study of ligand-protein interactions by UV-Vis absorption spectroscopy have been applied including direct comparison of spectra (protein versus ligand-protein) [Zhang et al. 2009], determination of binding constant by spectroscopic titration [Kanakis et al. 2006, Zsila et al. 2003] or a second derivative spectrophotometric method [Omran et al. 2011].

2.3.3.1.2 Fluorescence spectroscopy

Fluorescence spectroscopy is a powerful method to study molecular interactions involving proteins caused by the intrinsic protein fluorescence, which originates with the presence of aromatic amino acids. In proteins, the dominant fluorescent group is the indole nucleus of tryptophan residue that absorbs and emits near 295 nm and 340 nm, respectively. The emission of tryptophan is highly sensitive to its local environment (e.g. solvent polarity), and is often used as a reporter group for protein conformational changes. Spectral shifts of protein emission have been observed as a result of several phenomena, including binding of ligands, protein-protein association, and protein unfolding. The emission of tryptophan indole group may shift to shorter wavelengths (blue shift) if this group becomes more buried within a native protein (folded), and its emission may shift to longer wavelengths (red shift) when the protein is unfolded [Lakowicz 2006, Vivian and Callis 2001].

One of the most applied spectroscopic methods used for the studies of molecular interactions between proteins and low-molecular weight ligands is **fluorescence quenching methods**. Fluorescence quenching is the decrease of the quantum yield of fluorescence from a fluorophore induced by a variety of molecular interactions with quencher molecule such as excited-state reactions, molecular rearrangements, energy transfer, ground-state complex formation (static quenching), and collisional (dynamic) quenching. Dynamic (collisional) quenching occurs when the excited-state fluorophore is deactivated upon contact with some other molecule (quencher), and no molecule is

chemically altered during this process. In the case of static quenching, a non-fluorescent complex is formed between molecules of fluorophore and quencher. The static and dynamic quenching can be distinguished by the **Stern-Volmer analysis**.

Dynamic quenching of fluorescence is described by the well-known Stern-Volmer equation:

$$F_0/F = 1 + K_{SV}[Q] = 1 + K_q\tau_0[Q] \quad (1)$$

In this equation, F_0 and F are the fluorescence intensities of protein in the absence and presence of the quencher, respectively. [Q] is the quencher (low-molecular ligand) concentration, K_{SV} is the Stern-Volmer quenching constant ($K_{SV} = K_q\tau_0$), K_q is the bimolecular quenching rate constant ($K_q = K_{SV}\tau_0^{-1}$), and τ_0 is the lifetime of the fluorophore in the absence of the quencher. The value of τ_0 is about 5.10^{-9} s for serum albumin [Lakowicz 2006]. In the case, the Stern-Volmer plot (F_0/F versus [Q]) shows linear dependence, the quenching is either purely static or dynamic, whereas when the plot shows exponential dependence, both static and dynamic quenching is asserted [Lakowicz 2006].

The dynamic quenching depends on diffusion, while static quenching does not. One criterion for distinguishing the type of quenchinq is the fact that the bimolecular quenching constant k_q is larger than the limiting diffusion rate constant of the biomolecule (2.0×10^{10} $l.mol^{-1}.s^{-1}$), so the dynamic quenching is not the main reason that causes fluorescence quenching of protein, and the static quenching process can be postulated to obtain the binding parameters [Lakowicz 2006].

Binding parameters such as binding constants and number of binding sites can be obtained using one of these following logarithmic equations [Bi et al. 2005].

$$\log(F_0 - F)/F) = \log K_b + n\log[Q] \quad (2)$$

$$\log(F_0 - F)/F = n\log K_b - n\log(1/([Q_t] - (F_0 - F)[P_t]/F_0)) \quad (3)$$

where K_b represents the binding constant for quencher-protein interaction, n is the number of binding sites per protein, F_0 and F are the fluorescence intensities before and after the addition of the quencher, $[Q_t]$ and $[P_t]$ are the total quencher

concentration and the total protein concentration, respectively. The values of K_b and n could be thus obtained from the intercept and slope by plotting log $(F_0 – F)/F$ against log [Q] or nlog$(1/([Q_t] - (F_0 – F)[P_t]/F_0))$.

Utilizing K_b, the **free energy change** (ΔG^0) value can be estimated from the following equation and the negative sing of its value confirms the spontaneity of binding [Shang et al. 2006].

$$\Delta G^0 = -RTlnK_b \quad (4)$$

2.3.3.1.3 Fluorescence resonance energy transfer

Fluorescence resonance energy transfer (FRET) is a distance-dependent interaction in which the excitation energy is transferred non-radiatively from the donor molecule (protein) to the acceptor molecule (ligand). The efficiency of energy transfer can be used to evaluate the distance between the ligand and the tryptophan residues in the protein. According to Förster´s non-radiative energy transfer theory [Förster and Sinanoglu 1966], the efficiency of the energy transfer depends on: (a) the extent of overlap between the emission spectrum of the donor and the absorption spectrum of the acceptor, (b) the orientation of the transition dipole of the donor and the acceptor, and (c) the distance between the donor and the acceptor [Lakowicz 2006]. The efficiency of energy transfer (*E*) between the donor and the acceptor is given by:

$$E = 1 – (F/F_0) = R_0^6 / (R_0^6 + r_0^6) \quad (5)$$

where F_0 and F are the fluorescence intensities of protein in the absence and presence of ligand, r_0 is the distance between donor and acceptor, and R_0 is the critical distance when the transfer efficiency is 50%. The value of R_0^6 can be calculated using the equation:

$$R_0^6 = 8.8 \times 10^{-25} k^2 N^{-4} \Phi J \quad (6)$$

where k^2 is the spatial orientation factor describing the relative orientation in space of the transition dipoles of the donor and the acceptor, N is the refractive index for the medium, Φ is the fluorescence quantum yield of the donor in the absence of the

acceptor, and *J* is the overlap integral of the emission spectrum of the donor and acceptor absorption spectrum (cm^3 l mol^{-1}). J is given by:

$$J = \Sigma F(\lambda)\varepsilon(\lambda)\lambda^4\Delta\lambda / \Sigma F(\lambda)\Delta\lambda \quad (7)$$

where F(λ) is the fluorescence intensity of the donor at wavelength λ, ε(λ) is the molar absorption coefficient of the acceptor at wavelength λ to λ + Δλ (cm^{-1} mol^{-1} l).

Finally, the distance between donor and acceptor (r_0) is calculated using equation (5). In the case, it is lower than 8 nm and the condition $0.5R_0 < r_0 < 1.5R_0$ is fulfilled it indicates that non-radiation energy transfer from donor to acceptor occurred with high probability [Lakowicz 2006, Guo et al. 2009].

2.3.3.1.4 Polyacrylamide gel electrophoresis

Sodium dodecyl sulfate (SDS) and **native polyacrylamide gel electrophoresis** (PAGE) can be used for the analysis of the formation of water-soluble complexes from combinations of various polyphenolic compounds and plasma proteins (e.g. serum albumin). SDS PAGE is commonly used to estimate the molecular size of a protein. Samples for SDS PAGE analysis are generally denaturated by a treatment with sodium dodecyl sulfate (SDS), mercaptoethanol, and by heating. In contrast, native PAGE does not involve denaturation and the shape and charge of the protein is altered after the complex formation which is demonstrated by the changes in its mobility. Coupling of **SDS PAGE** with **western blotting** can significantly increase the sensitivity of this method [Ishii et al. 2011, Minoda et al. 2010].

Several formations of macromolecular complexes and changes in electrophoretic mobility of proteins were confirmed for some polyphenol-serum albumin systems [Kusuda et al. 2006, Minoda et al. 2010, Rawel et al. 2002]. Research has revealed that the polyphenol behavior during complexation with proteins depends on the polyphenol structure and used experimental conditions [Minoda et al. 2010]. The oxidation of polyphenols may contribute to the formation of more stable macromolecular complexes as has been described for epigallocatechin gallate-BSA system [Kusuda et al. 2006].

2.3.3.2 Examples of plant polyphenol-serum albumin interactions

Several studies dealing with the interaction of serum albumin with cinnamic acid and its hydroxyderivatives such as *p*-coumaric, caffeic, ferulic, sinapic, and chlorogenic acids have been carried out (Table 4). Different spectroscopic (e.g. UV-Vis absorption spectroscopy, fluorescence quenching, FRET, circular dichroism, FTIR) and non-spectroscopic (e.g. capillary electrophoresis, calorimetry, surface plasmon resonance, ultracentrifugation) methods were applied for evaluation of the interaction character, determination of the binding and thermodynamic parameters, and discussion concerning the binding affinity-structure relationships. One of the most outstanding and studied hydroxycinnamic acids is surely chlorogenic acid (ester of caffeic and quinic acid) (Table 4) and its derivatives [Singh and Mitra 2011, Tang et al. 2008a]. The relationships between the structure of seven naturally occurring HCAs and their binding affinities towards BSA are discussed in chapter 5.1.

Table 4: Examples of *in vitro* studies of HCA-serum albumin interactions.

Hydroxycinnamic acid	Protein	Applied techniques	References
Caffeic aid	BSA	UV-Vis absorption, fluorescence, equilibrium dialysis	[Adzet et al. 1988, Bartolomé et al. 2000, Li et al. 2010]
	HSA	fluorescence, FTIR	[Min et al. 2004]
Chlorogenic acid	BSA	UV-Vis absorption, fluorescence, FRET, CD, ultracentrifugation, SDS PAGE, isoelectric focussing, calorimetry, NMR	[Li et al. 2010, Prigent et al. 2003, Rawel et al. 2002, Seifert et al. 2004, Tang et al. 2008a, Wang et al. 2011, Yang et al. 1994]
	HSA	UV-Vis absorption, CD, fluorescence, FRET, FTIR, calorimetry, capillary electrophoresis, NMR	[Diniz et al. 2008, Hu et al. 2012, Kang et al. 2004, Muralidhara and Prakash 1995, Wang et al. 2010a, Yang et al. 1994]
Cinnamic acid	BSA	fluorescence, FRET, FTIR, CD	[Bian et al. 2007]
	HSA	fluorescence, FTIR	[Min et al. 2004]
p-Coumaric acid	HSA	fluorescence, FTIR	[Min et al. 2004]
Ferulic acid	BSA	UV-Vis absorption, affinity capillary electrophoresis, SPR	[Li et al. 2010, Zhang et al. 2007]

	HSA	fluorescence, FRET, FTIR	[Kang et al. 2004]
Sinapic acid	HSA	fluorescence, FTIR	[Liu et al. 2005]

CD (circular dichroism), FRET (fluorescence resonance energy transfer), FTIR (Fourier transform infrared specroscopy), NMR (nuclear magnetic resonance), SDS PAGE (sodium dodecyl sulfate polyacrylamide gel electrophoresis), SPR (surface plasmon resonance)

Studies of interactions between flavonoids and plasma proteins, especially serum albumin, have attracted a great attention in research community. It is caused by their biological and pharmacological activities which seem to be related to the formation of their complexes with proteins [Kusuda et al. 2006]. Various techniques and methods can be applied for study of flavonoid-serum albumin interactions including non-spectroscopic (e.g. calorimetry, capillary electrophoresis, equilibrium dialysis, size-exclusion chromatography, SDS and native PAGE) and spectroscopic (e.g. UV-Vis absorption and fluorescence spectroscopy, circular dichroism, FTIR) methods (**Table 5**). Catechins, also known as flavanols, are one of the most outstanding groups of flavonoids with a wide range of beneficial activities on human organism. The assessment of the relationships between eight naturally occurring catechins and their binding affinities towards human serum albumin is discussed in detail in chapter 5.2.

Table 5: Examples of *in vitro* studies of flavonoid-serum albumin interactions.

Flavones	Protein	Applied techniques	References
Apigenin	BSA	fluorescence	[Cao et al. 2008]
	HSA	UV-Vis absorption, CD, fluorescence, capillary electrophoresis	[Diniz et al. 2008, Xiao et al. 2010a, Yuan et al. 2007]
Baicalein	BSA	fluorescence	[Cao et al. 2008, Xiao et al. 2010b, Xiao et al. 2009]
	HSA	fluorescence	[Xiao et al. 2010b]
Baicalin	BSA	fluorescence	[Xiao et al. 2009]
	HSA	fluorescence, FRET	[Bi et al. 2004]
Chrysin	BSA	UV-Vis absorption, CD, fluorescence, FRET	[Xiao et al. 2010b, Zhang et al. 2009]
	HSA	fluorescence	[Xiao et al. 2010b]
Diosmetin	BSA, HSA	fluorescence	[Dufour and Dangles 2005]
Flavone	BSA	fluorescence	[Xiao et al. 2010b]
	HSA	capillary	[Diniz et al. 2008, Xiao et

		electrophoresis	al. 2010b]
3-Hydroxyflavone	BSA	fluorescence, fluorescence anisotropy	[Guharay et al. 2001]
7-Hydroxyflavone	BSA	fluorescence	[Xiao et al. 2010b]
	HSA	UV-Vis absorption, fluorescence, CD	[Banerjee et al. 2008, Xiao et al. 2010b]
Luteolin	BSA	UV-Vis absorption, CD, fluorescence	[Dufour and Dangles 2005, Shi et al. 2011, Zhang et al. 2011b]
	HSA	UV-Vis absorption, fluorescence, CD, Raman scattering spectroscopy, molecular modeling	[Dufour and Dangles 2005, Jurasekova et al. 2009, Xiao et al. 2010a]
Nevadensin	BSA	fluorescence, FRET, CD	[Yu et al. 2008]
	HSA	UV-Vis absorption, fluorescence, FRET, molecular modeling	[Li et al. 2007a]
Vicenin-2	HSA	capillary electrophoresis	[Diniz et al. 2008]
Vitexin	HSA	capillary electrophoresis	[Diniz et al. 2008]
Wogonin	BSA	fluorescence, CD, FTIR	[Tian et al. 2005]
	HSA	fluorescence spectroscopy, CD, FTIR	[Tian et al. 2004a]
Isoflavones	**Protein**	**Applied techniques**	**References**
Calycosin	BSA	UV-Vis absorption, fluorescence	[Liu et al. 2010]
Daidzein	BSA	fluorescence	[Bolli et al. 2010]
	HSA	CD, FTIR, fluorescence anisotropy, molecular modeling	[Li et al. 2007b, Mahesha et al. 2006]
Daidzin	BSA	fluorescence	[Xiao et al. 2009, Zhao and Ren 2009]
Genistein	BSA	fluorescence	[Bolli et al. 2010, Cao et al. 2008, Xiao et al. 2009]
	HSA	fluorescence, equilibrium dialysis, CD, molecular modeling	[Mahesha et al. 2006]
Genistin	BSA	fluorescence	[Xiao et al. 2009, Zhao and Ren 2009]
Irisflorentin	BSA	UV-Vis absorption, fluorescence, FRET	[Zhang et al. 2008a]
Puerarin	BSA	fluorescence	[Xiao et al. 2009]
	HSA	fluorescence, CD, FTIR,	[Li et al. 2008]

Sophoricoside	HSA	UV-Vis absorption, fluorescence, FTIR, molecular modeling	[Tang et al. 2008b]
Flavanones	**Protein**	**Applied techniques**	**References**
Alpinetin	BSA	UV-Vis absorption, fluorescence, FTIR	[Ni et al. 2010, Zhang et al. 2010]
	HSA	UV-Vis absorption, CD, FTIR, fluorescence, FRET, molecular modeling	[He et al. 2005]
Flavanone	HSA	capillary electrophoresis	[Diniz et al. 2008]
Hesperetin	BSA	UV-Vis absorption, fluorescence, CD, FTIR	[Hegde et al. 2011]
	HSA	UV-Vis absorption, FTIR, fluorescence	[Xie et al. 2005]
Naringenin	BSA	fluorescence	[Bolli et al. 2010, Dufour and Dangles 2005]
Flavonols	**Protein**	**Applied techniques**	**References**
Fisetin	BSA	fluorescence	[Sentchouk and Bondaryuk 2007]
Galangin	BSA	fluorescence	[Cao et al. 2008, Xiao et al. 2008]
Hyperin		fluorescence, FRET	[Bi et al. 2004]
Icariin	HSA	UV-Vis absorption, fluorescence	[Zhang et al. 2008b]
Isoquercetin	BSA, HAS	fluorescence	[Rawel et al. 2005, Rawel et al. 2006]
Isoquercitrin	BSA, HAS	fluorescence	[Dufour and Dangles 2005]
Isorhamnetin	BSA, HSA	fluorescence	[Dufour and Dangles 2005]
Kaempferol	BSA	fluorescence, CD, FTIR	[Cao et al. 2008, Dufour and Dangles 2005, Tian et al. 2004b, Xiao et al. 2008]
	HSA	UV-Vis absorption, fluorescence, CD, FTIR	[Dufour and Dangles 2005, Kanakis et al. 2006, Matei and Hillebrand 2010, Tajmir-Riahi 2007]
Morin	BSA	fluorescence	[Sentchouk and Bondaryuk 2007]
	HSA	UV-Vis absorption, fluorescence, FTIR	[Qi et al. 2008, Xie et al. 2006]
Myricetin	BSA	fluorescence	[Cao et al. 2008, Tian et al. 2009, Xiao et al. 2008]

Naringenin	HSA	fluorescence	[Dufour and Dangles 2005]
Naringin	HSA	UV-Vis absorption, CD, fluorescence, FTIR, molecular modeling	[Zhang et al. 2008c]
Quercetin	BSA	UV-Vis absorption, CD, fluorescence, cyclic voltammetry	[Bolli et al. 2010, Cao et al. 2008, Dufour and Dangles 2005, Liu et al. 2010, Ni et al. 2009, Papadopoulou et al. 2005, Rawel et al. 2005, Rawel et al. 2006, Sentchouk and Bondaryuk 2007, Shi et al. 2011, Xiao et al. 2008, Xiao et al. 2009, Zhang et al. 2011b]
	HSA	UV-Vis absorption, CD, fluorescence, FRET, capillary electrophoresis, molecular modeling	[Bi et al. 2004, Diniz et al. 2008, Dufour and Dangles 2005, Kaldas et al. 2005, Kanakis et al. 2006, Rawel et al. 2005, Rawel et al. 2006, Tajmir-Riahi 2007, Zsila et al. 2003]
Quercitrin	BSA	fluorescence	[Xiao et al. 2008, Xiao et al. 2009]
Rutin	BSA	UV-Vis absorption, fluorescence	[Dufour and Dangles 2005, Liu et al. 2010, Papadopoulou et al. 2005, Rawel et al. 2005, Rawel et al. 2006, Sentchouk and Bondaryuk 2007, Xiao et al. 2009]
	HSA	fluorescence, FRET, capillary electrophoresis	[Bi et al. 2004, Diniz et al. 2008, Dufour and Dangles 2005, Rawel et al. 2005, Rawel et al. 2006]
Tamarixetin	BSA, HSA	fluorescence	[Dufour and Dangles 2005]
Troxerutin	BSA	UV-Vis absorption, fluorescence	[Wang et al. 2009]
Taxifolin	BSA	UV-Vis absorption, CD, fluorescence	[Shi et al. 2011, Zhang et al. 2011b]

Flavanols	Protein	Applied techniques	References
(+)-Catechin	BSA	UV-Vis absorption, CD, fluorescence, equilibrium dialysis, size-exclusion chromatography, native PAGE, SDS-PAGE	[Arora et al. 1989, Bartolomé et al. 2000, Dufour and Dangles 2005, Hatano et al. 2003, Kusuda et al. 2006, Papadopoulou et al. 2005, Peng et al. 2012, Shi et al. 2011, Soares et al. 2007, Zhang et al. 2011b]
	HSA	HPLC analysis with immobilized albumin column, capillary electrophoresis	[Diniz et al. 2008, Dufour and Dangles 2005, Ishii et al. 2010a]
(-)-Catechin gallate	HSA	HPLC analysis with immobilized albumin column	[Ishii et al. 2010a]
(-)-Epicatechin	BSA	fluorescence	[Papadopoulou et al. 2005, Soares et al. 2007]
	HSA	isothermal titration calorimetry, HPLC analysis with immobilized albumin column, capillary electrophoresis	[Diniz et al. 2008, Frazier et al. 2006, Ishii et al. 2010a]
(-)-Epicatechin gallate	HSA	HPLC analysis with immobilized albumin column	[Ishii et al. 2010a]
(-)-Epigallocatechin	BSA	fluorescence	[Soares et al. 2007]
	HSA	HPLC analysis with immobilized albumin column	[Ishii et al. 2010a]
(-)-Epigallocatechin gallate	BSA	CD, size-exclusion chromatography, native PAGE, SDS-PAGE	[Hatano et al. 2003, Kusuda et al. 2006, Nozaki et al. 2009]
	HSA	fluorescence, CD, FTIR, docking study, native PAGE, SDS-PAGE, western blotting, HPLC analysis with immobilized albumin column, quartz crystal microbalance	[Bae et al. 2009, Ishii et al. 2010a, Ishii et al. 2011, Maiti et al. 2006, Minoda et al. 2010, Nozaki et al. 2009]
(-)-Gallocatechin	HSA	HPLC analysis with immobilized albumin column	[Ishii et al. 2010a]

(-)-Gallocatechin gallate	HSA	HPLC analysis with immobilized albumin column	[Ishii et al. 2010a]
Anthocyanidines	**Protein**	**Applied techniques**	**References**
Malvidin-3-glucoside	BSA	fluorescence	[Soares et al. 2007]
Delphinidin	HSA	UV-Vis absorption, FTIR, capillary electrophoresis, CD	[Kanakis et al. 2006, Tajmir-Riahi 2007]

CD (circular dichroism), FRET (fluorescence resonance energy transfer), FTIR (Fourier transform infrared specroscopy), HPLC (high performance liquid chromatography), SDS PAGE (sodium dodecyl sulfate polyacrylamide gel electrophoresis), SPR (surface plasmon resonance)

2.3.4 Protective activity of plant polyphenols against non-enzymatic glycation

Plant polyphenols with obvious antioxidant properties including hydroxycinnamic acids and flavonoids can act also as potential inhibitors of AGEs formation and thus reduce non-enzymatic glycation. It may take place by different mechanisms such as trapping of reactive oxygen species or reactive dicarbonyl compounds, chelating of transition metal ions [Gugliucci et al. 2009, Sang et al. 2007]. However, mechanisms of their anti-glycating actions have not been fully clarified [Wu and Yen 2005]. Several anti-glycating effects of hydroxycinnamic acids and flavonoids on different *in vitro* systems of glycation models have been already described and the examples are given in **Table 6**. It has been shown that the effectiveness of protection against protein non-enzymatic glycation by flavonoids is attributed to their structure and antioxidant properties [Sang et al. 2007, Wu and Yen 2005]. It seems that also binding ability of naturally occurring substances towards biological macromolecule such as proteins may play a role in their anti-glycating activity [Kusuda et al. 2006]. Possible inhibitory effects of plant materials, which are significant source of polyphenolic compounds, on various *in vitro* glycation models have been investigated (**Table 7**).

Table 6: Examples of *in-vitro* anti-glycating effect of HCAs and flavonoids.

Plant polyphenol	Protein + glycating agent	References
Baicalin	AST + fructose	[Boušová et al. 2005a]
Baicalein	AST + fructose	[Boušová et al. 2005a]
Caffeic acid	BSA + methylglyoxal	[Gugliucci et al. 2009, Lee et al. 2008]
	G.K. peptide + ribose	[Lee et al. 2008]

(+)-Catechin	BSA + fructose	[Jang et al. 2009]
	BSA + glucose	[Jang et al. 2009, Wu and Yen 2005]
	BSA + methylglyoxal	[Wu and Yen 2005]
	Collagen + glucose	[Urios et al. 2007]
	G.K. peptide + ribose	[Wu and Yen 2005]
	HbA_{1C} + δ-gluconolactone	[Wu and Yen 2005]
Chlorogenic acid	BSA + glucose	[Kim et al. 2011]
	BSA + methylglyoxal	[Gugliucci et al. 2009]
	Collagen + glucose	[Kim et al. 2011]
o-Coumaric acid	AST + fructose	[Boušová et al. 2005a]
p-Coumaric acid	AST + fructose	[Boušová et al. 2005a]
(-)-Epicatechin (-)-Epicatechin gallate (-)-Epigallocatechin (-)-Epigallocatechin gallate	BSA + fructose	[Jang et al. 2009]
	BSA + glucose	[Jang et al. 2009]
	BSA + glucose	[Wu and Yen 2005]
	BSA + methylglyoxal	[Wu and Yen 2005]
	G.K. peptide + ribose	[Wu and Yen 2005]
	HbA_{1C} + δ-gluconolactone	[Wu and Yen 2005]
Eriodictyol	BSA + glucose	[Morimitsu et al. 1995]
Feruloyl oligosaccharides	BSA + glucose	[Wang et al. 2009]
Ferulic acid	AST + fructose	[Boušová et al. 2005a]
Fisetin	BSA + glucose	[Lee et al. 2008]
Fustin	BSA + glucose	[Lee et al. 2008]
Genistein	HSA + methylglyoxal	[Lv et al. 2011]
Isoferulic acid	AST + fructose	[Boušová et al. 2005a]
Isovitexin	BSA + glucose	[Peng et al. 2008]
	BSA + methylglyoxal	[Peng et al. 2008]
Kaempferol	BSA + glucose	[Wu and Yen 2005]
	BSA + methylglyoxal	[Wu and Yen 2005]
	Collagen + glucose	[Urios et al. 2007]
	G.K. peptide + ribose	[Wu and Yen 2005]
	HbA_{1C} + δ-gluconolactone	[Wu and Yen 2005]
Luteolin	BSA + glucose	[Wu and Yen 2005]
	BSA + methylglyoxal	[Wu and Yen 2005]
	G.K. peptide + ribose	[Wu and Yen 2005]
	HbA_{1C} + δ-gluconolactone	[Wu and Yen 2005]
Morin	BSA + glucose	[Lee et al. 2008]
Myricetin	Collagen + glucose	[Urios et al. 2007]
Naringenin	BSA + glucose	[Wu and Yen 2005]
	BSA + methylglyoxal	[Wu and Yen 2005]
	G.K. peptide + ribose	[Wu and Yen 2005]
	HbA_{1C} + δ-gluconolactone	[Wu and Yen 2005]
Proanthocyanidin B-4	BSA + fructose	[Jang et al. 2009]
	BSA + glucose	[Jang et al. 2009]

Quercetin	BSA + glucose	[Lee et al. 2008, Morimitsu et al. 1995, Wu and Yen 2005]
	BSA + methylglyoxal	[Wu and Yen 2005]
	Collagen + glucose	[Cervantes-Laurean et al. 2006]
		[Urios et al. 2007]
	G.K. peptide + ribose	[Wu and Yen 2005]
	HbA_{1C} + δ-gluconolactone	[Wu and Yen 2005]
Rutin	BSA + glucose	[Peng et al. 2008, Wu and Yen 2005]
	BSA + methylglyoxal	[Peng et al. 2008, Wu and Yen 2005]
	Collagen + glucose	[Cervantes-Laurean et al. 2006, Muthenna et al. 2011, Urios et al. 2007]
	G.K. peptide + ribose	[Wu and Yen 2005]
	HbA_{1C} + δ-gluconolactone	[Wu and Yen 2005]
Vitexin	BSA + glucose	[Peng et al. 2008]
	BSA + methylglyoxal	[Peng et al. 2008]

AST (aspartate aminotransferase), G.K peptide (synthetic peptide containing lysine), HbA_{1C} (hemoglobin)

Table 7: Examples of *in-vitro* anti-glycating effect of plant extracts.

Plant extracts	Protein + glycating agent	References
Aged garlic extract	BSA + glucose	[Amad et al. 2007]
	Lysozyme + glucose	[Amad et al. 2007]
	Lysozyme + methylglyoxal	[Amad et al. 2007]
Apocynum venetum L. (Apocynaceae)	BSA + fructose	[Yokozawa and Nakagawa 2004]
	BSA + glucose	[Yokozawa and Nakagawa 2004]
Camellia sinensis (Theaceae)	BSA + fructose	[Nakagawa et al. 2002]
	BSA + glucose	[Nakagawa et al. 2002]
		[Ho et al. 2010]
	BSA + methylglyoxal	[Ho et al. 2010, Lunceford and Gugliucci 2005]
Chrysanthemum morifolium R. (Asteraceae)	BSA + fructose	[Tsuji-Naito et al. 2009]
	BSA + glucose	[Tsuji-Naito et al. 2009]
Chrysanthemum indicum L. (Asteraceae)	BSA + fructose	[Tsuji-Naito et al. 2009]
	BSA + glucose	[Tsuji-Naito et al. 2009]
Cymbopogon stratus (Cymbopogon)	BSA + glucose	[Ho et al. 2010]
	BSA + methylglyoxal	[Ho et al. 2010]
Cyperus rotundus (Cyperaceae)	BSA + fructose	[Ardestani and Yazdanparast 2007a]

Ilex paraguariensis (Aquifoliaceae)	BSA + methylglyoxal	[Lunceford and Gugliucci 2005]
Melissa officinalis (Lamiaceae)	BSA + glucose	[Ho et al. 2010]
	BSA + methylglyoxal	[Ho et al. 2010]
Mentha longifolia (Lamiaceae)	BSA + glucose	[Ho et al. 2010]
	BSA + methylglyoxal	[Ho et al. 2010]
Nelumbo nucifera (Nelumbonaceae)	BSA + fructose	[Jung et al. 2008]
	BSA + glucose	[Jung et al. 2008]
Passiflora alata (Passifloraceae)	BSA + fructose	[Rudnicki et al. 2007]
	BSA + glucose	[Rudnicki et al. 2007]
Passiflora edulis (Passifloraceae)	BSA + fructose	[Rudnicki et al. 2007]
	BSA + glucose	[Rudnicki et al. 2007]
Psidium guajava L. (Myrtaceae)	BSA + glucose	[Wu et al. 2009]
Rosmarinus officinalis (Lamiaceae)	BSA + glucose	[Ho et al. 2010]
	BSA + methylglyoxal	[Ho et al. 2010]
Salvia officinalis (Lamiaceae)	BSA + glucose	[Ho et al. 2010]
	BSA + methylglyoxal	[Ho et al. 2010]
Sorghum bicolor (Poaceae)	BSA + fructose	[Farrar et al. 2008]
	BSA + methylglyoxal	[Farrar et al. 2008]
Teucrium polium (Lamiaceae)	BSA + glucose	[Ardestani and Yazdanparast 2007b]
	BSA + ribose	[Ardestani and Yazdanparast 2007b]
Verbena officinalis (Verbenaceae)	BSA + glucose	[Ho et al. 2010]
	BSA + methylglyoxal	[Ho et al. 2010]
	BSA + ribose	[Ho et al. 2010]

2.4 MODEL PROTEINS TO STUDY GLYCATION AND LIGAND-PROTEIN INTERACTIONS

Several model proteins have been selected for purposes of the experiments dealing with protein-polyphenol interactions and non-enzymatic glycation processes. These include serum albumins and enzymes such as a multifunctional thiol-disulfide oxidoreductase ERp57 and a glutathione S-transferase. Their structures and properties are briefly described below.

2.4.1 Serum albumin

Serum albumin (65 kDa) is the most abundant protein in blood plasma with a typical concentration of 50 g/l and one of the most extensively studied proteins [Peters 1996]. The crystallographic analysis of serum albumin revealed that the protein contains three structurally similar domains (I–III), which assemble to form heart-shaped molecule. Each of these domains is further divided into two subdomains (A and B) [Carter and Ho 1994]. It was found out that aromatic and heterocyclic ligands bind within two hydrophobic pockets in subdomains IIA and IIIA corresponding to Sudlow´s site I and II, respectively [Otagiri 2005]. Human (HSA) and bovine (BSA) serum albumins are the most used model proteins. They are cross-linked with 17 disulfide bonds and comprise of 585 and 583 amino acid residues in their polypeptide chains for HSA and BSA, respectively. HSA differs from BSA by 24% of primary structure [Peters 1996].

Serum albumin possesses a wide range of physiological functions involving the binding, transport, and deposition of many endogenous and exogenous ligands such as nutrients, hormones, fatty acids, and many diverse drugs present in blood circulation. It is well known that the deposition, transportation, metabolism, and efficacy of drugs are strongly affected by their binding to serum albumin [Peters 1996, Varshney et al. 2010]. On the other hand, ligands can cause various changes in protein conformation influencing its physiological function and such impaired proteins may be consequently pathologically accumulated in body tissues. Thereby, the studies of serum albumin-drug interactions play an important role in pharmacology and pharmacodynamics [Bertucci and Domenici 2002].

From spectroscopic point of view, the presence of the aromatic amino acid residues in proteins, mainly tryptophan residue(s), are important for effective revealment of protein conformational changes due to the changes in the

microenvironment of the tryptophan residue(s) [Lakowicz 2006]. Bovine serum albumin (BSA) contains two tryptophan residues. One is located near the surface in domain IB (Trp-134) and the second one is buried in a hydrophobic (non-polar) pocket in the internal part of domain IIA (Trp-212). Although Trp-134 is more accessible to drug binding than Trp-212, the second one is known to bind a variety of ligands in its hydrophobic pocket. Readiness of the drug penetration to Trp-212 also depends on its structure and character. Human serum albumin (HSA) has only one tryptophan residue (Trp-214) within a hydrophobic binding pocket of subdomain IIA (**Figure 7**), which significantly contributes to the intrinsic fluorescence of this protein [Carter and Ho 1994].

Serum albumin is also a target for various glycating agents during non-enzymatic glycation process, i.e. formation of a Schiff base between ε-amino groups of lysine or arginine residues and reducing sugars or their metabolites. HSA and BSA contains 59 lysine residues, whereas 24 and 23 arginine residues, respectively [Westwood and Thornalley 1995].

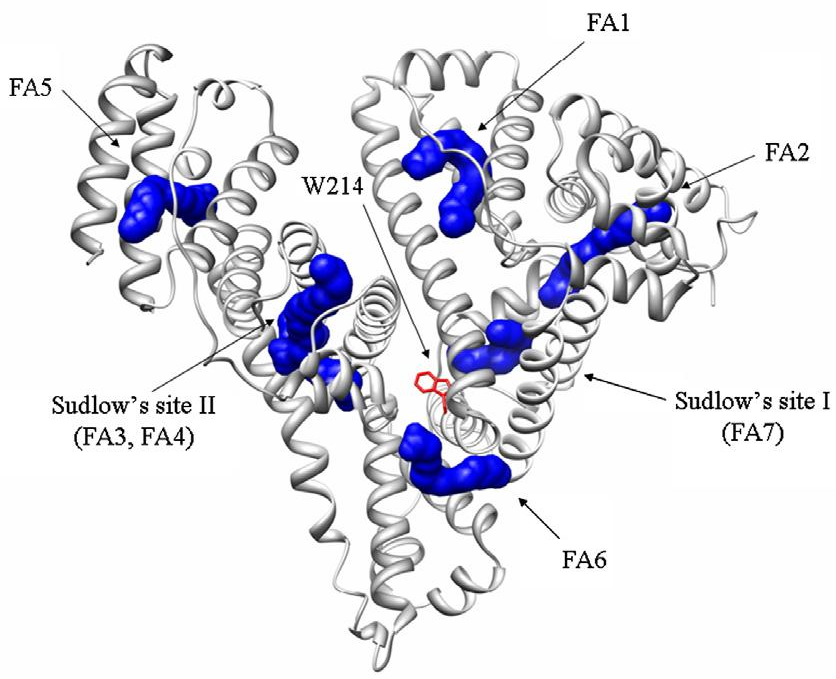

Figure 7: Structure of human serum albumin [Bolli et al. 2010]**.**
The sole tryptophan residue (Trp-214, W-214) residue in hydrophobic pocket is highlighted in red. Fatty acid binding sites are indicated by arrows and labeled. Oleate molecules bound to fatty acid sites (represented as space filled) are shown in blue. The Sudlow´s site I and II are showed.

2.4.2 Protein ERp57

ERp57 (58 kDa) is a multifunctional thiol-disulfide oxidoreductase (EC 5.3.4.1) that is highly similar to the protein disulfide isomerase (PDI) family members in terms of amino acid sequence and structural/functional domain organization [Wang et al. 2010]. However, it possesses some distinctive structural features that dictate its unique functions within the cells [Coe and Michalak 2010, Maattanen et al. 2006, Silvennoinen et al. 2004]. ERp57 is localized mainly in the endoplasmic reticulum (ER) of eukaryotic cells where it plays numerous physiological functions. Two major and the most studied roles of ERp57 are: (i) a key molecular player in the quality control of newly synthesized glycoproteins, together with the lectine-like ER chaperones calnexin and calreticulin [Jessop et al. 2007, Oliver et al. 1997], and (ii) involvement in the assembly of the MHC (Major Histocompatibility Complex) class I molecules [Dong et al. 2009, Wearsch and Cresswell 2008]. However, ERp57 has been found also outside of the ER in the nucleus, cytoplasm and cell surface, and involved in gene regulation [Coppari et al. 2002, Khanal and Nemere 2007, Turano et al. 2002]. Its numerous functions are linked to many disease states predicting cancer, prion disorders, Alzheimer's disease, and hepatitis, and it makes ERp57 as a probable target for developing novel strategies for treatment and early diagnosis of these diseases [Erickson et al. 2005, Hetz et al. 2005, Martin et al. 1993, Seliger et al. 2001].

The overall domain construction of ERp57 is *abb'a'c* (**Figure 8**), where domains *a* and *a´*are two thioredoxin-like catalytic domains, while *b* and *b´* are two thioredoxin-like non-catalytic domains, and *c* is a basic carboxyl terminal domain with C-terminal ER retention sequence (QEDL). Each of the *a* and *a´* domains contains the catalytically redox-active WCGHCK[1] motif and is capable of catalyzing simple oxido-reductions and thiol-disulfide exchange reactions [Frickel et al. 2004, Kozlov et al. 2006]. The *b* and *b´* domains provide the principal substrate binding sites for the lectine-like chaperones calnexin and calreticulin [Urade et al. 2004], the *a* domain is critical for forming disulfide bonds during interaction of ERp57 with chaperone tapasin within the MHC class I peptide-loading complex [Peaper et al. 2005]. The DNA binding activity of ERp57 is associated with the *a´* domain [Grillo et al. 2002] and related to its redox-dependent conformational changes [Grillo et al. 2007]. The ERp57 interacts also with Ref-1

[1] Amino acid sequence motif of redox-active sites of ERp57 (Trp–Cys–Gly–His–Cys–Lys).

protein, which is involved in DNA repair as well as in the reduction and activation of transcription factors [Grillo et al. 2006], Stat3[2] [Guo et al. 2002], and is involved in Stat3-DNA complexes [Eufemi et al. 2004]. High binding affinities of several antibiotics to ERp57 and their inhibitory effects on the reductase activity of the protein have been described [Gaucci et al. 2008]. From the spectroscopic point of view, the presence of three tryptophan residues in ERp57 molecule is important. They unequally contribute to the protein intrinsic (tryptophan) fluorescence. One residue is buried in a hydrophobic pocket of the *b´*domain, whereas the other two residues are located on the protein surface close to the active like-thioredoxin sites in domains *a* and *a´*, respectively. Hence these tryptophan residues differ in accessibility to molecule of a quencher.

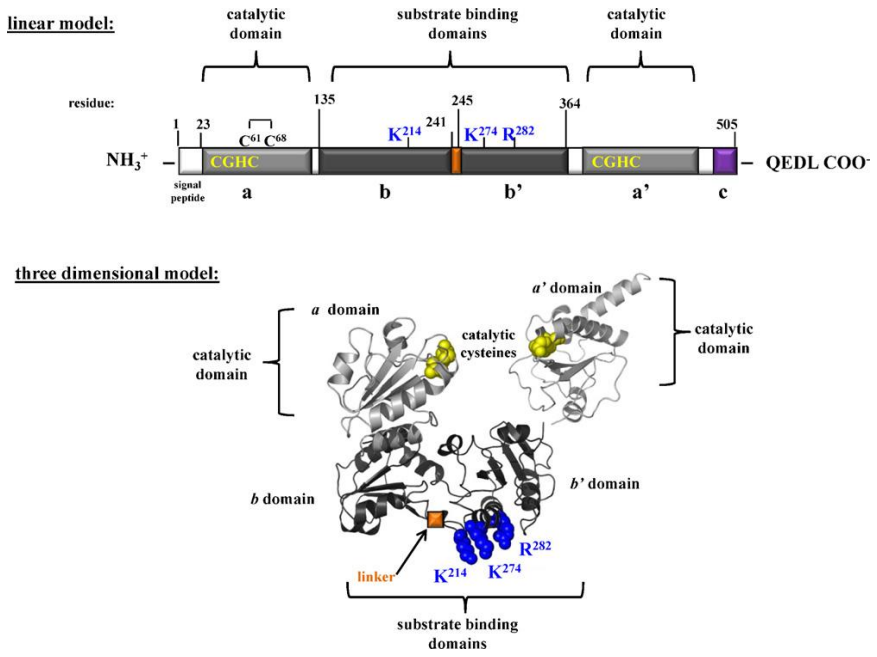

Figure 8: Structure and domain organization of ERp57 [Coe and Michalak 2010].
ERp57 has a N-terminal amino acid signal sequence (*white*), catalytic *a* and *a'* domains (*light grey*) with catalytic residues (CGHC, *yellow*), substrate binding *b* and *b'* domains (*dark grey*) connected with a linker region *(orange),* a basic C-terminal tail (*violet)* and a C-terminal ER-retention signal (QEDL). Amino acids involved in calnexin binding are indicated in blue and disulfide bond in the *a* domain is marked.

[2]Signal Transducer and Activator of Transcription 3 - a member of the STAT family of transcription factors, participates in the regulation of expression of genes involved in the immune response, in inflammation, in cell survival and in cell proliferation [Lee et al. 2011].

2.4.3 Gluthathione S-transferase

Glutathione S-transferases (GST, EC 2.5.1.18) represent a group of xenobiotic-metabolizing enzymes that play a crucial role in the phase II of detoxification. These enzymes catalyze conjugation of toxic compounds with endogenous tripeptide glutathione (GSH) in order to deactive them and increase their hydrophobilicity [Uetrecht and Trager 2007]. GSTs are extremely ubiquitous, e.g. constituting about 4% of soluble protein in the liver [van Bladeren 2000]. They can be divided into three subfamilies according to the cellular localization: cytosolic, microsomal, and mitochondrial. Among them, cytosolic GSTs are numerous and well described. Seven classes of mammalian cytoslic GSTs, called alpha, kappa, mu, omega, pi, theta, and zeta, have been identified and categorized based on a sequence identity (at least 40% sequence identity within a class) [Dourado at al. 2008, Nebert and Vasiliou 2004, Sheehan et al. 2001]. The most widely distributed GST isoforms come from alpha, mu, and pi classes [Dourado at al. 2008]. These enzymes exist as dimeric proteins, with an approximate molecular weight of 25 kDa for each subunit (**Figure 9**). Each of the subunits possesses a GSH binding site (G-site) as well as an adjacent relatively hydrophobic site (H-site) for the binding of the electrophilic substrate [van Bladeren 2000, Mannervik and Danielson 1988]. Other details are described in chapter 5.5.

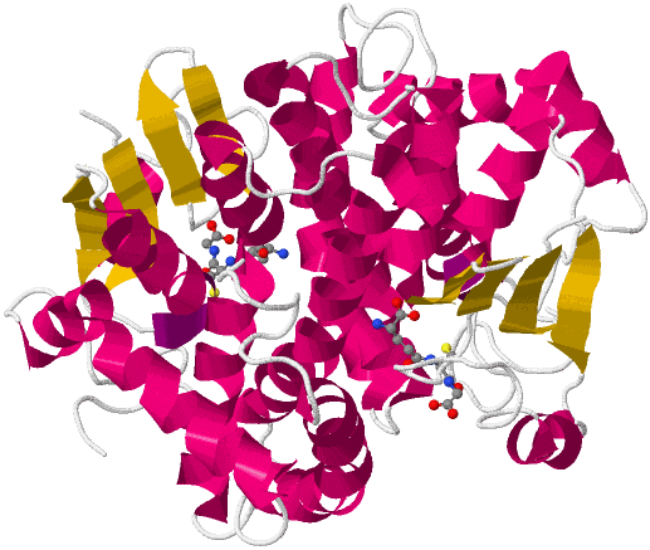

Figure 9: Structure of non-fusion GST from *Schistosoma japonicum* in complex with glutathione. GST contains α-helix parts (*ping*), ß-pleated sheet parts (*yellow*), and their connecting parts, e.g. loops or folds (*white*). Source: RCSB Protein Databank (1UA5, http://www.pdb.org/pdb/explore/jmol.do?structureId=1UA5&bionumber=1).

3 RESEARCH OBJECTIVES

The main aim of this work has been focused on study of effects of naturally occurring dietary polyphenols (i.e. hydroxycinnamic acids and catechins) on protein conformation, protein binding ability, enzyme activity, and protein glycation processes in the *in vitro* models to evaluate their structure-activity relationships. Moreover, study of methylglyoxal-mediated glycation of model protein has been also performed. Spectroscopic, especially fluorescence methods, and electrophoretic (native PAGE, SDS PAGE, western blotting) methods were applied for these purposes.

Interaction of selected dietary plant polyphenols with model proteins

(i) *In vitro* study of interaction between hydroxycinnamic acids (HCAs) and bovine serum albumin (BSA) by fluorescence quenching method

(ii) *In vitro* study of interaction between catechins and human serum albumin (HSA) by spectroscopic (fluorescence quenching method and UV-Vis spectroscopy) and electrophoretic methods (native PAGE and SDS PAGE)

(iii) *In vitro* study of interaction between green tea catechins (GTCs) and ERp57 protein by fluorescence quenching method

Effect of selected dietary plant polyphenols on enzyme activity of model protein

(i) *In vitro* study of effect of green tea catechins (GTCs) on disulfide reductase activity of the ERp57 protein by sensitive fluorescent assay

Methylglyoxal-mediated non-enzymatic glycation of model proteins

(i) *In vitro* study of methylglyoxal-mediated non-enzymatic glycation process of glutathione S-transferase by spectroscopic (fluorescence and UV-Vis spectroscopy) and electrophoretic (native PAGE and western blotting) methods

(ii) *In vitro* study of effect of green tea catechins (GTCs) on methylglyoxal-mediated non-enzymatic glycation process of human serum albumin by fluorescence methods

4 EXPERIMENTAL PART

4.1 CHEMICALS

Proteins

Albumin from bovine serum (min. 98% electrophoresis):

Sigma-Aldrich Co., St. Louis, USA

Albumin from human serum (lyophilized powder, ≥99%):

Sigma-Aldrich Co., St. Louis, USA

Endoplasmic reticulum protein 57 (ERp57):

protein preparation by prof. Altieri [Grillo et al. 2002]

Glutathione S-transferase (a recombinant enzyme from *Schistosoma japonicum*):

GenScript, New Jersey, USA

Hydroxycinnamic acids: Sigma-Aldrich Co., St. Louis, USA

Caffeic acid (min. 99% HPLC, crystalline)

Chlorogenic acid (min. 95% titration)

m-Coumaric acid (trans-3-hydroxycinnamic acid, 99%)

o-Coumaric acid (≥97% HPLC)

p-Coumaric acid (min. 98% HPLC)

Ferulic acid (trans-4-hydroxy-3-methoxy-cinnamic acid, 99%)

Rosmarinic acid (min. 96%)

Sinapic acid (p.a. matrix substance for MALDI-MS, 99%)

Catechins (flavan-3-ols) : Sigma-Aldrich Co., St. Louis, USA

(-)-Catechin (from green tea, ≥98%)

(-)-Catechin gallate (from green tea, ≥98%)

(-)-Epicatechin (from green tea, ≥98%)

(-)-Epicatechin gallate (from green tea, ≥98%)

(-)-Epigallocatechin (from green tea, ≥95%)

(-)-Epigallocatechin gallate (from green tea, ≥95%)

(-)-Gallocatechin (from green tea, ≥98%)

(-)-Gallocatechin gallate (from green tea, ≥98%)

Others chemicals

Acrylamide (for electrophoresis, ≥99%): Sigma-Aldrich Co., St. Louis, USA

β-alanine: Sigma-Aldrich Co., St. Louis, USA

Aminoguanidine hydrochloride (≥98%): Sigma-Aldrich Co., St. Louis, USA

Ammonium persulfate (for electrophoresis, ≥98%): Sigma-Aldrich Co., St. Louis, USA

Bromophenol blue: Riedel-de Haën, Steinheim, Germany

Chemiluminescent/fluorescent substrate for alkaline phosphatase DuoLux: Vector Laboratories, Burlingame, USA

1-Chloro-2,4-dinitrobenzene: Sigma-Aldrich Co., St. Louis, USA

Coomassie Blue G250 (EZBlue gel staining reagent): Sigma-Aldrich Co., St. Louis, USA

DL- Dithiothreitol (≥99%): Sigma-Aldrich Co., St. Louis, USA

Ethanol (p.a.): Sigma-Aldrich Co., St. Louis, USA

Ethylenediaminetetraacetic acid (anhydrous, ≥99%): Sigma-Aldrich Co., St. Louis, USA

N-Ethylmaleimide (purum p.a., ≥99%): Sigma-Aldrich Co., St. Louis, USA

Fixing and developing bath: Foma Bohemia, Hradec Králové, Czech Republic

L-Glutathione oxidized (≥98%): Sigma-Aldrich Co., St. Louis, USA

L-Glutathione reduced (≥98%): Sigma-Aldrich Co., St. Louis, USA

Glycerol (for molecular biology, ≥98%): Sigma-Aldrich Co., St. Louis, USA

Glycine for electrophoresis (≥99%): Sigma-Aldrich Co., St. Louis, USA

Goat polyclonal anti-rabbit IgG antibody conjugated with alkaline phosphatase (secondary antibody): Acris GmbH, Hiddenhausen, Germany

2-Mercaptoethanol (electrophoresis reagent, ≥98%): Sigma-Aldrich Co., St. Louis, USA

Methanol (p.a.): Penta, Prague, Czech Republic

N,N´-Methylenebisacrylamide (for electrophoresis, ≥98%): Sigma-Aldrich Co., St. Louis, USA

Methylglyoxal (aqueous solution, 40%): Sigma-Aldrich Co., St. Louis, USA

Mouse monoclonal antibody [3C] to MGO-derived AGEs (primary antibody): Abcam plc, Cambridge, UK

Non-fat dry milk: Bio-Rad Laboratories, Hercules, USA

Precision Plus molecular weight standards: Bio-Rad Laboratories, Hercules, USA

Rabbit polyclonal antibody to AGE (primary antibody):

Acris GmbH, Hiddenhausen, Germany

Rabbit polyclonal anti-mouse IgG antibody conjugated with alkaline phosphatase (secondary antibody): Abcam plc, Cambridge, UK

Sodium azide: Lachema, Brno, Czech Republic

Sodium dodecyl sulfate: Sigma-Aldrich Co., St. Louis, USA

Sodium isothiocyanate (ACS reagent, ≥98%): Sigma-Aldrich Co., St. Louis, USA

N,N,N´,N´-Tetramethylethylendiamine (for molecular biology): Sigma-Aldrich Co., St. Louis, USA

2,4,6-Trinitrobenzenesulfonic acid: Sigma-Aldrich Co., St. Louis, USA

Tris(hydroxymethyl)aminomethane (Tris, ACS reagent, ≥99.8%): Sigma-Aldrich Co., St. Louis, USA

Trolox ((±)-6-Hydroxy-2,5,7,8-tetramethylchromane-2-carboxylic acid, ≥97%): Sigma-Aldrich Co., St. Louis, USA

X-ray films CL-XPosure: Thermo Fisher Scientific, Rockford, USA

Buffers

Buffers were prepared using common chemicals of analytical grade and redistilled water.

Phosphate buffered saline system (PBS, 0.01 M, pH 7.4)

Sodium phosphate buffer (0.1 M, pH 7.4)

Sodium phosphate buffer with sodium azide (0.1 M, pH 7.4, 0.05% sodium azide)

Potassium phosphate buffer (0.1 M, pH 7.0, 2 mM EDTA)

Potassium phosphate buffer (0.1 M, pH 8.8, 2 mM EDTA)

Tris buffer (0.1 M, pH 8.0)

Tris buffer (0.1 M, pH 9.5, 5 mM $MgCl_2.6H_2O$)

Tris buffer saline (TBS)

Tris buffered saline-Tween-20 buffer (TBST)

Tris-HCl buffer (1.5 M, pH 8.8)

Tris-HCl buffer (0.5 M, pH 6.8)

Tris-glycine buffer (0.6 M, pH 8.3) (concentrated running buffer for native PAGE)

Tris-glycine buffer (0.6 M, pH 8.3, 10% SDS) (concentrated running buffer for SDS PAGE)

4.2 SOLUTION PREPARATIONS

Redistilled water was used for preparation of all aqueous solutions.

4.2.1 Stock protein solutions

Bovine serum albumin was dissolved in sodium phosphate buffer (0.1 M, pH 7.4, 0.05% sodium azide) in order to yield solution with concentration of 2×10^{-6} M. Human serum albumin was dissolved in sodium phosphate buffer (pH 7.4, 0.1 M, 0.05% sodium azide) in order to yield solutions with concentration of 4×10^{-6} M and 15×10^{-6} M for spectroscopic measurements and electrophoresis, respectively. ERp57 and GST were dissolved in PBS (0.01 M, pH 7.4) in order to yield stock solutions with concentrations of 5×10^{-7} M and 19×10^{-9} M (1 mg/ml), respectively.

4.2.2 Stock polyphenolic solutions

Individual polyphenols were dissolved in anhydrous methanol in order to yield 10 mM stock solutions that were stored at -20°C until use.

4.2.3 Sample preparation and incubation

4.2.3.1 Protein sample preparation

Stock protein solutions of BSA (2×10^{-6} M), HSA (4×10^{-6} M), and ERp57 (15×10^{-6} M) have been used for fluorescence quenching measurements without further dilution.

4.2.3.2 HSA sample preparation and incubation

Samples with and without (controls) tested catechins were prepared as follows. Protein concentration in all samples was 15×10^{-6} M and concentration of catechins was 6×10^{-4} M. Samples were incubated for 30 minutes at 37°C and further analyzed using polyacrylamide gel electrophoresis under non-denaturating (native PAGE) or denaturating (SDS PAGE) conditions.

4.2.3.3 GST sample preparation and incubation

Stock solution of GST (1 mg/ml) was diluted by sodium phosphate buffer (0.1 M, pH 7.4) in order to yield 0.025 mg/ml solution for enzyme activity assay.

GST (0.5 mg/ml) was incubated in the absence or presence of methylglyoxal (0.5, 1, and 2 mM) at 37 °C for up to 14 days in 100 mM phosphate-buffered saline (pH 7.4, 0.05% sodium azide). Low-molecular compounds were removed using Microcon centrifugal filtration device with 10 mM phosphate-buffered saline (pH 7.4). The protein content was determined using Bradford assay and adjusted to the concentration 0.5 mg/ml. Aliquots were stored frozen at -20 °C until analysis. All the samples were assessed in triplicates and experiments were repeated twice if not stated otherwise.

4.2.4 Stock solutions for polyacrylamide gel electrophoresis

4.2.4.1 Stock solution containing acrylamide and bis-acrylamide

Thirty g of acrylamide (AA) and 0.8 g of *N,N´*-methylenebisacrylamide (bis-AA) were dissolved in 100 ml of redistilled water.

4.2.4.2 Stock solution of bromophenol blue

Fifty mg of bromophenol blue (BPB) were dissolved in 10 ml of redistilled water in order to yield solution with concentration of 0.5%.

4.2.4.3 Stock solution of ammonium persulfate

Twenty-five mg of ammonium persulfate (APS) were dissolved in 250 µl of redistilled water in order to yield solution with concentration of 10%.

4.2.4.4 Stock solution of sodium dodecyl sulfate

Ten g of sodium dodecyl sulfate (SDS) were dissolved in 100 ml of redistilled water in order to yield solution with concentration of 10%.

4.2.4.5 Running buffers

Concentrated running buffers were diluted by redistilled water in ratio 1:4 in order to yield running buffers for native and SDS PAGE.

4.2.4.6 Sample buffers and samples

Sample buffer for native PAGE was prepared by mixing 1 ml of Tris-HCl buffer (0.5 M, pH 6.8), 4.3 ml of redistilled water, 2 ml of glycerol, and 0.6 ml of BPB (0.5%). Protein samples were diluted by sample buffer in ratio 1:1.

Sample buffer for SDS PAGE was prepared by mixing 1 ml of Tris-HCl buffer (0.5 M, pH 6.8), 1.3 ml of redistilled water, 2 ml of glycerol, 3 ml of SDS (10%), and 0.6 ml of BPB (0.5%). Consecutively, 50 µl of 2-mercaptoethanol was added into 1 ml of sample buffer with SDS. Protein sample (12 µl) was diluted by 3 µl of SDS (10%) and 15 µl of sample buffer containing SDS and 2-mercaptoethanol.

4.2.5 Preparation of polyacrylamide gels

Table 8: *Preparation of non-denaturating polyacrylamide gel for native PAGE.*

Preparation for 1 gel	Separating gel (10%)	Stacking gel (4%)
Redistilled water	4000 µl	3176 µl
Tris-HCl buffer (1.5 M, pH 8.8)	2500 µl	1250 µl
Solution (AA + bis-AA)	3400 µl	500 µl
APS (10%)	116 µl	100 µl
TEMED	8 µl	10 µl

Acrylamide (AA), ammonium persulfate (APS), *N,N´*-methylenebisacrylamide (bis-AA), *N,N,N´,N´*-tetramethylethylendiamine (TEMED).

Table 9: *Preparation of denaturating polyacrylamide gel for SDS PAGE.*

Preparation for 1 gel	Separating gel		Stacking gel
	10%	12.5%	4%
Redistilled water	2450 µl	1600 µl	1563 µl
Tris-HCl buffer (1.5 M, pH 8.8)	1250 µl	1250 µl	625 µl
Solution (AA + bis-AA)	50 µl	50 µl	25 µl
SDS (10%)	1250 µl	2100 µl	250 µl
APS (10%)	116 µl	116 µl	100 µl
TEMED	8 µl	8 µl	10 µl

Acrylamide (AA), ammonium persulfate (APS), *N,N´*-methylenebisacrylamide (bis-AA), sodium dodecyl sulfate (SDS), *N,N,N´,N´*-tetramethylethylendiamine (TEMED).

4.3 APPLIED METHODS AND INSTRUMENT EQUIPMENTS

4.3.1 UV-Vis absorption spectroscopy

All absorption spectra were recorded using a spectrophotometer Helios β (Spectronic Unicam, United Kingdom) in a 10 mm quartz cuvette.

4.3.1.1 Stability of polyphenolic solutions

UV-Vis absorption spectroscopy was employed to check stabilities of polyphenol solutions during long-term incubation. Fifty micromolar solutions of the tested catechins or HCAs in sodium phosphate buffer (pH 7.4, 0.1 M, 0.05% sodium azide) were incubated at 37°C for up to 15 or 28 days, respectively. The absorption spectra were recorded at the time 0 and in the selected time intervals from 190 to 550 nm at 37°C. Time-dependent changes in the characteristic spectra of individual polyphenols were observed to obtain information about their stabilities.

4.3.1.2 Complex formation between catechins and HSA

Possibility of complex formation between catechins and human serum albumin was probed by UV-Vis absorption spectroscopy as an additional method. Solutions containing HSA (4×10^{-6} M) and individual catechins (4×10^{-5} M) were incubated for 5 minutes at 37°C ([HSA]/[catechin] = 1/10) and consecutively absorption spectra were recorded from 190 to 550 nm at 37°C. The spectrum of sodium phosphate buffer (0.1 M, pH 7.4, 0.05% sodium azide) with or without appropriate catechin was substracted and the obtained differential spectrum was compared with protein spectrum in time 0.

4.3.1.3 Glutathione transferase activity assay

GST (0.025 mg/ml) was incubated in the absence or presence of methylglyoxal (0.5, 1, and 2 mM) for 180 min at 37°C in sodium phosphate buffer (0.1 M, pH 7.4). Sample aliquots were taken away at 0, 60, 120, and 180 min, diluted, and their activity was assessed by colorimetric method based on the GST-catalyzed reaction between GSH and GST substrate 1-chloro-2,4-dinitrobenzene at pH 6.5. Product of the reaction, S-(2,4-dinitrophenyl)glutathione, was detected spectrophotometrically at 340 nm

[Habig et al. 1974]. Catalytic activity of GST was expressed as percentage of control sample activity at all time intervals, which was considered 100% ± SD (%).

4.3.1.4 Determination of amino groups of GST

Amine content, which is a measure of protein glycation extent, was estimated spectrophotometrically with trinitrobenzenesulfonic acid using *β*-alanine as the standard [Steinbrecher 1987]. Sample containing 50 µg of GST was incubated with 0.1% trinitrobenzenesulfonic acid in alkaline conditions for 2 h at 37°C. The reaction was stopped by acidification (1 M HCl) and addition of 10% SDS. The absorbance of trinitrophenyl-amino acid complex was measured at 340 nm. The standard curve was linear in the range 5-100 nmol of NH_2.

4.3.2 Fluorescence spectroscopy

4.3.2.1 Fluorescence spectra of complex between catechins and HSA

Fluorescence emission spectra of individual catechins (4×10^{-5} M) with or without HSA (4×10^{-6} M) were recorded at the excitation wavelength of 330 nm corresponding to the absorption maximum of ground state complex.

4.3.2.2 Fluorimetric titration: polyphenol-serum albumin systems

Fluorescence spectra for study of polyphenol-serum albumin interactions were recorded using a luminescence spectrometer LS-50B (Perkin Elmer, United Kingdom) in a 10 mm quartz Suprasil fluorescence cuvette (Hellma, Germany) at 37°C. Fluorescence emission spectra were recorded from 300 to 530 nm with excitation wavelength of 295 nm (intrinsic/tryptophan protein fluorescence) while stirring. The excitation and emission slits were both set to 5 nm and scanning speed was 200 $nm.min^{-1}$. Quantitative analyses of the potential interaction between the studied polyphenols and serum albumin were performed by fluorimetric titration. Briefly, solutions of BSA (2×10^{-6} M) or HSA (4×10^{-6} M) were titrated in cuvette by successive additions of HCA or catechin solutions (1×10^{-2} M) to a final concentration of 2×10^{-5} M, respectively. Fluorescence of individual polyphenols ($0\text{-}2 \times 10^{-5}$ M) was recorded as blanks under the same experimental conditions and subtracted from the corresponding sample to

correct the fluorescence background. Fluorescence intensities were read at emission wavelength of 350 nm and 348 nm for HCA-BSA and catechin-HSA systems, respectively.

4.3.2.3 Fluorimetric titration: green tea catechin-ERp57 systems

Fluorescence emission spectra were recorded on a FluoroMax spectrofluorimeter (Horiba Jobin Yvon, UK) using a 1 cm path length quartz cuvette from 300 to 500 nm with excitation at 290 nm under continuous stirring. The excitation and emission slits were both set to 5 nm and scan speed was 120 nm·min^{-1}. Quantitative analyses of the potential interaction between green tea catechins and protein was performed by the fluorimetric titration in PBS (0.01 M, pH 7.4) containing dithiothreitol (DTT, 1 x 10^{-4} M) and ethylenediaminetetraacetic acid (EDTA, 2 x 10^{-4} M) at 25°C. Briefly, ERp57 (5 x 10^{-7} M) was titrated in cuvette by successive additions of individual catechin (1 x 10^{-3} M) to a final concentration of 2 x 10^{-5} M. Fluorescence intensities were read at protein emission maximum of 338 nm. Appropriate blanks (samples without proteins) under the same experimental conditions were subtracted from the corresponding samples to correct the fluorescence background. Quenching effect of the quenchers on ERp57 was calculated using the following equation:

$$Q = (1 - F/F_0) \times 100\% \quad (8)$$

where Q is the quenching fraction (%), F and F_0 are fluorescence intensities in the presence and absence of the quencher.

4.3.2.4 Fluorimetric titration: analysis of data

Fluorescence quenching spectra were used for appraisal of protein conformational changes induced by polyphenols. The obtained fluorescence data were used for Stern-Volmer analysis, determination of binding parameters, and estimation of the distances between protein and polyphenol by FRET. Principles and procedures of these analyses are briefly described in chapters "*2.3.3.1.2 Fluorescence spectroscopy"* and "*2.3.3.1.3 Fluorescence resonance energy transfer"*.

4.3.2.5 Disulfide reductase activity of ERp57

Disulfide reductase activity of ERp57 was monitored by sensitive fluorescent assay using dieosin glutathione disulfide (Di-E-GSSG) as fluorogenic probe. Di-E-GSSG was synthesized by the reaction of eosin isothiocyanate with glutathione disulfide (GSSG) according to the method of Raturi and Mutus [Raturi and Mutus 2007] with some modifications. Briefly, GSSG (1×10^{-4} M) was incubated with 10-fold molar excess of eosin isothiocyanate (1×10^{-3} M) in potassium phosphate buffer (0.1 M, pH 8.8, 2 mM EDTA) at room temperature. Two hundred microliters of the suspension was passed down the G-25 column (100 x 10 mm, 10 ml) using the potassium phosphate buffer (0.1 M, pH 7.0, 2 mM EDTA) and 1.5 ml of appropriate aliquots were collected. The final concentration of Di-E-GSSG was determined spectrophotometrically (ε_{525} = 88,000 M^{-1} cm^{-1}). ERp57 stock solution (1×10^{-6} M) was used to prepare four types of incubation samples: (a) with buffer only as control (potassium phosphate buffer, 0.1 M, pH 7.0, 2 mM EDTA); (b) with N-ethylmaleimide (NEM, 4×10^{-4} M) as positive control; (c) with vancomycin (VM, 1×10^{-4} M) as positive control; (d) with individual green tea catechins (GTCs, 1×10^{-4} M). The last incubation sample containing BSA (1 mg/ml) was used as negative control. Samples were incubated for 15 minutes at room temperature. Kinetic fluorescence measurements for determination of ERp57 disulfide reductase activity was monitored at 545 nm with excitation at 520 nm for 60 seconds at 25°C with continuous stirring. Scan speed was 60 $nm.min^{-1}$ and the excitation and emission slits were both set to 5 nm. Twenty microlitres of incubation sample aliquot was added into potassium phosphate buffer (0.1 M, pH 7.0, 2 mM EDTA) containing Di-E-GSSG (1.5×10^{-7} M) and DTT (5×10^{-6} M). The relative disulfide reductase activity (%) was calculated as: $(k_x - k_0)/(k_1 - k_0) \times 100\%$, where k_1, k_x, and k_0 are the slopes of ERp57 protein alone, ERp57 in the presence of GTC, NEM, or VM, and BSA protein alone, respectively.

4.3.2.6 Fluorescent AGEs formation in HSA induced by methylglyoxal

Human serum albumin (1 mg/ml) was preincubated with catechins at different concentrations (0-5 x 10^5 M) in PBS (0.01 M, pH 7.4, 0.05% sodium azide) at room temperature for 30 minutes. Consequently, methylglyoxal (1 mM MGO) was added into the mixtures which were then incubated at 37°C for 7 days. The aliquots were

taken away at time 0, 3 and 7 days, and stored frozen at -20°C. Low-molecular compounds were removed using Microcon centrifugal filtration device with PBS (0.01 M, pH 7.4). The protein content was determined using Lowry assay and adjusted to the concentration 0.5 mg/ml. Formation of total fluorescent AGEs and argpyrimidine were measured at the excitation/emission wavelength of 340/410 nm and 320/380 nm against corresponding blanks in 96-well-plate by a microplate reader (Tecan Infinity M200) using 0.2 mg of protein per well. The % inhibition of AGEs formation = [1-(fluorescence of the test group/fluorescence of the glycated control)] x 100%. Trolox (2.5 mM) and aminoguanidine (1 mM) were used as positive controls. Aliquots of time 0 were used as unincubated blanks. All the samples were assessed in triplicates and experiments were repeated twice if not stated otherwise.

4.3.2.7 Fluorescent AGEs formation and conformational changes in GST induced by methylglyoxal

Formation of total fluorescent AGEs and changes in tryptophan (intrinsic) fluorescence were determined using a microplate reader (Tecan Infinite M200). Fluorescence was measured at excitation and emission wavelengths of 370/440 nm (total fluorescent AGEs) and 295/386 nm (tryptofan fluorescence), respectively, in 96-well plate using 100 µg of GST per well. Emission wavelength for tryptophan fluorescence determination was found experimentally. Fluorescence data were expressed in relative fluorescence units ± SD.

4.3.3 Native polyacrylamide gel electrophoresis

4.3.3.1 Effect of catechins on molecular charge of HSA

Native PAGE was performed in discontinuous system with 4% stacking gel and 10% separating non-denaturating gel. All lanes were loaded with 8 µg of protein. Electrophoresis was performed at 30 mA using Mini ProteanIII apparatus (BioRad). The gel was stained with colloidal Coomassie Blue G250, scanned by GelDoc XR system (BioRad), and the relative mobilities (R_f) were calculated using Quantity One software (BioRad). Results were further expressed as a rise in percentage of sample mobility compared to the native protein (control): $[(R_f(\text{complex}) - R_f(\text{HSA}))/R_f(\text{HSA})] \times 100$ (%).

4.3.3.2 Effect of methylglyoxal on molecular charge of GST

Native PAGE was used to investigate the change in the molecular charge of GST due to glycation process. Electrophoresis was performed in Ornstein–Davies discontinuous system with 4% stacking gel and 10% separating non-denaturating gel [Ornstein 1964, Davies 1964]. All lanes were loaded with 10 µg of protein. Electrophoresis was performed at 30 mA for about 3 h using Mini ProteanIII apparatus. The gel was then stained by colloidal Coomassie Blue G250, scanned, and relative migration distances were calculated from R_f using Quantity One software (BioRad). Electrophoretic mobilities were expressed as a rise in percentage mobility compared with the native enzyme (control).

4.3.4 SDS PAGE and western blotting

4.3.4.1 Catechin-HSA systems: aggregation and cross-links formation

SDS-PAGE was performed using discontinuous system with 4% stacking gel and 7.5% separating non-denaturating gel. All lanes were loaded with 4 µg of protein. Electrophoresis was performed at 200 V using Mini ProteanIII apparatus (BioRad). Gels were visualized with colloidal Coomassie Blue G250, scanned, and their quantification was performed using Quantity One software (BioRad).

4.3.4.2 MGO-mediated glycation of GST: AGEs and cross-links formation

Formation of specific AGEs was assessed using western blotting with corresponding antibodies. Proteins were first separated by SDS PAGE on Mini ProteanIII apparatus (BioRad). SDS PAGE was performed using discontinuous system with 4% stacking gel and 12.5% separating gel according to the method of Laemmli [1970]. Lanes were loaded with 4 µg of protein. Proteins were then transferred to PVDF membrane (0.2 µm, Bio-Rad Laboratories, Hercules, USA) [Towbin et al. 1979] at a constant voltage of 100 V for 90 min (Mini Trans-Blot Electrophoretic Transfer Cell, Bio-Rad). After blotting, membranes were blocked in 8% non-fat dry milk in Tris buffered saline-Tween-20 buffer overnight at 4°C. After washing in Tris buffered saline-Tween-20 buffer, the membranes were reacted with either primary rabbit anti-AGE

antibody (dilution 1:1000) or primary mouse anti-MGO [3C] antibody (1:1000) for 45 min at room temperature. Subsequently, membranes were washed six times with Tris buffered saline-Tween-20 buffer and incubated with corresponding secondary antibody for 45 min (dilution 1:2000 for anti-rabbit IgG and 1:1000 for anti-mouse IgG). The blots were extensively washed in 0.1 M Tris buffer containing 5 mM $MgCl_2.6H_2O$ (pH 9.5), covered with chemiluminescent substrate DuoLux and incubated for 5 min. Protein bands were then detected by both chemiluminescent detection and staining with Ponceau S. Membranes and X-ray films (CL-XPosure film, Thermo Fisher Scientific) were scanned on GelDoc XR system and quantified by Quantity One software (BioRad).

4.3.5 Statistical analysis

Obtained values are given as means ± standard deviation ($n \leq 5$). Statistical significance was determined using Student's *t*-test and differences were regarded as significant when $p < 0.01$ or $p < 0.05$. Details of each statistical analysis are characterized in following chapters.

5 RESULTS AND DISCUSSION

5.1 INTERACTION BETWEEN HYDROXYCINNAMIC ACIDS AND BOVINE SERUM ALBUMIN

The possibility of binding of eight naturally occurring hydroxycinnamic acids (HCAs) to bovine serum albumin (BSA) has been studied using fluorescence quenching method under simulated physiological conditions (pH 7.4, 37°C) in the *in vitro* model. The main objective was to reveal the character of interactions and to evaluate the structure-binding activity relationships. The structures of the tested HCAs are shown in Table 2.

5.1.1 Stability of hydroxycinnamic acids

Firstly, stabilities of hydroxycinnamic acid solutions in phosphate buffer (0.1 M, pH 7.4, 0.05% NaN_3) during long-term incubation (28 days) at 37°C were checked by observation of changes in their characteristic UV-Vis absorption spectra (data not shown). No changes of absorbance in the characteristic profile of UV-Vis spectra of monosubstituted derivatives (coumaric acids) were observed during the incubation. Spectrum profile of ferulic acid was not altered throughout the incubation, but the intensity of absorbance in maximum slowly decreased. The spectra of other four tested derivatives (caffeic, sinapic, chlorogenic, and rosmarinic acid) showed remarkable changes which suggest that these compounds were decomposed probably to catechol and its substituted derivatives within first 24 hours of incubation [Müller et al. 2006, Jiang and Peterson 2010]. It can be concluded that coumaric acids are stable within the course of long term incubation, while di- and trisubstituted derivatives decompose easily and therefore they are not suitable for long lasting experiments. In the following experiment, the fluorimetric titration was carried out in phosphate buffer (0.1 M, pH 7.4, 0.05% sodium azide) during 45 minutes, where no changes in UV-Vis absorption profiles of the studied HCAs have been observed yet.

5.1.2 Fluorescence quenching spectra of BSA induced by hydroxycinnamic acids

Quenching of protein intrinsic (tryptophan) fluorescence was employed for more detailed study of HCA-BSA binding. First of all, fluorescence emission spectra of individual HCAs were measured as blanks. Only three HCAs (*o*-coumaric, sinapic, and ferulic acid) possessed apparent emission maxima at 498, 428, and 414, respectively. The most remarkable fluorescence intensity exerted *o*-coumaric acid (**Figure 10**).

Fluorescence intensity of BSA gradually decreased with increasing concentration of all HCAs (**Figure 10**). This may indicate alterations in microenvironment around tryptophan residues in protein molecule upon interaction with the tested compounds. Moreover, bathochromic (red) shifts of tryptophan emission maximum (350 nm) in dependence on increasing concentration of tested compounds were found in the case of ferulic, sinapic, chlorogenic, and rosmarinic acids. Emission maximum was slightly shifted towards longer wavelength by 2 nm for both ferulic and sinapic acid-BSA systems, and by 4 and 5 nm for chlorogenic and rosmarinic acid-BSA systems, respectively.

The red shift of protein emission band is caused by decrease in hydrophobic property of binding cavity near tryptophan in BSA (Trp-212) suggesting that tryptophan has been brought to more hydrophilic environment and thus protein secondary structure has been changed [Lakowicz 2006, Kang et al. 2004]. Li et al. [2010] have noticed the obvious red shifts of ferulic and chlorogenic acid-BSA systems by 5 and 20 nm under different conditions (e.g. temperature, pH, λ_{ex}, 0 - 7 x 10^{-5} M for HCAs), respectively. Significant red shifts by 12 and 18 nm were observed also by other authors upon interaction of HSA with sinapic [He et al. 2005] and chlorogenic [Kang et al. 2004] acids but the concentrations of tested compounds that caused so remarkable shift of emission maxima were as much as 1.5 x 10^{-4} M. Other four tested HCAs did not cause any spectral shift in the studied range of concentrations which indicates that they can bind to BSA without affecting the immediate environment of the tryptophan residues [Li et al. 2010, Tian et al. 2004b]. It can be concluded that red shift of protein emission band by HCAs depends on their structure, size and concentration. More pronounced red shift was noticed for bulkier molecules of HCAs such as chlorogenic or rosmarinic acids corresponding with the published data [Hu et al. 2012, Li et al. 2010].

Emission quenching spectra of BSA induced by *o*-coumaric, caffeic, ferulic, and sinapic acids involved isosbestic point, which might indicate that studied compounds exist both in bound and free form that are in equilibrium [Li et al. 2010, Rawel et al. 2006, Xie et al. 2006]. The bound form exerts fluorescence whereas the unbound form does not. It was noticed that emission spectra of these HCA-BSA systems above 430 nm correspond with emission spectra of individual HCAs.

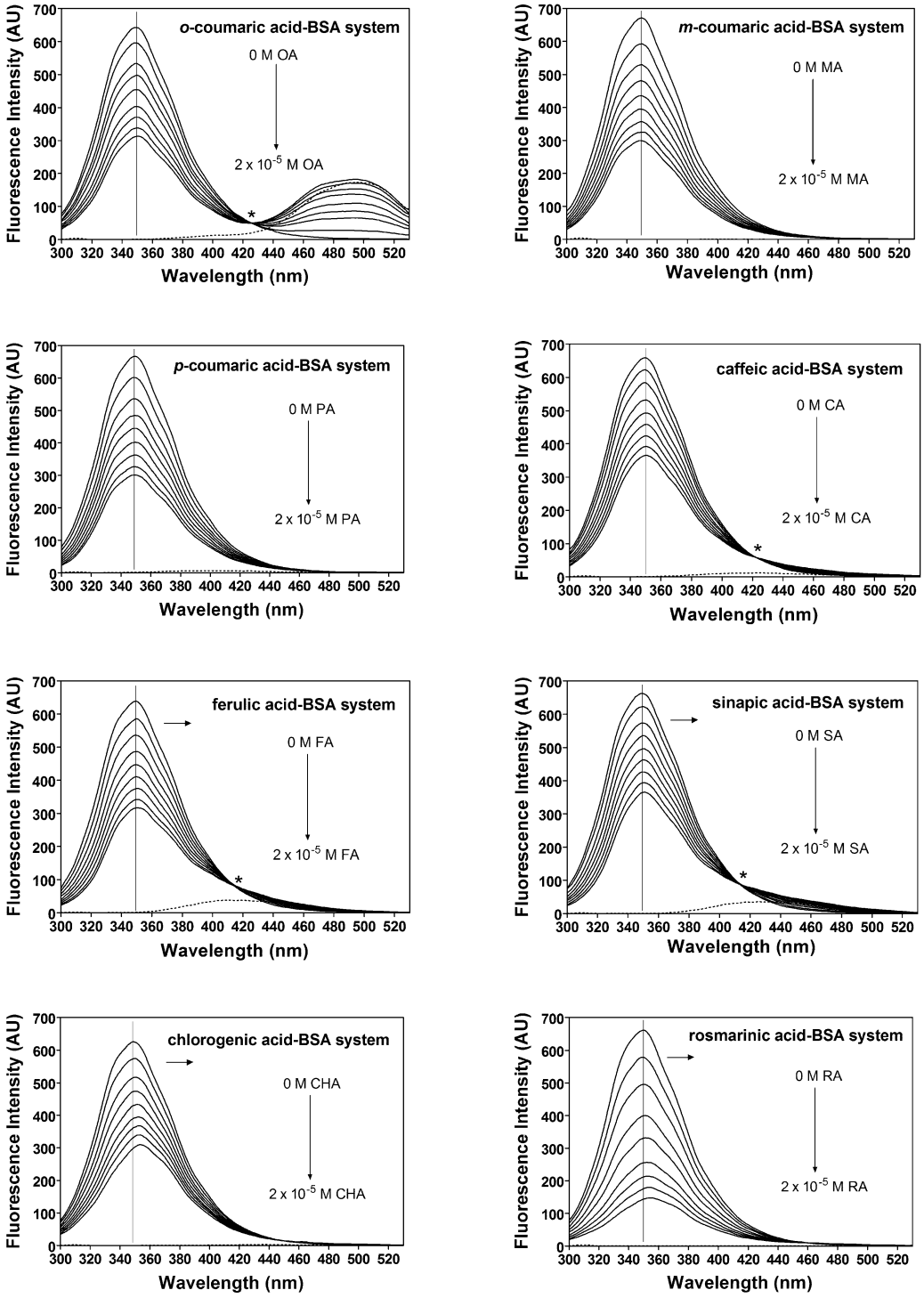

Figure 10: Fluorescence quenching spectra of HCA-BSA systems.
[BSA] = 2 x 10^{-6} M, [HCA] = 0 - 2 x 10^{-5} M, [HCA]/[HSA] = 0.625, 1.25, 1.875, 2.5, 3.125, 3.75, 4.375, and 5.00, pH 7.4, 37°C, and λ_{ex} = 295 nm. Dotted line and arrow display fluorescence spectrum of hydroxycinnamic acid (2 x 10^{-5} M) and shift, respectively. Isosbestic point is shown as asterisk.

5.1.3 Fluorescence quenching mechanism of hydroxycinnamic acid-BSA systems

The Stern-Volmer analysis was applied for determination of the type of fluorescence quenching mechanism of the HCA-BSA systems. The relevant Stern-Volmer plots (i.e. F_0/F versus [Q]) are displayed in the **Figure 11**. The most significant quenching effect (about 82.7%) was caused by rosmarinic acid but it exhibited the exponential dependence indicating that both types of quenching were asserted. For this reason, the constants (K_{SV} and K_q) were not determined. However, the linear dependence in the Stern-Volmer plots in the studied concentration range (0-2 x 10^{-5} M) was found out for all other HCAs. Consequently, the Stern-Volmer quenching constants (K_{SV}) and the bimolecular quenching rate constants (K_q) of these HCAs were determined from the slopes and are shown in **Table 10**. It was confirmed that the static quenching mechanism (i.e. non-fluorescent complex formation) is the main reason of protein fluorescence quenching because all K_q values were found to be higher than the diffusion-limited rate constant of a biomolecule (K_{diff} = 1 x 10^{10} $M^{-1}s^{-1}$) [Lakowicz 2006]. The highest value of K_q was determined for *p*-coumaric acid and further decreased in the order *p*-coumaric acid > *m*-coumaric acid ≥ *o*-coumaric acid > chlorogenic acid > ferulic acid > caffeic acid > sinapic acid.

Table 10: The Stern-Volmer constants (K_{SV}) and bimolecular quenching rate constants (K_q) of tested hydroxycinnamic-BSA systems (pH 7.4, 37°C).

Tested compound	K_{SV} [10^4 M^{-1}]	K_q [10^{13} $M^{-1}s^{-1}$]	R
o-Coumaric acid	5.95[b]	1.19[b]	0.995
m-Coumaric acid	5.96[b]	1.19[b]	0.998
p-Coumaric acid	7.13[a]	1.43[a]	0.993
Caffeic acid	4.30[e]	0.86[e]	0.997
Ferulic acid	4.86[d]	0.97[d]	0.996
Sinapic acid	4.25[f]	0.85[f]	0.997
Chlorogenic acid	5.36[c]	1.07[c]	0.997
Rosmarinic acid	-	-	-

$K_q = K_{SV}/\tau_0$; τ_0 = 5 x 10^{-9} s [Lakowicz 2006]. Standard deviations (mean value of three independent experiments) were lower than 10%. Data were analyzed by Student´s *t*-test and groups with different letters are significantly different ($p < 0.01$).

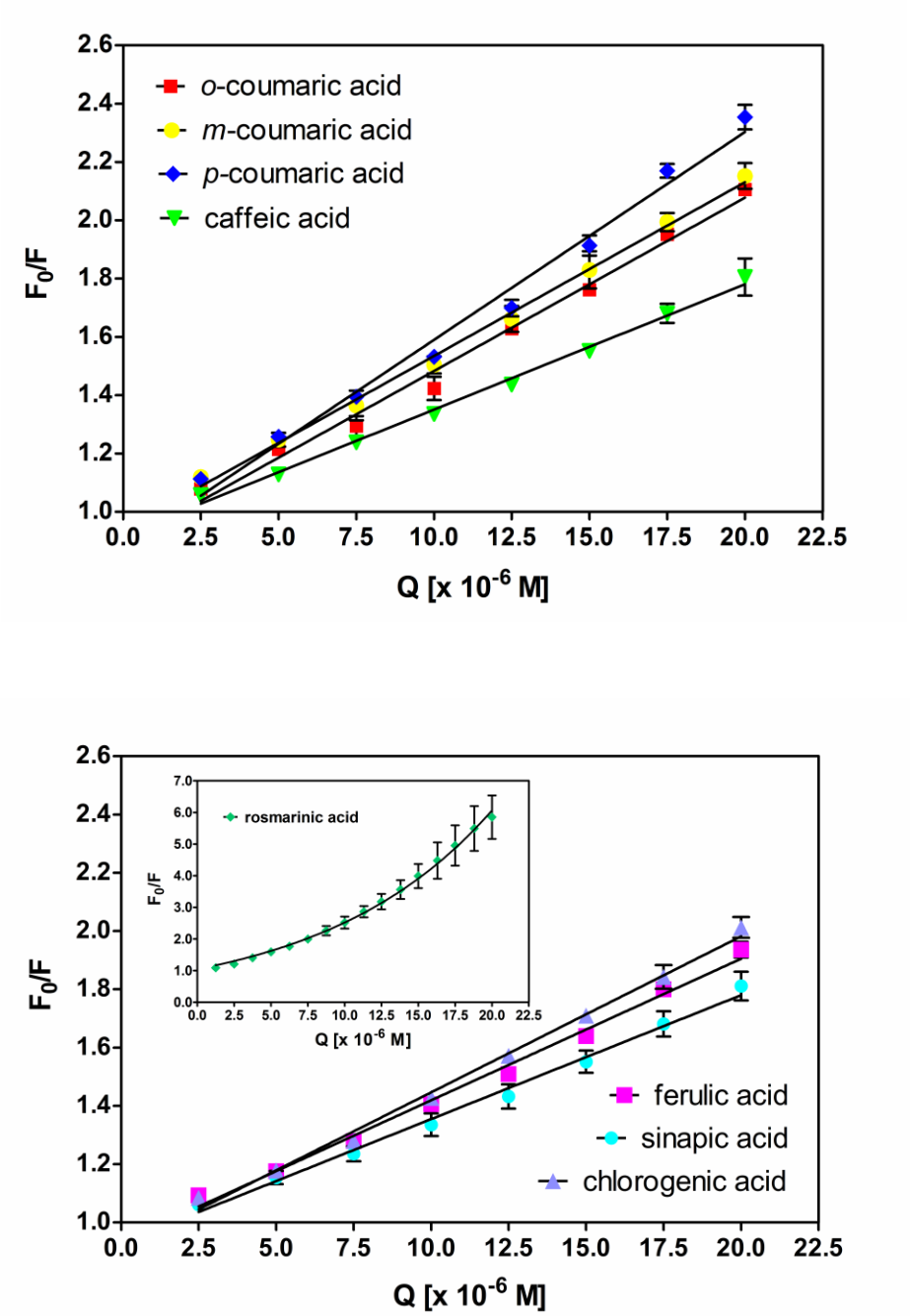

Figure 11: Stern-Volmer plots of tested hydroxycinnamic acid-BSA systems.
[BSA] = 2 x 10^{-6} M, [HCA] = 0 - 2 x 10^{-5} M, pH 7.4, 37°C, λ_{ex} = 295 nm, and λ_{em} = 350 nm. Correlation coefficients (R) were found in the range of 0.993 - 0.998.

Only small but significant differences among K_q values for the tested HCA-BSA systems were observed. All tested HCAs exerted better quenching effect than cinnamic acid (2.26 x 10^{12} $M^{-1}s^{-1}$ for $\tau = 10^{-8}$ s) [Bian et al. 2007]. Rosmarinic acid caused the most outstanding decrease in fluorescence intensity of BSA in the range of studied

concentrations but it exhibited exponential dependence in the Stern-Volmer diagram and thus was not considered in overall comparison. Coumaric acids showed stronger quenching activity than the other more substituted HCAs. In the case of coumaric acids, this effect was probably dependent upon the position of hydroxyl group on aromatic ring and *p*-position seems to be the most suitable structural feature for quenching fluorescence of BSA. The K_q value of chlorogenic acid was similar to K_q of coumaric acids and slightly higher than K_q of more substituted derivatives. It was probably caused by its spatial arrangement and the presence of aromatic ring and five hydroxyls in its molecule [Kang et al. 2004]. The lowest quenching effect was observed for sinapic and caffeic acid followed by ferulic acid. Presence of the methoxyl group in HCA seemed to play a role in quenching activity too. Ferulic acid showed higher effect than caffeic acid, while the K_q of sinapic acid was slightly lower compared to caffeic acid. This was perhaps caused by steric hindrance in the molecule of sinapic acid. The obtained bimolecular quenching rate constants for caffeic, ferulic, and chlorogenic acid-BSA systems are in good agreement with data found in literature [Hu et al. 2012, Liu et al. 2010, Tang et al. 2008a]. However, no quenching of BSA induced by chlorogenic acid was also observed [Rawel et al. 2006]. Several studies were published for HCA-HSA systems too. The highest K_q was obtained for chlorogenic acid followed by caffeic and sinapic, while ferulic and *p*-coumaric acid possessed lower K_q values. Data obtained for HCA-BSA systems in this study correspond with the findings published by other authors [Hu et al. 2012, Jiang et al. 2004, Kang et al. 2004].

5.1.4 Determination of binding parameters of hydroxycinnamic acid-BSA systems

In general, the binding constant (K_b) reflects the power of ligand-protein association and thus can be used for comparison of binding affinities of structurally-related ligands to protein molecule connected with alterations of its secondary structure. Number of binding sites (n) is another important parameter that contributes to better understanding of ligand-protein interaction [Lakowicz 2006].

Except for the rosmarinic acid-BSA system, the binding constants (K_b), number of binding sites (n), and free energy changes (ΔG^0) of all other HCA-BSA systems have been determined according to the equations (2) and (4), respectively. Obtained values are presented in **Table 11**. Logarithmic plots of the tested HCA-BSA systems are

displayed in Figure 12. The binding affinity was the strongest for chlorogenic acid and ranked in the order chlorogenic acid > sinapic acid > caffeic acid > ferulic acid ≥ *o*-coumaric acid > *p*-coumaric acid > *m*-coumaric acid. The negative value of free enthalpy (ΔG^0) indicating spontaneous process of HCA-BSA binding was determined for all studied interactions (Table 11).

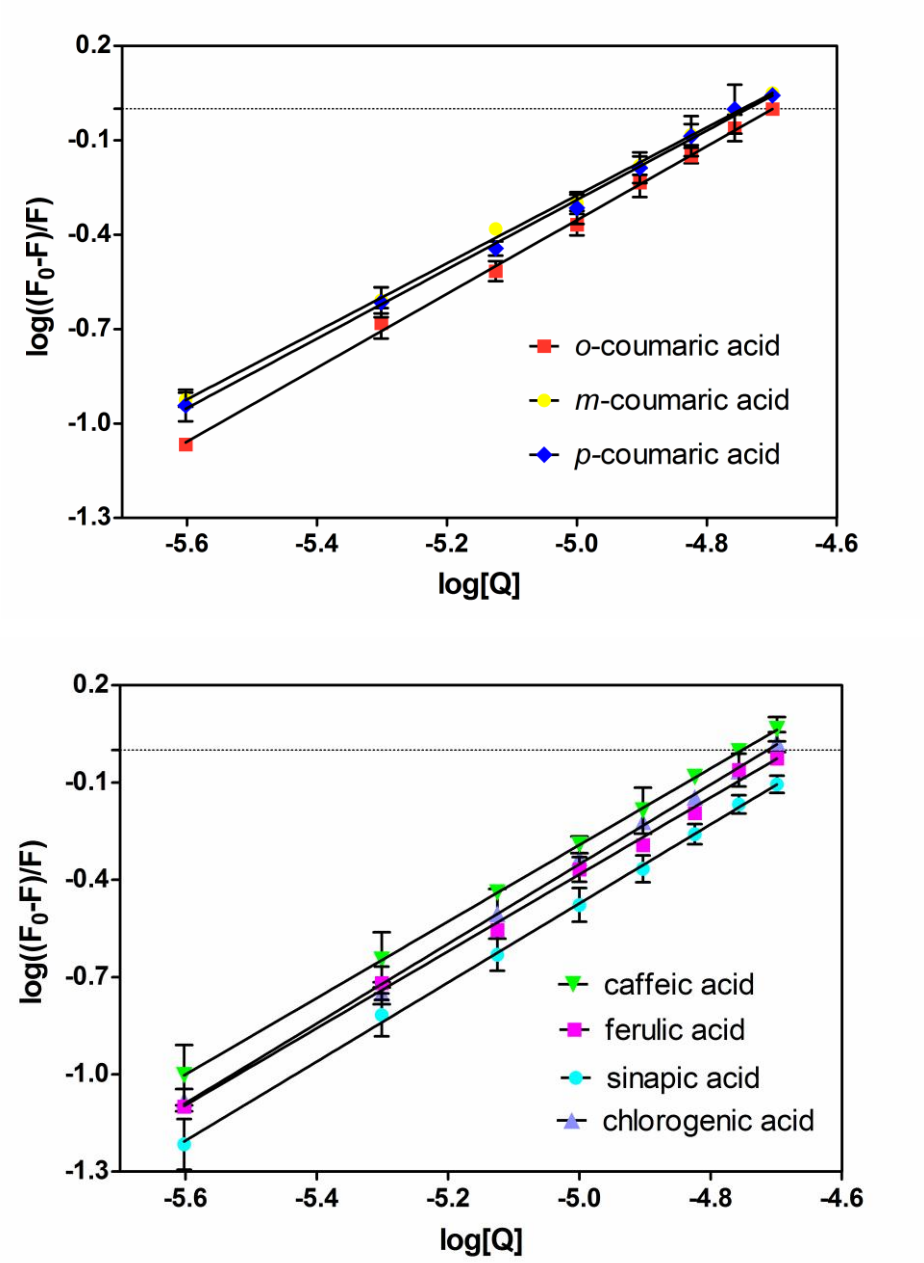

Figure 12: Logarithmic plots of tested hydroxycinnamic acid-BSA systems.
[BSA] = 2 x 10^{-6} M, [HCA] = 0 - 2 x 10^{-5} M, pH 7.4, 37°C, λ_{ex} = 295 nm, and λ_{em} = 350 nm. Correlation coefficients (R) were found in the range of 0.993 - 0.999.

Table 11: **The binding constants (K_b), number of binding sites (n), and free energy change (ΔG^0) of tested hydroxycinnamic acid-BSA systems (pH 7.4, 37°C).**

Tested compound	K_b [x10^5 M^{-1}]	n	R	ΔG^0 [kJ.mol^{-1}]
o-Coumaric acid	3.34^{b}	1.17	0.997	-32.73^{ab}
m-Coumaric acid	1.31^{e}	1.08	0.998	-30.36^{b}
p-Coumaric acid	1.81^{d}	1.10	0.993	-30.98^{ab}
Caffeic acid	4.16^{c}	1.18	0.995	-33.12^{a}
Ferulic acid	3.33^{b}	1.18	0.994	-32.75^{ab}
Sinapic acid	4.19^{b}	1.21	0.997	-33.36^{ab}
Chlorogenic acid	6.67^{a}	1.23	0.998	-34.55^{a}

Standard deviations (mean value of three independent experiments) were found in the range of 3 - 40%. Data were analyzed by Student´s *t*-test and groups with different letters are significantly different ($p < 0.05$). Differences in the number of binding sites were not statistically significant.

The binding constant (K_b) for cinnamic acid-BSA system mentioned in the literature [Bian et al. 2007, He et al. 2010, Jiang et al. 2004] is lower than values obtained in our experiments for HCA-BSA systems, which may confirm significance of hydroxyl groups in the process of binding. Moreover, binding affinity of cinnamic acid is higher for BSA than for HSA, which indicates that also binding of HCAs to BSA may be more pronounced [Jiang et al. 2004]. The same result was noticed for chlorogenic acid-HSA and chlorogenic acid-BSA systems using nuclear magnetic resonance (NMR) [Wang et al. 2011]. It was demonstrated that interaction of HCAs with protein molecule depends mainly on the ligand size and structure, especially on the number and position of hydroxyl groups on the aromatic ring [Rawel et al. 2006, Bartolomé et al. 2000]. Hydroxyl groups of studied compounds can form hydrogen bonds with amino acid residues in the protein molecule. Another important factor influencing ligand-protein binding is aromaticity of the ligand molecule because hydrophobic interactions can be asserted between aromatic rings of ligand and aromatic amino acid residues of proteins [Liu et al. 2005]. Chlorogenic acid with two aromatic hydroxyls and three hydroxyls on cyclohexane ring exerted the strongest binding affinity towards BSA because it can from hydrogen bonds with protein more easily than other less-substituted HCAs, e.g. ferulic acid. Thus esterification of carboxyl group with quinic acid increased this affinity. The similar results have been published for comparison of binding affinities of ferulic and chlorogenic acids towards BSA or HSA [He et al. 2010, Liu et al. 2010, Kang et al. 2004]. It is evident that the hydroxyls substituted on

aromatic ring of the HCAs play an important role in the binding affinity towards BSA. Monosubstituted HCAs possessed the lowest binding affinities of all HCAs studied. In the case of coumaric acids, the position of hydroxyl group on aromatic ring seems to play a role in binding affinity to BSA. The most suitable structural feature was determined *o*-position followed by *p*- and *m*-position. In comparison of caffeic, ferulic, and sinapic acids, it was noticed that substitution of hydroxyl on aromatic ring by methoxyl group lowered binding ability to BSA which is also supported by other authors [He et al. 2010, Liu et al. 2010].

The binding parameters of chlorogenic and ferulic acids with bovine serum albumin have been intensively studied. The value of K_b reported by Tang et al. [2008a] for chlorogenic acid-BSA system using fluorescence quenching method is lower than the value obtained in our experiments, which is probably due to different experimental conditions. Liu et al. [2010] compared binding affinity of caffeic, ferulic, and chlorogenic acids to BSA by fluorescence quenching method and their data are consistent with our results. However, Rawel et al. [2005, 2006] reported that chlorogenic acid does not quench tryptophan fluorescence of BSA and determined its binding constant by Hummel-Dreyer/size exclusion chromatography, which showed significantly lower K_b value in comparison with results presented by Tang et al. [2008a]. Non-covalent interactions of chlorogenic acid with BSA have been studied by Prigent et al. [2003], who reported that these interactions decrease with the increasing temperature, while pH and ionic strength had no pronounced effect. Zhang et al. [2007] reported the K_b for ferulic acid-BSA system determined by affinity capillary electrophoresis, which is in good agreement with our result. By contrast, Rawel et al. [2006] determined binding constant of ferulic acid-BSA system by fluorescence quenching method and Hummel-Dreyer/size exclusion chromatography, where first method gave similar results to our data and K_b obtained by second method was significantly lower. Several studies dealing with binding of *p*-coumaric, caffeic, ferulic, sinapic, and chlorogenic acids with HSA have been also published [Hu et al. 2012, Jiang et al. 2004, Kang et al. 2004, Liu et al. 2005].

The results showed that the number of binding sites ranged between 1.08 and 1.23 suggesting that one molecule of BSA was associated with one molecule of HCA in the drug to protein ratio up to 10 for the tested HCAs apart. The number of binding

sites rose with increasing number of hydroxyl groups in the ligand molecule, but their differences were not statistically significant. The similar results have been described in literature [He et al. 2010, Li et al. 2010].

The relatively strong binding enthalpy underlines the stability of HCA-BSA complexes from the energetic point of view. These findings are supported by data found in literature [Bian et al. 2007, He et al. 2010, Rawel et al. 2005, Rawel et al. 2006].

Interactions of HCAs with BSA differed in their binding affinities depending on the ligand size and structure. Binding affinities of HCAs towards BSA increased with increasing number of hydroxyl groups in their molecules which is consistent with the published data [He et al. 2005, Liu et al. 2010]. Coumaric acids containing only one hydroxyl group showed the lowest binding affinity to BSA. Substitution of hydroxyl by methoxyl group lowered the binding affinity towards BSA, whereas esterification of carboxyl group with quinic acid increased this binding ability. Obtained results also showed that tryptophan residues in BSA are not equally accessible to individual HCAs. Number of binding sites depended upon concentration of HCA. Ligands first bind to Trp-134, which is located on the surface of protein. With increasing concentration of HCAs, the microenvironment of Trp-212 changes to more hydrophilic, which leads to alterations in protein structure and results in better accessibility of Trp-212 for interaction with ligand.

5.2 INTERACTION BETWEEN CATECHINS AND HUMAN SERUM ALBUMIN

In this part, the binding affinity of eight naturally occurring catechins to HSA has been investigated in detail predominantly by fluorescence spectroscopy in combination with UV-Vis absorption spectroscopy and electrophoretic methods under simulated physiological conditions (pH 7.4, 37°C) in the *in vitro* models. The main objective was to reveal the character of interactions and consecutively to evaluate the relationships between the structure characteristics of the studied catechins (i.e. the presence of galloyl moiety on the C-ring, the number of hydroxyl groups on the B-ring, and the spatial arrangement of the substituents on the C-ring) and their binding affinities to HSA. The structures of tested catechins are displayed in **Figure 13**.

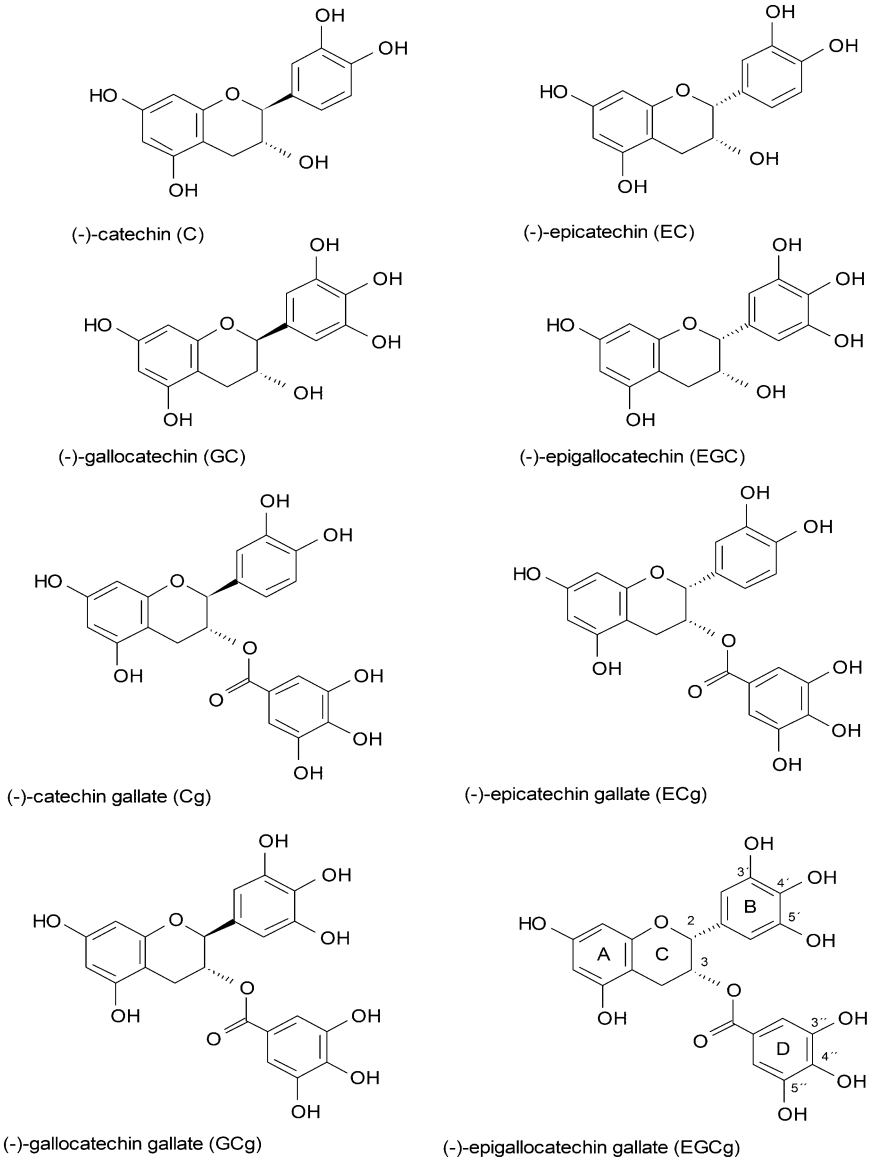

Figure 13: Chemical structures of tested catechins.

5.2.1 Stability of catechins

As for hydroxycinnamic acids, stabilities of the catechin solutions in phosphate buffer (0.1 M, pH 7.4, 0.05% NaN_3) were verified during long-term incubation (15 days) at 37°C by observation of changes in their characteristic UV-Vis absorption spectra. Slight changes in the spectra of all catechins appeared already after one hour of incubation and decomposition of the compounds significantly proceeded during 7 following days (data not shown). The obtained data are consistent with literature [Mochizuki et al. 2002, Roginsky and Alegria 2005, Sang et al. 2005]. Since the time-

dependent solution instabilities can influence the results of interaction between HSA and tested compounds in phosphate buffer (pH 7.4), the spectroscopic and fluorimetric measurements were carried out up to 30 minutes.

In addition, protection of (-)-epigallocatechin gallate by the sulfhydryl group of HSA (Cys-34), which act as an antioxidant, against its oxidation under aerobic conditions has been described [Bae et al. 2009]. The similar effect may be expected also for some other flavonoids. On the other hand, catechins can cause protein carbonyl formation in HSA via their pro-oxidant action [Ishi et al. 2010b].

5.2.2 Complex formation between catechins and HSA

In the present study, the absorption spectra of HSA in the absence and presence of individual catechins were recorded after 5 min of interaction. No changes were noticed in absorption spectra of HSA after interaction with catechins lacking the galloyl moiety on the C-ring (C, EC, GC, and EGC). On the other hand, the obvious changes, such as slight decrease of absorbance between 200 and 280 nm, significant growth of absorbance between 300 and 360 nm (λ_{max} = 330 nm) and slight red shift, in absorption spectrum of HSA after addition of the galloylated catechins (Cg, ECg, GCg, and EGCg) confirmed the complex formation [Guo et al. 2009]. The differential absorption spectra of HSA before and after interaction with epicatechin gallate are displayed in **Figure 14**.

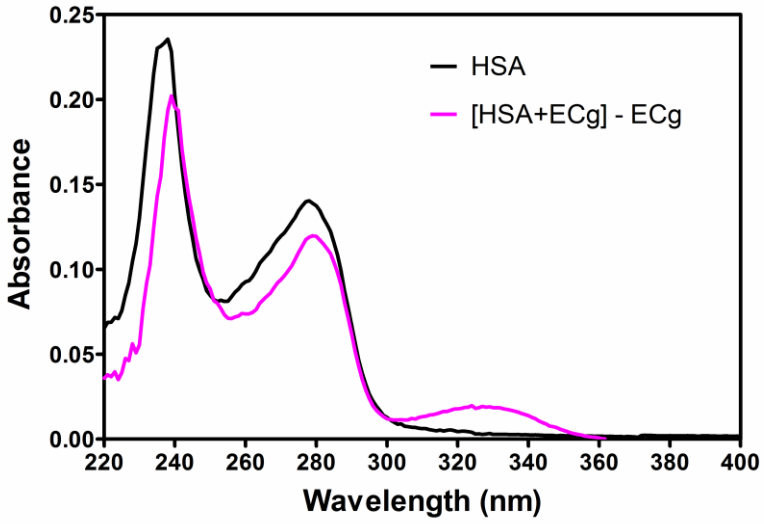

Figure 14: UV-Vis absorption spectra of HSA before and after interaction with epicatechin gallate. [HSA] = 4 x 10^{-6} M, [ECg] = 4 x 10^{-5} M, pH 7.4, 37°C, and 5 min of interaction.

It can be concluded that the presence of galloyl group in the molecules of catechins is responsible for their complex formation with HSA. It was not possible to gain more detailed information because UV-Vis absorption spectroscopy represents less sensitive technique.

5.2.3 Fluorescence spectra of catechins and catechin-HSA systems

As was described above, the complex formations between HSA and catechin gallates were noticed upon analyzing their UV-Vis absorption spectra. Subsequently, the emission spectra of these complexes were recorded with the excitation at 330 nm, which corresponds with the observed absorption maximum. All complexes emitted light between 374 and 377 nm (Figure 15), whereas catechin gallates as well as other catechins alone were not emissive under these experimental conditions.

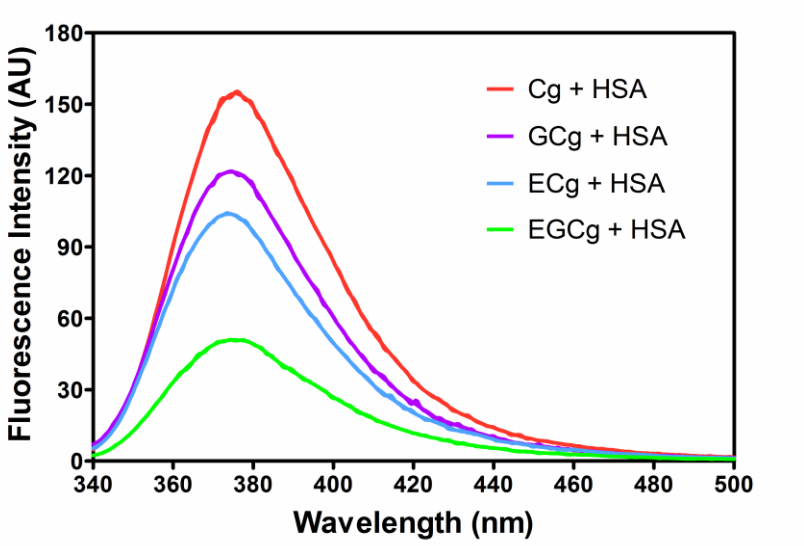

Figure 15: Fluorescence emission spectra of complex formation between catechin gallates and HSA. [HSA] = 4 x 10^{-6} M, [catechin gallate] = 4 x 10^{-5} M, pH 7.4, 37°C, λ_{ex} = 330 nm, and 5 min of interaction.

Fluorescence emission spectra of individual catechins were recorded at excitation wavelength of 295 nm, which corresponds to the tryptophan residue (Figure 16). Only, catechin and epicatechin possessed intrinsic fluorescence and both displayed the similar spectra with emission maximum of 318 nm. The observed wavelength of their emission maximum is consistent with literature [Papadopoulou et al. 2005]. Other catechins showed no emission spectra at this excitation wavelength.

5.2.4 Fluorescence quenching spectra of HSA induced by catechins

Quenching of protein intrinsic (tryptophan) fluorescence was employed for more detailed study of catechin-HSA interactions. Fluorescence intensity of HSA was gradually decreased with rising concentration of all tested compounds. All catechin gallates (Cg, ECg, GCg, and EGCg) caused more pronounced decrease in the tryptophan fluorescence of the HSA emission maximum (348 nm) than other catechins (C, EC, GC, and EGC). Furthermore, remarkable red shifts in their fluorescence quenching spectra were observed (**Figure 16**). Emission maximum of HSA was shifted towards longer wavelength by 25 nm for both catechin gallate-HSA and epicatechin gallate-HSA system, and by 23 nm for gallocatechin gallate-HSA system as well as for epigallocatechin gallate-HSA system. Generally, red shift in the emission maximum of a tryptophan residue, which is located in a hydrophobic pocket, indicates changes in its microenvironment, i.e. a polypeptide strand of a protein molecule is more extended and the hydrophobicity around this tryptophan residue is decreased [Lakowicz 2006]. These data suggest that Trp-214, which is the sole tryptophan residue in the HSA molecule, has been brought to a more hydrophilic environment and the protein secondary structure has been changed. No shifts in the emission maximum of HSA were observed after gradual additions of the non-galloylated catechins. Red shift in the fluorescence quenching spectra of (-)-epigallocatechin gallate-HSA system was also reported [Maiti et al. 2006]. By contrast, no shifts in the emission spectra of bovine serum albumin after titration with increasing amounts of (+)-catechin, (-)-epicatechin, and (-)-epicatechin gallate were noticed [Papadopoulou et al. 2005, Soares et al. 2007]. No isosbestic points were observed in the quenching specta of the studied systems.

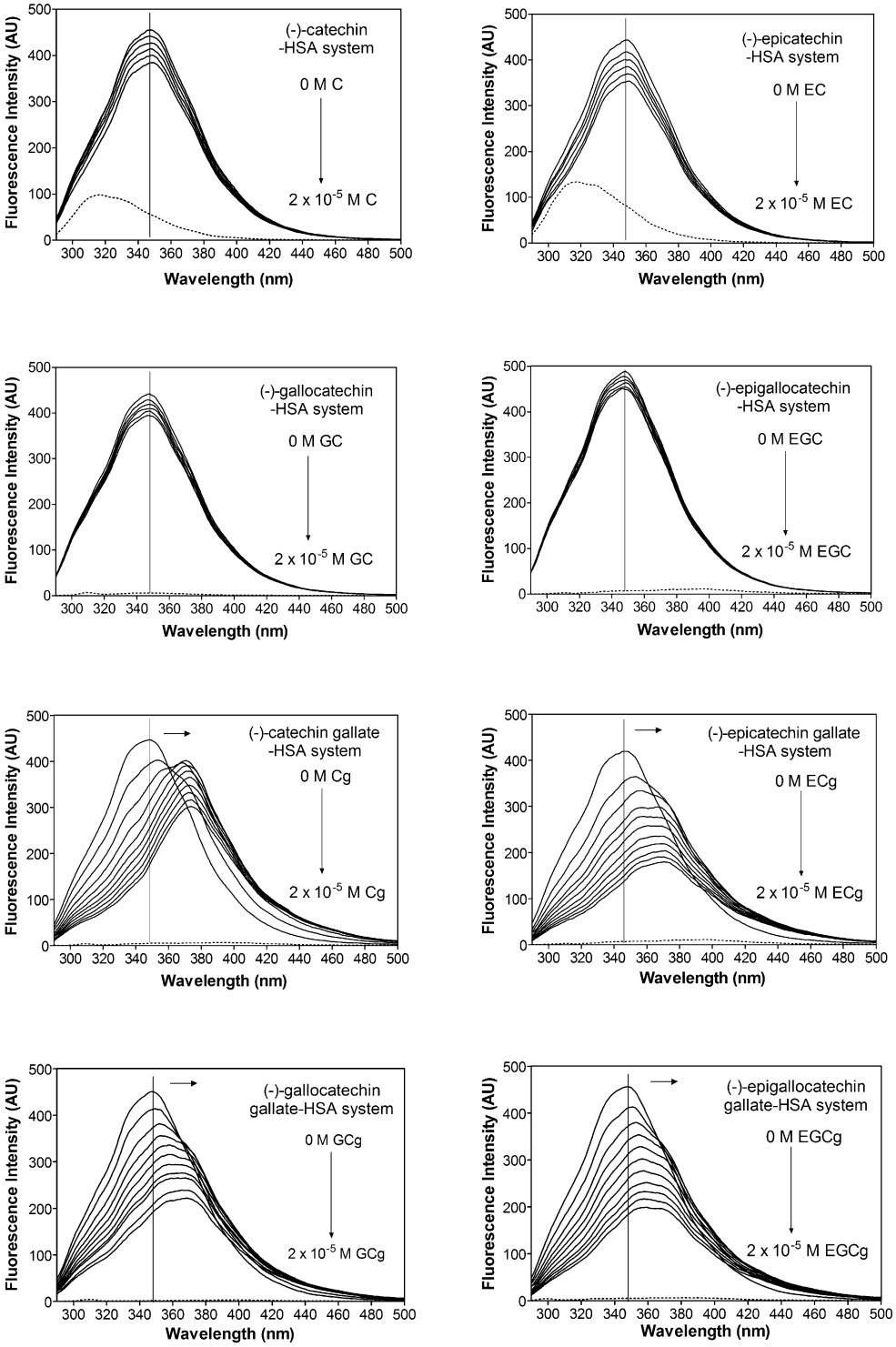

Figure 16: Fluorescence quenching spectra of catechin-HSA systems.
[HSA] = 4 x 10^{-6} M, [catechin] = 0 - 2 x 10^{-5} M, [non-galloylated catechin]/[HSA] = 0, 1, 2, 3, 4, and 5; [galloylated catechin]/[HSA] = 0, 0.5, 1, 1.5, 2, 2.5, 3, 3.5, 4, 4.5, and 5; pH 7.4, 37°C, and λ_{ex} = 295 nm. Dotted line and horizontal arrow display fluorescence spectrum of catechin (2 x 10^{-5} M) and red shift, respectively.

5.2.5 Fluorescence quenching mechanism of catechin-HSA systems

In order to clarify the fluorescence quenching mechanism induced by individual catechins, the fluorescence quenching data were analyzed using the Stern-Volmer analysis [Lakowicz 2006]. Fluorescence intensities were read at emission wavelength of 348 nm where the emission maximum of HSA was located. The Stern-Volmer plots (F_0/F versus [Q]) were linear in the range of studied concentrations (0 - 2 x 10^{-5} M) for all tested systems and the Stern-Volmer constants (K_{SV}) and consecutively the bimolecular quenching rate constants (K_q) were determined from their slopes (**Figure 17**). Values of the above mentioned constants are summarized in the **Table 12**.

The bimolecular quenching constant (K_q) reflects an efficiency of quenching or an accessibility of the fluorophores to a quencher. One of the criterions for determination of a static quenching mechanism is that the value of K_q is higher than the value of a diffusion-limited rate constant of a biomolecule (K_{diff} = 1.0 x 10^{10} $M^{-1}s^{-1}$) [Lakowicz 2006]. The values of K_q for all tested systems were higher that of K_{diff}, which confirmed that the static quenching mechanism is likely the main reason of protein fluorescence quenching [Lakowicz 2006]. The highest value of K_q was determined for epicatechin gallate and further decreased in the order ECg > Cg ≥ EGCg ≥ GCg >> EC ≥ C > GC > EGC.

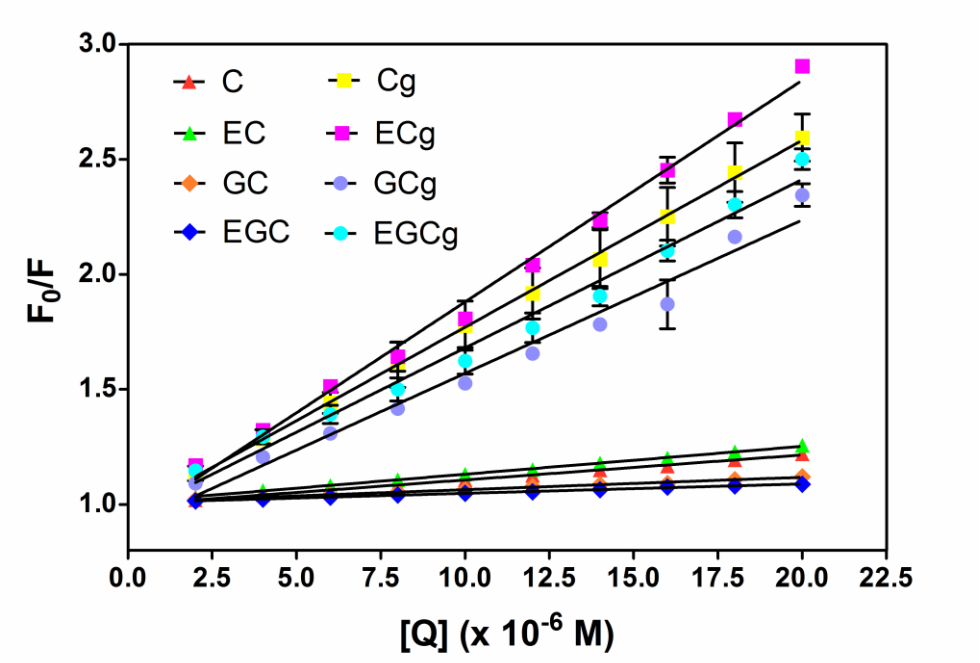

Figure 17: Stern-Volmer plots of tested catechin-HSA systems.
[HSA] = 4 x 10^{-6} M, [catechin] = 0 - 2 x 10^{-5} M, pH 7.4, 37°C, λ_{ex} = 295 nm, and λ_{em} = 348 nm. Correlation coefficients (R) were found in the range of 0.992 - 0.999.

Table 12: The Stern-Volmer constants (K_{SV}) and bimolecular quenching rate constants (K_q) of tested catechin-HSA systems (pH 7.4, 37°C).

Tested compound	K_{SV} [10^4 M^{-1}]	K_q [10^{12} $M^{-1}s^{-1}$]	R
Catechin	1.07^{c}	2.15^{c}	0.992
Epicatechin	1.22^{c}	2.44^{c}	0.995
Gallocatechin	0.55^{b}	1.10^{b}	0.989
Epigallocatechin	0.42^{a}	0.84^{a}	0.993
Catechin gallate	8.12^{de}	16.25^{de}	0.996
Epicatechin gallate	9.63^{e}	19.26^{e}	0.999
Gallocatechin gallate	6.66^{d}	13.33^{d}	0.995
Epigallocatechin gallate	7.32^{d}	14.65^{d}	0.995

$K_q = K_{SV}/\tau_0$; $\tau_0 = 5 \times 10^{-9}$ s [Lakowicz 2006]. Correlation coefficients (R) were higher than 0.990. Standard deviations (mean value of three independent experiments) were lower than 10%. Data were analyzed by Student´s *t*-test and groups with different letters are significantly different ($p < 0.01$).

The importance of the presence of the galloyl moiety on the C-ring was evident because quenching constants for all catechin gallates (Cg, ECg, GCg, and EGCg) were significantly higher than those of catechins lacking the galloyl group (C, EC, GC, and EGC). Catechin gallates with 2,3-*cis* structure (ECg and EGCg) possessed greater K_q values than catechin gallates with 2,3-*trans*-structure (Cg and GCg). Catechins with the catechol group on the B-ring (C, EC, ECg, and Cg) showed more pronounced quenching effect than their analogs with pyrogallol moiety (GC, EGC, EGCg, and GCg).

5.2.6 Determination of binding parameters of catechin-HSA systems

In general, a binding constant K_b reflects the power of ligand-protein association and thus can be used for comparison of the binding affinities of structurally-related ligands to a protein molecule connected with the alterations in its secondary structure. Number of binding sites (n) and free energy change (ΔG^0) are other important parameters that contribute to better understanding of ligand-protein interactions [Lakowicz 2006, Bi et al. 2004].

In this case, the binding constants (K_b), binding sites (n), and free energy changes (ΔG^0) of all catechin-HSA systems have been determined according to the equations (3) and (4). The obtained values are presented in **Table 13** and the logarithmic plots for determination of binding parameters are displayed in **Figure 18**. The binding affinity was the strongest for epicatechin gallate and decreased in the order ECg ≥ Cg > EGCg ≥ GCg >> EC ≥ C > GC ≥ EGC. The non-galloylated catechins possessed significantly lower

binding constants. The value of the number of binding sites (n) ranged from 0.87 to 1.10. Negative values of free energy changes (ΔG^0) for all studied interactions indicate that the binding between HSA and individual catechins proceeds spontaneously.

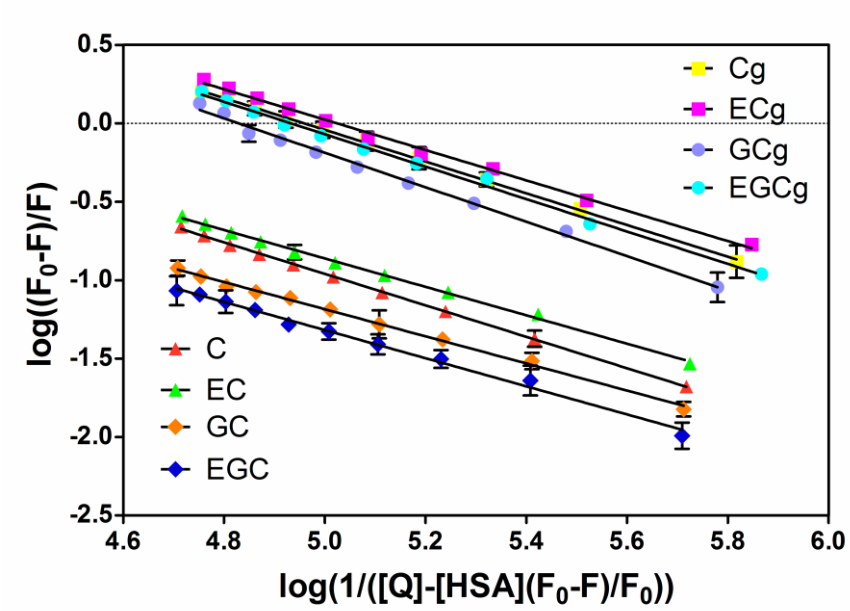

Figure 18: Logarithmic plots of studied catechin-HSA systems.
[HSA] = 4 x 10^{-6} M, [catechin] = 0 - 2 x 10^{-5} M, pH 7.4, 37°C, λ_{ex} = 295 nm, and λ_{em} = 348 nm. Correlation coefficients (R) were found in the range 0.993 - 0.999.

Table 13: The binding constants (K_b), number of binding sites (n) and free energy change (ΔG^0) of tested catechin-HSA systems (pH 7.4, 37°C).

Tested compound	K_b [x10^4 M^{-1}]	n	R	ΔG^0 [kJ.mol^{-1}]
Catechin	1.10^{b}	1.00	0.997	-23.99^{b}
Epicatechin	1.12^{b}	0.91	0.998	-24.03^{b}
Gallocatechin	0.43^{a}	0.87	0.993	-21.54^{a}
Epigallocatechin	0.34^{a}	0.89	0.994	-20.93^{a}
Catechin gallate	9.21^{de}	1.01	0.999	-29.46^{de}
Epicatechin gallate	10.57^{e}	0.97	0.996	-29.82^{e}
Gallocatechin gallate	6.75^{c}	1.10	0.998	-28.66^{c}
Epigallocatechin gallate	7.79^{d}	1.03	0.997	-29.03^{d}

Standard deviations (mean value of three independent experiments) were lower than 10%. Data were analyzed by Student´s *t*-test and groups with different letters are significantly different (p < 0.01). Differences in the number of binding sites were not statistically significant.

In general, the hydrophobicity, presence or absence of some functional group, steric hindrance, and spatial arrangement seem to be the key factors in the affinity of natural polyphenols towards plasmatic proteins [Diniz et al. 2008, Ishii et al. 2010a]. These compounds probably form reversible non-covalent complexes with the molecule

of serum albumin mainly through hydrogen bonding of their hydroxyl groups with amino acid residues and hydrophobic interactions between their aromatic rings and amino acid residues in the protein chain [Diniz et al. 2008, Otagiri 2005].

The galloylated catechins (Cg, ECg, GCg, and EGCg) showed significantly higher binding ability than the non-galloylated catechins (C, EC, GC, and EGC). It confirmed the importance of the galloyl moiety on the C-ring in the binding affinity of catechins to HSA due to a presence of additional aromatic ring with three hydroxyl groups, which can establish hydrophobic interactions and hydrogen bonds, respectively. The effect of this structural feature was clearly underlined by all applied methods. Also data found in literature support these findings, e.g. Ishii et al. [2010a] who studied binding affinities of catechins to the HSA with respect to their structural features using high-performance affinity chromatography with immobilized albumin column.

In addition, catechol-type catechins (ECg ≥ Cg > EC ≥ C) possessed stronger binding affinity than pyrogallol-type catechins (EGCg > GCg > GC > EGC). It suggests that the insertion of an additional hydroxyl group at the 5-position on the B-ring did not contribute to their binding affinities in the experimental model used, which is in conflict with literature data [Ishii et al. 2010a]. The effect of the spatial arrangement of catechins (i.e. *cis*- and *trans*-structure) on the binding to HSA was not explicit. Ishii et al. [2010a] observed that the *trans*-type catechins (C, GC, Cg, and GCg) had rather higher binding abilities than their epimers (EC, EGC, ECg, and EGCg). In this study, the opposite effect was observed in the case of the galloylated catechins. Diniz et al. [2008] found out using capillary electrophoresis that (-)-epicatechin showed no affinity towards HSA whilst (+)-catechin had intermediate binding ability to HSA (K_b = 2.2 x 10^3 M^{-1} and n = 1), which the authors attributed to the spatial arrangement of tested catechins. Ishii et al. [2010a] noticed negligible differences in binding affinities among (+)-catechin, (-)-catechin, and (-)-epicatechin obtained by affinity HPLC on immobilized HSA column. The latter results well correspond with our data where insignificant difference between binding constants of (-)-catechin and (-)-epicatechin was observed. One of the most studied flavan-3-ols is (-)-epigallocatechin gallate and the results obtained by Maiti et al. [2006] for the system EGCg-HSA are in good agreement with our data although the experimental conditions were slightly different. Binding of (-)-

epigallocatechin gallate to serum albumins was also studied in detail also by circular dichroism [Nozaki et al. 2009].

Further factor, which could contribute to binding affinity of tested catechins to HSA, is deprotonation of hydroxyl groups in their molecules. It is supposed that the catechins lacking the galloyl moiety (C, EC, GC, and EGC) are fully protonated at the tested pH (i.e. pH 7.4) because their first dissociation constants reach higher values (about pH 9) [Herrero-Martínez et al. 2005, Muzolf et al. 2008]. On the other hand, catechins with the galloyl moiety in C-ring (Cg, ECg, GCg, and EGCg) have the first dissociation constants near pH 7.4 [Muzolf et al. 2008], thus partial deprotonation can play role in the increase of their binding affinity to HSA.

Number of binding sites determined for catechin-HSA systems ranged from 0.87 to 1.10 suggesting that one molecule of HSA is associated with one molecule of catechin in the drug to protein ratio up to 5:1. The spontaneity of HSA-catechin interactions was confirmed by the negative values of ΔG^0. These findings are supported by the previous report [Maiti et al. 2006].

5.2.7 Estimation of distances between catechins and HSA

The distances between Trp-214 in molecule of HSA (donor) and the catechins (acceptor) were estimated by fluorescence resonance energy transfer (FRET) method. The overlaps of the UV-Vis absorption spectra of individual catechins with the fluorescence spectrum of HSA occurred for all tested systems. There was noticed significant effect of the galloyl moiety on the extent of spectral overlapping. The galloylated catechins (Cg, ECg, GCg, and EGCg) caused much greater spectral overlap than the non-galloylated catechins (C, EC, GC, and EGC) (**Figure 19**). In the present case, k^2 =2/3, N = 1.336, Φ = 0.118 [Yuan et al. 2007], the values of J, E, R_0, and r_0 for the tested systems have been calcuated according to the equations (5) - (7). The obtained values are stated in **Table 14**.

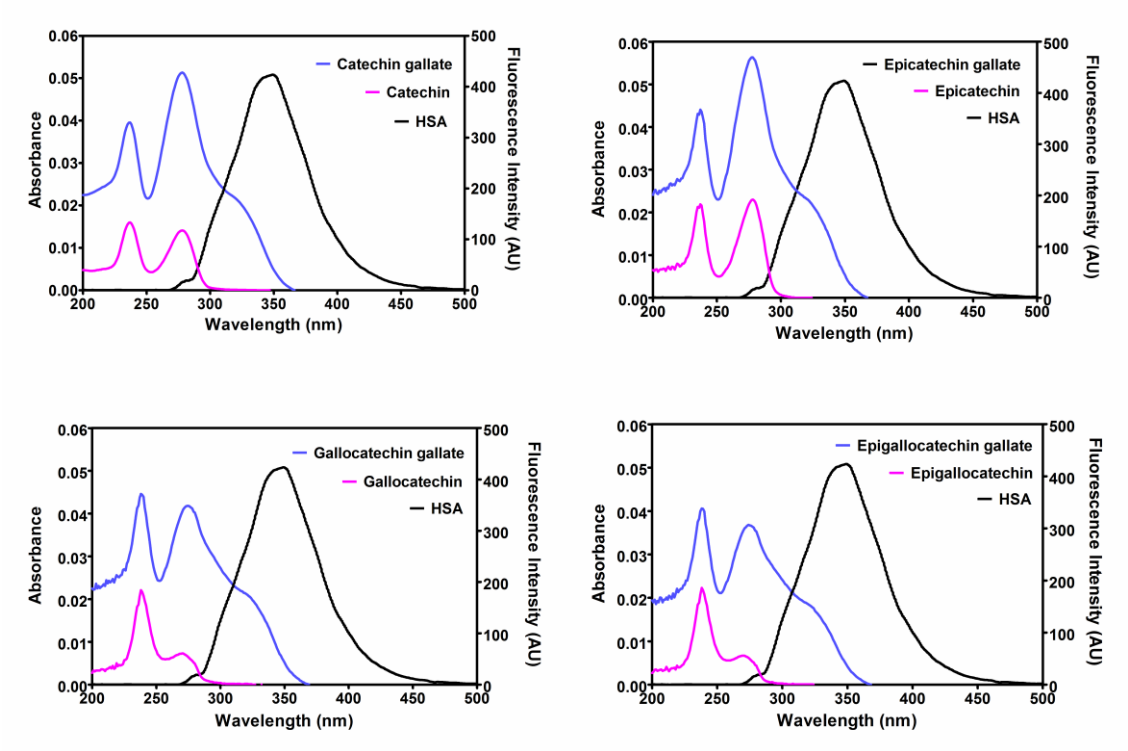

Figure 19: Spectral overlaps between the fluorescence emission spectrum of HSA and the absorption specra of catechins. [HSA] = [catechin] = 4 x 10^{-6} M, pH 7.4, 37°C, and λ_{ex} = 295 nm.

Table 14: The overlap integral (J), efficiency of energy transfer (E), critical distance (R_0), and distance between donor (HSA) and acceptor (catechin) (r_0) (pH 7.4, 37°C).

Tested compound	J [x 10^{-16} cm^3.l.mol^{-1}]	E	R_0 [nm]	r_0 [nm]
Catechin	0.40^{c}	0.18^{b}	0.98^{bc}	1.26^{a}
Epicatechin	0.44^{bc}	0.20^{c}	0.99^{c}	1.25^{a}
Gallocatechin	0.16^{ab}	0.11^{a}	0.84^{ab}	1.19^{a}
Epigallocatechin	0.12^{a}	0.08^{a}	0.80^{a}	1.20^{a}
Catechin gallate	26.04^{de}	0.61^{de}	1.96^{d}	1.82^{b}
Epicatechin gallate	28.15^{e}	0.66^{e}	1.98^{d}	1.78^{b}
Gallocatechin gallate	25.80^{de}	0.57^{d}	1.96^{d}	1.85^{b}
Epigallocatechin gallate	22.00^{d}	0.60^{d}	1.91^{d}	1.78^{b}

Standard deviations (mean value of three independent experiments) were lower than 10%. Data were analyzed by Student´s *t*-test and groups with different letters are significantly different ($p < 0.01$).

All binding distances (r_0) were much lower than 8 nm, and fulfilled the following condition $0.5R_0 < r_0 < 1.5R_0$, which indicates that non-radiation energy transfer from HSA to catechins occurred with high probability [Guo et al. 2009]. The galloyl moiety in the C-ring proved to have significant effect on the extent of spectral overlapping as

was described in literature for catechin-HSA systems using high-performance affinity chromatography with immobilized albumin column [Ishii et al. 2010a].

5.2.8 Effect of catechins on molecular charge of HSA

Native PAGE was used to investigate the changes in the molecular charge of HSA due to interactions with the catechins (**Figure 20**). The results were expressed as increment in electrophoretic mobility of individual samples compared to the native protein (control). The changes in the HSA molecule were exerted as broadening of protein band as well as increased sample mobility towards anode, which indicated that the molecule of HSA became more anionic due to the interaction with catechin gallates (Cg, ECg, GCg, EGCg). On the other hand, the non-galloylated catechins (C, EC, GC, and EGC) caused no significant changes in electrophoretic mobility of HSA. The electrophoretic mobility of tested systems decreased in the following order: EGCg (6.25%) > GCg (5.05%) > ECg (3.61%) > Cg (3.37%) ≈ EC (3.13%) > C (1.53%) ≥ GC (0.51%) ≈ EGC (0.24%).

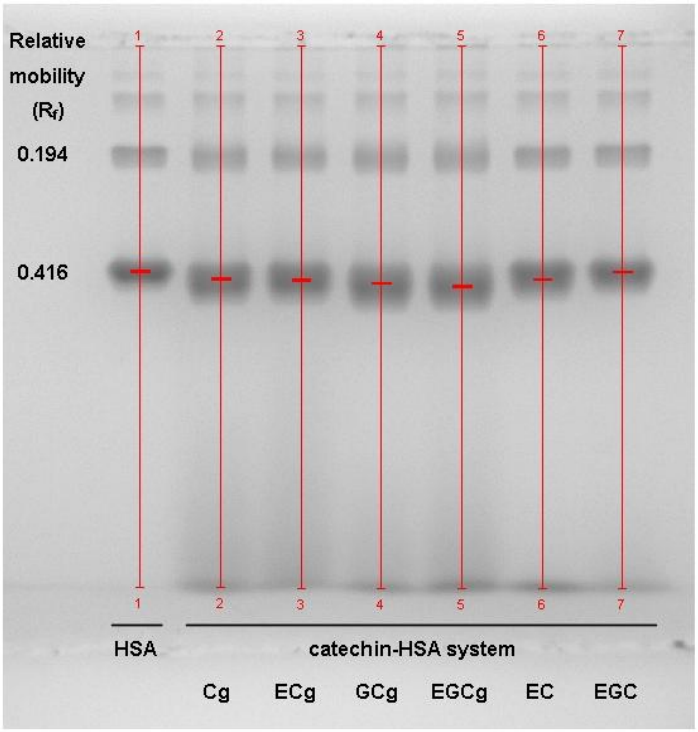

Figure 20: Effect of selected catechins on a molecular charge of HSA. [HSA] = 15 x 10^{-6} M, [catechin] = 6 x 10^{-4} M. Samples were incubated for 30 minutes at 37°C. Electrophoretic mobilities were expressed as a rise in percentage mobility compared to the native protein (control).

The loss of positive charges in HSA molecule was in a good agreement with a number of hydroxyl groups and molecular weight of the galloylated catechins. Moreover, catechin gallates with the pyrogallol group on the B-ring (GCg and EGCg) showed more pronounced effect on mobility than catechin gallates with the catechol moiety (Cg and ECg). The similar results were described for (+)-catechin-BSA and epigallocatechin gallate-BSA systems [Kusuda et al. 2006].

5.2.9 Protein cross-linking and aggregation induced by catechins

SDS PAGE analysis can provide some information on the binding stability and strength of the macromolecular complexes formed between serum albumin and plant polyphenols. The ability of aggregation and cross-link formation between the studied catechins and HSA was not proved by this method. No formation of high molecular weight protein adducts was observed (data not shown).

The same result was obtained for (+)-catechin-BSA system. By contrast, the formation of water-soluble, macromolecular complex of (-)-epigallocatechin gallate-BSA system has been proved by SDS PAGE after the incubation of 24 hours. It was also considered that the oxidation of (-)-epigallocatechin gallate contributes to its complex formation with BSA [Kusuda et al. 2006].

5.3 INTERACTION BETWEEN GREEN TEA CATECHINS AND ERP57 PROTEIN

Revelation of ERp57 conformation changes induced by GTCs, namely epicatechin, epigallocatechin, epicatechin gallate, epigallocatechin gallate (**Figure 12**), and evaluation of their binding affinities to the studied protein in its reducing state were explored using fluorescence quenching method in the *in vitro* model (pH 7.4, 25°C). The effect of tested catechins on disulfide reductase activity of ERp57 has been investigated by sensitive fluorescent method. The structure-binding and structure-activity relationships of GTCs were assessed.

5.3.1 Fluorescence quenching spectra of ERp57 induced by green tea catechins

Fluorescence quenching of protein intrinsic (tryptophan) fluorescence was employed for evaluation of ERp57 conformational changes induced by GTCs and for

detailed study of the GTC-ERp57 interactions. ERp57 possesses three tryptophan residues in its molecule differing in accessibility of a quencher to its molecule and thus unequally contributing to the protein intrinsic fluorescence. One tryptophan residue is buried in a hydrophobic pocket in the *b´*domain whereas the other two are located on the protein surface close to active thioredoxin-like sites in domains *a* and *a´*, respectively. ERp57 was reduced using dithiothreitol (DTT), which is used to reduce disulfide bonds of proteins, and thus to prevent formation of intramolecular and intermolecular disulfide bonds between cysteine residues of ERp57 in its redox active sites.

The tryptophan fluorescence emission of ERp57 was significantly decreased only with rising concentration of the galloylated GTCs (Figure 21). Quenching effect of GTCs on ERp57 was determinated using equation (8) (Table 15) and reached 27.1 and 26.1% at the highest concentration of ECg and EGCg, respectively. Also slight red shifts were noticed in the case of ECg and EGCg-ERp57 systems.

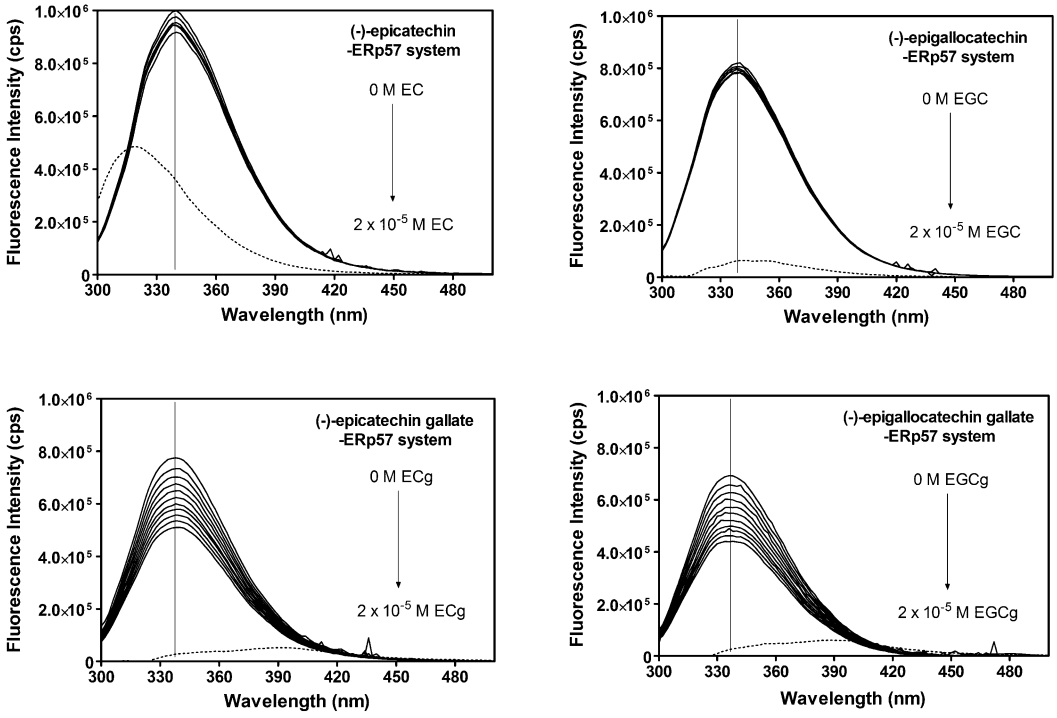

Figure 21: Fluorescence quenching spectra of GTC-ERp57 systems.
[ERp57] = 5 x 10^{-7} M, [GTC] = 0 - 2 x 10^{-5} M, [non-galloylated GTC]/[ERp57] = 0, 8, 16, 24, 32, and 40; [galloylated GTC]/[ERp57] = 0, 4, 8, 12, 16, 20, 24, 28, 32, 36, and 40; pH 7.4, 25°C, and λ_{ex} = 290 nm. Dotted line displays fluorescence spectrum of GTC (2 x 10^{-5} M).

The obtained results indicates that the presence of galloyl moiety in molecule of GTCs plays an important role in their binding affinity to ERp57 and the galloylated GTCs are able to evoke slight changes in the protein secondary structure.

5.3.2 Determination of binding parameters of green tea catechin-ERp57 systems

The obtained fluorescence quenching data were analyzed in the same way as in the previous chapter dealing with catechin-HSA interactions. The Stern-Volmer analysis was used only for the galloylated GTC-ERp57 systems where significant quenching effect has been remarked. Fluorescence intensities were read at emission maximum wavelength of 338 nm. The Stern-Volmer plots were linear in the range of studied concentrations (0-2 x 10^{-5} M) (Figure 22) and the Stern-Volmer constants were obtained from equation (1). Also the binding constants (K_b), number of binding sites (n), and free energy changes (ΔG^0) of the galloylated GTC-ERp57 systems were determined according to the equations (3) and (4) (Figure 23). The obtained values are summarized in Table 15.

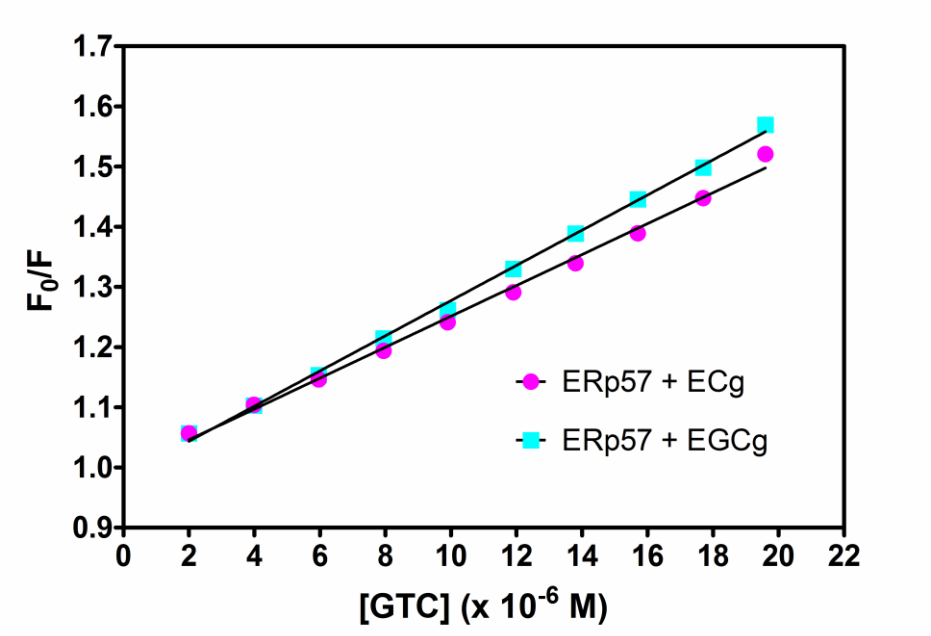

Figure 22: Stern-Volmer plots of galloylated GTC-ERp57 systems.
[ERp57] = 5 x 10^{-7} M, [GTC] = 0 - 2 x 10^{-5} M, pH7.4, 25°C, λ_{ex} = 290 nm, and λ_{em} = 338 nm. Correlation coefficients were better than 0.997. Plots are displayed as means (three independent experiments) and standard deviations were better than 10%.

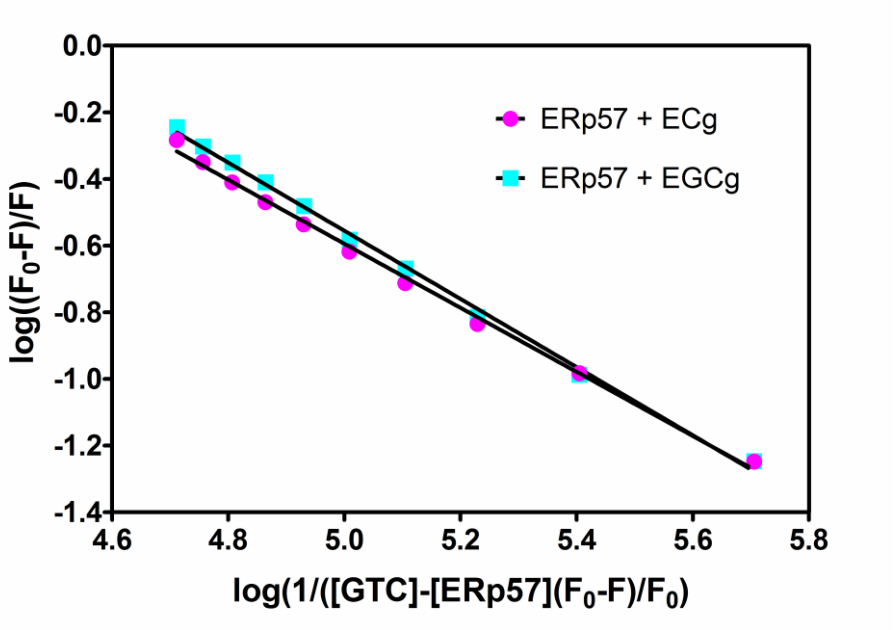

Figure 23: Logarithmic plots of galloylated GTC-ERp57 systems.
[ERp57] = 5 x 10^{-7} M, [GTC] = 0 - 2 x 10^{-5} M, pH7.4, 25°C, λ_{ex} = 290 nm, and λ_{em} = 338 nm. Correlation coefficients were better than 0.997. Plots are displayed as means (three independent experiments) and standard deviations were better than 10%.

Table 15: **Fluorescence quenching effects of GTCs on ERp57 (Q), Stern-Volmer constants (K_{SV}), number of binding sites (n), binding constants (K_b), and free energy change (ΔG^0) of tested systems (pH 7.4, 25°C).**

Tested system	Q (%)	K_{sv} (M^{-1})	n	K_b (M^{-1})	ΔG^0 (kJ.mol^{-1})
ERp57 + EC	6.65[b]	-	-	-	-
ERp57 + EGC	4.35[a]	-	-	-	-
ERp57 + ECg	27.13[c]	25647[a]	0.961	24063[a]	-24.99[a]
ERp57 + EGCg	26.07[c]	29219[a]	1.023	28650[b]	-25.43[a]

ERp57:GTC = 1:40. Standard deviations were lower than 10%. Data were analyzed by Student´s *t*-test and groups with different letters are significantly different ($p < 0.05$). Differences in the number of binding sites were not statistically significant.

The obtained data confirmed that the galloyl moiety in molecule of GTCs is the important structural feature which significantly contributes to the binding affinity of GTCs to ERp57. The number of hydroxyl groups in the galloylated GTCs does not seem to play any role in their binding capability to the tested protein (differences are not statistically significant). The results well correspond with the data obtained by us and other authors dealing with interaction between catechins and human serum albumin [Ishii et al. 2010a]. Higher binding affinities of several antibiotics (e.g. vancomycin, streptomycin) to ERp57 have been already described [Gaucci et al. 2008].

5.3.3 Effect of green tea catechins on disulfide reductase activity of ERp57

Disulfide reductase activity of ERp57 was monitored by sensitive fluorescent assay using fluorogenic probe, dieosin glutathione disulfide (Di-E-GSSG) [Raturi and Mutus 2007]. This probe displays low fluorescence (λ_{ex} = 520 nm and λ_{em} = 545 nm) which significantly increased (approximately 70-fold) on reduction of its disulfide bond. Effect of green tea catechins (GTCs), *N*-ethylmaleimide (NEM) and vancomycin (VM) on reduction of Di-E-GSSG by reduced enzyme of ERp57 was investigated. Bovine serum albumin was used as negative control (blank). Linear increase of fluorescence of the probe during the defined time interval was found for all tested systems. The slopes were used for calculation of the relative disulfide reductase activity (%) (Figure 24).

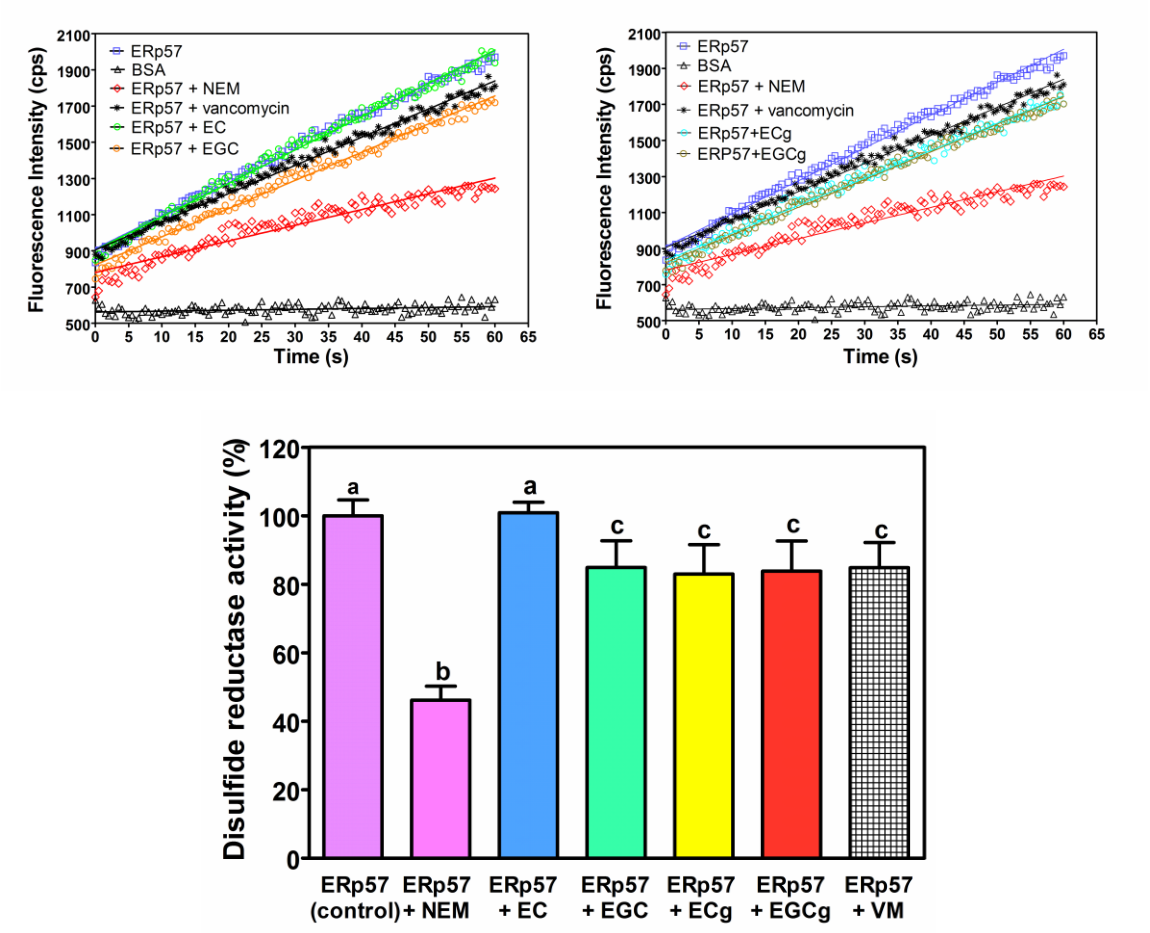

Figure 24: Effect of green tea catechins on disulfide reductase activity of ERp57. [ERp57] = 1 x 10^{-6} M, [NEM] = 4 x 10^{-3} M, [VM] = 1 x 10^{-4} M, and [GTC] = 1 x 10^{-4} M. Samples were incubated for 15 minutes at 25°C. Standard deviations (mean value of six independent experiments) were lower than 11%. Data were analyzed by Student´s t-test and groups with different letters are significantly different ($p < 0.05$).

Disulfide reductase activity of ERp57 in the presence of green tea catechins was determined as 100.9%, 84.9%, 83.8%, and 84.8% for epicatechin, epigallocatechin, epicatechin gallate, and epigallocatechin gallate in comparison with ERp57 activity alone (100%), respectively. The three last mentioned catechins decreased the reductase activity of ERp57 by 15% (differences were not statistically significant), whilst epicatechin did not. The studied catechins except epicatechin had the similar decreasing effect on reductase activity of the protein as vancomycin (15.1%, not statistically significant), the antibiotic which binds to ERp57 and moderately inhibits its reductase activity [Gaucci et al. 2008]. All green tea catechins possessed much less pronounced effect in comparison with NEM (53.8%, statistically significant), the agent used for inhibition of cysteine residues in proteins. BSA did not show any disulfide reductase activity. The obtained results show that apart from epicatechin, all studied GTCs are able to reduce disulfide reductase activity of ERp57. Besides these natural compounds, also several antibiotics (e.g. vancomycin, erythromycin, or streptomycin) can lower the disulfide reductase activity of ERp57 [Gaucci et al. 2008].

5.4 EFFECT OF GREEN TEA CATECHINS ON METHYLGLYOXAL-MEDIATED GLYCATION OF HUMAN SERUM ALBUMIN

Green tea catechins (GTCs), especially (-)-EGCg, have attracted a great attention in last two decades due to their beneficial effects on living organisms. The potential inhibitory activities of GTCs on MGO-mediated glycation of HSA were assessed by determination of AGEs with fluorescent properties. **Figure 25** displays courses of fluorescence emission spectra of total ("non-specific") fluorescent AGEs (λ_{ex} = 330 nm) and argpyrimidine (λ_{ex} = 320 nm) formation during MGO-mediated glycation of HSA in the absence and presence of different EGCg concentrations. The obvious anti-glycating effect was noticed for EGCg in the concentration range of 0.01 - 0.05 mM in the case of total fluorescent AGEs formation (A), whereas only the highest EGCg concentration seems to cause a very slightly influence the argpyrimidine formation (B).

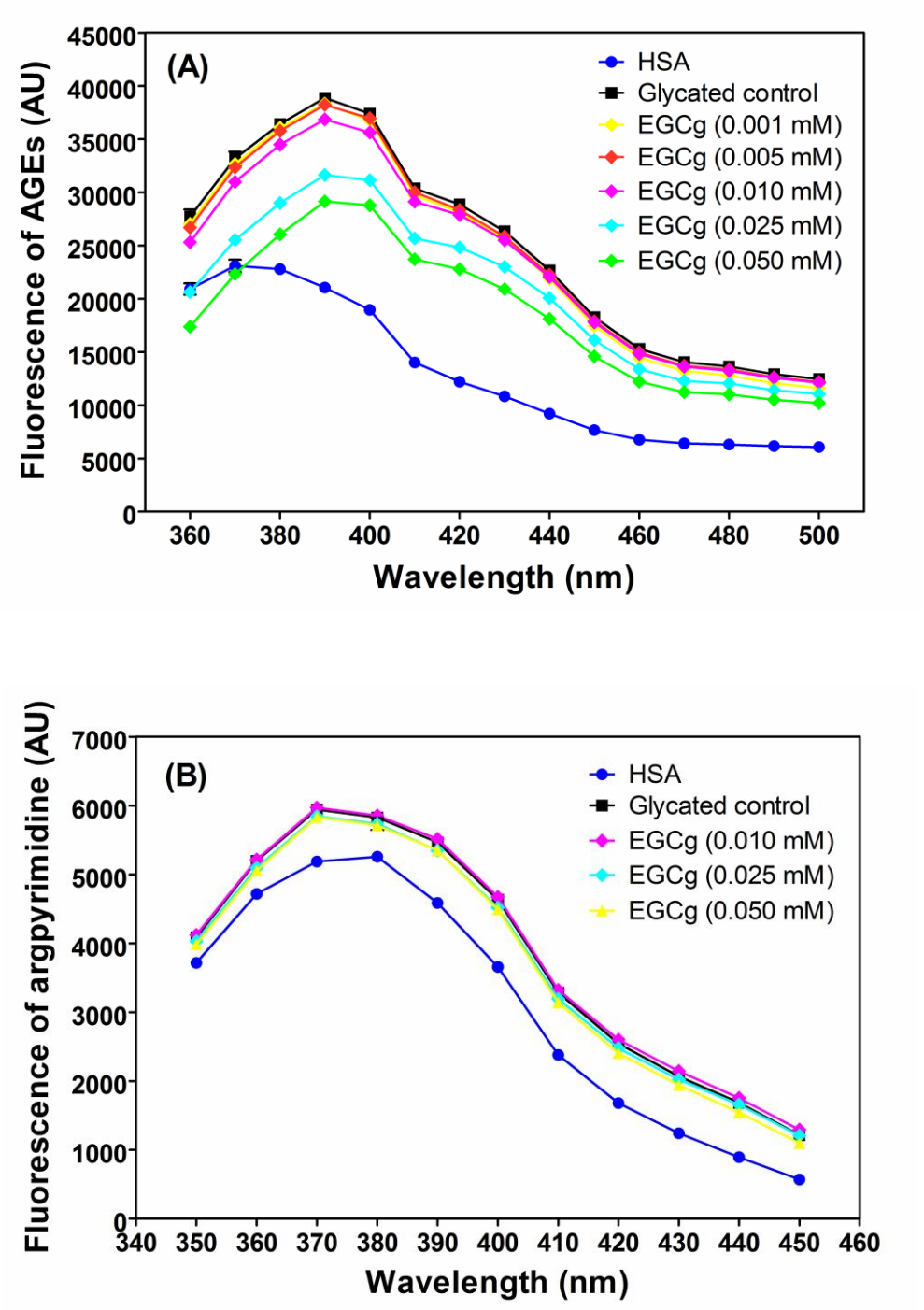

Figure 25: Fluorescence spectra of total fluorescent AGEs (A) and argpyrimidine (B) formation after incubation of HSA with MGO in the absence and presence of different EGCg concentrations. [HSA] = 1 mg/ml, [MGO] = 1 mM, [EGCg] = 0.001 - 0.050 mM, pH 7.4, 37°C, 7 days of incubation, λ_{ex} = 330 nm (A), and λ_{em} = 320 nm (B).

The effects of different GTCs concentrations on the formation of “non-specific” fluorescent AGEs are shown in **Figure 26** and the obtained results (% inhibition of AGEs formation) are summarized in **Table 16**. The samples containing HSA and MGO exerted about 66.0% and 116.5% higher fluorescence intensity than the control sample without MGO after 3 and 7 days of incubation, respectively. Aminoguanidine (1.0 mM) and Trolox (2.5 mM) were used as positive controls. They reached obvious inhibitory effect on MGO-mediated glycation of HSA among 62.6 - 66.6% and 16.3 - 25.4%, respectively. All tested GTCs did not cause any significant decline in AGEs formation at the lowest concentration (0.010 mM). Epicatechin exhibited anti-glycating effect only at its highest concentration (0.050 mM) after 3 days of incubation (about 20%). Other GTCs (0.025 and 0.050 mM) showed more pronounced inhibition after 3 days of incubation than after 7 days. The galloylated GTCs (ECg and EGCg) demonstrated the similiar decrease in the AGEs formation and showed more significant anti-glycating effect than the non-galloylated GTCs and Trolox (2.5 mM).

The effects of GTCs on the argpyrimidine formation during MGO-mediated glycation of HSA are displayed in **Figure 27** and the obtained results (% inhibition of argpyrimidin formation) are given in **Table 16**. Methylglyoxal caused low but statistically significant increase in concentration of agrpyrimidine with fluorescent properties (by 11%) compared to the control sample (HSA alone). The non-galloylated GTCs (EC and EGC) exhibited no anti-glycating effect as well as the galloylated GTCs (ECg and EGCg) at concetrations of 0.010 and 0.025 mM. More pronounced inhbition of argpyrimidine formation was noticed in the case of the galloylated GTCs at concentration of 0.050 mM. It was reduced by 38% and 25% for ECg and EGCg, respectively, and higher inhibitory effect was noticed after 3 days of incubation than after 7 days. Aminoguanidine (1.0 mM) and Trolox (2.5 mM) reached anti-glycating effects approximately about 64% and 14%, respectively.

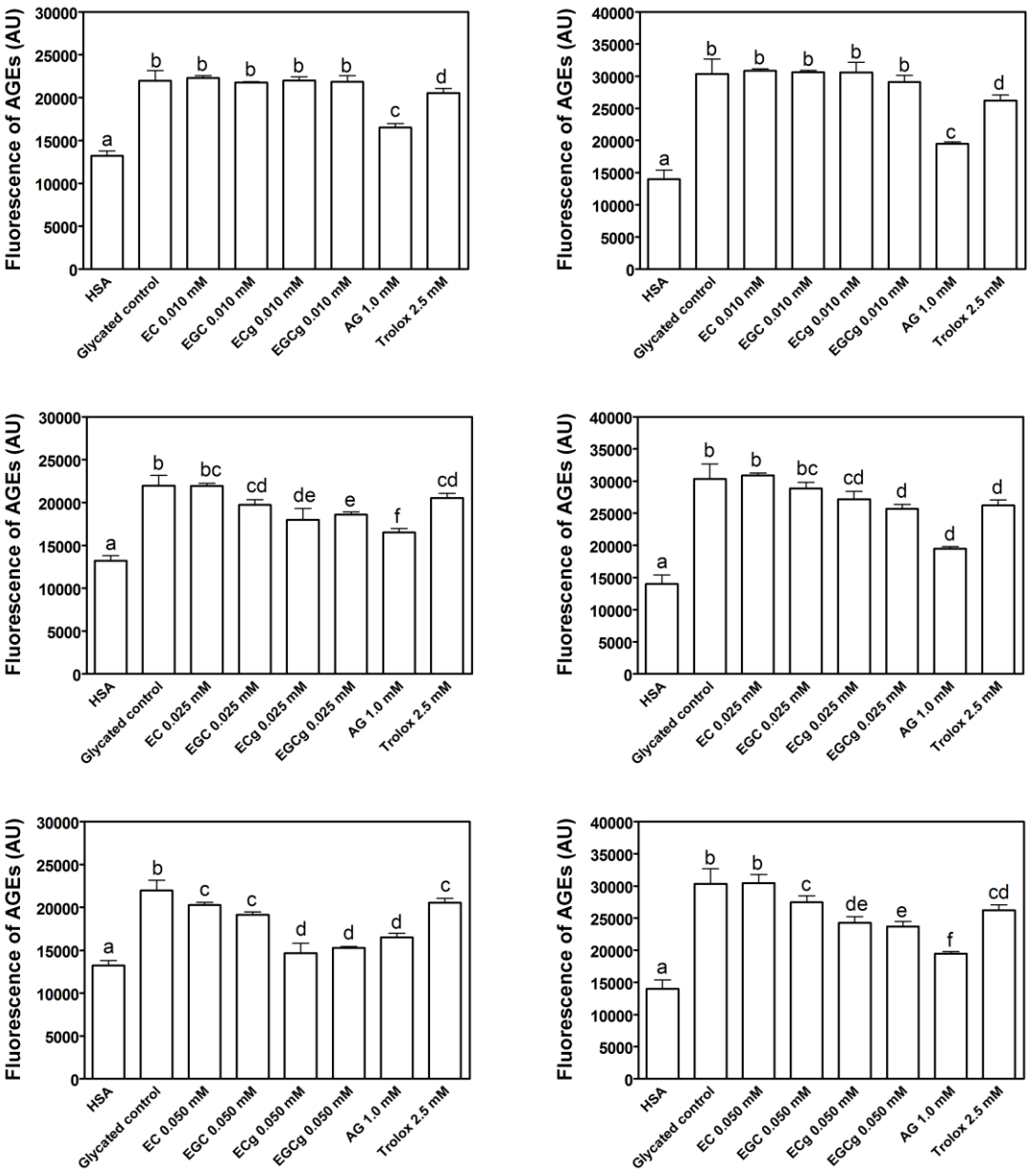

Figure 26: Inhibitory effect of GTCs on total fluorescent AGEs formation during MGO-mediated glycation of HSA (pH 7.4, 37°C). [HSA] = 1 mg/ml, [MGO] = 1 mM, λ_{ex} = 330 nm, and λ_{em} = 410 nm. The first and second columns represent inhibitory effects after 3 and 7 days of incubation time, respectively. Standard deviations were lower than 10%. Data were analyzed by Student´s *t*-test and groups with different letters are significantly different ($p < 0.05$).

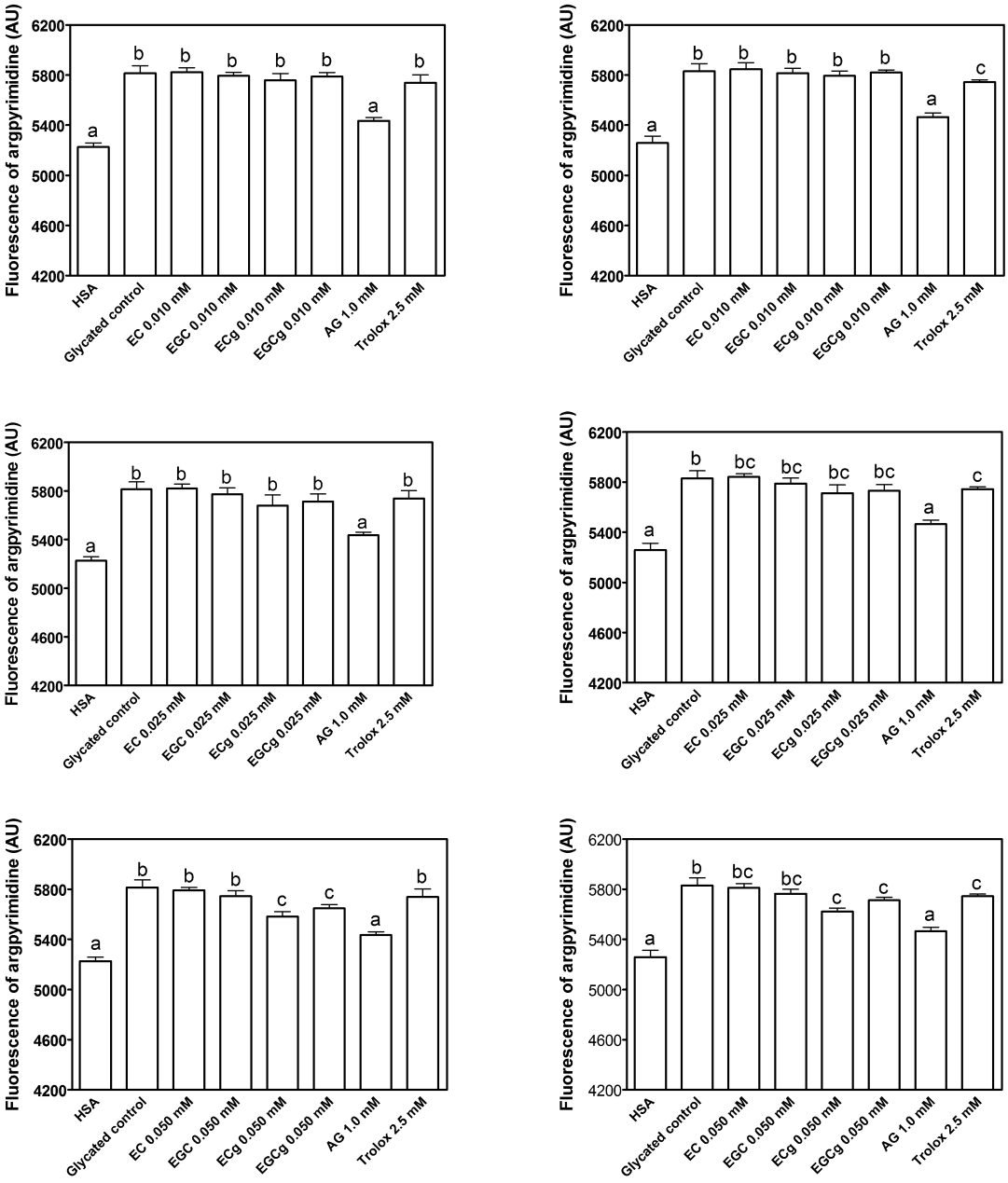

Figure 27: Inhibitory effect of GTCs on argpyrimidine formation during MGO-mediated glycation of HSA (pH 7.4, 37°C). [HSA] = 1 mg/ml, [MGO] = 1 mM, λ_{ex} = 320 nm, and λ_{em} = 380 nm. The first and second columns represent inhibitory effects after incubation of 3 and 7 days, respectively. Standard deviations were lower than 10%. Data were analyzed by Student´s *t*-test and groups with different letters are significantly different ($p < 0.01$).

Tables 16: Inhibitory effect of green tea catechins on total fluorescent AGEs and argpyrimidine formation during MGO-mediated glycation (pH 7.4, 37°C). [HSA] = 1 mg/ml and [MGO] = 1 mM, $\lambda_{ex}/\lambda_{em}$ = 330/410 nm (fluorescent AGEs), and $\lambda_{ex}/\lambda_{em}$ = 320/380 nm (argpyrimidine).

Compounds	Concentration (x 10^{-3} M)	% inhibition of total AGEs formation		% inhibition of argpyrimidine formation	
		3 days	*7 days*	*3 days*	*7 days*
Epicatechin	0.010	-3.58	-2.93	-1.23	-2.87
	0.025	0.37	-3.19	-1.16	-2.25
	0.050	19.6	-0.52	3.87	3.11
Epigallocatechin	0.010	2.58	-1.50	3.65	2.78
	0.025	25.8	9.18	7.09	6.91
	0.050	32.3	17.6	12.2	11.5
Epicatechin gallate	0.010	-0.29	-1.36	9.66	6.22
	0.025	45.7	19.5	22.9	20.4
	0.050	83.4	37.4	39.6	36.2
Epigallocatechin gallate	0.010	-1.36	7.61	4.74	1.29
	0.025	39.0	28.7	17.3	16.9
	0.050	76.61	40.8	28.5	20.6
Aminoguanidine	1.0	62.6	66.6	64.5	63.7
Trolox	2.5	16.3	25.4	13.1	15.0

The anti-glycating effects of green tea catechins on middle stage of protein glycation were investigated using the *in vitro* model system containing human serum albumin as a model protein, methylglyoxal as a glycating agent, and GTCs as studied compounds with potential anti-glycating properties. Serum albumin belongs to the most used model proteins for assessment of anti-glycating activity of various compounds [Lunceford and Gugliucci 2005, Tsuji-Naito et al. 2009]. Methylglyoxal represents one of the reactive α-dicarbonyls, which are important precursors in the formation of AGEs *in vivo*, and are far more reactive than the parent sugars concerning their abilities to form inter- and intramolecular protein cross-links [Nass et al. 2007, Yim et al. 2001]. The increased levels of MGO have been reported in patients suffering from diabetes mellitus [McLellan et al. 1994]. This compound reacts irreversibly with lysine and arginine residues to form *N*-ε-(1-carboxyethyl)lysine (CEL), 1,3- di(*N*-ε-lysino)-4-methyl-imidazolium (MOLD), argpyrimidine, and three structural isomers of hydroimidazolone [Ahmed et al. 2003]. One of the approaches in diabetes prevention or treatment is to develop effective compounds in removing α-dicarbonyls, and thus

forestall formation of AGEs. Aminoguanidine could serve as a prototype of such drugs because of its antioxidant and anti-glycating properties. However, its side adverse effects on human body have been indicated [Thornalley 2003]. Trolox is a water-soluble derivative of vitamin E which shows also inhibitory activity in protein glycation [Tarwadi and Agte 2011]. Aminoguanidine (1.0 mM) and Trolox (2.5 mM) were used as positive controls for the assessment of potential anti-glycating effects of green tea catechins (flavanols) as outstanding representatives of flavonoids.

Flavonoids show many biological and pharmacological activities including anti-glycating properties. Inhibitory effects of several flavonoids on different glycating systems in the *in vitro* models have been already described (**Table 6**). The results obtained by flurescence measurement of the extent of total fluorescent AGEs formation revealed that the most pronounced inhibitory effect against MGO-mediated glycation of HSA possessed the galloylated GTCs (ECg and EGCg) predominantly at higher GTCs concentrations (0.025 mM and 0.050 mM). ECg showed a slightly higher anti-glycating effect than EGCg but it was not statistically significant. Inhibitory effects of several flavonoids including GTCs (0.10 mM) on methylgyloxal-mediated glycation of BSA have been investigated by Wu and Yen [2005]. It was noticed that the galloylated GTCs (ECg and EGCg) were more effective anti-glycating agents than the non-galoylated GTCs (EC and EGC), which is in good agreement with our results. However, the most pronounced anti-glycating effect was described for EGCg (about 69%). Only the galloylated GTCs (ECg and EGCg) at the highest concentration (0.050 mM) caused obvious inhibitory effect on argpyrimidine generation during MGO-mediated glycation of HSA. ECg and EGCg were more effective anti-glycating agents than Trolox (2.5 mM) but less effective than aminoguanidine (1.0 mM). It can be concluded that the presence of the galloyl moiety in GTCs seems to be an important structural feature for their anti-glycating activities. It suggests that the binding affinity of GTCs may contribute to their anti-glycating properties [Kusuda et al. 2006, Wu and Yen 2005]. Also anti-glycating effects of green tea (*Camellia sinensis*, Theaceae) on glycation of BSA by different glycating agents glucose, fructose, and methylglyoxal) have been investigated in detail [Ho et al. 2010, Lunceford and Gugliucci 2005, Nakagawa et al. 2002].

Anti-glycating activity of GTCs, especially EGCg, has been attributed to their trapping ability of reactive oxygen [Lunceford and Gugliucci 2005] and dicarbonyl species (e.g. GO and MGO) [Lo et al. 2006, Sang et al. 2007]. However, some other mechanisms such as chelating of transition metals or interaction with proteins can take place [Gugliucci et al. 2009]. Therefore, the mechanisms of actions of plant polyphenols including flavonoids need to be more elucidated. It is very important to note that the use of fluorescence methods for evaluation of protein glycation is limited by its imprecision. The measurement of total or some well-identified AGEs (e.g. argpyrimidine and CML) by techniques such as ELISA or HPLC could give more precise information on this matter.

5.5 EFFECT OF METHYLGLYOXAL ON STRUCTURAL AND CATALYTIC PROPERTIES OF GST

In this study, the effect of MGO on structural and catalytic properties of recombinant cytosolic GST from *Schistosoma japonicum* was investigated. This enzyme shares striking sequence homology, the characteristics of the amino acid residues in the G-site, and a common GSH-binding mode with mammalian mu-class GSTs [Ji et al. 1997, Lim et al. 1994]. Glutathione metabolism and GST distribution in the tissues of diabetics may be crucial in the etiology, pathology, and prevention of diabetes [Raza et al. 2004]. Furthermore, the long-term hyperglycemia results in the decrease of GST enzymatic activity in tissues of diabetic animals [Lapshina et al. 2006, Petlevski et al. 2003, Saito-Yamanaka et al. 1993, Thomas et al. 1989]. Administration of MGO to Swiss albino mice reduced GSH content and inhibited catalytic activity of several enzymes including GST, superoxide dismutase, glyoxalase I and II, and catalase [Choudhary et al. 1997]. All these findings indicate that ongoing diabetes may modify the detoxification metabolism. They also suggest that GST may be modified by non-enzymatic glycation *in vivo*, and hence, provide a rationale of this enzyme use for studying glycation reactions. Reactive α-dicarbonyls (e.g. GO, MGO, 3-DG) are important precursors in the formation of AGEs *in vivo*. These compounds are far more reactive than the parent sugars (e.g. glucose) concerning their abilities to form inter- and intramolecular protein cross-links [Matsumoto et al. 2000, Kang 2006]. MGO is mainly generated not only by the fragmentation of triosephosphates, but also by the

catabolism of ketone bodies and threonine and the degradation of glucose-modified proteins *in vivo*. MGO has been identified as an intermediate in non-enzymatic glycation, and increased levels of MGO have been reported in patients suffering from diabetes mellitus [West 2000].

5.5.1 Effect of MGO-mediated glycation on GST catalytic activity

Enzymatic activity of control sample (GST alone) was stable throughout the experiment. Methylglyoxal caused an irreversible decrease in enzymatic activity of GST (Figure 28). When GST was incubated with MGO (0.5, 1.0, and 2.0 mM) up to 180 min at 37°C its activity decreased by 12.1, 20.3, and 27.6%, respectively. The rate of enzyme inactivation increased with increasing concentrations of MGO.

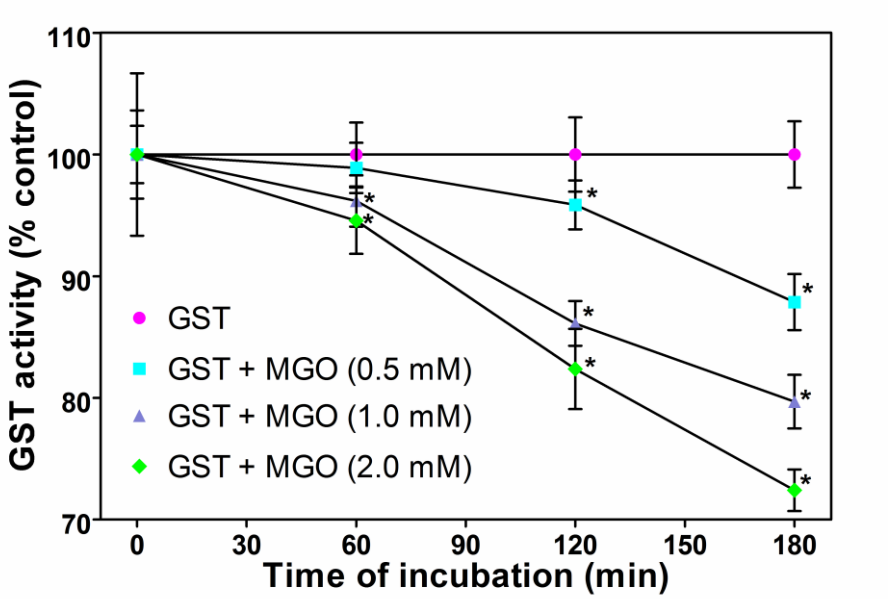

Figure 28: **Effect of glycation by MGO on GST catalytic activity**. [GST] = 0.025 mg/ml and [MGO] = 0 - 2 mM. Samples were incubated for 180 min at pH 7.4 and 37°C. Catalytic activity of GST was expressed as percentage of control sample activity at all time intervals, which was 100% ± SD (%). Every point represents an average of two independent experiments, in which assays were performed in hexaplicates (*$p < 0.05$, Student's *t*-test).

It can be concluded that the incubation of GST with MGO led to the inhibition of its catalytic activity, which is probably caused by the lysine residues modification and the intramolecular cross-links formation induced by AGEs (further discuss below). This effect of MGO was concentration-dependent.

5.5.2 Effect of MGO-mediated glycation on primary amine content in GST

Protein glycation, the chemical modification of primary amines (i.e. ε-amino group of lysine residues and α-amino group of *N*-terminal amino acids), leads to the decrease in amine content. Incubation of GST with all concentrations of MGO led to the gradual reduction in amine content (Table 17).

Table 17: **Amine content and number of primary amino groups after incubation (pH 7.4, 37°C, and 7 days).**

Sample	Amine content [mol NH_2/mol GST]	Number of primary amino groups
GST	52.76 ± 1.17^{a}	44
GST + MGO (0.5 mM)	46.19 ± 2.68^{b}	39
GST + MGO (1.0 mM)	40.70 ± 1.22^{c}	34
GST + MGO (2.0 mM)	36.44 ± 1.42^{d}	30

Groups with different letters are significantly different ($p < 0.01$, Student´s *t*-test).

Incubation of GST with MGO (0.5, 1.0, and 2.0 mM) for 7 days caused 12.5%, 22.9%, and 30.9% decrease in amine content due to chemical modification of primary amines, respectively. GST in its native dimeric form contains 44 primary amino groups, suggesting that about 5, 10, and 14 amino groups were modified during its 7-day incubation with increasing concentration of MGO.

MGO chemically modified GST by a process with the generally accepted features of glycation as evidenced by a decrease in amine content. Lysine and arginine residues are target sites for reducing sugars as well as MGO modification via the Maillard reaction [Seidler and Kowalewski 2003]. Typical arising products of MGO-mediated glycation of lysine and arginine residues are CEL, MOLD, argpyrimidine, and three structural isomers of hydroimidazolone. All of these compounds were described and quantified *in vivo* [Thornalley 1996]. The GST dimer contains 44 lysine and 20 arginine residues with four Lys–Lys and two Lys–Arg sequence pairs, which are possible targets for glycating agents. Approximately 10 Lys residues per GST molecule were irreversibly modified during 7-day incubation with MGO 1.0 mM.

5.5.3 AGEs formation and conformational changes of GST induced by MGO

Incubation of GST with MGO led to the increase in fluorescence intensity due to the formation of non-specific AGEs with fluorescent properties (Figure 29) and the decrease in tryptophan fluorescence (Figure 30). The 7-day incubation of GST with MGO (0.5, 1.0, and 2.0 mM) at 37 °C caused an increase in AGEs formation by 32.0, 55.1, and 85.3% and a decrease in tryptophan fluorescence by 11.3, 16.6, and 27.7% compared with the control sample (GST alone), respectively.

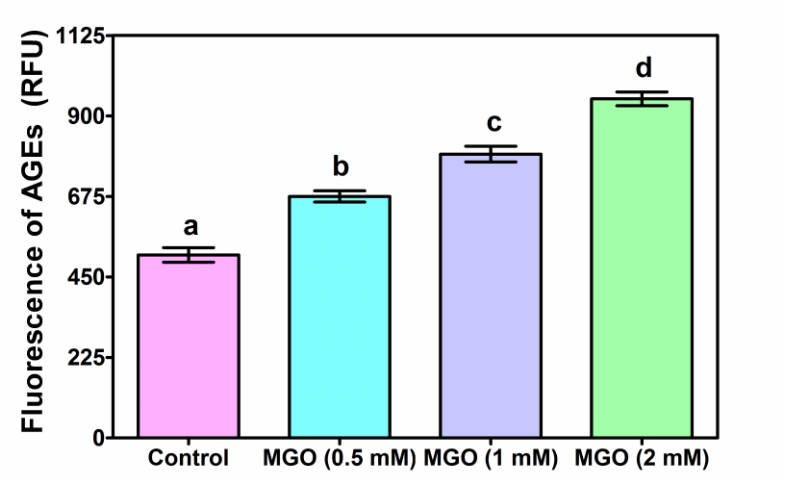

Figure 29: **Effect of glycating agents on the formation of fluorescent AGEs**.
[GST] = 0.5 mg/ml, [MGO] = 0 - 2.0 mM, pH 7.4, 37 °C, 7 days of incubation, λ_{ex} = 370 nm, and λ_{em} = 440 nm. Every point represents an average of two independent experiments (six samples). Groups with different letters are significantly different (p < 0.01, Student's t-test).

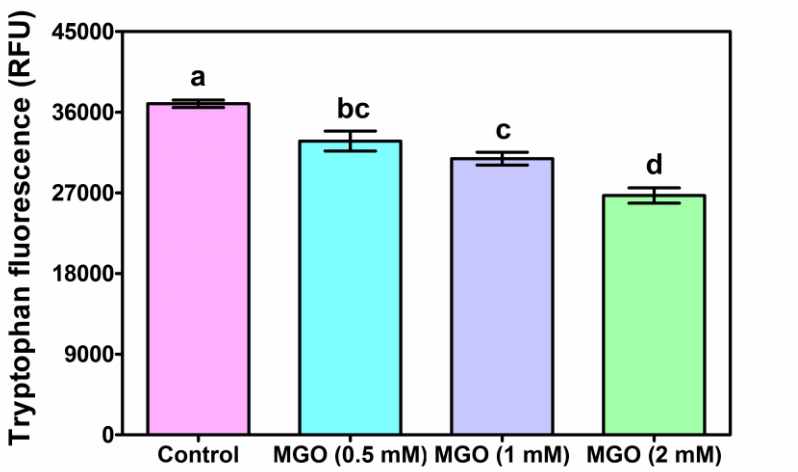

Figure 30: **Effect of glycating agents on the tryptophan fluorescence**.
[GST] = 0.5 mg/ml, [MGO] = 0 - 2.0 mM, pH 7.4, 37 °C, 7 days of incubation, λ_{ex} = 295 nm, and λ_{em} = 386 nm. Every point represents an average of two independent experiments (six samples). Groups with different letters are significantly different (p < 0.01, Student's t-test).

In order to determine whether the changes in tryptophan fluorescence observed in the samples containing various concentrations of MGO (0 - 2.0 mM) correlated with the loss of primary amino groups in these samples, the fluorescence intensity was plotted as a function of amine content. The decrease in fluorescence emission ($\lambda_{ex}/\lambda_{em}$ = 295/386 nm) varied directly with the loss of primary amino groups (R = 0.987, p < 0.013, Figure 31A). Changes in tryptophan fluorescence also correlated well with the formation of fluorescent AGEs (R = 0.997, p < 0.003, Figure 31B). In addition, the amine content was plotted as a function of AGEs fluorescence (Figure 31C), indicating that MGO-induced formation of AGEs was directly proportional to an irreversible loss of primary amino groups in GST molecule (R = 0.995, p < 0.005).

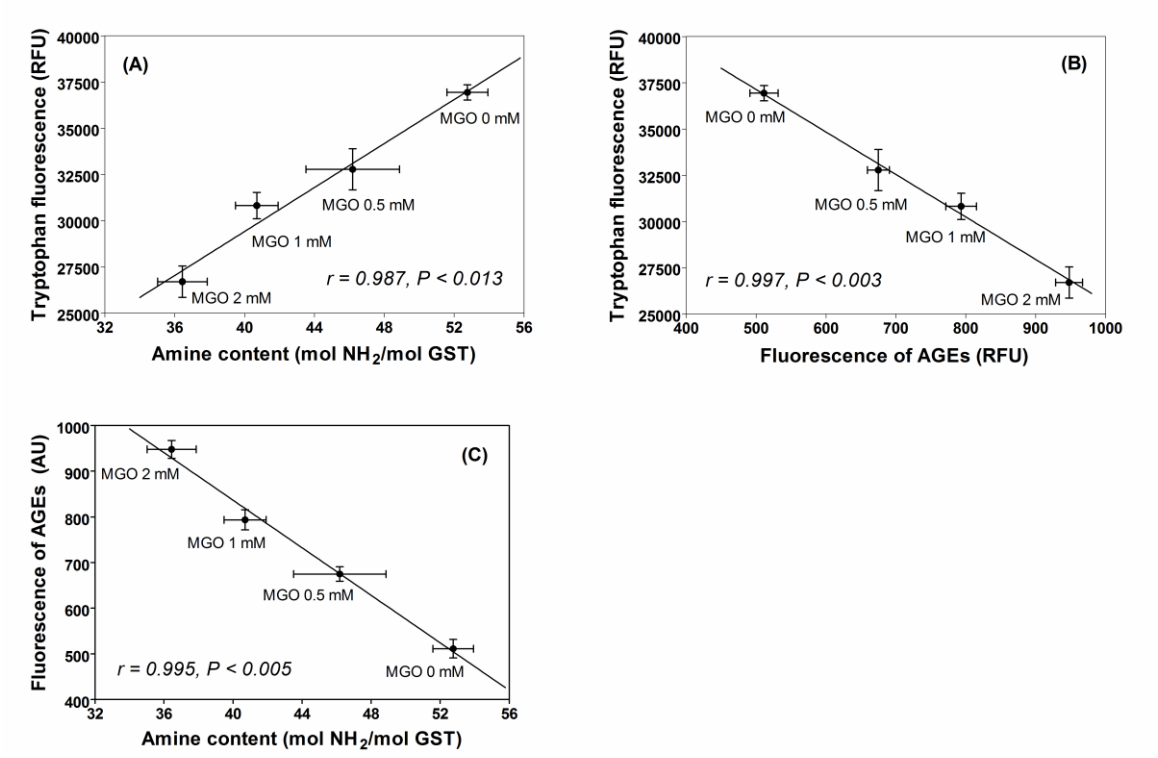

Figure 31: Correlations between amine content, tryptophan fluorescence, and formation of fluorescent AGEs in the samples containing GST and various concentrations of MGO. MGO-induced decrease in tryptophan fluorescence intensity correlated with the loss of primary amino groups (A) (R = 0.987, p < 0.013). Correlation between the decrease in tryptophan fluorescence and formation of AGEs (B) (R = 0.997, p < 0.003). Plot of an increase in AGEs formation as a function of amine content (C) (R = 0.995, p < 0.005).

The glycation-induced conformational changes in protein topography and modification of lysine residues, which may play a role in the enzyme catalysis (e.g. Lys-44 is involved in the formation of G-site), probably contribute to enzyme inhibition (Figure 29). Also the formation of intramolecular cross-links induced by AGEs (Figure 33) may be accompanied by progressive localized compaction of protein molecule that may result in its dysfunction (e.g. creation of surface to interior channels, impairment of conformational transition, and inhibition of domain movement during catalysis). Moreover, introducing AGEs, which are hydrophobic, would also promote a local condensation of substructures [Ulrich and Cerami 2001, Seidler 2005].

5.5.4 Effect of MGO-mediated glycation on molecular charge of GST

Native PAGE was used to investigate the changes in the molecular charge of GST due to glycation process by MGO. The results were expressed as a rise in percentage mobility of samples compared to the native protein (control). Native PAGE was run three times and the obtained mean values of protein relative mobility are presented in Table 18. Incubation of GST with MGO in all tested concentrations caused significantly increased mobility of the sample towards the positive electrode (Figure 32). This phenomenon was noticeable since the first day of incubation and the electrophoretic mobility of GST was gradually increased with increasing concentration of MGO. After 14-day incubation, it reached about 17.4, 21.7, and 22.6% for MGO (0.5, 1, and 2 mM), respectively.

Table 18: **Effect of MGO-mediated glycation on molecular charge of GST.**

Sample	Relative mobility (%)				
	day 0	day 1	day 3	day 7	day 14
GST	100.0	100.0	100.0	100.0	100.0
GST + MGO (0.5 mM)	99.8	106.1	113.9	116.2	117.4
GST + MGO (1.0 mM)	99.5	109.1	115.5	118.9	121.7
GST + MGO (2.0 mM)	99.3	111.6	116.8	121.9	122.6

Standard deviations (mean value of three independent experiments) were lower than 4.1%. Relative mobilities of all the samples were compared with the relative migration of the main protein band (R_f = 0.517).

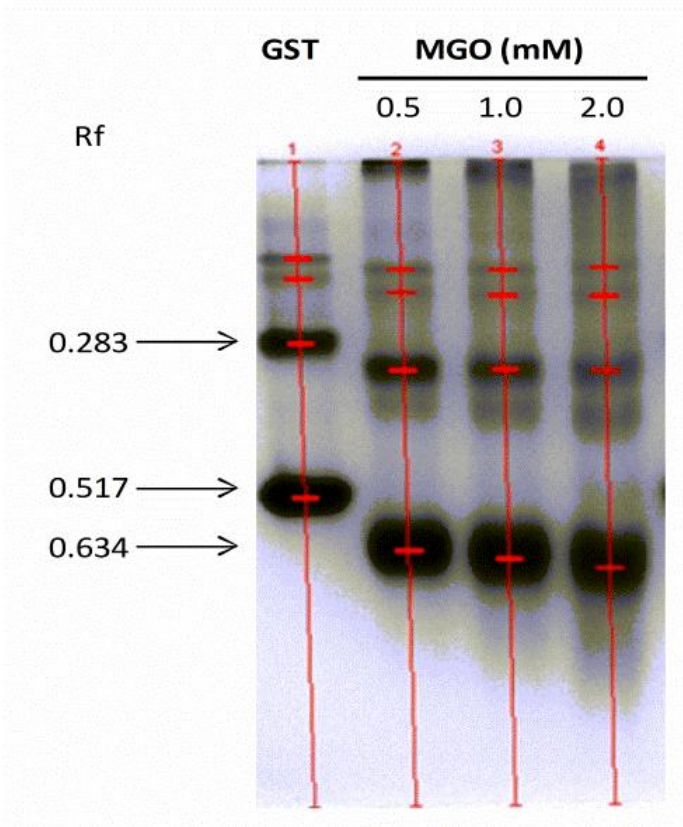

Figure 32: **Effect of MGO-mediated glycation on molecular charge of GST.**
GST (0.5 mg/ml) was incubated with or without MGO (0 – 2 mM) in sodium phosphate buffer (0.1 M, pH 7.4) at 37°C for 14 days and then subjected to native PAGE. Proteins were visualized by Coomassie Blue G250. Electrophoretic mobilities were expressed as a rise in percentage mobility compared to the native protein (control).

MGO-induced chemical modifications led to a change in molecular charge of GST, which became more anionic as revealed by native PAGE. These results indicate the progressive loss of the positive charge in the glycation modified GST molecule, which is caused by the irreversible modification of arginine and lysine residues [Kang 2006, Nagai et al. 2000] as was confirmed by determination of amine content. MGO proved to be potent and fast-acting glycating agent because it progressively modified molecular charge of GST within the first 3 days of incubation.

5.5.5 Protein cross-linking and aggregation

Western blotting with specific antibody against advanced glycation end products and against AGEs derived from MGO (anti-MGO [3C]) was employed to confirm the formation of protein aggregates as a result of glycating agent's activity. The presence

of high molecular protein cross-links in samples containing GST and MGO was observed using the both antibodies. These protein aggregates had molecular weight about 50 and 75 kDa (Figure 33A) corresponding to GST dimer and trimer, respectively. Also cleavage to shorter peptides (≈ 14 kDa) occurred in immunoblots that were incubated with anti-MGO primary antibody. Membranes were then stained with Ponceau S and changes in the migration of the main GST band (26 kDa) towards higher molecular weight and loss of its intensity was observed in all the samples containing MGO (Figure 33B). These results suggest that glycation by MGO was accompanied mainly by cross-linking, formation of high molecular protein aggregates containing AGEs, and as well as protein fragmentation.

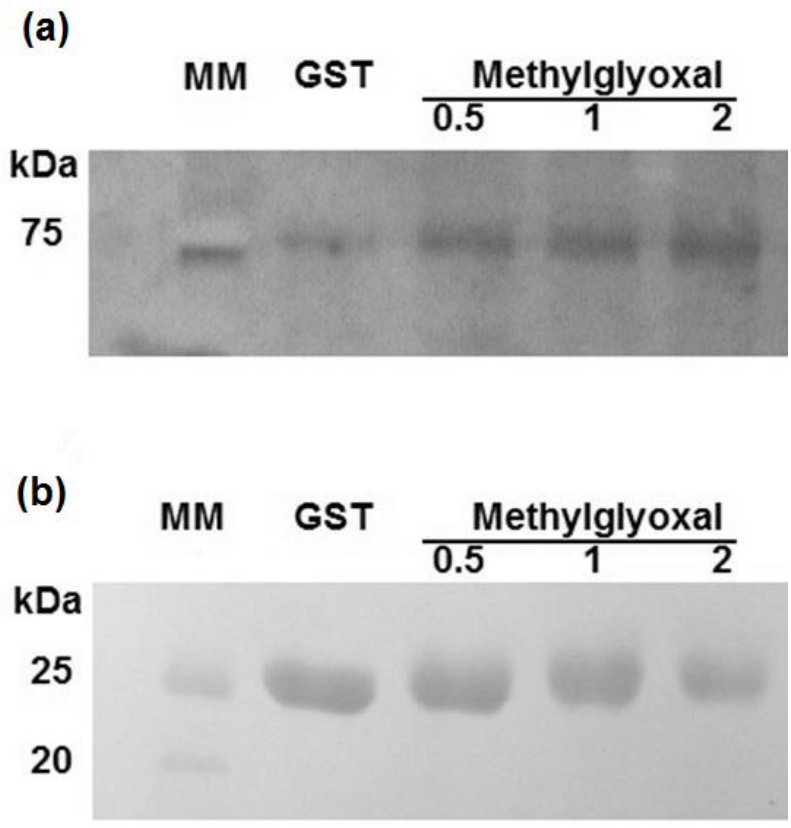

Figure 33: **Western blotting of GST samples treated with MGO.** GST (0.5 mg/ml) was incubated with or without MGO (0 - 2 mM) in sodium phosphate buffer (0.1 M, pH 7.4) at 37°C for 11 days and then subjected to SDS PAGE with subsequent western blotting. Blot was reacted with rabbit anti-AGE primary antibody. Molecular weight standard (MM) and protein bands were marked by goat anti-rabbit IgG using a chemiluminescent detection with an alkaline phosphatase substrate (a). Membrane was further stained with Ponceau S (b).

The SDS PAGE and subsequent western blotting clearly showed formation of protein cross-links with higher molecular weight (75 kDa) than native enzyme in the samples containing MGO. Also, the migration of the main protein band towards higher molecular weight was observed in all the samples containing MGO after 11 days of incubation. These results suggest that glycation by MGO was accompanied by cross-linking and formation of high molecular protein aggregates containing AGEs. Such glycation modified sites on proteins act as trapping agents that bind transition metals and proteins, which may provide a nucleation center for extracellular plaque or intracellular inclusion body formation [Seidler 2005]. Protein aggregation takes part in the development and progress of various diseases including cataract [Argirova and Breipohl 2002, Harding 2007] and Alzheimer's disease [Apostolova and Cumings 2007].

6 CONCLUSIONS

Plant polyphenols are naturally occurring substances with a wide range of biological and pharmacological properties, which constitute a significant part of the human diet. They are readily able to react with various proteins including serum albumin which acts as a carrier of various endogenous and exogenous low molecular compounds in blood stream. One of the main goals of this thesis was to study structure-binding affinity relationships between serum albumin and two selected groups of polyphenolic compounds such as hydroxycinnamic acids and catechins (flavanols) in the *in vitro* models using spectroscopic (UV-Vis absorption and fluorescence spectroscopy) and electrophoretic (native and SDS PAGE) methods.

Apart from rosmarinic acid, all tested HCAs quenched tryptophan fluorescence of BSA in the studied range of concentrations mainly by static quenching mechanism and thus showed the formation of non-fluorescent HCA-BSA complexes. The obtained results suggest that the binding affinity and number of binding sites of HCA-BSA systems depended on the size and structure of HCA and on the number and position of hydroxyls in the molecule of HCA. Their binding affinity towards BSA increased with increasing number of hydroxyls in their molecules. Coumaric acids containing only one hydroxyl showed the lowest binding affinity. Substitution of hydroxyl by methoxyl group lowered the binding affinity, whereas esterification of carboxyl group with quinic acid increased this ability. It was shown that one molecule of BSA associated with one molecule of HCA and all HCA-BSA interactions were spontaneous processes.

All studied catechins quenched tryptophan fluorescence of HSA in the studied range of concentrations mainly by static quenching mechanism and thus the non-fluorescent catechin-HSA complexes were formed. The complex formation for the galloylated catechins and HSA was confirmed also by UV-Vis absorption spectroscopy. All catechins bound spontaneously to the molecule of HSA with different binding affinity. The most important structural features of the studied catechins contributing to HSA binding were the galloyl group on the C-ring, followed by the number of hydroxyl groups on the B-ring, and the spatial arrangement (*cis*- and *trans*-structure). The number of binding sites was roughly one for all systems suggesting that one molecule of HSA associated with one molecule of catechin. The non-radiation energy transfer from HSA to all studied catechins was also occurred. The galloylated catechins

increased the electrophoretic mobility of HSA while the ability of aggregation and cross-linking of the tested catechins was not proved.

Results imply that the studied plant polyphenols can be stored and transported in blood by serum albumin which may influence their biological and pharmacological activities. On the other hand, physiological functions of this protein could be altered by ligand binding.

Green tea catechins (EC, EGC, ECg, and EGCg) were selected as representatives of the most outstanding plant polyphenols. Effects of GTCs on catalytic and structural properties of ERp57 enzyme have been investigated using fluorescence methods. The presence of galloyl moiety in the molecules of GTCs was an important structural feature which significantly contributed to the binding affinity of GTCs to ERp57 and evoked the protein conformational changes. By contrast, the number of hydroxyl groups in GTCs did not seem to play any role in their binding capability to ERp57. The GTCs except epicatechin were able to inhibit disulfide reductase activity of the protein. Their inhibitory activities were probably related to their binding affinity to the protein.

Effects of green tea catechins on methylglyoxal-mediated non-enzymatic glycation of HSA in the *in vitro* models have been investigated by fluorescence methods and their structure-activity relationships were discussed. It can be concluded that the galloylated GTCs, namely epicatechin gallate and epigallocatechin gallate, were able to partially inhibit methylglyoxal-induced modification of HSA and thus prevent their deleterious action in the human organism. It was probably due to their antioxidant and chelating activities. However, other mechanisms may be take place.

Finally, effects of methylglyoxal as a very potent glycating agent on structural and catalytic properties of recombinant cytosolic glutathion S-transferase from *S. japonicum* have been investigated in the *in vitro* model using spectroscopic (UV-Vis absorption and fluorescence spectroscopy) and electrophoretic (native PAGE, SDS PAGE/western blotting) methods. Methylglyoxal has proved to be the potent glycating agent, which caused concentration-dependent inhibition of GST catalytic activity, decrease in amine content of GST, enzyme conformational changes, generation of fluorescent AGEs and cross-links, as well as changes in molecular charge of the studied enzyme.

7 REFERENCES

Abdel-Rahman E and Bolton WK. 2002. Pimagedine: a novel therapy for diabetic nephropathy. Expert Opin Investig Drugs. 11(4):565-574.

Adzet T, Camarasa J, Escubedo E, Merlos M. 1988. *In vitro* study of caffeic acid-bovine serum albumin interaction. Eur J Drug Metab Pharmacokinet. 13(1):11-14.

Ahmad MS, Pischetsrieder M, Ahmed N. 2007. Aged garlic extract and S-allyl cysteine prevent formation of advanced glycation endproducts. Eur J Pharmacol. 561(1-3):32-38.

Ahmed N. 2005. Advanced glycation endproducts - role in pathology of diabetic complications. Diabetes Res Clin Pract. 67(1):3-21.

Ahmed N and Thornalley PJ. 2005. Peptide mapping of human serum albumin modified minimally by methylglyoxal *in vitro* and *in vivo*. Ann NY Acad Sci. 1043:260–266.

Ahmed N, Thornalley PJ, Dawczynski J, Franke S, Strobel J, Stein G, Haik GM. 2003. Methylglyoxal-derived hydroimidazolone advanced glycation endproducts of human lens proteins. Invest Ophthalmol Vis Sci. 44:5287–5292.

Apostolova LG and Cummings JL. 2007. The pathogenesis of Alzheimer's disease: general overview. In: Uversky VN, Fink AL (eds) Protein misfolding, aggregation, and conformational diseases. Part B: molecular mechanisms of conformational diseases, 1st ed. Springer Science, New York, pp 3-29.

Ardestani A and Yazdanparast R. 2007a. *Cyperus rotundus* suppresses AGE formation and protein oxidation in a model of fructose-mediated protein glycoxidation. Int J Biol Macromol. 41(5):572-578.

Ardestani A and Yazdanparast R. 2007b. Inhibitory effects of ethyl acetate extract of *Teucrium polium* on *in vitro* protein glycoxidation. Food Chem Toxicol. 45(12):2402-2411.

Argirova M and Breipohl W. 2002. Comparison between modifications of lens proteins resulted from glycation with methylglyoxal, glyoxal, ascorbic acid, and fructose. J Biochem Mol Toxicol. 16:140-145.

Arora JP, Singhal VK, Chand M, Laxmi, Pal C. 1989. Study of interaction between catechin and native and modified bovine serum albumin by physico-chemical methods. Indian J Biochem Biophys. 26(1):14-18.

Bae JW and Lee MH. 2004. Effect and putative mechanism of action of ginseng on the formation of glycated hemoglobin *in vitro*. J Ethnopharmacol. 91(1):137-140.

Bae M-J, Ishii T, Minoda K, Kawada Y, Ichikawa T, Mori T, Kamihira M, Nakayama T. 2009. Albumin stabilizes (-)-epigallocatechin gallate in human serum: Binding capacity and antioxidant property. Mol Nutr Food Res. 53:709-715.

Banerjee A, Basu K, Sengupta PK. 2008. Interaction of 7-hydroxyflavone with human serum albumin: a spectroscopic study. J Photochem Photobiol B. 90(1):33-40.

Barnaby OS, Cerny RL, Clarke W, Hage DS. 2011. Comparison of modification sites formed on human serum albumin at various stages of glycation. Clin Chim Acta. 412(3-4):277-285.

Bartolomé B, Estrella I, Hernández MT. 2000. Interaction of low molecular weight phenolics with proteins (BSA). J Food Sci. 65:617-621.

Bastianetto S, Dumont Y, Han Y, Quirion R. 2009. Comparative neuroprotective properties of stilbene and catechin analogs: action via a plasma membrane receptor site? CNS Neurosci Ther. 15(1):76-83.

Baynes JW. 1991. Role of oxidative stress in development of complications in diabetes. Diabetes. 40(4):405-412.

Beisswenger PJ, Howell SK, Nelson RG, Mauer M, Szwergold BS. 2003. Alpha-oxoaldehyde metabolism and diabetic complications. Biochem Soc Trans. 31(6):1358-1363.

Beránek M, Držata J, Palička V. 2001. Inhibitory effect of glycation on catalytic activity of alanine aminotransferase. Mol Cell Biochem. 218(1-2):35-39.

Berg JM, Tymoczko JL, Stryer L. 2002. 5th ed. Biochemistry. Chapter 3: Protein Structure and Function. New York: W H Freeman. 541 p.

Bertucci C and Domenici E. 2002. Reversible and covalent binding of drugs to human serum albumin: methodological approaches and physiological relevance. Curr Med Chem. (15):1463-81.

Bi S, Ding L, Tian Y, Song D, Zhou X, Liu X, Zhang H. 2004. Investigation of the interaction between flavonoids and human serum albumin. J Mol Struct. 703:37-45.

Bi S, Song D, Tian Y, Zhou X, Liu Z, Zhang H. 2005. Molecular spectroscopic study on the interaction of tetracyclines with serum albumins. Spectrochim Acta Part A. 61:629-636.

Bian H, Zhang H, Yu Q, Chen Z, Liang H. 2007. Studies on the interaction of cinnamic acid with bovine serum albumin. Chem Pharm Bull. 55:871-875.

Blakytny R and Harding JJ. 1992. Glycation (non-enzymic glycosylation) inactivates glutathione reductase. Biochem J. 288(1):303-307.

Bolli A, Marino M, Rimbach G, Fanali G, Fasano M, Ascenzi P. 2010. Flavonoid binding to human serum albumin. Biochem Biophys Res Commun. 398(3):444-449.

Bolton WK, Cattran DC, Williams ME, Adler SG, Appel GB, Cartwright K, Foiles PG, Freedman BI, Raskin P, Ratner RE, Spinowitz BS, Whittier FC, Wuerth JP; ACTION I Investigator Group. 2004. Randomized trial of an inhibitor of formation of advanced glycation end products in diabetic nephropathy. Am J Nephrol. 24(1):32-40.

Booth AA, Khalifah RG, Hudson BG. 1996. Thiamine pyrophosphate and pyridoxamine inhibit the formation of antigenic advanced glycation end-products: comparison with aminoguanidine. Biochem Biophys Res Commun. 220(1):113-119.

Boušová I, Bacílková E, Dobrijević S, Držata J. 2009. Glycation of aspartate aminotransferase by methylglyoxal, effect of hydroxycitric and uric acid. Mol Cell Biochem. 331(1-2):215-223.

Boušová I, Bakala H, Chudáček R, Palička V, Držata J. 2005b. Glycation-induced inactivation of aspartate aminotransferase, effect of uric acid. Mol Cell Biochem. 278(1-2):85-92.

Boušová I, Martin J, Jahodář L, Dušek J, Palička V, Držata J. 2005a. Evaluation of *in vitro* effects of natural substances of plant origin using a model of protein glycoxidation. J Pharm Biomed Anal. 37(5):957-962.

Bunn HF, Gabbay KH, Gallop PM. 1978. The glycosylation of hemoglobin: relevance to diabetes mellitus. Science. 200(4337):21-27.

Cabrera C, Artacho R, Gimenez R. 2006. Beneficial effects of green tea - A review. J Am Coll Nutr. 25 (2):79-99.

Cantero A-V, Portero-Otín M, Ayala V, Auge N, Sanson M, Elbaz M, Thiers J-C, Pamplona R, Salvayre R, Anne Nègre-Salvayre A. 2007. Methylglyoxal induces advanced glycation end product (AGEs) formation and dysfunction of PDGF receptor-β: implications for diabetic atherosclerosis. FASEB J. 21:3096-3106.

Cao H, Liu Q, Shi J, Xiao J, Xu M. 2008. Comparing the affinities of flavonoid isomers with protein by fluorescence spectroscopy. Anal Lett. 41(4): 521-532.

Carter DC and Ho JX. 1994. Structure of serum albumin. Adv Protein Chem. 45:153-203.

Cervantes-Laurean D, Schramm DD, Jacobson EL, Halaweish I, Bruckner GG, Boissonneault GA. 2006. Inhibition of advanced glycation end product formation on collagen by rutin and its metabolites. J Nutr Biochem. 17(8):531-540.

Choudhary D, Chandra D, Kale RK. 1997. Influence of methylglyoxal on antioxidant enzymes and oxidative damage. Toxicol Lett. 93:141-152.

Clere N, Faure S, Martinez MC, Andriantsitohaina R. 2011. Anticancer properties of flavonoids: roles in various stages of carcinogenesis. Cardiovasc Hematol Agents Med Chem. 9(2):62-77.

Coe H and Michalak M. 2010. ERp57, a multifunctional endoplasmic reticulum resident oxidoreductase. Int J Biochem Cell Biol. 42:796-799.

Cohen RA and Tong X-Y. 2010. Vascular oxidative stress: the common link in hypertensive and diabetic vascular disease. J Cardiovasc Pharmacol. 55(4):308-316.

Coppari S, Altieri F, Ferraro A, Chichiarelli S, Eufemi M, Turano C. 2002. Nuclear localization and DNA interaction of protein disulfide isomerase ERp57 in mammalian cells. J Cell Biochem. 85(2):325-333.

Crespy V and Williamson G. 2004. A review of the health effects of green tea catechins *in vivo* animal models. J Nutr. 134(12):3431S-3440S.

Croft KD. 1998. The chemistry and biological effects of flavonoids and phenolic acids. Ann N Y Acad Sci. 854:435-442.

Davies BJ. 1964. Disc electrophoresis. II. Method and application to human serum proteins. Ann NY Acad Sci. 121:404–427.

Dewick PM. 2002. Medicinal natural products: A biosynthetic approach. 2nd ed. Wiley & Sons Ltd. 520 p.

Dhar A, Desai K, Liu J, Wu L. 2009. Methylglyoxal, protein binding and biological samples: Are we getting the true measure? J Chromatr B. 877:1093-1100.

Dickancaité E, Nemeikaitè A, Kalvelytè A, Cènas N. 1998. Prooxidant character of flavonoid cytotoxicity: structure-activity relationships. Biochem Mol Biol Int. 45(5):923-930.

Diniz A, Escuder-Gilabert L, Lopes NP, Villanueva-Camañas RM, Sagrado S, Medina-Hernández MJ. 2008. Characterization of interactions between polyphenolic compounds and human serum proteins by capillary electrophoresis. Anal Bioanal Chem. 391:625-632.

Dong G, Wearsch PA, Peaper DR, Cresswell P, Reinisch KM. 2009. Insights into MHC class I peptide loading from the structure of the tapasin/ERp57 heterodimer. Immunity. 30(1):21–32.

Dourado DF, Fernandes PA, Ramos MJ. 2008. Mammalian cytosolic glutathione transferases. Curr Protein Pept Sci. 9:325-337.

Drew B and Leeuwenburgh C. 2002. Aging and the role of reactive nitrogen species. Ann NY Acad Sci. 959:66-81.

Dröge W. 2002. Free Radicals in the physiological control of cell function. Physiol Rev. 82:47-95.

Dršata J, Beránek M, Palička V. 2002. Inhibition of aspartate aminotransferase by glycation *in vitro* under various conditions. J Enzyme Inhib Med Chem. 17(1):31-36.

Dufour C and Dangles O. 2005. Flavonoid-serum albumin complexation: determination of binding constants and binding sites by fluorescence spectroscopy. Biochim Biophys Acta. 1721:164-173.

Durham JT and Herman IM. 2011. Microvascular modifications in diabetic retinopathy. Curr Diab Rep. 11(4):253-264.

Dyer DG, Dunn JA, Thorpe SR, Lyons TJ, McCance DR, Baynes JW. 1992. Accumulation of Maillard reaction products in skin collagen in diabetes and aging. Ann NY Acad Sci. 663:421–422.

Ďuráčková Z. 2010. Some current insights into oxidative stress. Physiol Res. 59:459-469.

Elahi MM, Kong YX, Matata BM. 2009. Oxidative stress as a mediator of cardiovascular disease. Oxid Med Cell Longev. 2(5):259-269.

Erickson RR, Dunning LM, Olson DA, Cohen SJ, Davis AT, Wood WG, Kratzke RA, Holtzman JL. 2005. In cerebrospinal fluid ER chaperones ERp57 and calreticulin bind beta-amyloid. Biochem Biophys Res Commun. 332(1):50-57.

Espinosa-Mansilla A, Durán-Merás I, Cañada FC, Márquez MP. 2007. High-performance liquid chromatographic determination of glyoxal and methylglyoxal in urine by prederivatization to lumazinic rings using in serial fast scan fluorimetric and diode array detectors. Anal Biochem. 371(1):82-91.

Eufemi M, Coppari S, Altieri F, Grillo C, Ferraro A, Turano C. 2004. ERp57 is present in STAT3-DNA complexes. Biochem Biophys Res Commun. 323:1306-1312.

Farrar JL, Hartle DK, Hargrove JL, Greenspan P. 2008. A novel nutraceutical property of select sorghum (*Sorghum bicolor*) brans: inhibition of protein glycation. Phytother Res. 22(8):1052-1056.

Ferguson LR. 2010. Chronic inflammation and mutagenesis. Mutat Res. 690(1-2):3-11.

Finkel T and Holbrook NJ. 2000. Oxidants, oxidative stress and the biology of ageing. Nature 408:239-247.

Förster T and Sinanoglu O. 1966. Modern quantum chemistry, vol. 3, Academic Press, New York, 1966. 93 p.

Frazier RA, Papadopoulou A, Green RJ. 2006. Isothermal titration calorimetry study of epicatechin binding to serum albumin. J Pharm Biomed Anal. 41:1602-1605.

Frickel E-M, Frei P, Bouvier M, Stafford WF, Helenius A, Glockshuber R, Ellgaard L. 2004. ERp57 is a multifunctional thiol-disulfide oxidoreductase. J Biol Chem. 279(18):18287-18287.

Friedman M. 2007. Overview of antibacterial, antitoxin, antiviral, and antifungal activities of tea flavonoids and teas. Mol Nutr Food Res. 51:116-134.

Frost L, Chaudhry M, Bell T, Cohenford M. 2011. *In vitro* galactation of human serum albumin: analysis of the protein's galactation sites by mass spectrometry. Anal Biochem. 410(2):248-256.

Fujimura Y, Umeda D, Yamada K, Tachibana H. 2008. The impact of the 67 kDa laminin receptor on both cell-surface binding and anti-allergic action of tea catechins. Arch Biochem Biophys. 476:133-138.

Galleano M, Verstraeten SV, Oteiza PI, Fraga CG. 2010. Antioxidant actions of flavonoids: Thermodynamic and kinetic analysis. Arch Biochem Biophys. 501:23-30.

Gaucci E, Chichiarelli S, Grillo C, Del Vecchio E, Eufemi M, Turano C. 2008. The binding of antibiotics to ERP57/GRP58. J Antibiot. 61(6):400-402.

Gella A and Durany N. 2009. Oxidative stress in Alzheimer disease. Cell Adh Migr. 3(1):88-93.

Ghanem AA, Elewa A, Arafa LF. 2011. Pentosidine and N-carboxymethyl-lysine: biomarkers for type 2 diabetic retinopathy. Eur J Ophthalmol. 21(1):48-54.

Giacco F and Brownlee M. 2010. Oxidative stress and diabetic complications. Circ Res. 107(9):1058-1070.

Glenn JV and Stitt AW. 2009. The role of advanced glycation end products in retinal ageing and disease. Biochim Biophys Acta. 1790:1109-1116.

Graf E. 1992. Antioxidant potential of ferulic acid. Free Rad Biol Med. 13(4):435-448.

Golbidi S, Ebadi SA, Laher I. 2011. Antioxidants in the treatment of diabetes. Curr Diabetes Rev. 7(2):106-125.

Grillo C, Coppari S, Turano C, Altieri F. 2002. The DNA-binding activity of protein disulfide isomerase ERp57 is associated with the a´ domain. Biochem Biophys Res Comm. 295:67-73.

Grillo C, D´Ambrosio C, Consalvi V, Chiaraluce R, Scaloni A, Maceroni M, Eufemi M, Altieri F. 2007. DNA-binding activity of the ERp57 C-terminal domain is related to a redox-dependent conformational change. J Biol Chem. 282(14):10299-10310.

Grillo C, D´Ambrosio C, Scaloni A, Maceroni M, Merluzzi S, Turano C, Altieri F. 2006. Cooperative activity of Ref-1/APE and ERp57 in reductive activation of transcription factors. Free Radic Biol Med. 41:1113-1123.

Gugliucci A, Bastos DH, Schulze J, Souza MF. 2009. Caffeic and chlorogenic acids in *Ilex paraguariensis* extracts are the main inhibitors of AGE generation by methylglyoxal in model proteins. Fitoterapia. 80(6):339-344.

Guharay J, Sengupta B, Sengupta PK. 2001. Protein-flavonol interaction: Fluorescence spectroscopic study. Proteins. 43:75-81.

Guo GG, Patel K, Kumar V, Shah M, Fried VA, Etlinger JD, Sehgal PB. 2002. Association of the chaperone glucose-regulated protein 58 (GRP58/ER-60/ERp57) with Stat3 in cytosol and plasma membrane complexes. J Interferon Cytokine Res. 22(5):555-563.

Guo X, Zhang L, Sun X, Han X, Guo C, Kang P. 2009. Spectroscopic studies on the interaction between sodium ozagrel and bovine serum albumin. J Mol Struct. 928:114-120.

Habig WH, Pabst MJ, Jakoby WB. 1974. Glutathione S-transferase: the first enzymatic step in mercapturic acid formation. J Biol Chem. 249:7130-7139.

Halliwell B and Gutteridge JMC. 1998. Free radicals in biology and medicine. 3rd ed. Oxford University Press, Oxford. 851 p.

Harborne JB and Williams CA. 2000. Advances in flavonoid research since 1992. Phytochem. 55(6):481-504.

Harding JJ. 2007. Protein glycation and cataract: a conformational disease. In: Uversky VN, Fink AL (eds) Protein misfolding, aggregation, and conformational diseases. Part B: molecular mechanisms of conformational diseases, 1st ed. Springer Science, New York, pp 499-514.

Hashimoto T, Kumazawa S, Nanjo F, Hara Y, Nakayama T. 1999. Interaction of green tea catechins with lipid bilayers investigated with liposome systems. Biosci Biotechnol Biochem. 63(12):2252-2255.

Hatano T, Hori M, Hemingway RW, Yoshida T. 2003. Size exclusion chromatographic analysis of polyphenol-serum albumin complexes. Phytochem. 63(7):817-823.

He W, Li Y, Xue C, Hu Z, Chen X, Sheng F. 2005. Effect of Chinese medicine alpinetin on the structure of human serum albumin. Bioorg Med Chem. 13:1837-1845.

He T, Liang Q, Luo T, Wang Y, Luo G. 2010. Study on interactions of phenolic acid-like drug candidates with bovine serum albumin by capillary electrophoresis and fluorescence spectroscopy. J Solution Chem. 39: 1653-1664.

Hegde AH, Sandhya B, Seetharamappa J. 2011. Evaluation of binding and thermodynamic characteristics of interactions between a citrus flavonoid hesperitin with protein and effects of metal ions on binding. Mol Biol Rep. 38(8):4921-4929.

Herges T, Merlitz H, Wenzel W. 2002. Stochastic optimization metods for biomolecular structure prediction. In: Chakraborty T, Peeters F, Sivan U (eds). Nano-Physics & Bio-Electronics: A New Odyssey. Elsevier Science, Amsterdam, pp 281-303.

Herrero-Martínez JM, Sanmartin M, Rosés M, Bosch E, Ràfols C. 2005. Determination of dissociative constants of flavonoids by capillary electrophoresis. Electrophoresis. 26:1886-1895.

Hetz C, Russelakis-Carneiro M, Wälchli S, Carboni S, Vial-Knecht E, Maundrell K, Castilla J, Soto C. 2005. The disulfide isomerase Grp58 is a protective factor against prion neurotoxicity. J Neurosci. 25(11):2793-2802.

Ho S-C, Wu S-P, Lin S-M, Tang Y-L. 2010. Comparison of anti-glycation capacities of several herbal infusions with that of green tea. Food Chem. 122:768-774.

Hodgson JM and Croft KD. 2011. Tea flavonoids and cardiovascular health. Mol Aspects Med. 31(6):495-502.

Hu YJ, Chen CH, Zhou S, Bai AM, Ou-Yang Y. 2012. The specific binding of chlorogenic acid to human serum albumin. Mol Biol Rep. 39:2781-2787.

Hudson BI, Bucciarelli LG, Wendt T, Sakaguchi T, Lalla E, Qu W, Lu Y, Lee L, Stern DM, Naka Y, Ramasamy R, Yan SD, Yan SF, D'Agati V, Schmidt AM. 2003. Blockade of receptor for advanced glycation endproducts: a new target for therapeutic intervention in diabetic complications and inflammatory disorders. Arch Biochem Biophys. 419(1):80-88.

Hunt JV, Dean RT, Wolff SP. 1988. Hydroxyl radical production and autoxidative glycosylation. Glucose autoxidation as the cause of protein damage in the experimental glycation model of diabetes mellitus and ageing. Biochem J. 256(1):205-212.

Hwang SL, Shih PH, Yen GC. 2012. Neuroprotective effects of citrus flavonoids. J Agric Food Chem. 60(4):877-885.

Ishii T, Ichikawa T, Minoda K, Kusaka K, Ito S, Suzuki Y, Akagawa M, Mochizuki K, Goda T, Nakayama T. 2011. Human serum albumin as an antioxidant in the oxidation of (-)-epigallocatechin gallate: Participation of reversible covalent binding for interaction and stabilization. Biosci Biotechnol Biochem. 75(1):100-106.

Ishii T, Minoda K, Bae M-J, Mori T, Uekusa Y, Ichikawa T, Aihara Y, Furuta T, Wakimoto T, Kan T, Nakayama T. 2010a. Binding affinity of tea catechins for HSA: Characterization by high-performance affinity chromatography with immobilized albumin column. Mol Nutr Food Res. 54:816–822.

Ishii T, Mori T, Ichikawa T, Kaku M, Kusaka K, Uekusa Y, Akagawa M, Aihara Y, Furuta T, Wakimoto T, Kan T, Nakayama T. 2010b. Structural characteristics of green tea catechins for formation of protein carbonyl in human serum albumin. Bioorg Med Chem. 18: 4892-4896.

Ishii T, Mori T, Tanaka T, Mizuno D, Yamaji R, Kumazawa S, Nakayama T, Akagawa M. 2008. Covalent modification of proteins by green tea polyphenol (-)-epigallocatechin-3-gallate through autoxidation. Free Rad Biol Med. 45:1384–1394.

Izuhara Y, Miyata T, Ueda Y, Suzuki D, Asahi K, Inagi R, Sakai H, Kurokawa K. 1999. A sensitive and specific ELISA for plasma pentosidine. Nephrol Dial Transplant. 14:576-580.

Janebová M, Zima T, Tesař V. 1999. AGEs – produkty pokročilé glykace, advances glycation (glycosylation) end-products. Remedia. 9(2):94-103.

Jang DS, Lee GY, Lee YM, Kim YS, Sun H, Kim DH, Kim JS. 2009. Flavan-3-ols having a gamma-lactam from the roots of Actinidia arguta inhibit the formation of advanced glycation end products *in vitro*. Chem Pharm Bull. 57(4):397-400.

Jessop CE, Chakravarthi S, Garbi N, Hämmerling GJ, Lovell S, Bulleid NJ. 2007. ERp57 is essential for efficient folding of glycoproteins sharing common structural domains. EMBO J. 26:28-40.

Ji X, Tordova M, O'Donnell R, Parsons JF, Hayden JB, Gilliland, GL, Zimniak P. 1997. Structure and function of the xenobiotic substrate-binding site and location of a potential non substratebinding site in a class pi glutathione S-transferase. Biochemistry. 36:9690-9702.

Jiang D and Peterson DG. 2010. Role of hydroxycinnamic acids in food flavor: a brief overview. Phytochem Rev. 9(1):187-193.

Jiang M, Xie MX, Zheng D, Liu Y, Li XY, Chen X. 2004. Spectroscopic studies on the interaction of cinnamic acid and its hydroxyl derivatives with human serum albumin. J Mol Struct. 692:71-80.

Jomová K, Vondrakova D, Lawson M, Valko M. 2010. Metals, oxidative stress and neurodegenerative disorders. Mol Cell Biochem. 345:91-104.

Jono T, Nagai R, Lin X, Ahmed N, Thornalley PJ, Takeya M, Horiuchi S. 2004. Nepsilon (Carboxymethyl)lysine and 3-DG-imidazolone are major AGE structures in protein modification by 3-deoxyglucosone. J Biochem. 136(3):351-358.

Jung HA, Jung YJ, Yoon NY, Jeong DM, Bae HJ, Kim D-W, Na DH, Choi JS. 2008. Inhibitory effects of *Nelumbo nucifera* leaves on rat lens aldose reductase, advanced glycation endproducts formation, and oxidative stress. Food Chem Tox. 46:3818–3826.

Jurasekova Z, Marconi G, Sanchez-Cortes S, Torreggiani A. 2009. Spectroscopic and molecular modeling studies on the binding of the flavonoid luteolin and human serum albumin. Biopolymers. 91(11):917-927.

Kaku M and Nakagawa K. 2009. (+)-Catechin with Cu^{2+} induces protein modifications via reactive oxygen species-independent pathway. J Health Sci. 55(3):441-446.

Kaldas MI, Walle UK, van der Woude H, McMillan JM, Walle T. 2005. Covalent binding of the flavonoid quercetin to human serum albumin. J Agric Food Chem. 53:4194-4197.

Kanakis CD, Tarantilis PA, Polissiou MG, Diamantoglou S, Tajmir-Riahi HA. 2006. Antioxidant flavonoids bind human serum albumin. J Mol Struct. 798:69-74.

Kang JH. 2006. Oxidative modification of human ceruloplasmin by methylglyoxal: an *in vitro* study. J Biochem Mol Biol. 39:335-338.

Kang J, Liua Y, Xie M-X, Lia S, Jiang M, Wang Y-D. 2004. Interactions of human serum albumin with chlorogenic acid and ferulic acid. Biochim Biophys Acta. 1674:205-214.

Katwal AB and Dokun AO. 2011. Peripheral arterial disease in diabetes: is there a role for genetics? Curr Diab Rep. 11(3):218-225.

Kawai M, Hirano T, Higa S, Arimitsu J, Maruta M, Kuwahara Y, Ohkawara T, Hagihara K, Yamadori T, Shima Y, Ogata A, Kawase I, Tanaka T. 2007. Flavonoids and related compounds as anti-allergic substances. Allergol Int. 56(2):113-123.

Kelly FJ. 2004. Dietary antioxidants and environmental stress. Proc Nutr Soc. 63:579-585.

Khan N and Mukhtar H. 2007. Tea polyphenols for health promotion. Life Sci. 81:519-533.

Khanal RC and Nemere I 2007. The ERp57/GRp58/1,25D3-MARRS receptor: multiple functional roles in diverse cell systems. Curr Med Chem. 14(10):1087-1093.

Kim J, Jeong IH, Kim CS, Lee YM, Kim JM, Kim JS. 2011. Chlorogenic acid inhibits the formation of advanced glycation end products and associated protein cross-linking. Arch Pharm Res. 34(3):495-500.

Klaunig JE, Kamendulis LM, Hocevar BA. 2010. Oxidative stress and oxidative damage in carcinogenesis. Toxicol Pathol. 38:96-109.

Kondo T, Hirose M, Kageyama K. 2009. Role sof oxidative stress and redox regulation in atherosclerosis. J Atheroscler Thromb. 16:532-538.

Kozlov G, Maattanen P, Schrag JD, Pollock S, Cygler M, Nagar B, Thomas DY, Gehring K. 2006. Crystal structure of the *bb*' domains of the protein disulfide isomerase ERp57. Structure. 14(8):1331-1339.

Kusuda M, Hatano T, Yoshida T. 2006. Water-soluble complexes formed by natural polyphenols and bovine serum albumin: evidence from gel electrophoresis. Biosci Biotechnol Biochem. 70(1):152-160.

Laemmli UK. 1970. Cleavage of structural proteins during the assembly of the head of bacteriophage T4. Nature. 227:680-685.

Lakowicz JR. 2006. Principles of Fluorescence Spectroscopy, 3rd ed. Springer, New York, 953 p.

Lambert JD and Elias RJ. 2010. The antioxidant and pro-oxidant activities of green tea polyphenols: A role in cancer prevention. Arch Biochem Biophys. 501:65-72.

Lapolla A, Flamini R, Dalla Vedova A, Senesi A, Reitano R, Fedele D, Basso E, Seraglia R, Traldi P. 2003. Glyoxal and methylglyoxal levels in diabetic patients: quantitative determination by a new GC/MS method. Clin Chem Lab Med. 41(9):1166-1173.

Lapshina EA, Sudnikovich EJ, Maksimchik JZ, Zabrodskaya SV, Zavodnik LB, Kubyshin VL, Nocun M, Kazmierczak P, Dobaczewski M, Watala C, Zavodnik IB. 2006. Antioxidative enzyme and glutathione S-transferase activities in diabetic rats exposed to long-term ASA treatment. Life Sci. 79:1804-1811.

Lee BS, Jayathilaka GD, Huang JS, Vida LN, Honig GR, Gupta S. 2011. Analyses of *in vitro* nonenzymatic glycation of normal and variant hemoglobins by maldi-tof mass spectrometry. J Biomol Tech. 22(3):90-94.

Lee YS, Kang YH, Jung JY, Lee S, Ohuchi K, Shin KH, Kang IJ, Park JH, Shin HK, Lim SS. 2008. Protein glycation inhibitors from the fruiting body of *Phellinus linteus*. Biol Pharm Bull. 31(10):1968-1972.

Li B, Zhang Z, ZhaoL. 2002. Flow-injection chemiluminescence detection for studying protein binding for drug with ultrafiltration sampling. Anal Chim Acta. 468:65-70.

Li D, Zhu J, Jin J, Yao X. 2007a. Studies on the binding of nevadensin to human serum albumin by molecular spectroscopy and modeling. J Mol Struct. 846(1-3):34-41.

Li J, Ren C, Zhang Y, Liu X, Yao X, Hu Z. 2008. Spectroscopic studies on binding of Puerarin to human serum albumin. J Mol Struct. 885:64-69.

Li S, Huang K, Zhong M, Guo J, Wang WZ, Zhu R. 2010. Comparative studies on the interaction of caffeic acid, chlorogenic acid and ferulic acid with bovine serum albumin. Spectrochim Acta A Mol Biomol Spectrosc. 77(3):680-686.

Li Y, He W, Liu H, Yao X, Hu Z. 2007b. Daidzein interaction with human serum albumin studied using optical spectroscopy and molecular modeling methods. J Mol Struct. 831:144-150.

Lim K, Ho JX, Keeling K, Gilliland GL, Ji X, Rüker F, Carter DC. 1994. Three-dimensional structure of *Schistosoma japonicum* glutathione S-transferase fused with a six-amino acid conserved neutralizing epitope of gp41 from HIV. Protein Sci. 3:2233-2244.

Liu E-Hu, Qi L-W, Li P. 2010. Structural relationship and binding mechanisms of five flavonoids with bovine serum albumin. Molecules. 15:9092-9103.

Liu Y, Xie M-X, Li S, Jiang M, Wang YD. 2005. Spectroscopic investigation of the interaction between human serum albumin and three organic acids. Spectrochim Acta Part A. 61:2245-2251.

Lo CY, Li S, Tan D, Pan MH, Sang S, Ho CT. 2006. Trapping reactions of reactive carbonyl species with tea polyphenols in simulated physiological conditions. Mol Nutr Food Res. 50(12):1118-1128.

Lu N, Chen P, Yang Q, Peng YY. 2011. Anti- and pro-oxidant effects of (+)-catechin on hemoglobin-induced protein oxidative damage. Toxicol In Vitro. 25(4):833-838.

Lunceford N and Gugliucci A. 2005. *Ilex paraguariensis* extracts inhibit AGE formation more efficiently than green tea. Fitoterapia. 76(5):419-427.

Lv L, Shao X, Chen H, Ho CT, Sang S. 2011. Genistein inhibits advanced glycation end product formation by trapping methylglyoxal. Chem Res Toxicol. 24(4):579-586.

Lyons TJ. 1995. Glycation, oxidation, and glycoxidation reactions in the development of diabetic complications. Contrib Nephrol. 112:1-10.

Maattanen P, Kozlov G, Gehring K, Thomas DY. 2006. ERp57 and PDI: multifunctional PDIs with similar domain architectures but differing substrate-partner associations. Biochem Cell Biol. 84:881-889.

Mahesha HG, Singh SA, Srinivasan N, Rao AGA. 2006. A spectroscopic study of the interaction of isoflavones with human serum albumin. FEBS J. 273:451-467.

Maiti TK, Ghosh KS, Dasgupta S. 2006. Interaction of (-)-epigallocatechin-3-gallate with human serum albumin: fluorescence, Fourier transform infrared, circular dichroism, and docking studies. Proteins. 64:355-362.

Mannervik B and Danielson UH. 1988. Glutathione transferases - structure and atalitic activity. Crit Rev Biochem. 23:283-337.

Martin JL, Kenna JG, Martin BM, Thomassen D, Reed GF, Pohl LR. 1993. Halothane hepatitis patients have serum antibodies that react with protein disulfide isomerase. Hepatology. 18(4):858-863.

Martini LA, Catania AS, Ferreira SR. 2010. Role of vitamins and minerals in prevention and management of type 2 diabetes mellitus. Nutr Rev. 68(6):341-354.

Martínez A, Portero-Otin M, Pamplona R, Ferrer I. 2010. Protein targets of oxidative damage in human neurodegenerative diseases with abnormal protein aggregates. Brain Pathol. 20(2):281-297.

Matei I and Hillebrand M. 2010. Interaction of kaempferol with human serum albumin: a fluorescence and circular dichroism study. J Pharm Biomed Anal. 51(3):768-773.

Matsumoto K, Sano H, Nagai R, Suzuki H, Kodama T, Yoshida M, Ueda S, Smedsrød B, Horiuchi S. 2000. Endocytic uptake of advanced glycation end products by mouse liver sinusoidal endothelial cells is mediated by a scavenger receptor distinct from the macrophage scavenger receptor class A. Biochem J. 352:233-240.

McLellan AC, Thornalley PJ, Benn J, Sonksen PH. 1994. Glyoxalase system in clinical diabetes mellitus and correlation with diabetic complications. Clin Sci. 87:21-29.

Mercer N, Ahmed H, McCarthy AD, Etcheverry SB, Vasta GR, Cortizo AM. 2004. AGE-R3/galectin-3 expression in osteoblast-like cells: regulation by AGEs. Mol Cell Biochem. 266(1-2):17-24.

Mikulíková K, Eckhardt A, Kunes J, Zicha J, Mikšík I. 2008. Advanced glycation end-product pentosidine accumulates in various tissues of rats with high fructose intake. Physiol. Res. 57:89-94.

Mikulíková K, Eckhardt A, Pataridis S, Mikšík I. 2007. Study of posttranslational non-enzymatic modifications of collagen using capillary electrophoresis/mass spectrometry and high performance liquid chromatography/mass spectrometry. J Chromatogr A. 1155(2):125-133.

Mikulíková K, Mikšík I, Deyl Z. 2005. Non-enzymatic posttranslational modifications of bovine serum albumin by oxo-compounds investigated by chromatographic and electrophoretic methods. J Chromatogr B Analyt Technol Biomed Life Sci. 815(1-2):315-331.

Min J, Meng-Xia X, Dong Z, Yuan L, Xiao-Yu L, Xing C. 2004. Spectroscopic studies on the interaction of cinnamic acid and its hydroxyl derivatives with human serum albumin. J Mol Struct. 692:71-80.

Minoda K, Ichikawa T, Katsumata T, Onobori K-i, Mori T, Suzuki Y, Ishii T, Nakayama. 2010. Influence of the galloyl moiety in tea catechins on binding affinity for human serum albumin. J Nutr Sci Vitaminol. 56:331-334.

Mochizuki M, Yamazaki S, Kano K, Ikeda T. 2002. Kinetic analysis and mechanistic aspects of autoxidation of catechins. Biochim Biophys Acta. 1569:35-44.

Monnier VM. 1989. Toward a Maillard reaction theory of aging. Prog Clin Biol Res. 304:1-22.

Moreira PI, Smith MA, Zhu X, Nunomura A, Castellani RJ, Perry G. 2005. Oxidative stress and neurodegeneration. Ann N Y Acad Sci. 1043:545-552.

Morimitsu Y, Yoshida K, Esaki S, Hirota A. 1995. Protein glycation inhibitors from thyme (*Thymus vulgaris*). Biosci Biotechnol Biochem. 59(11):2018-2021.

Muralidhara BK and Prakash V. 1995. Interaction of 3'-O-caffeoyl D-quinic acid with human serum albumin. Int J Pept Protein Res. 46(1):1-8.

Muthenna P, Akileshwari C, Saraswat M, Bhanuprakash Reddy G. 2011. Inhibition of advanced glycation end-product formation on eye lens protein by rutin. Br J Nutr. 25:1-9.

Muzolf M, Szymusiak H, Gliszczyńska-Świgło A, Rietjens IMCM, Tyrakowska B. 2008. pH-Dependent radical scavenging capacity of green tea catechins. J Agric Food Chem. 56:816-823.

Müller C, Hemmersbach S, van't Slot G, Hofmann T. 2006. Synthesis and structure determination of covalent conjugates formed from the sulfury−roasty-smelling 2-

furfurylthiol and di- or trihydroxybenzenes and their identification in coffee brew. J Agric Food Chem. 54(26):10076-10085.

Nagai R, Fujiwara Y, Mera K, Yamagata K, Sakashita N, Takeya M. 2008. Immunochemical detection of Nepsilon-(carboxyethyl)lysine using a specific antibody. J Immunol Methods. 332(1-2):112-120.

Nagai R, Matsumoto K, Ling X, Suzuki H, Araki T, Horiuchi S. 2000. Glycolaldehyde, a reactive intermediate for advanced glycation end products, plays an important role in the generation of an active ligand for the macrophage scavenger receptor. Diabetes. 49:1714-1723.

Nakagawa T, Yokozawa T, Terasawa K, Shu S, Juneja LR. 2002. Protective activity of green tea against free radical- and glucose-mediated protein damage. J Agric Food Chem. 50(8):2418-2422.

Nass N, Barting B, Navarrete Santos A, Sccheubel RJ, Börgermann J, Silber RE, Simm A. 2007. Advanced glycation end products, diabetes and aging. Z Gerontol Geriat. 40:349–356.

Natarajan K, Singh S, Burke TR, Grunberger D, Aggarwal BB. 1996. Caffeic acid phenethyl ester is a potent and specific inhibitor of activation of nuclear transcription factor NF-kappa B. Proc Nat Acad Sci USA. 93(17):9090-9095.

Natella F, Nardini M, Di Felice M, Scaccini CJ. 1999. Benzoic and cinnamic acid derivatives as antioxidants: Structure-activity relation. J Agric Food Chem. 47(4):1453-1459.

Nebert DW and Vasiliou V. 2004. Analysis of the glutatione S-transferase (GST) gene family. Hum Genomics 1:460-464.

Ni Y, Shuangshuang Wang S, Kokot S. 2010. Spectrometric study of the interaction between alpinetin and bovine serum albumin using chemometrics approaches. Anal Chim Acta. 663:139-146.

Ni Y, Zhang X, Kokot S. 2009. Spectrometric and voltammetric studies of the interaction between quercetin and bovine serum albumin using warfarin as site marker with the aid of chemometrics. Spectrochim Acta A Mol Biomol Spectrosc. 71(5):1865-1872.

Nicolle E, Souard F, Faure P, Boumendjel A. 2011. Flavonoids as promising lead compounds in type 2 diabetes mellitus: molecules of interest and structure-activity relationship. Curr Med Chem. 18(17):2661-2672.

Niwa T. 1999. 3-Deoxyglucosone: metabolism, analysis, biological activity, and clinical implication. J Chrom B: Biomed Sci Appl. 731(1):23-36.

Nozaki A, Hori M, Kimura T, Ito H, Hatano T. 2009. Interaction of polyphenols with proteins: Binding of (-)-epigallocatechin gallate to serum albumin, estimated by induced circular dichroism. Chem Pharm Bull. 57(2):224-228.

Nursten H. 2005. The Maillard reation: Chemistry, biochemistry and implications. 1st ed. Cambridge: The Royal Society of Chemistry, Great Britain. 214 p.

Oliver JD, van der Wal FJ, Bulleid NJ, High S. 1997. Interaction of the thiol-dependent reductase ERp57 with nascent glycoproteins. Science. 275:86-88.

Omran AA, El-Sayed AA, Shehata A. 2011. Binding of benzodiazepine drugs to bovine serum albumin: a second derivative spectrophotometric study. Spectrochim Acta A Mol Biomol Spectrosc. 83(1):362-367.

Ornstein L: Disc electrophoresis. 1964. I. Background and theory. Ann NY Acad Sci. 121:321-349.

Otagiri M. 2005. A molecular functional study on the interactions of drugs with plasma proteins. Drug Metab Pharmacokinet. 20(5):309-323.

Pan JS, Hong M-Z, Ren J-L. 2009. Reactive oxygen species: A double-edged sword in oncogenesis. World J Gastroenterol. 15(14):1702-1707.

Pannala AS, Razaq R, Halliwell B, Singh S, Rice-Evans CA. 1998. Inhibition of peroxynitrite dependent tyrosine nitration by hydroxycinnamates: Nitration or electron donation? Free Rad Biol Med. 24(4):594-606.

Papadopoulou A, Green RJ, Frazier RA. 2005. Interaction of flavonoids with bovine serum albumin: A fluorescence quenching study. J Agric Food Chem. 53:158-163.

Pastore RL and Fratellone P. 2006. Potential health benefits of green tea (*Camellia sinensis*): A narrative review. Explore. 2(6):531-539.

Peaper DR, Wearsch PA, Cresswell P. 2005. Tapasin and ERp57 form a stable disulfide-linked dimer within the MHC class I peptide-loading complex**.** EMBO J. 24:3613-3623.

Peng M, Shi S, Zhang Y. 2012. Influence of Cd^{2+}, Hg^{2+} and Pb^{2+} on (+)-catechin binding to bovine serum albumin studied by fluorescence spectroscopic methods. Spectrochim Acta A Mol Biomol Spectrosc. 85(1):190-197.

Peng X, Zheng Z, Cheng K-W, Shan F, Ren G-X, Chen F, Wang M. 2008. Inhibitory effect of mung bean extract and its constituents vitexin and isovitexin on the formation of advanced glycation endproducts. Food Chem. 106:475-481.

Peters T. 1996. All About Albumin: Biochemistry, genetics, and medical applications, Academic Press, San Diego(CA). 435 p.

Petlevski R, Hadzija M, Slijepcević M, Juretić D, Petrik J. 2003. Glutathione S-transferases and malondialdehyde in the liver of NOD mice on short-term treatment with plant mixture extract P-9801091. Phytother Res. 17:311-314.

Petrovic R, Futas J, Chandoga J, Jakus V. 2005. Rapid and simple method for determination of Nepsilon-(carboxymethyl)lysine and Nepsilon-(carboxyethyl)lysine in urine using gas chromatography/mass spectrometry. Biomed Chromatogr. 19(9):649-654.

Pietta PG. 2000. Flavonoids as antioxidants. J Nat Prod. 63:1035-1042.

Pinzur MS. 2011. Diabetic peripheral neuropathy. Foot Ankle Clin. 16(2):345-349.

Portero-Otin M, Nagaraj RH, Monnier VM. 1995. Chromatographic evidence for pyrraline formation during protein glycation *in vitro* and *in vivo*. Biochim Biophys Acta. 1247(1):74-80.

Prigent SVE, Gruppen H, Visser AJWG, van Koningsveld GA, de Jong GAH, Voragen AGJ. 2003. Effects of non-covalent interactions with 5-O-caffeoylquinic acid (chlorogenic acid) on the heat denaturation and solubility of globular proteins. J Agric Food Chem. 51(17):5088-5095.

Procházková D, Boušová I, Wilhelmová N. 2011. Antioxidant and prooxidant properties of flavonoids. Fitoterapia. 82(4):513-523.

Qi Z-d, Zhang Y, Liao F-l, Ou-Yang Y-w, Liu Y, Yang X. 2008. Probing the binding of morin to human serum albumin by optical spectroscopy. J Pharm Biomed Anal. 46:699–706.

Rahimi R, Nikfar S, Larijani B, Abdollahi M. 2005. A review on the role of antioxidants in the management of diabetes and its complications. Biomed Pharmacother. 59(7):365-373.

Rathee P, Chaudhary H, Rathee S, Rathee D, Kumar V, Kohli K. 2009. Mechanism of action of flavonoids as anti-inflammatory agents: a review. Inflamm Allergy Drug Targets. 8(3):229-235.

Raturi A and Mutus B. 2007. Characterization of redox state and reductase activity of protein disulfide isomerase under different redox environments using a sensitive fluorescent assay. Free Rad Biol Med. 43:62-70.

Rawel HM, Frey SK, Meidtner K, Kroll J, Schweigert FJ. 2006. Determining the binding affinities of phenolic compounds to proteins by quenching of the intrinsic tryptophan fluorescence. Mol Nutr Food Res. 50:705-713.

Rawel HM, Meidtner K, Kroll J. 2005. Binding of selected phenolic compounds to proteins. J Agric Food Chem. 53:4228-4235.

Rawel HM, Rohn S, Kruse H-P, Kroll J. 2002. Structural changes induced in bovine serum albumin by covalent attachment of chlorogenic acid. Food Chem. 78:443-455.

Raza H, Ahmed I, John A. 2004. Tissue specific expression and immunohistochemical localization of glutathione S-transferase in streptozocin induced diabetic rats: modulation by *Momordica charantia* (karela) extract. Life Sci .74:1503-1511.

Rice-Evans CA, Miller NJ, Paganga G. 1996. Structure-antioxidant activity relationships of flavonoids and phenolic acids. Free Rad Biol Med. 20(7):933-956.

Rice-Evans CA, Miller N, Paganga G. 1997. Antioxidant properties of phenolic compounds. Trends Plant Sci. 2(4):152-159.

Ristow M. 2004. Neurodegenerative disorders associated with diabetes mellitus. J Mol Med. 82(8):510-529.

Roginsky V and Alegria AE. 2005. Oxidation of tea extracts and tea catechins by molecular oxygen. J Agric Food Chem. 53:4529-4535.

Romano AD, Serviddio G, de Matthaeis A, Bellanti F, Vendemiale G. 2010. Oxidative stress and aging. J Nephrol. 23(15):S29-S36.

Rudnicki M, de Oliveira MR, da Veiga Pereira T, Reginatto FH, Dal-Pizzol F, Fonseca Moreira JC. 2007. Antioxidant and antiglycation properties of *Passiflora alata* and *Passiflora edulis* extracts. Food Chem. 100(2):719-724.

Saito-Yamanaka N, Yamanaka H, Nagasawa S. 1993. Glutathione-related detoxication functions in streptozocin-induced diabetic rats. J Vet Med Sci. 55:991-994.

Sang S, Lee M-J, Hou Z, Ho C-T, Yang CS. 2005. Stability of tea polyphenol (-)-epigallocatechin-3-gallate and formation of dimers and epimers under common experimental conditions. J Agric Food Chem. 53:9478-9484.

Sang S, Shao X, Bai N, Lo CY, Yang CS, Ho CT. 2007. Tea polyphenol (-)-epigallocatechin-3-gallate: a new trapping agent of reactive dicarbonyl species. Chem Res Toxicol. 20(12):1862-1870.

Sato T, Iwaki M, Shimogaito N, Wu X, Yamagishi S, Takeuchi M. 2006a. TAGE (toxic AGEs) theory in diabetic complications. Curr Mol Med. 6(3):351-358.

Sato T, Shimogaito N, Wu X, Kikuchi S, Yamagishi S, Takeuchi M. 2006b. Toxic advanced glycation end products (TAGE) theory in Alzheimer's disease. Am J Alzheimers Dis Other Demen. 21(3):197-208.

Schalkwijk CG, Stehouwer CD, van Hinsbergh VW. 2004. Fructose-mediated non-enzymatic glycation: sweet coupling or bad modification. Diabetes Metab Res Rev. 20(5):369-382.

Scheijen JLJM, van deWaarenburg MPH, Stehouwer CDA, Schalkwijk CG. 2009. Measurement of pentosidine in human plasma protein by a single-column high-performance liquid chromatography method with fluorescence detection. J Chrom B. 877:610–614.

Schmalhausen EV, Zhlobek EB, Shalova IN, Firuzi O, Saso L, Muronetz VI. 2007. Antioxidant and prooxidant effects of quercetin on glyceraldehyde-3-phosphate dehydrogenase. Food Chem Toxicol. 45(10):1988-1993.

Schmitt A, Schmitt J, Münch G, Gasic-Milencovic J. 2005. Characterization of advanced glycation end products for biochemical studies: side chain modifications and fluorescence characteristics. Anal Biochem. 338(2):201-215.

Schröder P and Krutmann J. 2005. Environmental oxidative stress - Environmental sources of ROS. In: Grune T (ed) The Handbook of Environmental Chemistry, 1st ed. Springer, Heidelberg, pp 645-820.

Seidler NW. 2005. Carbonyl-induced enzyme inhibition: mechanism and new perspectives. Curr Enzyme Inhib. 1:21-27.

Seidler NW and Kowalewski C. 2003. Methylglyoxal-induced glycation affects protein topography. Arch Biochem Biophys. 410(1):149-154.

Seidler NW and Seibel I. 2000. Glycation of aspartate aminotransferase and conformational flexibility. Biochem Biophys Res Commun. 277(1):47-50.

Seifert A, Rawel HM, Harding SE, Kroll J. 2004. Characterization of bovine serum albumin/chlorogenic acid solution mixtures by analytical ultracentrifugation. Progr Colloid Polym Sci. 127:83-88.

Seliger B, Wollscheid U, Momburg F, Blankenstein T, Huber C. 2001. Characterization of the major histocompatibility complex class I deficiencies in B16 melanoma cells. Cancer Res. 61:1095-1099.

Sell DR, Nagaraj RH, Grandhee SK, Odetti P, Lapolla A, Fogarty J, Monnier VM. 1991. Pentosidine: a molecular marker for the cumulative damage to proteins in diabetes, aging, and uremia. Diabetes Metab Rev. 7(4):239-251.

Sentchouk VV and Bondaryuk EV. 2007. Fluorescent analysis of interation of flavonols with hemoglobin and bovine serum albumin. J Appl Spectrosc. 74(5):731-737.

Shang L, Jiang X, Dong S. 2006. *In vitro* study on the binding of neutral red to bovine serum albumin by molecular spectroscopy. J Photochem Photobiol A. 184(1-2):93-97.

Sharangi AB. 2009. Medical and therapeutic potentialities of tea (*Camellia sinensis* L.) – A review. Food Res Int. 42:529-535.

Sheehan D, Meade G, Foley VM, Dowd CA. 2001. Structure, function and evolution of glutathione transferases: implications for classification of non-mammalian members of an ancient enzyme superfamily. Biochem J. 360:1-16.

Shi S, Zhang Y, Chen X, Peng M. 2011. Investigation of flavonoids bearing different substituents on ring C and their Cu^{2+} complex binding with bovine serum albumin: structure-affinity relationship aspects. J Agric Food Chem. 59(19):10761-10769.

Silvennoinen L, Myllyharju J, Ruoppolo M, Orrù S, Caterino M, Kivirikko KI, Koivunen P. 2004. Identification and characterization of structural domains of human ERp57. J Biol Chem. 279(14):13607-13615.

Simm A, Wagner J, Gursinsky T, Nass N, Friedrich I, Schinzel R, Czeslik E, Silber RE, Scheubel RJ. 2007. Advanced glycation endproducts: a biomarker for age as an outcome predictor after cardiac surgery? Exp Gerontol. 42:668-675.

Singh R, Akhtar N, Haqqi TM. 2010. Green tea polyphenol epigallocatechin-3-gallate: Inflamation and arthritis. Life Sci. 86:907-918.

Singh R, Barden A, Mori T, Beilin L. 2001. Advanced glycation end-products: a review. Diabetologia. 44(2):129-46.

Singh TS and Mitra S. 2011. Interaction of cinnamic acid derivatives with serum albumins: a fluorescence spectroscopic study. Spectrochim Acta A Mol Biomol Spectrosc. 78(3):942-948.

Soares S, Mateus N, de Freitas V. 2007. Interaction of different polyphenols with bovine serum albumin (BSA) and human salivary α-amylase (HSA) by fluorescence quenching. J Agric Food Chem. 55:6726-6735.

Song JM and Seong BL. 2007. Tea catechins as a potential alternative anti-infectious agent. Expert Rev. Anti Infect Ther. 5(3):497-506.

Srey C, Haughey SA, Connolly L, del Castillo MD, Ames JM, Elliott CT. 2010. Immunochemical and mass spectrometric analysis of *N*-*ε*-(carboxymethyl)lysine content of AGE-BSA systems prepared with and without selected antiglycation agents. J Agric Food Chem. 58(22):11955-11961.

Sun Y, Hung W-C, Chen F-Y, Lee C-C, Huang HW. 2009. Interaction of tea catechin (-)-epigallocatechin gallate with lipid bilayers. Biophys J. 96:1026-1035.

Stadtman ER. 2004. Role of oxidant species in aging. Curr Med Chem. 11:1105-1112.

Stadtman ER and Levine RL. 2000. Protein oxidation. Ann NY Acad Sci. 899:191-208.

Stadtman ER and Levine RL. 2003. Free radical-mediated oxidation of free amino acids and amino acid residues in proteins. Amino Acids. 25:207-218.

Steinbrecher UP. 1987. Oxidation of human low density lipoprotein results in derivatization of lysine residues of apolipoprotein B by lipid peroxide decomposition products. J Biol Chem. 262:321-349.

Stote KS and Baer DJ. 2008. Tea comsuption may improve biomarkers of insulin sensitivity and risk factor for diabetes. J Nutr. 138:1584S–1588S.

Stuchbury G and Münch G. 2005. Alzheimer's associated inflammation, potential drug targets and future therapies. J Neural Transm. 112(3):429-453.

Suarez G, Rajaram R, Oronsky Al, Gawinowicz MA. 1989. Nonenzymatic glycation of bovine serum albumin by fructose (fructation). Comparison with the Maillard reaction initiated by glucose. J Biol Chem. 264(7): 3674-3679.

Sztanke K and Pasternak K. 2003. The Maillard reaction inhibitors and their biological and therapeutic significance. Ann Univ Mariae Curie Sklodowska Med. 58(2):156-158.

Štípek S, Borovanský J, Čejková J, Homolka J, Klener P, Lukáš M, Špičák J, Tesař V, Zeman M, Zima T, Žák A. 2000. Antioxidants and Free Radicals in Health and Disease. 1st ed. Grada Publishing, Prague. 320 p.

Tajmir-Riahi HA. 2007. An overview of drug binding to human serum albumin: protein folding and unfolding. Scientia Iranica. 14(2):87-95.

Tanaka T, Ishii T, Mizuno D, Mori T, Yamaji R, Nakamura Y, Kumazawa S, Nakayama T, Akagawa M. 2011. (-)-Epigallocatechin-3-gallate suppresses growth of AZ521 human gastric cancer cells by targeting the DEAD box RNA helicase p68. Free Rad Biol Med. 50(10):1324-1335.

Taneda S and Monnier VM. 1994. ELISA of pentosidine, an advanced glycation end product, in biological specimens. Clin Chem. 40(9):1766-1773.

Tang D, Li H-J, Wen X-D, Qian Z-M. 2008a. Interaction of bioactive components caffeoylquinic acid derivatives in Chinese medicines with bovine serum albumin. Chem Pharm Bull. 56(3):360-365.

Tang J, Lian N, He X, Zhang G. 2008b. Investigation of the interaction between sophoricoside and human serum albumin by optical spectroscopy and molecular modeling methods. J Mol Struct. 889:408-414.

Tarwadi KV and Agte VV. 2011. Effect of micronutrients on methylglyoxal-mediated *in vitro* glycation of albumin. Biol Trace Elem Res. 143(2):717-725.

Thielecke F and Boschmann M. 2009. The potential role of green tea catechins in the prevention of the metabolit syndrome - A review. Phytochem. 70:11–24.

Thomas H, Schladt L, Knehr M, Oesch F. 1989. Effect of diabetes and starvation on the activity of rat liver epoxide hydrolases, glutathione S-transferases and peroxisomal beta-oxidation. Biochem Pharmacol. 38:4291-4297.

Thornalley PJ. 1996. Pharmacology of methylglyoxal: formation, modification of proteins and nucleic acids, and enzymatic detoxification - a role in pathogenesis and antiproliferative chemotherapy. Gen Pharmacol. 27:565-573.

Thornalley PJ. 2003. Use of aminoguanidine (Pimagedine) to prevent the formation of advanced glycation endproducts. Arch Biochem Biophys. 419(1):31-40.

Thornalley PJ, Langborg A, Harjit S. 1999. Formation of glyoxal, methylglyoxal and 3-deoxyglucosone in the glycation of proteins by glucose. Biochem J. 344:109-116.

Tian J, Liu J, Hu Z, Chen X. 2005. Interaction of wogonin with bovine serum albumin. Bioorg Med Chem. 13:4124-4129.

Tian J, Liu J, Xie J, Yao X, Hu Z, Chen X. 2004a. Binding of wogonin to human serum albumin: a common binding site of wogonin in subdomain IIA. J Photochem Photobiol B. 74(1):39-45.

Tian J, Liu J, Tian X, Hu Z, Chen X. 2004b. Study of the interaction of kaempferol with bovine serum albumin. J Mol Struct. 691:197-202.

Tian J, Zhao Y, Liu X, Zhao S. 2009. A steady-state and time-resolved fluorescence, circular dichroism study on the binding of myricetin to bovine serum albumin. Luminiscence. 24:386-393.

Towbin H, Stachlin T, Gordon J. 1979. Electrophoretic transfer of proteins from polyacrylamide gels to nitrocellulose sheets: procedure and some applications. Proc Natl Acad Sci USA. 76:4350-4354.

Tsuji-Naito K, Saeki H, Hamano M. 2009. Inhibitory effects of *Chrysanthemum* species extracts on formation of advanced glycation end products. Food Chem. 116:854–859.

Turano C, Coppari S, Altieri F, Ferraro A. 2002. Proteins of the PDI family: unpredicted non-ER locations and functions. J Cell Physiol. 193:154–163.

Uetrecht JP and Trager W. 2007. Drug metabolism: chemical and enzymatic aspects. 1st ed. Informa Healthcare, New York. 200 p.

Ulrich P and Cerami A. 2001. Protein glycation, diabetes, and aging. Recent Prog Horm Res. 56:1-21.

Urade R, Okudo H, Kato H, Moriyama T, Arakaki Y. 2004. ER-60 domains responsible for interaction with calnexin and calreticulin. Biochemistry. 43(27):8858-8868.

Urios P, Grigorova-Borsos AM, Sternberg M. 2007. Flavonoids inhibit the formation of the cross-linking AGE pentosidine in collagen incubated with glucose, according to their structure. Eur J Nutr. 46(3):139-146.

van Bladeren PJ. 2000. Glutathione conjugation as a bioactivation reaction. Chem Biol Interact. 129:61-76.

Vasan S, Zhang X, Zhang X, Kapurniotu A, Bernhagen J, Teichberg S, Basgen J, Wagle D, Shih D, Terlecky I, Bucala R, Cerami A, Egan J, Ulrich P. 1996. An agent cleaving glucose-derived protein crosslinks *in vitro* and *in vivo*. Nature. 382(6588):275-278.

Varshney A, Sen P, Ahmad E, Rehan M, Subbarao N, Khan RH. 2010. Ligand binding strategies of human serum albumin: how can the cargo be utilized? Chirality. 22(1):77-87.

Velayutham P, Babu A, Liu D. 2008. Green tea catechins and cardiovascular health: an update. Curr Med Chem. 15(18):1840-1850.

Verzijl N, DeGroot J, Oldehinkel E, Bank RA, Thorpe SR, Baynes JW, Bayliss MT, Bijlsma JW, Lafeber FP, Tekoppele JM. 2000. Age-related accumulation of Maillard reaction products in human articular cartilage collagen. Biochem J. 350(2):381-387.

Vetter SW and Indurthi VS. 2011. Moderate glycation of serum albumin affects folding, stability, and ligand binding. Clin Chim Acta. 412(23-24):2105-2116.

Vivian JT and Callis PR. 2001. Mechanisms of tryptophan fluorescence shifts in proteins. Biophys J. 80:2093-2109.

Vlassara H. 1997. Recent progress in advanced glycation end products and diabetic complications. Diabetes. 46(Suppl 2):S19-S25.

Wang C, Chen S, Wang X, Wang L, Wallis AK, Freedman RB, Wang C-C. 2010. Plasticity of human protein disulfide isomerase. J Biol Chem. 285(35):26788-26797.

Wang J, Sun B, Cao Y, Tian Y. 2009. Protein glycation inhibitory activity of wheat bran feruloyl oligosaccharides. Food Chem. 112(2):350-353.

Wang T, Zhao Z, Zhang L, Ji L. 2009. Spectroscopic studies on the interaction between troxerutin and bovine serum albumin. J Mol Struct. 937(1-3):65-69.

Wang Y, Zhang T, Xu J, Du W. 2011. Comparison of the binding affinity of chlorogenic acid with two serum albumins. Int J Biol Macromol. 48(1):81-86.

Wearsch PA and Cresswell P. 2008. The quality control of MHC class I peptide loading. Curr Opin Cell Biol. 20(6):624–631.

West IC. 2000. Radicals and oxidative stress in diabetes. Diabetic Medicine. 17:171-180.

Westwood ME and Thornalley PJ. 1995. Molecular characteristics of methylglyoxal-modified bovine and human serum albumins. Comparison with glucose-derived advanced glycation endproduct-modified serum albumins. J Protein Chem. 14(5):359-372.

Whaley-Connell A, McCullough PA, Sowers JR. 2011. The role of oxidative stress in the metabolic syndrome. Rev Cardiovasc Med. 2(1):21-29.

Wilker SC, Chellan P, Arnold BM, Nagaraj RH. 2001. Chromatographic quantification of argpyrimidine, a methylglyoxal-derived product in tissue proteins: Comparison with pentosidine. Anal Biochem. 290:353-358.

Willemsen S, Hartog JW, Hummel YM, Posma JL, van Wijk LM, van Veldhuisen DJ, Voors AA. 2010. Effects of alagebrium, an advanced glycation end-product breaker, in patients with chronic heart failure: study design and baseline characteristics of the beneficiak trial. Eur J Heart Fail. 12(3):294-300.

Winlove CP, Parker KH, Avery NC, Bailey AJ. 1996. **I**nteractions of elastin and aorta with sugars *in vitro* and their effects on biochemical and physical properties. Diabetologia. 39(10):1131-1139.

Wolff SP and Dean RT. 1987. Glucose autoxidation and protein modification. The potential role of 'autoxidative glycosylation' in diabetes. Biochem J. 245(1):243-250.

Wu C and Yen GC. 2005. Inhibitory effect of naturally occuring flavonoids on the formation of advanced glycation end products. J Agric Food Chem. 53:3167-3173.

Wu J-W, Hsieh C-L, Wang H-Y, Chen H-Y. 2009. Inhibitory effects of guava (*Psidium guajava L.*) leaf extracts and its active compounds on the glycation process of protein. Food Chem. 113:78–84.

Wu MY, Chen BG, Chang CD, Huang MH, Wu TG, Chang DM, Lee YJ, Wang HC, Lee CI, Chern CL, Liu RH. 2008. A novel derivatization approach for simultaneous determination of glyoxal, methylglyoxal, and 3-deoxyglucosone in plasma by gas chromatography-mass spectrometry. J Chromatogr A. 1204(1):81-86.

Xiao J, Cao H, Wang Y, Yamamoto K, Wei X. 2010b. Structure-affinity relationship of flavones on binding to serum albumins: effect of hydroxyl groups on ring A. Mol Nutr Food Res. 54(Suppl 2):S253-S260.

Xiao J, Cao H, Wang Y, Zhao J, Wei X. 2009. Glycosylation of dietary flavonoids decreases the affinities for plasma protein. J Agric Food Chem. 57:6642-6648.

Xiao J, Chen L, Yang F, Liu C, Bai Y. 2010a. Green, yellow and red emitting CdTe QDs decreased the affinities of apigenin and luteolin for human serum albumin *in vitro*. J Hazard Mater. 182(1-3):696-703.

Xiao J, Suzuki M, Jiang X, Chen X, Yamamoto K, Ren F, Xu M. 2008. Influence of B-ring hydroxylation on interactions of flavonols with bovine serum albumin. J Agric Food Chem. 56:2350-2356.

Xie M-X, Long M, Liu Y, Qin C, Wang Y-D. 2006. Characterization of the interaction between human serum albumin and morin. Biochim Biophys Acta. 1760:1184-1191.

Xie M-X, Xu X-Y, Wang Y-D. 2005. Interaction between hesperetin and human serum albumin revealed by spectroscopic methods. Biochim Biophys Acta. 1724:215-224.

Yamagishi S, Nakamura K, Matsui T, Ueda S, Noda Y, Imaizumi T. 2008. Inhibitors of advanced glycation end products (AGEs): Potential utility for the treatment of cardiovascular disease. Cardiovasc Ther. 26(1):50-58.

Yamagishi S-i and Matsui T. 2010. Advanced glycation end products, oxidative stress and diabetic nephropathy. Oxid Med Cell Longev. 3(2):101-108.

Yan H and Harding JJ. 1997. Glycation-induced inactivation and loss of antigenicity of catalase and superoxide dismutase. Biochem J. 328(2):599-605.

Yang CS, Lambert JD, Sang S. 2009 Antioxidative and anti-carcinogenic activities of tea polyphenols. Arch Toxicol. 83:11–21.

Yang MM, Yang P, Zhang L-W 1994. Study on interaction of caffeic acid series medicine and albumin by fluorescence method. Chin Sci Bull. 39(9):734-739.

Yegin A, Ozben T, Yegin H. 1995. Glycation of lipoproteins and accelerated atherosclerosis in non-insulin-dependent diabetes mellitus. Int J Clin Lab Res. 25(3):157-161.

Yim MB, Yim HS, Lee C, Kang SO, Chock PB. 2001. Protein glycation: creation of catalytic sites for free radical generation. Ann N Y Acad Sci. 928:48-53.

Yokozawa T and Nakagawa T. 2004. Inhibitory effects of Luobuma tea and its components against glucose-mediated protein damage Food Chem Toxicol. 42:975-981.

Yu Z, Li D, Ji B, Chen J. 2008. Characterization of the binding of nevadensin to bovine serum albumin by optical spectroscopic technique. J Mol Struct. 889:422-428.

Yuan J-L, Iv Z, Liu Z-G, Hu Z, Zou G-L. 2007. Study on interaction between apigenin and human serum albumin by spectroscopy and molecular modeling. J Photochem Photobiol A: Chem. 191:104-113.

Zargar SJ and Rabbani A. 2002. Interaction of daunomycin antibiotic with histone H1: ultraviolet spectroscopy and equilibrium dialysis studies. Int J Biol Macromol. 30:113-117.

Zeng J and Davies MJ. 2005. Evidence for the formation of adducts and S-(carboxymethyl)cysteine on reaction of alpha-dicarbonyl compounds with thiol groups on amino acids, peptides, and proteins. Chem Res Toxicol. 18:1232-1241.

Zeng J, Dunlop RA, Rodgers KJ, Davies MJ. 2006. Evidence for inactivation of cysteine proteases by reactive carbonyls via glycation of active site thiols. Biochem J. 398(2):197-206.

Zhang G, Chen X, Guo J, Wang J. 2009. Spectroscopic investigation of the interaction between chrysin and bovine serum albumin. J Mol Struct. 921:346-351.

Zhang G, Que Q, Pan J, Guo J. 2008b. Study of the interaction between icariin and human serum albumin by fluorescence spectroscopy. J Mol Struct. 881:132-138.

Zhang G, Wang A, Jiang T, Guo J. 2008a. Interaction of the irisflorentin with bovine serum albumin: A fluorescence quenching study. J Mol Struct. 891:93-97.

Zhang G, Zhao N, Hu X, Tian J. 2010. Interaction of alpinetin with bovine serum albumin: Probing of the mechanism and binding site by spectroscopic methods. Spectrochim Acta A Mol Biomol Spectrosc. 76(3-4):410-417.

Zhang G, Huang G, Xiao L, Mitchell AE. 2011a. Determination of advanced glycation endproducts by LC-MS/MS in raw and roasted almonds (*Prunus dulcis*). J Agric Food Chem. 59(22):12037-12046.

Zhang Y, Li Y, Dong L, Li J, He W, Chen X, Hu Z. 2008c. Investigation of the interaction between naringin and human serum albumin. J Mol Struct. 875:1-8.

Zhang Y, Shi S, Sun X, Xiong X, Peng M. 2011b. The effect of Cu(2+) on interaction between flavonoids with different C-ring substituents and bovine serum albumin: Structure-affinity relationship aspect. J Inorg Biochem. 105(12):1529-1537.

Zhang Y, Xu M, Du M, Zhou F. 2007. Comparative studies of the interaction between ferulic acid and bovine serum albumin by ACE and surface plasmon resonance. Electrophoresis. 28(11):1839-1845.

Zhao J and Ren F. 2009. Influence of hydroxylation and glycosylation in ring A of soybean isoflavones on interaction with BSA. Spectrochim Acta A Mol Biomol Spectrosc. 72(3):682-685.

Zhao HR, Smith JB, Jiang XY, Abraham EC. 1996. Sites of glycation of beta B2-crystallin by glucose and fructose. Biochem Biophys Res Commun. 229(1):128-133.

Zhao W, Devamanoharan PS, Varma SD. 2000. Fructose induced deactivation of antioxidant enzymes: preventive effect of pyruvate. Free Radic Res. 33(1):23-30.

Zmatliková Z, Sedláková P, Lacinová K, Eckhardt A, Pataridis S, Mikšík I. 2010. Non-enzymatic posttranslational modifications of bovine serum albumin by oxo-compounds investigated by high-performance liquid chromatography-mass spectrometry and capillary zone electrophoresis-mass spectrometry. J Chromatogr A. 1217(51):8009-8015.

Zsila F, Bikádi Z, Simonyi M. 2003. Probing the binding of the flavonoid, quercetin to human serum albumin by circular dichroism, electronic absorption spectroscopy and molecular modelling methods. Biochem Pharmacol. 65(3):447-456.

ABSTRACT

Charles University in Prague, Faculty of Pharmacy in Hradec Králové
Department of Biochemical Sciences
Candidate **Ing. Lucie Trnková**
Supervisor **Prof. MUDr. Jaroslav Dršata, CSc.**
Title of Doctoral thesis **Interaction of proteins with low-molecular substances *in vitro*. Effect of glycation, substances of plant origin, and combination of these factors on function and spectral properties of selected proteins.**

Plant polyphenolic compounds naturally occurring in human diet possess a wide range of biological and pharmacological properties. They can interact with various proteins including enzymes. Their interaction with serum albumin has a great significance because of its ability to bind, transport and store many endogenous and exogenous low-molecular compounds present in blood circulation. One of the objectives of this thesis was to study chemical structure-binding affinity relationships of two important groups of polyphenolic substances, namely hydroxycinnamic acids and catechins (flavanols), with the molecule of serum albumin in the in vitro models using spectroscopic (UV-Vis absorption spectroscopy, fluorescence quenching method) and electrophoretic (native and SDS PAGE) methods. Some polyphenols caused the changes in protein conformation and the relationships between their structures and obtained binding affinities to serum albumin were noticed.

Green tea catechins (flavanols) represent one of the most important plant polyphenolic substances. Interaction between these compounds and ERp57 enzyme in the in vitro model has been studied by fluorescence quenching method. Effects of green tea catechins on disulfide reductase activity of ERp57 enzyme in the in vitro model was monitored by sensitive fluorescent assay using dieosin glutathione disulfide as a fluorescent probe. This probe displays low fluorescence at the excitation/emission wavelength of 520 nm/545 nm, respectively, which significantly increases on reduction of its disulfide bonds (i.e. the presence of ERp57). Relationships between structures of the studied catechins and their binding affinities or their inhibitory effects on reductase activity of ERp57 were discussed.

Alpha-dicarbonyl compounds (e.g. methylglyoxal) are formed during various metabolic processes and also by non-enzymatic protein glycation by glucose. They are thought to be principal precursors in generation of AGEs in vivo. Methylglyoxal can readily react with amino groups of proteins to form covalent cross-links and reactive oxygen species (ROS). It contributes to the onset and progression of many human diseases including diabetes mellitus and its related complications. Plant polyphenolic

compounds can reduce formation of AGEs and thus slow down the process of non-enzymatic glycation by different mechanisms such as trapping of reactive α-dicarbonyl compounds or ROS. Another aim of this thesis was to study the effects of green tea catechins on methylglyoxal-mediated non-enzymatic glycation of serum albumin in the in vitro models using fluorescence methods for determination of total ("non-specific") AGEs (λex/λem = 330/410 nm) and argpyrimidine as specific AGE (λex/λem = 320/380 nm). Antiglycating activity of the studied catechins was dependent on their structure and concentration.

Glutathione S-transferases (GSTs) represent a group of enzymes which catalyze conjugation of reduced glutathione to various hydrophobic compounds. They are important enzymes in detoxification of various xenobiotics. Effect of methylglyoxal on the structural and catalytic properties of GST from Schistosoma japonicum was investigated in the in vitro model using spectroscopic (UV-Vis absorption and fluorescence spectroscopy) and electrophoretic (native PAGE, SDS PAGE/western blotting) methods. It was found out that methylglyoxal reduced catalytic activity of GST and caused changes in the molecular charge of the enzyme as well as changes in its structure (i.e. conformational changes, formation of AGEs and cross-links) in dependence on the concentration.

ABSTRAKT

Univerzita Karlova v Praze, Farmaceutická fakulta v Hradci Králové

Katedra	Katedra biochemických věd
Kandidát	**Ing. Lucie Trnková**
Školitel	**Prof. MUDr. Jaroslav Dršata, CSc.**
Název disertační práce	**Interakce proteinů s nízkomolekulárními látkami *in vitro*. Vliv glykace, látek přírodního původu a kombinace těchto faktorů na funkci a spektrální vlastnosti vybraných bílkovin.**

Rostlinné polyfenolické látky se přirozeně vyskytují v lidské stravě a vyznačují se řadou biologických a farmakologických vlastností. Mají schopnost reagovat s nejrůznějšími proteiny včetně enzymů. Velký význam má jejich interakce se sérovým albuminem, jehož jednou z nejvýznamnějších funkcí je vázání, přenos a ukládání řady endogenních a exogenních nízkomolekulárních látek v krevním řečišti. Jedním z cílů práce bylo prostudovat vztahy mezi chemickou strukturou a vazebnými afinitami dvou významných skupin polyfenolických látek, konkrétně hydroxyskořicových kyselin a katechinů (flavanolů), s molekulou sérového abuminu v in vitro modelech pomocí spektrálních (UV-Vis absorpční spektroskopie, metoda zhášení fluorescence) a elektroforetických (nativní a SDS PAGE) metod. Některé polyfenoly způsobily změny v konformaci proteinu a byly zaznamenány určité vztahy mezi jejich strukturou a zjištěnými vazebnými afinitami k sérovému albuminu.

Mezi nejvýznamnější rostlinné polyfenolické látky patří katechiny (flavanoly) zeleného čaje. Byla studována možnost interakce těchto katechinů s enzymem ERp57 v in vitro modelu metodou zhášení fluorescence. Pro studování vlivu katechinů zeleného čaje na reduktasovou aktivitu enzymu ERp57 v in vitro modelu byla použita citlivá fluorescenční metoda využívající dieosinglutathiondisulfid jako fluorescenční sondu. Sonda vykazuje nízkou fluorescenci při vlnové délce excitace a emise 520 nm/545 nm, která významně vzroste po redukci disulfidové vazby, tedy v přítomnosti enzymu ERp57. Na základě získaných výsledků byl diskutován vztah mezi strukturou studovaných katechinů a jejich vazebnou afinitou, popř. jejich inhibičním účinkem na reduktasovou aktivitu ERp57.

Alfa-dikarbonylové sloučeniny (např. methylglyoxal) vznikají během řady metabolických procesů a také neenzymovou glykací proteinů glukosou. Jsou považovány za důležité prekurzory vzniku AGEs in vivo. Methylglyoxal se snadno váže na aminoskupiny proteinů za tvorby kovalentních zesítěných agregátů (crosslinků) a reaktivních forem kyslíku (ROS). Tím přispívá ke vzniku a rozvoji různých onemocnění

včetně diabetu mellitu a jeho pozdních komplikací. Rostlinné polyfenolické látky mohou snižovat tvorbu AGEs a tím zpomalovat proces neenzymové glykace různými mechanismy, např. vychytáváním reaktivních α-dikarbonylových sloučenin nebo ROS. Dalším cílem práce bylo studium vlivu katechinů zeleného čaje na neenzymovou glykaci sérového albuminu zprostředkovanou methylglyoxalem v modelech in vitro pomocí fluorescenčních metod pro stanovení množství celkových ("nespecifických") AGEs (λex/λem = 330/410 nm) a argpyrimidinu jako specifického AGE (λex/λem = 320/380 nm). Antiglykační účinek studovaných katechinů závisel na jejich struktuře a koncentraci.

Glutathion-S-transferasy (GSTs) představují skupinu enzymů, které katalyzují konjugaci redukovaného glutathionu s řadou hydrofobních látek. Jedná se o důležité enzymy v detoxikaci různých xenobiotik. V rámci této práce byl studován účinek methylglyoxalu na strukturní a katalytické vlastnosti rekombinantní cytosolické GST z Schistosoma japonicum v in vitro modelu pomocí spektroskopických (UV-Vis absorpční a fluorescenční spektroskopie) a elektroforetických (nativní PAGE, SDS PAGE/western blotting) metod. Bylo zjištěno, že methylglyoxal snižuje katalytickou aktivitu GST a způsobuje změny v náboji molekuly enzymu stejně tak jako změny v jeho struktuře (tj. změna konformace, tvorba AGEs a crosslinků) v závislosti na koncentraci.

Papers closely related to the topic of doctoral thesis

1. **Trnková L.**, Boušová I., Ryšánková L., Vrabcová P., Držata J. 2009. Antioxidants and environmental stress: Spectroscopic study on stability of natural compounds and their interaction with a molecule of protein in an *in vitro* model. *Proceedings of ECOpole.* 3(1):27-34. ISSN 1898-617X. ***p. 140***

2. **Trnková L.**, Boušová I., Kubíček V., Držata J. 2010. Binding of naturally occurring hydroxycinnamic acids to bovine serum albumin. *Natural Science.* 6(2):563-570. ISSN 2150-4091. ***p. 148***

3. **Trnková L.**, Boušová I., Staňková V., Držata J. 2011. Study on the interaction of catechins with human serum albumin using spectroscopic and electrophoretic techniques. *Journal of Molecular Structure*. 985(2-3):243-250. ISSN 0022-2860. ***p. 156***

4. Boušová I., Průchová Z., **Trnková L.**, Držata J. 2011. Comparison of glycation of glutathione S-transferase by methylglyoxal, glucose or fructose. *Molecular and Cellular Biochemistry.* 357(1-2):323-330. ISSN 0300-8177. ***p. 164***

Other papers

Mueller-Harvey I, Feucht W, Polster J, **Trnková L**, Burgos P, Parker AW, Botchway SW. 2012. Two-photon excitation with pico-second fluorescence lifetime imaging to detect nuclear association of flavanols. *Analytica Chimica Acta.* (*in press*).

SUPPLEMENTS

Copies of published papers related to the topic of this doctoral thesis

Proceedings of ECOpole
Vol. 3, No. 1 2009

Lucie TRNKOVÁ[1,2], Iva BOUŠOVÁ[2], Lucie RYŠÁNKOVÁ[1], Petra VRABCOVÁ[1] and Jaroslav DRŠATA[1,2]

ANTIOXIDANTS AND ENVIRONMENTAL STRESS: SPECTROSCOPIC STUDY ON STABILITY OF NATURAL COMPOUNDS AND THEIR INTERACTION WITH A MOLECULE OF PROTEIN IN AN *IN VITRO* MODEL

ANTYOKSYDANTY A STRES ŚRODOWISKOWY, BADANIA SPEKTRALNE STABILNOŚCI SUBSTANCJI NATURALNYCH I ICH ODDZIAŁYWANIE Z MOLEKUŁĄ BIAŁKA

Abstract: The stability of eight hydroxycinnamic acids (HCAs) during long-term incubation under physiological conditions was studied by UV-VIS absorption spectroscopy and their possibility of binding to a model protein (bovine serum albumin, BSA) under physiological conditions was investigated by tryptophan fluorescence quenching method. The obtained results suggest that the stability of hydroxycinnamic acids is dependent upon its individual structure and duration of incubation. The monosubstituted derivatives (coumaric acids) were stable within the course of long-term incubation, while di- and trisubstituted derivatives decomposed easily. It was found out that all studied compounds changed fluorescence emission spectrum of BSA. The Stern-Volmer analysis was employed in order to explore binding of HCAs to BSA in details. The binding constants (K_b), number of binding sites (n) and the free energy changes (ΔG^0) were determined. The binding affinity was strongest for rosmarinic acid and ranked in the following order rosmarinic acid > chlorogenic acid > sinapic acid > caffeic acid > ferulic acid > *o*-coumaric acid > *p*-coumaric acid > *m*-coumaric acid. All free energy changes (ΔG^0) possessed negative sign indicating the spontaneity of HCAs binding to BSA.

Keywords: oxidative stress, antioxidant, hydroxycinnamic acid, serum albumin, protein-ligand binding

There is a large amount of air pollutants in our environment and many of them show adverse oxidative effects on living organisms [1]. Although the properties of air pollutants vary markedly, they all have one common feature. They can cause oxidative stress, a state in which the prooxidant-antioxidant balance is seriously impaired. This imbalance can occur when the generation of reactive oxygen species overwhelms endogenous antioxidant systems. Oxidative stress can have serious impact on human health [1, 2]. Recently, considerable attention has been focused on the study of naturally occurring compounds with antioxidant effects (eg flavonoids, hydroxycinnamic acids, carotenoids) which can protect body against environmental pollutants. Hydroxycinnamic acids (HCAs) are natural compounds widely distributed in higher plants and are used in folk medicine because of their antioxidant and other effects [3, 4]. Serum albumin was used as a model protein because it is one of the most abundant proteins in circulatory system of a wide variety of organisms and one of the most extensively studied proteins at all. It possesses a wide range of physiological functions involving the binding, transport and deposition of many endogenous and exogenous ligands present in blood circulation [5, 6]. It is well known that

[1] Department of Chemistry, Faculty of Education, University of Hradec Králové, Rokitanského 62, 500 03 Hradec Králové, Czech Republic, tel. +420 49 333 11 59, fax +420 49 333 11 66, email: lucie.trnkova@uhk.cz
[2] Department of Biochemical Sciences, Charles University in Prague, Faculty of Pharmacy, Heyrovského 1203, 500 05 Hradec Králové, Czech Republic

many drugs are bound to serum albumin and that their effectiveness depends on their binding ability [6]. But on the other hand, drugs can cause various changes in protein conformation, which may influence its physiological function and these impaired proteins may be consequently pathologically accumulated in body tissues. Spectroscopic techniques are an ideal tool to observe conformational changes in structure of protein since it allows non-destructive measurements of compounds present at low concentration under physiological conditions. In the presented study the interactions of HCAs with the molecule of BSA were studied using UV-VIS absorption spectroscopy and fluorescence quenching method which is based on quenching of protein fluorescence by drug. The Stern-Volmer analysis is often used in order to analyze obtained data and to elucidate protein-drug (ligand) binding mechanism [7].

Experimental

Chemicals and preparation of stock solutions

Bovine serum albumin and all hydroxycinnamic acids (Fig. 1) were obtained from Sigma-Aldrich GmbH, Germany. All other chemicals were of analytical grade. Bovine serum albumin was dissolved in sodium phosphate buffer (pH 7.4; 0.1 M; 0.05% sodium azide) in order to yield solution with concentration of 2 μM for fluorescence spectroscopic experiments. Individual HCAs were dissolved in 20 mM NaOH in order to yield 10 mM stock solutions. BSA and HCA solutions were freshly prepared before each measurement.

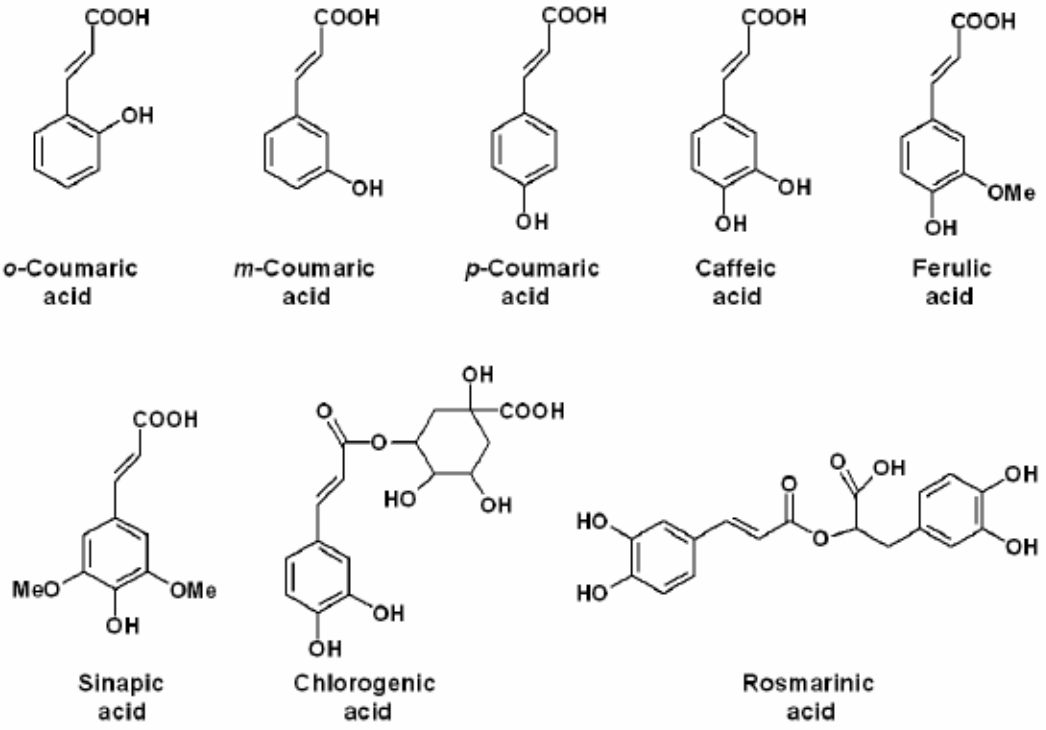

Fig. 1. Chemical structures of tested hydroxycinnamic acids

UV-VIS absorption spectroscopy

Absorption spectra were measured using spectrophotometers Lambda 25 (Perkin Elmer, United Kingdom) and Helios β (Spectronic Unicam, United Kingdom) in a 10 mm quartz cuvette. 50 μM solutions of HCAs in sodium phosphate buffer (pH 7.4; 0.1 M; 0.05% sodium azide) were incubated for up to 28 days at 37°C. The absorption UV-VIS spectra were recorded from 190 to 550 nm at the time 0, 1 hour and day 1, 7, 14, 21, and 28. The sample temperature was maintained at 37°C.

Fluorescence spectroscopy

Fluorescence spectra were recorded using a luminescence spectrometer LS 50B (Perkin Elmer, United Kingdom) in a 10 mm quartz Suprasil cuvette. Quantitative analysis of the potential interaction between individual HCA and BSA was performed by the fluorimetric titration. Briefly, solution of BSA (2 μM) was titrated in cuvette by successive additions of HCA solution (10 mM) to a final concentration of 20 μM. Fluorescence emission spectra were recorded from 300 to 530 nm with excitation at 295 nm while stirring. The excitation and emission slits were both set to 5 nm and scanning speed to 200 nm/min. All experiments were carried out at 37°C. Fluorescence intensity was read at emission wavelength of 350 nm.

Principles of fluorescence quenching

Dynamic (collisional) quenching occurs when the excited-state fluorophore is deactivated upon contact with some other molecule (quencher) and no molecule is chemically altered during this process. In the case of static quenching, a non-fluorescent complex is formed between molecules of fluorophore and quencher. Collisional quenching of fluorescence is described by the well-known Stern-Volmer equation as follows [7]

$$\frac{F_0}{F} = 1 + k_q \tau_0 [Q] = 1 + K_{SV}[Q] \quad (1)$$

In this equation, F_0 and F are the fluorescence intensities of BSA in the absence and presence of quencher, respectively, [Q] is the quencher concentration, k_q is the bimolecular quenching constant, and τ_0 is the lifetime of the fluorophore in the absence of quencher. The Stern-Volmer quenching constant (K_{SV}) is given by $k_q\tau_0$. The static and dynamic quenching can be distinguished by the Stern-Volmer diagram (dependence of F_0/F on quencher concentration). When the plot of Stern-Volmer diagram shows exponential dependence, both static and dynamic quenching is present. In case the plot shows linear dependence, the quenching is either purely static or dynamic. One criterion for distinguishing of type of quenching is the fact that the obtained bimolecular quenching constant k_q is larger than the limiting diffusion rate constant of the biomolecule (2.0×10^{10} $dm^3 \cdot mol^{-1} \cdot s^{-1}$) [7], and so the static quenching process can be postulated to obtain the binding parameters according to the following equation

$$\log \frac{F_0 - F}{F} = \log K_b + n \log [Q] \quad (2)$$

where K_b represents binding constant for quencher-protein interaction, n the number of binding sites per BSA, and F_0, F have the same meaning as in Eq. (1). The values of K_b and

n could be measured from the intercept and slope by plotting log $(F_0 - F)/F$ against log [Q] [2]. Utilizing K_b, the free energy change (ΔG^0) value can be estimated from the following equation [8]

$$\Delta G^0 = -R\ T \ln K_b \quad (3)$$

Results and discussion

Changes in UV-VIS absorption spectra were employed to check stabilities of stock solutions of hydroxycinnamic acids. Each HCA has characteristic profile of its UV-VIS spectrum at physiological conditions (pH 7.40; 37°C). No changes in UV-VIS spectra of monosubstituted derivatives (coumaric acids) were observed during their incubation. Profile of spectrum of ferulic acid was not altered throughout the incubation, but the intensity of absorbance in maximum slowly decreased. The spectra of other four tested derivatives (caffeic, sinapic, chlorogenic, and rosmarinic acid) showed remarkable changes (Fig. 2) which suggest that these compounds were decomposed probably to catechol and its substituted derivatives within first 24 hours of incubation. It can be concluded that coumaric acids are stable within the course of long term incubation, while di- and trisubstituted derivatives decompose easily and therefore they are not suitable for long lasting experiments.

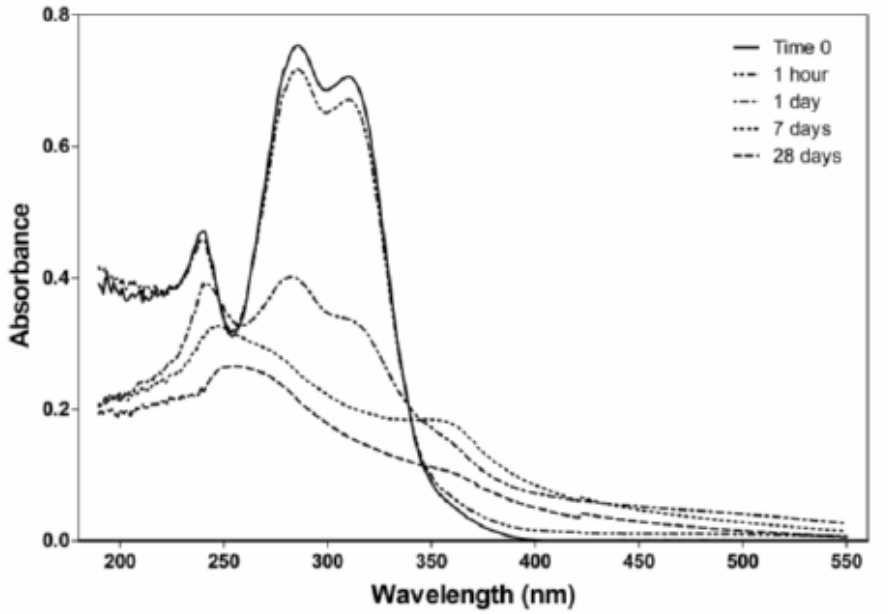

Fig. 2. Effect of long term incubation (28 days at 37°C) on characteristic UV-VIS absorption spectrum of 50 μM caffeic acid in sodium phosphate buffer (pH 7.4; 0.1 M; 0.05% sodium azide)

Quenching of protein intrinsic (tryptophan) fluorescence was employed for more detailed study of HCA-BSA binding. Fluorescence emission spectra were recorded upon excitation at 295 nm and possessed maximum at 350 nm. The excitation at 295 nm was used to ensure that the light was absorbed by tryptophan residues only [7]. Protein solution was titrated by successive additions of individual HCAs solutions. Fluorescence intensitiy

of BSA gradually decreased with increasing concentration of hydroxycinnamic acid (Fig. 3). This may indicate alterations in microenvironment around tryptophan residues in protein molecule upon interaction with tested compound. Red shifts of protein fluorescence emission bands in dependence on increasing concentration of tested compound were observed in the case of sinapic, chlorogenic and rosmarinic acids. Emission maximum of BSA was shifted by 2, 4 and 5 nm towards longer wavelength after BSA interaction with sinapic, chlorogenic, and rosmarinic acids in 20 μM concentration, respectively. Significant red shifts by 12 and 18 nm were observed by other authors upon interaction of human serum albumin with sinapic acid [9] and chlorogenic acid [10] but the concentrations of tested compounds that caused so remarkable shifts of emission maxima were as much as 150 μM. The red shift of protein emission band is caused by decrease in hydrophobic property of binding cavity near tryptophan in BSA suggesting that tryptophan has been brought to more hydrophilic environment [10] and protein secondary structure has been changed [11]. Other tested HCAs did not show any shifts in their spectra, which indicates that these HCAs can bind to BSA without affecting the immediate environment of the tryptophan residues [8].

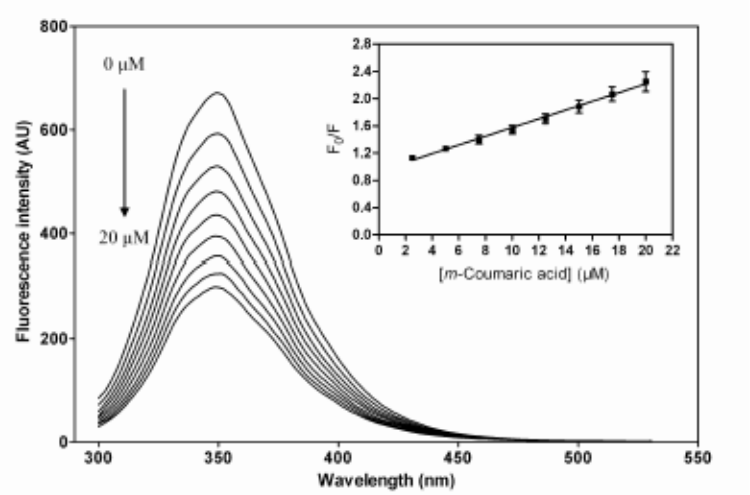

Fig. 3. Fluorescence emission spectra of BSA (2 μM) in the absence and in the presence of increasing amounts of *m*-coumaric acid (0÷20 μM) in sodium phosphate buffer (pH 7.4; 0.1 M; 0.05% sodium azide) at λ_{ex} = 295 nm and 37°C. The insert shows the corresponding Stern-Volmer diagram of the *m*-coumaric acid-BSA system (λ_{em} = 350 nm), R^2 = 0.9951

The type of fluorescence quenching was determined using the Stern-Volmer diagrams. Apart from rosmarinic acid the linear dependence in the Stern-Volmer diagram was found out in all tested HCAs and type of quenching was distinguished by the bimolecular quenching constants (k_q). In the case of rosmarinic acid the plot exhibited exponential dependence (Fig. 4) indicating that both static and dynamic type of quenching was asserted. The bimolecular quenching constants (k_q) of the rosmarinic acid-BSA system were obtained from the linear range (concentrations of 0÷10 μM) of the diagram. The bimolecular quenching constants of all HCAs (Table 1) were found to be higher than 10^{10} $dm^3 \cdot mol^{-1} \cdot s^{-1}$ [7] which is the maximum value of k_q for a diffusion controlled quenching process. This fact suggests that the static quenching mechanism between each

HCA and BSA is the main reason of protein fluorescence quenching and binding parameters can be determined according to the equation (2) (Fig. 5). The binding constants (K_b), binding sites (n) and free energy change (ΔG^0) are showed in Table 1. The binding affinity was the strongest for rosmarinic acid and ranked in the order rosmarinic acid > chlorogenic acid > sinapic acid > caffeic acid > ferulic acid > *o*-coumaric acid > *p*-coumaric acid > *m*-coumaric acid. The obtained results suggest that the binding affinity depends on the number and the position of hydroxyl groups. Di- and trisubstituted derivatives have stronger binding affinity than monosubstituted derivatives. Binding of rosmarinic acid to BSA proceeds the most easily due to higher number and suitable position of hydroxyl groups on the aromatic ring. The negative sign for ΔG^0 indicates that the binding of HCAs to the molecule of BSA is spontaneous process.

Table 1

The bimolecular quenching constants (k_q), the binding constants (K_b), the number of binding sites (n) and the free energy change (ΔG^0) of the HCA-BSA system at 37°C

Tested compound	k_q[1] [x10^{13} dm^3·mol^{-1}s^{-1}]	K_b [x10^5 dm^3·mol^{-1}]	n	ΔG^0 [kJ·mol^{-1}]
o-coumaric acid	1.19	3.34	1.17	–32.73
m-coumaric acid	1.19	1.31	1.08	–30.36
p-coumaric acid	1.43	1.81	1.10	–30.98
caffeic acid	0.86	4.16	1.18	–33.12
ferulic acid	0.97	3.39	1.18	–32.75
sinapic acid	0.85	4.19	1.21	–33.36
chlorogenic acid	1.07	6.67	1.23	–34.55
rosmarinic acid	16.39[2]	96.16	1.40	–41.43

Standard deviation (mean value of three independent measurements) was lower than 10%.
[1] $k_q = K_{SV}/\tau_0$; $\tau_0 = 5x10^{-9}$ s [7]
[2] assessed in the linear range (1÷10 μM)

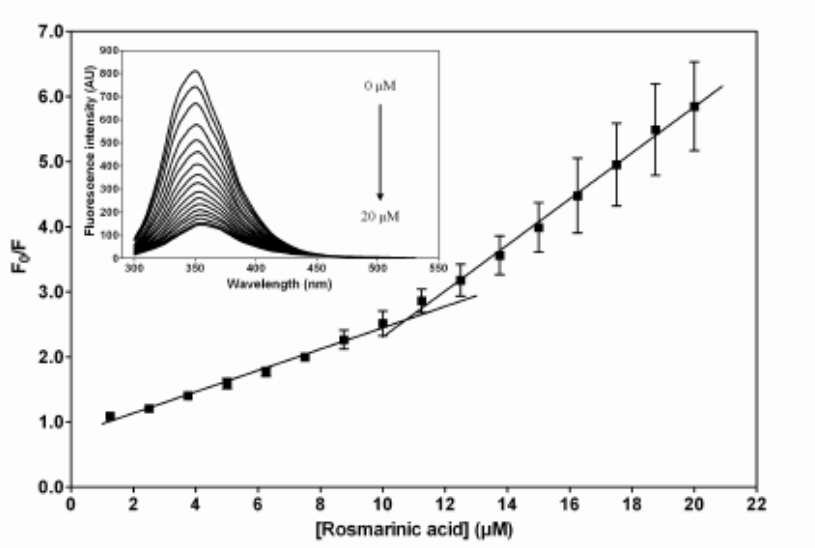

Fig. 4. The Stern-Volmer diagram of the rosmarinic acid-BSA system obtained by the titration with rosmarinic acid at physiological conditions (37°C; pH 7.4). [BSA] = 2 μM, [rosmarinic acid] = 0÷20 μM, λ_{ex} = 295 nm and λ_{em} = 350 nm. R_1^2 = 0.9895 and R_2^2 = 0.9957. The insert shows the corresponding fluorescence quenching spectra

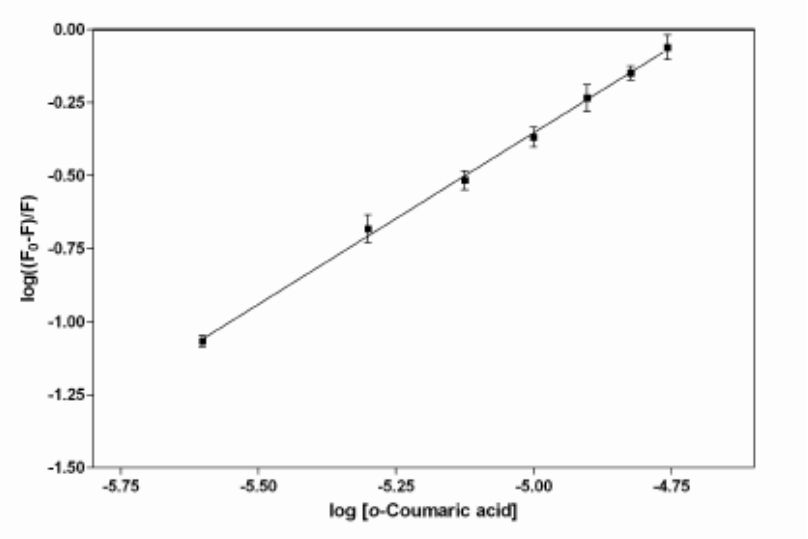

Fig. 5. Logarithmic plots of fluorescence quenching of BSA treated with different concentrations of *o*-coumaric acid at physiological conditions (37°C; pH 7.4). [BSA] = 2 μM, [*o*-coumaric acid] = 0÷20 μM, λ_{ex} = 295 nm and λ_{em} = 350 nm. R^2 = 0.9983

Conclusions

It can be concluded that coumaric acids are stable within the course of long term incubation, while di- and trisubstituted derivatives decompose easily and therefore they are not suitable for long lasting experiments. All HCAs are able to bind spontaneously to the protein molecule with different affinity depending on the number and the position of hydroxyl groups. This binding may influence physiological function of altered protein.

Acknowledgements

The presented study was supported by the Specific research 2008 of the University of Hradec Králové and by the Development project of Czech Ministry of Education No. 141/2008.

References

[1] Kelly F.J.: Proc. Nutr. Soc., 2004, **63**, 579-585.
[2] Stadtman E.R. and Levine R.L.: Ann. N.Y. Acad. Sci., 2000, **899**, 191-208.
[3] Kikuzaki H., Hisamoto M., Hirose K., Akiyama K. and Taniguchi H.: J. Agric. Food Chem., 2002, **50**, 2161-2168.
[4] Halliwell B., Aeschbach R., Löliger J. and Aruoma O.I.: Food Chem. Toxicol., 1995, **33**(7), 601-617.
[5] Peters T.: All About Albumin: Biochemistry, Genetics, and Medical Applications. Academic Press, San Diego 1996.
[6] Carter D.C. and Ho J.X.: Adv. Protein Chem., 1994, **45**, 153-203.
[7] Lakowicz J.R.: Principles of Fluorescence Spectroscopy. Kluwer Academic/Plenum Press, New York 1999.
[8] Liu Y., Xie M.X., Jiang M. and Wang Y.D.: Spectr. Acta Pt. A - Mol. Biomol. Spectr., 2005, **61**, 2245-2251.
[9] Kang J., Liu Y., Xie M.X., Li S., Jiang M. and Wang Y.D.: Biochim. Biophys. Acta-Gen. Subj., 2004, **1674**, 205-214.
[10] He W., Li Y., Xue Ch., Hu Z., Chen X. and Sheng F.: Bioorg. Med. Chem., 2005, **13**, 1837-1845.
[11] Shang L., Jiang X. and Dong S.: J. Photochem. Photobiol. A - Chemistry, 2006, **184**, 93-97.

ANTYOKSYDANTY A STRES ŚRODOWISKOWY, BADANIA SPEKTRALNE STABILNOŚCI SUBSTANCJI NATURALNYCH I ICH ODDZIAŁYWANIE Z MOLEKUŁĄ BIAŁKA

Abstrakt: Badano trwałość ośmiu kwasów hydrooksycynamonowych, HCAs, podczas inkubacji długoterminowej w warunkach fizjologicznych i możliwość ich wiązania się z modelowym białkiem (albuminą, BSA). Uzyskane wyniki pokazały, że trwałość tych kwasów zależy od ich indywidualnej budowy oraz czasu inkubacji. Wyznaczono stałe trwałości (K_b), liczbę miejsc wiązania (n) oraz zmianę wartości energii Gibbsa (ΔG^0) wiązania HCAs do BSA, który to proces przebiegał samorzutnie.

Słowa kluczowe: stres oksydacyjny, antyoksydant, kwas hydrooksycynamonowy, albumina (BSA), wiązanie białka z ligandem

Vol.2, No.6, 563-570 (2010)
doi:10.4236/ns.2010.26071

Natural Science

Binding of naturally occurring hydroxycinnamic acids to bovine serum albumin

Lucie Trnková[1,2], Iva Boušová[1*], Vladimír Kubíček[1], Jaroslav Dršata[1,2]

[1]Charles University in Prague, Faculty of Pharmacy, Hradec Králové, Czech Republic; *Corresponding Author: Iva.Bousova@faf.cuni.cz
[2]University of Hradec Králové, Faculty of Education, Hradec Králové, Czech Republic

Received 22 February 2010; revised 12 April 2010; accepted 13 May 2010.

ABSTRACT

Hydroxycinnamic acids (HCAs) possess numerous biological effects including antioxidant, antiallergic, antimicrobial, and immunomodulatory activities and due to these properties are widely used in folk medicine. Nevertheless, they can interact with protein molecules and cause some structural and functional changes. The possibility of HCAs binding to bovine serum albumin (BSA) under physiological conditions was investigated by the UV-VIS absorption spectroscopy and fluorescence quenching method. Apart from rosmarinic acid, all tested HCAs quenched tryptophan fluorescence of BSA in the studied range of concentrations (0-20 μM) mainly by static quenching mechanism (formation of non-fluorescent HCA-BSA complexes). The binding constants, number of binding sites and free energy changes were determined. The binding affinities of HCAs were ranked in the order: chlorogenic acid > sinapic acid ≥ caffeic acid > ferulic acid > *o*-coumaric acid > *p*-coumaric acid ≥ *m*-coumaric acid, which was confirmed by spectral overlaps of BSA emission spectrum with absorption spectrum of HCA. All free energy changes possessed negative sign indicating the spontaneity of HCA-BSA interaction.

Keywords: Bovine Serum Albumin; Hydroxycinnamic Acid; Fluorescence Quenching; Protein-Ligand Binding

1. INTRODUCTION

Recently, considerable attention has been focused on the study of the interaction between small molecules (drugs) and biological macromolecules (e.g. proteins), especially discussing the thermodynamic quality, binding force quality, and mechanism of interactions [1-3]. These studies play crucial role in promoting research on proteins because they can provide useful information for study of pharmacological and biological effects of drugs as well as conformational changes of proteins caused by drugs.

Serum albumin is one of the most abundant proteins in circulatory system of a wide variety of organisms and one of the most extensively studied proteins at all [4,5]. Bovine serum albumin (BSA) consists of 583 amino acids in a single polypeptide chain cross-linked with 17 disulfide bonds. It is composed of three homologous domains (I-III), each of which comprises of two subdomains (A and B). BSA has two tryptophan residues, which significantly contribute to the intrinsic fluorescence of this protein: Trp-134 is located near the surface in domain IB and Trp-212 is buried in a hydrophobic (non-polar) pocket in the internal part of domain IIA [6]. HSA differs from BSA by 24% of primary structure and the most important difference from spectroscopic point of view seems to be presence of only one tryptophan residue (Trp-214) in its molecule [4,5]. Serum albumin possesses a wide range of physiological functions involving the binding, transport and deposition of many endogenous and exogenous ligands present in blood circulation [4,7]. Perhaps, its most outstanding property is the ability to bind a variety of ligands. It is well known that many drugs bind to serum albumin and their effectiveness depends on the binding ability [5,8]. On the other hand, drugs can cause various changes in protein conformation influencing its physiological function and such impaired proteins may be consequently pathologically accumulated in body tissues.

Plant polyphenols represent a heterogeneous group of natural compounds with one or more hydroxyl groups attached to the benzene ring. These substances possess several important physiological roles in plants, such as defense against herbivores and pathogens, pigmentation, and attraction of pollinating insects [9]. The most widely distributed polyphenolic compounds in plant tissues are hydroxycinnamic acids. Some of the most common

naturally occurring HCAs are *p*-coumaric acid, ferulic acid, sinapic acid, and caffeic acid. These can be found in a free form but more often in various conjugated forms resulting from enzymatic hydroxylation, *O*-glycosylation, *O*-methylation or esterification [10,11]. Hydroxycinnamic acids have been reported to possess antimicrobial, antiallergic and anti-inflammatory activities, as well as antimutagenic and immunomodulatory effects [12,13] and due to these properties are widely used in folk medicine. They exert also antioxidant and anti-radical activities [14-16]. Their biological effects are strongly dependent on the number and position of hydroxyl groups [15]. Just the presence of hydroxyl groups suggests the possibility of HCAs binding with molecules of proteins.

Spectroscopic techniques, such as ultraviolet-visible (UV-VIS) absorption spectroscopy [17], fluorescence spectroscopy [1,6], circular dichroism [18], and attenuated total reflectance-Fourier transform infrared spectroscopy [19] are commonly used tools to observe conformational changes in structure of proteins because of non-destructive measurements of substances in low concentration under physiological conditions, high sensitivity, rapidity and ease of implementation. Fluorescence spectroscopy is widely used to study mechanism of the binding between drugs and plasma proteins [6].

Nowadays, the investigation of the binding of naturally occurring polyphenolic compounds with various proteins attracts a great attention. Several spectroscopic studies on the interaction between bovine serum albumin and cinnamic acid [1], ferulic acid [20,21], chlorogenic acid [19,22] or various flavonoids [18,19,24] have been published. Also several studies dealing with the interaction of human serum albumin (HSA) with derivatives of cinnamic acid or flavonoids have been carried out [2,3,17,25-29]. The data obtained in several studies concerning the HCAs-BSA binding parameters (especially caffeic, chlorogenic, and ferulic acid) are hardly comparable because these studies were performed under various conditions (e.g. pH, temperature).

The aim of the presented work was to study interactions of eight naturally occurring hydroxycinnamic acids with bovine serum albumin under physiological conditions (pH 7.4; 37℃) using UV-VIS absorption spectroscopy and fluorescence quenching method, reveal their character, evaluate structure-activity relationships, and compare obtained results with already published spectroscopic data on interaction of HCAs with BSA or HSA. The presented study contributes to the current knowledge in the area of protein-ligand binding, particularly bovine serum albumin-hydroxycinnamic acids interactions.

2. EXPERIMENTAL

2.1. Chemicals

Bovine serum albumin and all hydroxycinnamic acids were obtained from Sigma-Aldrich GmbH, Germany. The chemical structures of tested HCAs are presented in **Figure 1**. All other chemicals were of analytical grade.

2.2. Preparation of Stock Solutions

Bovine serum albumin was dissolved in sodium phosphate buffer (pH 7.4; 0.1 M; 0.05% sodium azide) in order to yield solutions with concentration 16 μM and 2 μM for UV-VIS absorption and fluorescence spectroscopic experiments, respectively. Individual HCAs were dissolved in anhydrous methanol in order to yield 10 mM stock solutions. BSA and HCA solutions were prepared fresh before each measurement.

2.3. UV-VIS Absorption Spectroscopy

The UV-VIS spectra were recorded by a spectrophotometer Helios β (Spectronic Unicam, United Kingdom) in a 10 mm quartz cuvette. Quantitative analysis of the potential interaction between HCAs and BSA was performed by the spectroscopic titration. Briefly, solution of BSA (16 μM) was titrated in cuvette by successive additions of HCA solution (10 mM) to a final concentration of 50 μM (the drug to protein molar ratios were 0; 0.25; 0.5; 0.75; 1.0; 1.25; 1.5; 1.75; 2.0; 2.5; and 3.125) and the absorption spectra were recorded from 190 to 550 nm at 37℃.

2.4. Fluorescence Spectroscopy

Fluorescence spectra were recorded using a luminescence spectrometer LS-50B (Perkin Elmer, United Kingdom) in a 10 mm quartz Suprasil fluorescence cuvette (Hellma,

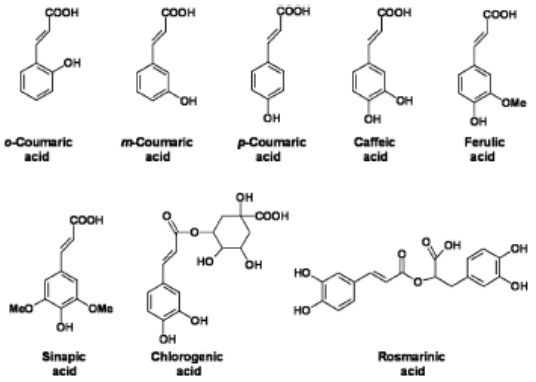

Figure 1. Chemical structures of tested hydroxycinnamic acids.

Germany). Fluorescence emission spectra of individual HCA solutions (25 μM) in sodium phosphate buffer (pH 7.4; 0.1 M; 0.05% sodium azide) were recorded. Quantitative analysis of the potential interaction between HCA and BSA was performed by the fluorimetric titration. Briefly, solution of BSA (2 μM) was titrated in cuvette by successive additions of HCA solution (10 mM) to a final concentration of 20 μM (the drug to protein molar ratios were 0; 1.25; 2.5; 3.75; 5.0; 6.25; 7.5; 8.75; and 10.0). Fluorescence emission spectra were recorded from 300 to 530 nm with excitation at 295 nm while stirring. The excitation and emission slits were both set to 5 nm and scanning speed to 200 nm/min. All experiments were carried out at 37℃. Fluorescence intensity was read at emission wavelength of 350 nm.

2.5. Principles of Fluorescence Quenching

The intensity of fluorescence can be decreased as a result of a wide variety of processes. Such declines in intensity are called quenching and can be caused by different molecular interactions. Dynamic quenching occurs when the excited-state fluorophore is deactivated upon contact with some other molecule (quencher) and no molecule is chemically altered during this process. In the case of static quenching, a non-fluorescent complex is formed between molecules of fluorophore and quencher. The static and dynamic quenching can be distinguished by the Stern-Volmer analysis. In the case the quenching is either purely static or dynamic, the plot shows linear dependence. When the plot of Stern-Volmer diagram shows exponential dependence, both static and dynamic quenching are exerted [6].

Dynamic quenching of fluorescence is described by the well-known Stern-Volmer equation as follows.

$$F_0 / F = 1 + k_q \tau_0 [Q] = 1 + K_D [Q] \quad (1)$$

In this equation, F_0 and F are the fluorescence intensities of BSA in the absence and presence of quencher, respectively, [Q] is the quencher concentration, k_q is the bimolecular quenching constant, and τ_0 is the lifetime of the fluorophore in the absence of quencher (τ_0 is about 5.10^{-9} s, as to Ref. [6 page 256]). The Stern-Volmer quenching constant is given by $k_q\tau_0$. In case the quenching is known to be dynamic, the Stern-Volmer constant will be presented by K_D otherwise this constant will be described as K_S [2,6]. The dynamic quenching depends on diffusion, while static quenching does not. One criterion for distinguishing the type of quenching is the fact that the bimolecular quenching constant k_q is larger than diffusion-limited rate constant of the biomolecule (1×10^{10} $M^{-1} \cdot s^{-1}$) [6], so the static mechanism is the main reason that causes the fluorescence quenching (formation of a complex).

When small molecules bind independently to a set of equivalent sites on a macromolecule, the equilibrium between free and bound molecules is given by the equation:

$$\log(F_0 - F) / F = \log K_b + n \log[Q] \quad (2)$$

where K_b represents binding constant for quencher-protein interaction, n the number of binding sites per BSA, and F_0, F, have the same meaning as in (1) [2]. The values of K_b and n could be determined from the intercept of y-axe and slope by plotting log (F_0 – F)/F against log [Q]. Utilizing K_b, the free energy change (ΔG^0) value can be estimated from the following equation [30]:

$$\Delta G^0 = -RT \ln K_b \quad (3)$$

The negative sing ΔG^0 value confirms the spontaneity of binding.

3. RESULTS

3.1. Spectroscopic Study of Interactions between BSA and HCAs

The UV-VIS absorption spectra of BSA titrated by individual HCAs solution were monitored in order to explore the structural changes of BSA caused by addition of these compounds. Spectral shifts were observed in all HCA-BSA systems with rising concentration of tested compound. Six HCAs (*p*-coumaric, caffeic, ferulic, sinapic, chlorogenic, and rosmarinic acid) induced move of Trp absorption maximum (280 nm) to longer wavelengths which is called bathochromic (red) shift. Maximal spectral shift was about 6 nm. The opposite phenomenon (blue shift) occurred in the absorption spectrum of BSA after interaction with *o*- or *m*-coumaric acid. Absorbance maximum moved about 5 nm towards shorter wavelengths in both cases (data not shown).

3.2. Fluorescence Quenching of BSA in the Presence of HCAs

Quenching of protein intrinsic (tryptophan) fluorescence was employed for more detailed study of HCA-BSA binding. Fluorescence emission spectra were recorded upon excitation at 295 nm, which is attributed to tryptophan residues only. Four individual HCAs (*o*-coumaric, caffeic, sinapic and ferulic acid) possessed remarkable emission maximum at 498, 432, 428 and 414 nm, respectively. The most significant fluorescence intensity showed *o*-coumaric acid. Fluorescence intensities of HCA-BSA systems were read at emission wavelength of 350 nm, where the emission maximum of BSA was located. Protein solution was titrated by successive additions of individual HCA solutions and its fluorescence

intensity gradually decreased with rising concentration of HCA. This may indicate that the microenvironment around tryptophan residues in BSA molecule was altered due to the interaction with tested compound. Fluorescence emission spectrum of *p*-coumaric acid-BSA system is shown in **Figure 2**.

Red shifts of tryptophan emission maximum (350 nm) in dependence on increasing concentration of tested compounds were found in the case of *o*-coumaric, sinapic, chlorogenic, and rosmarinic acid. Emission maximum was slightly shifted towards longer wavelength by 2 nm for both *o*-coumaric and sinapic acid-BSA systems, and by 4 and 5 nm for chlorogenic and rosmarinic acid-BSA system, respectively. Other four tested HCAs did not cause any spectral shift. Emission spectra of *o*-coumaric, caffeic, ferulic, and sinapic acid involved isosbestic point, which might indicate that studied compounds exist both in bound and free form that are in equilibrium. The bound form exerts fluorescence whereas the unbound form does not (**Figure 3**).

It was noticed that emission spectra of these HCA-BSA systems above 430 nm corresponding with emission spectra of individual HCAs.

The type of fluorescence quenching of HCA-BSA systems was distinguished using the Stern-Volmer diagrams in the range of HCA concentrations of 0-20 μM. It was confirmed that the static quenching mechanism is the main reason of protein fluorescence quenching and consecutively the K_S and k_q (1) were determined from the slope of the linear regression curve of F_0/F versus [Q] (**Table 1**). The representative Stern-Volmer diagram of *o*-coumaric-BSA system is displayed in the inset of **Figure 3**. Rosmarinic acid exhibited exponential dependence (**Figure 4**) indicating that both types of quenching

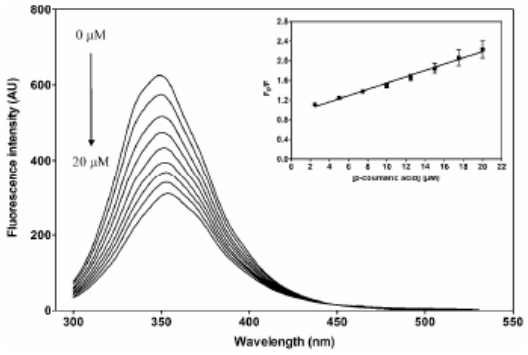

Figure 2. Fluorescence emission spectra of BSA (2 μM) in the absence and in the presence of increasing amounts of *p*-coumaric acid (0-20 μM) in sodium phosphate buffer (pH 7.4; 0.1 M; 0.05% sodium azide) at λ_{ex} = 295 nm and 37℃. The inset shows the corresponding Stern-Volmer diagram of the *p*-coumaric acid-BSA system (λ_{em} = 350 nm), R^2 = 0.9908.

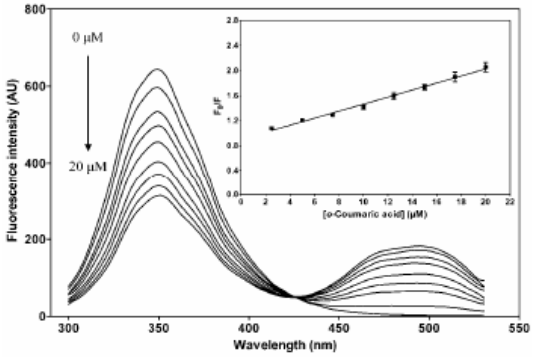

Figure 3. Fluorescence emission spectra of BSA (2 μM) in the absence and in the presence of increasing amounts of *o*-coumaric acid (0-20 μM) in sodium phosphate buffer (pH 7.4; 0.1 M; 0.05% sodium azide) at λ_{ex} = 295 nm and 37℃. The inset shows the corresponding Stern-Volmer diagram of the *o*-coumaric acid-BSA system (λ_{em} = 350 nm), R^2 = 0.9921.

Table 1. The Stern-Volmer quenching constants (K_S) and the bimolecular quenching constants (k_q) of the system of HCA-BSA at 37℃.

Tested compound	$K_S \pm$ S.D.[a] [$\times 10^4$ l.mol^{-1}]	k_q[b] $\pm$ S.D.[a] [$\times 10^{13}$ M^{-1}s^{-1}]
o-coumaric acid	5.95 ± 0.155	1.19 ± 0.031
m-coumaric acid	5.96 ± 0.170	1.19 ± 0.034
p-coumaric acid	7.13 ± 0.190	1.43 ± 0.038
caffeic acid	4.30 ± 0.263	0.86 ± 0.053
ferulic acid	4.86 ± 0.090	0.97 ± 0.018
sinapic acid	4.25 ± 0.209	0.85 ± 0.042
chlorogenic acid	5.36 ± 0.195	1.07 ± 0.039

[a]standard deviation (mean value of three independent experiments); [b]$k_q = K_S/\tau_0$; $\tau_0 = 5.10^{-9}$ s. [6]

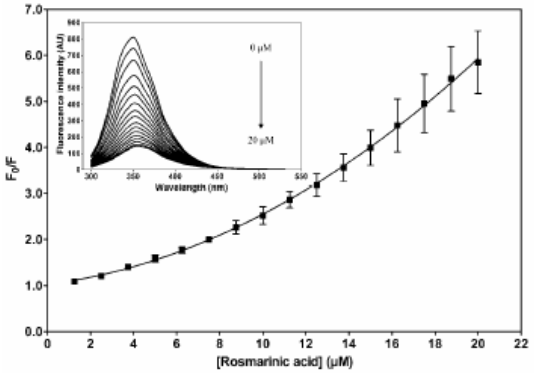

Figure 4. The Stern-Volmer diagram of the rosmarinic acid-BSA system obtained by the titration with rosmarinic acid at 37℃. [BSA] = 2 μM, [rosmarinic acid] = 0-20 μM, pH 7.4, λ_{ex} = 295 nm, λ_{em} = 350 nm. The inset shows the corresponding fluorescence quenching spectra.

were asserted and for this reason the K_S (k_q) of the rosmarinic acid-BSA system was not determined.

It was noticed that emission spectra of these HCA-BSA systems above 430 nm corresponding with emission spectra of individual HCAs.

The type of fluorescence quenching of HCA-BSA systems was distinguished using the Stern-Volmer diagrams in the range of HCA concentrations of 0-20 μM. It was confirmed that the static quenching mechanism is the main reason of protein fluorescence quenching and consecutively the K_S and k_q (1) were determined from the slope of the linear regression curve of F_0/F versus [Q] (**Table 1**). The representative Stern-Volmer diagram of *o*-coumaric-BSA system is displayed in the inset of **Figure 3**. Rosmarinic acid exhibited exponential dependence (**Figure 4**) indicating that both types of quenching were asserted and for this reason the K_S (k_q) of the rosmarinic acid-BSA system was not determined.

3.3. Binding parameters and Binding Mode of BSA-HCA Complexes

Except for the rosmarinic acid-BSA system, the binding constants (K_b), binding sites (n), and free energy changes (ΔG^0) of all other HCA-BSA systems have been determined according to the Equations (2) and (3), respectively. Obtained values are presented in **Table 2** and representative example of binding parameters determination for sinapic acid is displayed in **Figure 5**. The binding affinity was strongest for chlorogenic acid and ranked in the order chlorogenic acid > sinapic acid ≥ caffeic acid > ferulic acid > *o*-coumaric acid > *p*-coumaric acid ≥ *m*-coumaric acid. This order of binding affinities of HCA to BSA was confirmed also by spectral overlaps of BSA emission spectrum with absorption spectrum of individual HCAs. Example of spectral overlap for chlorogenic acid is shown in **Figure 6**. The negative value of ΔG^0 indicating spontaneous process of HCA-BSA binding was determined for all studied interactions (**Table 2**).

Table 2. The binding constants (K_b), the number of binding sites (n) and the free energy change (ΔG^0) of the HCA-BSA system at 37℃ which showed the static quenching mechanism.

Tested compound	$K_b \pm$ S.D.[a] [x10^5 l.mol^{-1}]	n ± S.D.[a]	$\Delta G^0 \pm$ S.D.[a] [kJ.mol^{-1}]
o-coumaric acid	3.34 ± 0.720	1.17 ± 0.012	−32.73 ± 0.563
m-coumaric acid	1.31 ± 0.045	1.08 ± 0.002	−30.36 ± 0.088
p-coumaric acid	1.81 ± 0.728	1.10 ± 0.027	−30.98 ± 1.096
caffeic acid	4.16 ± 1.659	1.18 ± 0.011	−33.12 ± 1.088
ferulic acid	3.39 ± 0.802	1.18 ± 0.019	−32.75 ± 0.621
sinapic acid	4.19 ± 0.117	1.21 ± 0.004	−33.36 ± 0.072
chlorogenic acid	6.67 ± 0.837	1.23 ± 0.016	−34.55 ± 0.325

[a]standard deviation (mean value of three independent experiments)

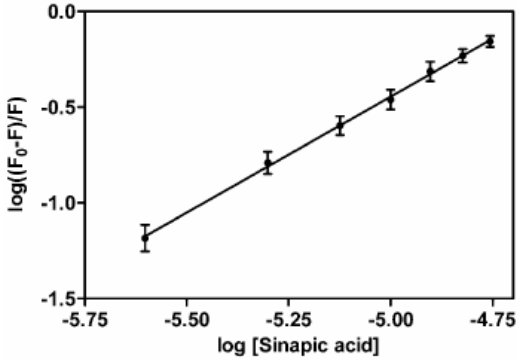

Figure 5. Logarithmic plots of fluorescence quenching of BSA treated with different concentrations of sinapic acid at physiological conditions (37℃; pH 7.4). [BSA] = 2 μM, [sinapic acid] = 0 – 20 μM, λ_{ex} = 295 nm and λ_{em} = 350 nm. R^2 = 0.9988.

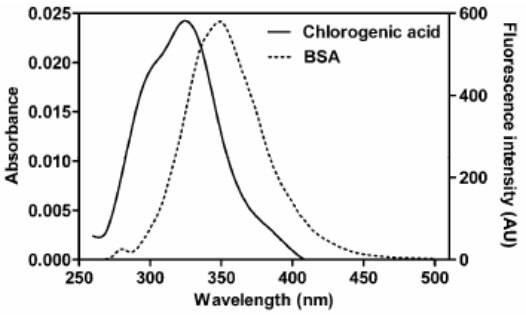

Figure 6. Overlap between the fluorescence emission spectrum of BSA and the absorption spectrum of chlorogenic acid at physiological conditions (37℃; pH 7.4). [BSA] = 2 μM, [chlorogenic acid] = 2 μM, λ_{ex} = 295 nm and λ_{em} = 350 nm.

4. DISCUSSION

Red shift in absorption maximum of tryptophan residues indicates changes in its microenvironment, where the polypeptide strand of BSA molecule is less extended and the hydrophobicity around Trp is increased. The conformational stability, rigidity, mechanical strength, and contributions of electrostatic interactions are enhanced by absence of water in the molecular interior [31]. On the other hand, blue shift implies that the BSA polypeptide strands are more extended and the hydrophocibity of Trp vicinity is decreased.

The changes in tryptophan microenvironment polarity are probably related to chemical structure of each HCA, namely to the number and position of hydroxyl groups. Hydrophobicity around tryptophan residues rose with increasing number of hydroxyl groups in the molecule of

HCA. However, the position of hydroxyl groups on the benzene ring seemed to be also important. Only *o*- and *m*-monosubstituted derivatives of cinnamic acid (*o*-coumaric and *m*-coumaric acid) caused increase in the polarity of Trp environment, while *p*-monosubstituted (*p*-coumaric acid), di- and tri-substituted derivatives showed opposite effect.

Emission spectra of BSA were measured using excitation wavelength at 295 nm to ensure that the light caused excitation only of tryptophan residues. These are highly susceptible to any change in their local environment resulting in appearance of a substantial spectral shift [6]. In contrast to absorption spectroscopy, the red shift of Trp emission band is caused by decrease in hydrophobic property of its environment in protein molecule suggesting that tryptophan residue has been brought to more hydrophilic environment [3] and protein secondary structure has been changed [26].

Red shift in emission spectra of four studied hydroxycinnamic acids (*o*-coumaric, sinapic, chlorogenic, and rosmarinic acid), which indicated that binding of these compounds to BSA was associated with changes in the dielectric environment of at least one of its two indole rings, was observed. Only slight blue shift and no shift were noticed during interaction of cinnamic acid with BSA and HSA, respectively [1,2]. It can be expected that changes found in emission spectra of HCA-BSA systems were connected with alterations in microenvironment of Trp-134 because Trp-212 in BSA molecule is in the similar position as Trp-214, where cinnamic acid caused no spectral shift of its emission band. Increasing number of hydroxyl groups in the molecule of HCA was accompanied by decline of hydrophobicity around Trp. The significant changes in BSA emission spectrum were observed after its interaction with chlorogenic or rosmarinic acid. Other authors described red shifts by 3 to 18 nm in HSA spectrum upon reaction with *p*-coumaric, ferulic, sinapic, and chlorogenic acid [2,3,25] but the concentrations applied in these experiments were higher (up to 150 μM) than those used in presented work.

The natural lifetime for the biological macromolecules (τ_0) is generally given as 10^{-8} s [1,3]. However, the value for BSA is more precisely estimated as 5×10^{-9} s [6]. The latter mentioned value was used in this study for calculation of bimolecular quenching constants (k_q) which reflect efficiency of quenching or the accessibility of the fluorophores to the quencher. The fact that the value of k_q is higher than the value of the diffusion-limited rate constant of the biomolecule (1×10^{10} $M^{-1} \cdot s^{-1}$) is one of the criterions for determination of static mechanism of quenching [1,6].

Only small but significant differences among k_q values for the tested HCA-BSA systems were observed. All tested HCAs exerted better quenching effect than cinnamic acid (2.26×10^{12} $M^{-1} \cdot s^{-1}$ for $\tau_0 = 10^{-8}$ s) [1]. Rosmarinic acid caused the most outstanding decrease in fluorescence intensity of BSA in the range of studied concentrations but it exhibited exponential dependence in the Stern-Volmer diagram and thus was not considered in overall comparison. Coumaric acids showed stronger quenching activity than the other more substituted HCAs. This effect was probably dependent upon the position of hydroxyl group on aromatic ring and *p*-position was determined as the most suitable location of hydroxyl group. The k_q value of chlorogenic acid was similar to k_q of coumaric acids and slightly higher than k_q of more substituted derivatives (**Table 1**). It was probably caused by the presence of five hydroxyl groups in its molecule and their spatial arrangement [3]. The lowest quenching effect was observed for sinapic and caffeic acid followed by ferulic acid. Presence of methoxy group seemed to be important for quenching activity too. Ferulic acid showed higher effect than caffeic acid, while the k_q of sinapic acid was slightly lower compared to caffeic acid. This was perhaps caused by steric hindrance in molecule of sinapic acid. The obtained bimolecular quenching constant for chlorogenic acid-BSA system is in good agreement with data found in literature [19]. However, published data are inconsistent and even in one case no quenching by chlorogenic acid was observed [20]. More studies were published for some HCA-HSA systems. The highest k_q was obtained for chlorogenic acid followed by caffeic and sinapic, while ferulic and *p*-coumaric acid possessed lower k_q values. Data obtained for HCA-BSA systems in this study corresponded with these findings by other authors [2,3].

In general, the binding constant K_b reflects the power of ligand-protein association and thus can be used for comparison of binding affinities of structurally-related ligands to protein molecule connected with alterations of its secondary structure. Number of binding sites is another important parameter that contributes to better understanding of ligand-protein interaction [1-3].

The binding constant K_b for cinnamic acid-BSA system mentioned in the literature [1,2] is lower than values obtained in our experiments for HCA-BSA systems, which may confirm significance of hydroxyl groups in the process of binding. Moreover, binding affinity of cinnamic acid is higher for BSA than for HSA, which indicates that also binding of HCAs to BSA may be more pronounced [2]. It was demonstrated that interaction of HCAs with protein molecule depends mainly on the size and structure of ligand, especially on the number and position of hydroxyl groups on the aromatic ring [20,32]. Hydroxyl groups of studied compounds form hydrogen bonds with amino acid residues in the protein

molecule. Another important factor influencing ligand-protein binding is aromaticity of the ligand molecule because hydrophobic interactions are formed between aromatic rings of ligand and amino acid residues [25]. Chlorogenic acid with two aromatic hydroxyls and three hydroxyls on cyclohexane ring exerted the strongest binding affinity because this compound can form hydrogen bonds with protein more easily than other less-substituted HCAs, e.g. ferulic acid. Similar results were published also for ferulic acid-HSA and chlorogenic acid-HSA system [3]. It is evident that the hydroxyls substituted on aromatic ring of the HCAs play an important role in the changes of BSA secondary structure. Monosubstituted HCAs possessed the lowest binding affinities of all HCAs studied. The differences among binding affinities of sinapic, ferulic and caffeic acid were not statistically significant.

The binding parameters of chlorogenic and ferulic acid with bovine serum albumin have been intensively studied by other authors, while no information about other HCAs was found in the literature. The value of K_b reported by Tang *et al.* [19] for chlorogenic acid-BSA system using fluorescence quenching method is lower than value obtained in performed experiments, but the authors used higher concentrations of chlorogenic acid and different experimental conditions. Moreover, Rawel *et al.* [20,21] reported that chlorogenic acid does not quench Trp fluorescence in BSA and determined its binding constant by Hummel-Dreyer/size exclusion chromatography which showed significantly lower value of K_b in comparison with results presented by Tang *et al.* [19]. Non-covalent interactions of chlorogenic acid with BSA have been studied by Prigent *et al.* [33], who reported that these interactions decrease with the increasing temperature while pH and ionic strength had no pronounced effect. Zhang *et al.* [34] reported the K_b for ferulic acid-BSA system determined by affinity capillary electrophoresis which is in good agreement with our result. By contrast, Rawel *et al.* [20] determined binding constant of ferulic acid-BSA system by fluorescence quenching method and Hummel-Dreyer/size exclusion chromatography, where first method gave similar results to our data and K_b obtained by second method was significantly lower. However, several studies dealing with binding of *p*-coumaric, caffeic, ferulic, sinapic acid, and chlorogenic acid with HSA have been published [2,3,25].

The results showed that the numbers of binding sites ranged between 1.08 and 1.23 suggesting that one molecule of BSA was associated with one molecule of HCA in the drug to protein ratio up to 10 for the tested HCAs apart. The number of binding sites rose with increasing number of hydroxyl groups in the ligand molecule.

The free enthalpy had negative sign for all studied interactions which indicates the spontaneity of the interaction between BSA and hydroxycinnamic acids. The relatively strong binding enthalpy underlines the stability of BSA-HCA complexes from the energetic point of view. These findings are supported by data found in literature [1,20,21].

5. CONCLUSIONS

Apart from rosmarinic acid, all tested HCAs quenched tryptophan fluorescence of BSA in the studied range of concentrations (0-20 μM) mainly by static quenching mechanism and thus showed the formation of non-fluorescent HCA-BSA complexes. For this reason the rosmarinic acid-BSA system was not concluded in the overall assessment of binding affinities. The obtained results suggest that the binding affinity and number of binding sites depend on the number and position of hydroxyl groups in the molecule of HCA. Disubstituted and trisubstituted derivatives exhibited stronger binding affinity than monosubstituted derivatives. The number of binding sites for all HCAs ranged from 1.08 to 1.23 suggesting that one molecule of BSA associates with one molecule of HCA. All HCA-BSA interactions were spontaneous processes based on ΔG^0. The results imply that HCAs could be stored and transported in blood by serum albumin which may influence their biological and pharmacological activities. On the other hand, physiological functions of this protein could be altered by ligand binding.

6. ACKNOWLEDGEMENTS

The presented study was supported by the Specific research 2009 of the University of Hradec Králové.

REFERENCES

[1] Bian, H., Zhang, H., Yu, Q., Chen, Z. and Liang, H. (2007) Studies on the interaction of cinnamic acid with bovine serum albumin. *Chemical & Pharmaceutical Bulletin*, **55(6)**, 871-875.

[2] Jiang, M., Xie, M.X., Zheng, D., Liu, Z., Li, X.Y. and Chen, X. (2004) Spectroscopic studies on the interaction of cinnamic acid and its hydroxyl derivatives with human serum albumin. *Journal of Molecular Structure*, **692(1-2)**, 71-80.

[3] Kang, J., Liu, Y., Xie, M.X., Li, S., Jiang, M. and Wang, Y.D. (2004) Interactions of human serum albumin with chlorogenic acid and ferulic acid. *Biochimica et Biophysica Acta*, **1674(2)**, 205-214.

[4] Peters, T. (1996) All about albumin: Biochemistry, genetics, and medical applications. Academic Press, San Diego.

[5] Carter, D.C. and Ho, J.X. (1994) Structure of serum albumin. *Advances in Protein Chemistry*, **45**, 153-203.
[6] Lakowicz, J. R. (2004) Principles of Fluorescence Spectroscopy, 2nd Edition. Springer, New York.
[7] Behrens, P.Q., Spiekerman, A.M. and Brown, J.R. (1975) Structure of bovine serum-albumin. *Federation Proceedings*, **34(3)**, 591.
[8] Kragh-Hansen, U. (1981) Molecular aspects of ligand binding to serum albumin. *Pharmacological Reviews*, **33(1)**, 17-53.
[9] Dewick, P. M. (2002) Medicinal natural products: A biosynthetic approach, 2nd Edition. Wiley, Chichester.
[10] Harborne, J.B. and Williams, C.A. (2000) Advances in flavonoid research since 1992. *Phytochemistry*, **55(6)**, 481-504.
[11] Rice-Evans, C.A., Miller, N. and Paganga, G. (1997) Antioxidant properties of phenolic compounds. *Trends in Plant Science*, **2(4)**, 152-159.
[12] Natarajan, K., Singh, S., Burke, T.R., Grunberger, D. and Aggarwal, B.B. (1996) Caffeic acid phenethyl ester is a potent and specific inhibitor of activation of nuclear transcription factor NF-kappa B. *Proceedings of the National Academy of Sciences of the United States of America*, **93(17)**, 9090-9095.
[13] Pannala, A.S., Razaq, R., Halliwell, B., Singh, S. and Rice-Evans, C.A. (1998) Inhibition of peroxynitrite dependent tyrosine nitration by hydroxycinnamates: Nitration or electron donation? *Free Radical Biology and Medicine*, **24(4)**, 594-606.
[14] Natella, F., Nardini, M., Di Felice, M. and Scaccini, C.J. (1999) Benzoic and cinnamic acid derivatives as antioxidants: Structure-activity relation. *Journal of Agricultural and Food Chemistry*, **47(4)**, 1453-1459.
[15] Rice-Evans, C.A., Miller, N.J. and Paganga, G. (1996) Structure-antioxidant activity relationships of flavonoids and phenolic acids. *Free Radical Biology and Medicine*, **20(7)**, 933-956.
[16] Graf, E. (1992) Antioxidant potential of ferulic acid. *Free Radical Biology and Medicine*, **13(4)**, 435-448.
[17] Kanakis, C.D., Tarantilis, P.A., Polissiou, M.G., Diamantoglou, S. and Tajmir-Riahi, H.A. (2006) Antioxidant flavonoids bind human serum albumin. *Journal of Molecular Structure*, **798(1-3)**, 67-74.
[18] Tian, J., Liu, J., Hu, Z. and Chen, X. (2005) Interaction of wogonin with bovine serum albumin. *Bioorganic & Medicinal Chemistry*, **13(12)**, 4124-4129.
[19] Tang, D., Li, H.J., Wen, X.D. and Qian, Z.M. (2008) Interaction of bioactive components caffeoylquinic acid derivatives in chinese medicines with bovine serum albumin. *Chemical & Pharmaceutical Bulletin*, **56(3)**, 360-365.
[20] Rawel, H.M, Frey, S.K., Meidtner, K., Kroll, J. and Schweigert, F.J. (2006) Determining the binding affinities of phenolic compounds to proteins by quenching of the intrinsic tryptophan fluorescence. *Molecular Nutrition & Food Research*, **50(8)**, 705-713.
[21] Rawel, H.M, Meidtner, K. and Kroll, J. (2005) Binding of selected phenolic compounds to proteins. *Journal of Agricultural and Food Chemistry*, **53(10)**, 4228-4235.
[22] Rawel, H.M, Rohn, S., Kruse, H.P. and Kroll, J. (2002) Structural changes induced in bovine serum albumin by covalent attachment of chlorogenic acid. *Food Chemistry*, **78(4)**, 443-455.
[23] Tian, J., Liu, J., Tian, X., Hu, Z. and Chen, X. (2004) Study of the interaction of kaempferol with bovine serum albumin. *Journal of Molecular Structure*, **691(1-3)**, 197-202.
[24] Papadopoulou, A., Green, R.J. and Frazier, R.A. (2005) Interaction of flavonoids with bovine serum Albumin: A fluorescence quenching study. *Journal of Agricultural and Food Chemistry*, **53(1)**, 158-163.
[25] Liu, Y., Xie, M.X., Jiang, M. and Wang, Y.D. (2005) Spectroscopic investigation of the interaction between human serum albumin and three organic acids. *Spectrochimica Acta Part A*, **61(9)**, 2245-2251.
[26] He, W., Li, Y., Xue, C., Hu, Z., Chen, X. and Sheng, F. (2005) Effect of Chinese medicine alpinetin on the structure of human serum albumin. *Bioorganic & Medicinal Chemistry*, **13(5)**, 1837-1845.
[27] Xie, M.X., Long, M., Liu, Y., Qin, C. and Wang, Y.D. (2006) Characterization of the interaction between human serum albumin and morin. *Biochimica et Biophysica Acta*, **1760(8)**, 1184-1191.
[28] Xie, M.X., Xu, X.Y. and Wang, Y.D. (2005) Interaction between hesperetin and human serum albumin revealed by spectroscopic methods. *Biochimica et Biophysica Acta*, **1724(1-2)**, 215-224.
[29] Liu, J., Tian, J., Li, Y., Yao, X., Hu, Z. and Chen, X. (2004) Binding of the bioactive component daphnetin to human serum albumin demonstrated using tryptophan fluorescence quenching. *Macromolecular Bioscience*, **4(5)**, 520-525.
[30] Shang, L., Jiang, X. and Dong, S. (2006) In vitro study on the binding of neutral red to bovine serum albumin by molecular spectroscopy. *Journal of Photochemistry and Photobiology A*, **184(1-2)**, 93-97.
[31] Hu, Y.J., Liu, Y., Zhao, R.M., Dong, J.X. and Qu, S.S. (2006) Spectroscopic studies on the interaction between methylene blue and bovine serum albumin. *Journal of Photochemistry and Photobiology A*, **179(3)**, 324-329.
[32] Bartolome, B., Estrella, I. and Hernandez, M.T. (2000) Interaction of low molecular weight phenolics with proteins (BSA). *Journal of Food Science*, **65(4)**, 617-621.
[33] Prigent, S.V.E., Gruppen, H., Visser, A.J.W.G., van Koningsveld, G.A., de Jong, G.A.H. and Voragen, A.G.J. (2003) Effects of non-covalent interactions with 5-O-caffeoylquinic acid (chlorogenic acid) on the heat denaturation and solubility of globular proteins. *Journal of Agricultural and Food Chemistry*, **51(17)**, 5088-5095.
[34] Zhang, Y., Xu, M., Du, M. and Zhou, F. (2007) Comparative studies of the interaction between ferulic acid and bovine serum albumin by ACE and surface plasmon resonance. *Electrophoresis*, **28(11)**, 1839-1845.

Journal of Molecular Structure 985 (2011) 243–250

Contents lists available at ScienceDirect

Journal of Molecular Structure

journal homepage: www.elsevier.com/locate/molstruc

Study on the interaction of catechins with human serum albumin using spectroscopic and electrophoretic techniques

Lucie Trnková [a,b,*], Iva Boušová [a], Veronika Staňková [a], Jaroslav Dršata [a,b]

[a] Department of Biochemical Sciences, Charles University in Prague, Faculty of Pharmacy, Heyrovského 1203, 500 05 Hradec Králové, Czech Republic
[b] Department of Chemistry, Faculty of Science, University of Hradec Králové, Rokitanského 62, 500 03 Hradec Králové, Czech Republic

ARTICLE INFO

Article history:
Received 26 August 2010
Received in revised form 31 October 2010
Accepted 1 November 2010
Available online 6 November 2010

Keywords:
Human serum albumin
Catechin
Fluorescence quenching
UV–Vis absorption spectroscopy
Electrophoresis
Protein–ligand binding

ABSTRACT

The interaction between eight naturally occurring flavanols (catechin, epicatechin, gallocatechin, epigallocatechin, catechin gallate, epicatechin gallate, gallocatechin gallate, and epigallocatechin gallate) and human serum albumin (HSA) has been investigated by spectroscopic (fluorescence quenching and UV–Vis absorption) and electrophoretic (native and SDS PAGE) techniques under simulated physiological conditions (pH 7.40, 37 °C). The spectroscopic results confirmed the complex formation for the tested systems. The binding constants and the number of binding sites were obtained by analysis of fluorescence data. The strongest binding affinity to HSA was found for epicatechin gallate and decreased in the order epicatechin gallate ⩾ catechin gallate > epigallocatechin gallate > gallocatechin gallate ⩾ epicatechin ⩾ catechin > gallocatechin ⩾ epigallocatechin. All free energy changes possessed negative sign indicating the spontaneity of catechin–HSA systems formation. The binding distances between the donor (HSA) and the acceptors (catechins) estimated by the Förster theory revealed that non-radiation energy transfer from HSA to catechins occurred with high possibility. According to results obtained by native PAGE, the galloylated catechins increased the electrophoretic mobility of HSA, which indicated the change in the molecular charge of HSA, whilst the non-galloylated catechins caused no changes. The ability of aggregation and cross-linking of tested catechins with HSA was not proved by SDS–PAGE. The relationship between the structure characteristics of all tested catechins (e.g. presence of the galloyl moiety on the C-ring, the number of hydroxyl groups on the B-ring, and the spatial arrangement of the substituents on the C-ring) and their binding properties to HSA is discussed. The presented study contributes to the current knowledge in the area of protein–ligand binding, particularly catechin–HSA interactions.

1. Introduction

The interaction between macromolecules (e.g. proteins) and drugs (e.g. flavonoids) has attracted a great interest among researchers for several decades [1–4]. Serum albumin is the most abundant protein in the circulatory system and one of its most outstanding properties is the ability to reversibly bind a large variety of endogenous and exogenous ligands, such as nutrients, hormones, fatty acids, and many diverse drugs [5]. It is well known that the deposition, transportation, metabolism, and efficacy of drugs are strongly affected by their binding to serum albumin [6]. On the other hand, drugs can cause various changes in protein conformation influencing its physiological functions. Such impaired proteins may be consequently accumulated in body tissues. Therefore, the studies of serum albumin–drug interactions play an important role in pharmacology and pharmacodynamics.

Human serum albumin (HSA) consists of 585 amino acids in a single polypeptide chain cross-linked with 17 disulfide bonds. The crystallographic analysis of HSA revealed that the protein contains three structurally similar domains (I–III), which assemble to form heart-shaped molecule. Each of these domains is further divided into two subdomains (A and B). It was found out that aromatic and heterocyclic ligands bind within two hydrophobic pockets in subdomains IIA and IIIA [7]. HSA has only one tryptophan residue (Trp-214) within a hydrophobic binding pocket of subdomain IIA, which significantly contributes to the intrinsic fluorescence of the protein. Therefore, the fluorescence spectroscopy can easily reveal changes in the microenvironment of the tryptophan residue and be used for determining the binding affinities [8].

Catechins (flavan-3-ols) are plant polyphenolic compounds occurring in higher concentrations in beans, black grapes, cherries, pears and chocolate [9]. The most important and rich natural source of catechins is undoubtedly green tea (*Camellia sinensis*,

* Corresponding author at: Department of Biochemical Sciences, Charles University in Prague, Faculty of Pharmacy, Heyrovského 1203, CZ-500 05 Hradec Králové, Czech Republic. Tel.: +42 0493331159; fax: +42 0495512665.
E-mail addresses: Lucie.Trnkova@faf.cuni.cz (L. Trnková), Iva.Bousova@faf.cuni.cz (I. Boušová), STANV5AA@faf.cuni.cz (V. Staňková), Jaroslav.Drsata@faf.cuni.cz (J. Dršata).

0022-2860/$ - see front matter © 2010 Elsevier B.V. All rights reserved.
doi:10.1016/j.molstruc.2010.11.001

Theaceae), which is one of the most widely consumed beverages in the world. The major green tea catechins are (−)-epigallocatechin, (−)-epicatechin, (−)-epicatechin gallate and (−)-epigallocatechin gallate, the most important active compound. They are responsible for beneficial health effects of the green tea in the prevention or treatment of various diseases such as cancer, heart diseases, diabetes and neurodegenerative disease. These active compounds have been reported to possess also antioxidant, anti-inflammatory, antimicrobial and antiviral effects [10,11]. However, catechins were noticed to show also negative effects such as pro-oxidative, cyto- and phytotoxic activities [11–14]. It is well known that structural features, namely the number of the galloyl and hydroxyl groups in the molecule of catechins, play an important role in their biological activities, particularly antioxidant properties [15,16]. The catechin structures also suggest the possibility of their binding to the molecules of enzymes and other proteins [17].

The spectroscopic techniques, such as fluorescence spectroscopy, UV–Vis absorption spectroscopy, circular dichroism spectroscopy (CD), and Fourier transform infrared spectroscopy (FTIR), have become popular methods for revealing drug–protein interactions because of their high sensitivity, rapidity, and ease of implementation. They allow non-destructive measurements of substances in low concentration under various experimental conditions [18–23]. These techniques provide the binding information and reflect the conformation changes of proteins in various environments.

Some spectroscopic studies on the interaction between serum albumin and catechins have been published, namely catechin and epicatechin [2,24], epigallocatechin [24] and epigallocatechin gallate [18,25], as well as some non-spectroscopic studies, e.g. determination of binding parameters by capillary electrophoresis (catechin and epicatechin) [3] or isothermal titration calorimetry (epicatechin) [26]. Nevertheless, these data are hardly comparable because of different techniques used and various experimental conditions (e.g. pH, temperature, excitation wavelength used). Recently, binding ability of tea catechins and their analogs with HSA have been investigated by HPLC analysis with immobilized albumin column [17].

In the presented work, the binding affinity of eight naturally occurring catechins to HSA has been investigated in detail by fluorescence spectroscopy in combination with UV–Vis absorption spectroscopy and electrophoretic methods under simulated physiological conditions (pH 7.4; 37 °C). The main objective of the study was to reveal the character of interactions and evaluate structure–activity relationships within the group of catechins (effect of the galloyl moiety on the C-ring, the number of hydroxyl groups in the B-ring and the spatial arrangement of the substituents on the C-ring). The presented study contributes to the current knowledge in the area of protein–ligand binding, particularly catechins–HSA interactions.

2. Experimental

2.1. Chemicals and preparation of stock solutions

Human serum albumin and all catechins were obtained from Sigma–Aldrich GmbH, Germany. The chemical structures of tested compounds are presented in Fig. 1. All other chemicals were of analytical grade.

Human serum albumin was dissolved in sodium phosphate buffer (pH 7.4; 0.1 M; 0.05% sodium azide) in order to yield solutions with concentration 4×10^{-6} M and 15×10^{-6} M for spectroscopic measurements, and electrophoresis, respectively. Individual catechins were dissolved in methanol in order to yield 1×10^{-2} M stock solutions.

2.2. UV–Vis absorption spectroscopy

The UV–Vis absorption measurements were carried out using a spectrophotometer Helios β (Spectronic Unicam, United Kingdom) in a 10 mm quartz cuvette. The concentrations of HSA and individual catechins were 4×10^{-6} M and 4×10^{-5} M, respectively. All samples were incubated for 5 min at 37 °C. The UV–Vis absorption spectra were recorded from 190 to 550 nm at 37 °C. The spectrum of sodium phosphate buffer (pH 7.4; 0.1 M; 0.05% sodium azide) with or without appropriate catechin was subtracted.

2.3. Fluorescence spectroscopy

Fluorescence spectra were recorded using a luminescence spectrometer LS-50B (Perkin Elmer, United Kingdom) in a 10 mm quartz Suprasil fluorescence cuvette (Hellma, Germany). Quantitative analysis of the potential interaction between catechins and HSA was performed by the fluorimetric titration. Briefly, solution of HSA (4×10^{-6} M) was titrated in cuvette by successive additions of individual catechin solutions (1×10^{-2} M) to a final concentration of 2×10^{-5} M. Fluorescence emission spectra were recorded from 290 to 530 nm with excitation at 295 nm under continuous stirring. The excitation and emission slits were both set to 5 nm and scanning speed was 200 nm/min. All experiments were carried out at 37 °C. Fluorescence intensity was read at protein emission maximum of 348 nm. Fluorescence spectra of individual catechins in buffer (0–2×10^{-5} M) were recorded as blanks under the same experimental conditions and subtracted from the corresponding sample to correct the fluorescence background [2].

Fluorescence emission spectra of individual catechins (4×10^{-5} M) with or without HSA (4×10^{-6} M) were also recorded at the excitation wavelength of 330 nm, which corresponds to the absorption maximum of ground state complex.

2.4. Preparation of incubation mixtures for electrophoresis

Samples with and without (controls) tested catechins were prepared. Protein concentration in all samples was 15×10^{-6} M and concentration of catechins was 6×10^{-4} M. Samples were incubated for 30 min at 37 °C and further analyzed using polyacrylamide gel electrophoresis under denaturating (SDS–PAGE) or non-denaturating (native PAGE) conditions.

2.5. Native electrophoresis

Native PAGE was performed in discontinuous system with 4% stacking gel and 10% separating non-denaturating gel. All lanes were loaded with 8 μg of protein. Electrophoresis was performed at 30 mA using Mini ProteanIII apparatus (BioRad). The gel was stained with colloidal Coomassie Blue G250, scanned by GelDoc XR system (BioRad), and the relative mobilities (R_f) were calculated using Quantity One software (BioRad). Results were further expressed as a rise in percentage of sample mobility compared to the native protein (control): $[(R_f(\text{complex}) - R_f(\text{HSA}))/R_f(\text{HSA})] \times 100$ (%).

2.6. SDS–PAGE electrophoresis

SDS–PAGE was performed using discontinuous system with 4% stacking gel and 7.5% separating non-denaturating gel. All lanes were loaded with 4 μg of protein. Electrophoresis was performed at 200 V using Mini ProteanIII apparatus (BioRad). Gels were visualized with colloidal Coomassie Blue G250, scanned, and their quantification was performed using Quantity One software (BioRad).

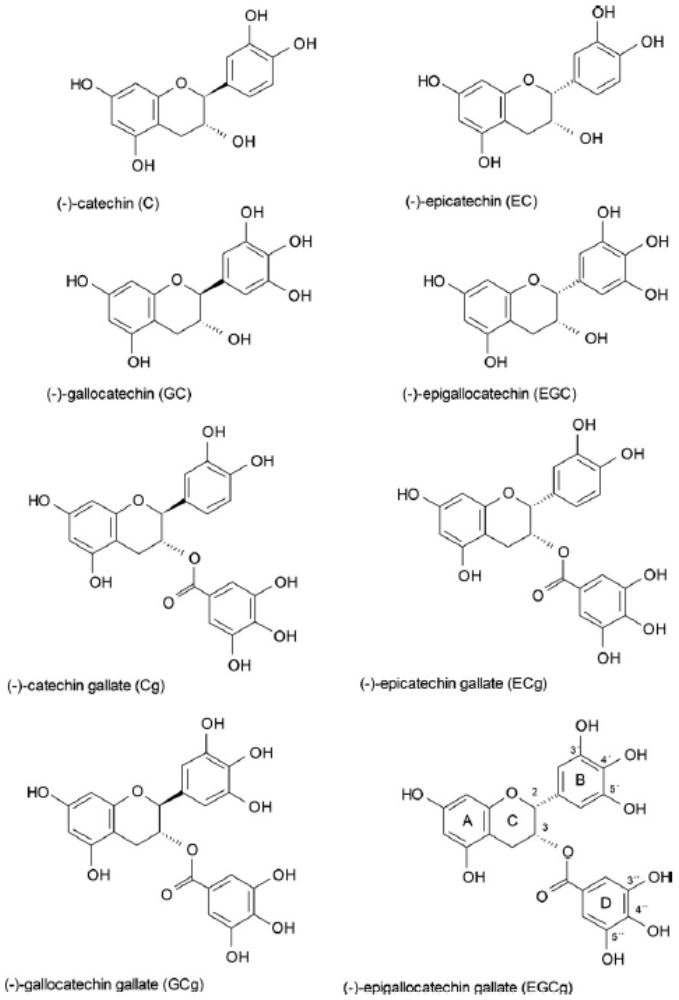

Fig. 1. Chemical structures of tested catechins.

2.7. Statistical analysis

All measurements were performed in triplicates and the mean values of determined constants were calculated. All standard deviations (S.D.) were lower than 10%. Statistical significance was determined using Student's *t*-test and differences were significant when $p < 0.01$.

3. Results

3.1. UV–Vis absorption spectra of catechin–HSA systems

UV–Vis absorption measurement is a very simple but effective method to explore the structural change and the complex formation [20]. In the present study, the absorption spectra of HSA in the absence and presence of individual catechins were recorded after 5 min of interaction. Stabilities of all compounds under experimental conditions (pH 7.4, 37 °C) were verified by recording their individual UV–Vis absorption spectra after 5 min of incubation. No changes in UV–Vis spectra were observed.

No changes were noticed in absorption spectra of HSA after interaction with catechins lacking the galloyl moiety on the C-ring (catechin, epicatechin, gallocatechin, and epigallocatechin). On the other hand, the obvious changes, such as slight decrease of absorbance between 200 and 280 nm, significant growth of absorbance between 300 and 360 nm (λ_{max} = 330 nm) and slight red shift, in absorption spectrum of HSA after addition of the galloylated catechins (catechin gallate, epicatechin gallate, gallocatechin gallate, and epigallocatechin gallate) confirmed the complex formation [27]. The differential absorption spectrum of HSA after interaction with epicatechin gallate is displayed in Fig. 2.

3.2. Fluorescence spectra of catechins and catechin–HSA systems

As was described above, the complex formation between HSA and catechin gallates was noticed at their UV–Vis absorption

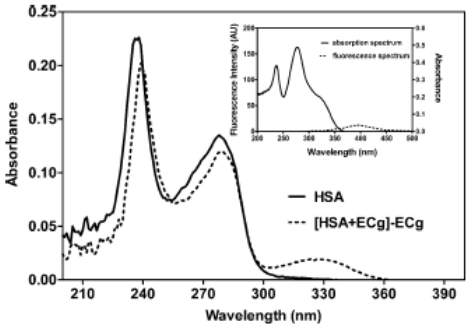

Fig. 2. UV–Vis absorption spectra of HSA before and after interaction with epicatechin gallate (pH 7.4, 37 °C, 5 min). The inset shows the absorption and fluorescence spectrum of epicatechin gallate. [HSA] = 4×10^{-6} M and [ECg] = 4×10^{-5} M, and λ_{ex} = 295 nm.

spectra. Subsequently, the emission spectra of these complexes were recorded with the excitation at 330 nm, which corresponds with the observed absorption maximum. All complexes emitted light between 374 and 377 nm (Fig. 3), whereas catechin gallates as well as other catechins alone were not emissive under these experimental conditions.

Fluorescence emission spectra of individual catechins were recorded at excitation wavelength of 295 nm, which corresponds to the tryptophan. Only, catechin and epicatechin possessed intrinsic fluorescence and both displayed the similar spectra with emission maximum of 318 nm (Fig. 4A). The observed wavelength of their emission maximum is consistent with literature [2]. Other catechins showed no significant emission spectra at this excitation wavelength (the inset of Figs. 2 and 4B).

3.3. Fluorescence quenching spectra of HSA induced by catechins

Quenching of protein intrinsic (tryptophan) fluorescence was employed for more detailed study of catechin–HSA interactions. Fluorescence emission spectra were recorded upon excitation at 295 nm, which is attributed to tryptophan residues only. Fluorescence intensity of HSA gradually decreased with rising concentration of all tested compounds (Fig. 4). This may indicate that the microenvironment of tryptophan residue (Trp-214) in HSA molecule was altered due to the interaction with tested compounds. Catechin gallates induced considerable red shift of the HSA emission maximum (348 nm) depending on increasing concentration

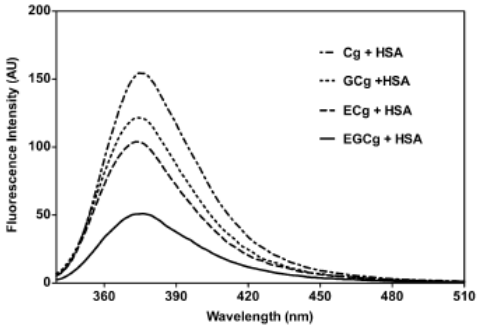

Fig. 3. Fluorescence emission spectra of tested catechin gallate–HSA systems (pH 7.4, 37 °C). [HSA] = 4×10^{-6} M, [catechin gallate] = 4×10^{-5} M, and λ_{ex} = 330 nm.

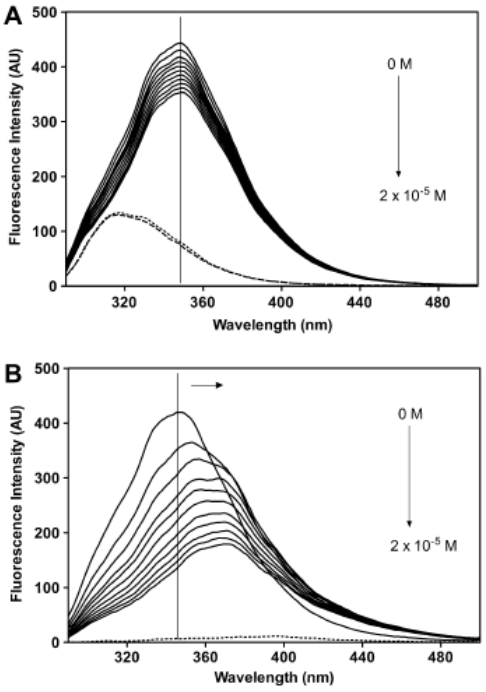

Fig. 4. Fluorescence quenching spectra of selected catechin–HSA systems (pH 7.4, 37 °C). (A) epicatechin–HSA system, epicatechin (2×10^{-5} M, dotted line), and catechin (2×10^{-5} M, dashed line), (B) epicatechin gallate–HSA system and epicatechin gallate (2×10^{-5} M, dotted line). [HSA] = 4×10^{-6} M, [EC] = [ECg] = 0–2×10^{-5} M, and λ_{ex} = 295 nm.

of tested compounds (Fig. 4B). Emission maximum of HSA was shifted towards longer wavelength by 25 nm for both catechin gallate–HSA and epicatechin gallate–HSA system, and by 23 nm for gallocatechin gallate–HSA system as well as for epigallocatechin gallate–HSA system. No isosbestic points were noticed.

3.4. Fluorescence quenching mechanism of catechin–HSA systems

In order to clarify the fluorescence quenching mechanism induced by individual catechins, the fluorescence quenching data were analyzed using the Stern–Volmer equation [8].

$$F_0/F = 1 + K_q\tau_0[Q] = 1 + K_{SV}[Q] \quad (1)$$

In this equation, F_0 and F are the fluorescence intensities of HSA in the absence and presence of the quencher, respectively. [Q] is the quencher concentration, K_{SV} is the Stern–Volmer quenching constant ($K_{SV} = K_q \times \tau_0$), K_q is the bimolecular quenching rate constant, and τ_0 is the lifetime of the fluorophore in the absence of the quencher (τ_0 is about 5×10^{-9} s [8]).

Fluorescence intensities were read at emission wavelength of 348 nm where the emission maximum of HSA was located. The Eq. (1) was applied to determine the bimolecular quenching rate constants (K_q) by linear regression of plots of F_0/F versus [Q] (Fig. 5). Plots were linear in the range of concentration of 0–2×10^{-5} M for all tested systems. The quenching rate constants are summarized in Table 1. The values of K_q for all tested systems are higher than the diffusion-limited rate constant of the biomolecule ($K_{diff} = 1.0 \times 10^{10}$ l mol^{-1} s^{-1}) which confirmed that the static quenching

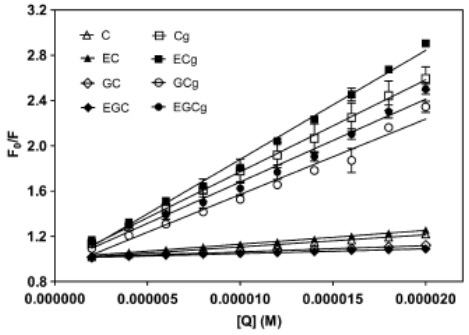

Fig. 5. Stern–Volmer plots of tested catechin–HSA systems (pH 7.4, 37 °C). [HSA] = 4×10^{-6} M, [catechin] = 0–2×10^{-5} M, λ_{ex} = 295 nm, and λ_{em} = 348 nm. Correlation coefficients (R) were found in the range 0.992–0.999.

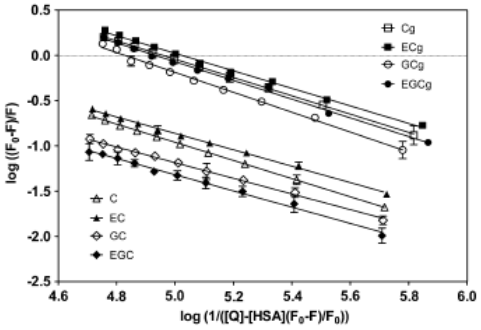

Fig. 6. Logarithmic plots of tested catechin–HSA systems (pH 7.4, 37 °C). [HSA] = 4×10^{-6} M, [catechin] = 0–2×10^{-5} M, λ_{ex} = 295 nm, and λ_{em} = 348 nm. Correlation coefficients (R) were found in the range 0.993–0.999.

mechanism is the main reason of protein fluorescence quenching [8]. The highest value of K_q was determined for epicatechin gallate and further decreased in the order ECg > Cg ⩾ EGCg ⩾ GCg ≫ EC ⩾ C > GC > EGC.

3.5. Determination of binding parameters of catechin–HSA systems

The apparent binding constants (K_b) and the number of binding sites (n) can be calculated using the following equation [19]:

$$\log(F_0 - F)/F = n \log K_b - n \log(1/([Q_t] - (F0 - F)[P_t]/F_0)) \quad (2)$$

where F_0 and F are the fluorescence intensities before and after the addition of the quencher, $[Q_t]$ and $[P_t]$ are the total quencher concentration and the total protein concentration, respectively. The number of binding sites and binding constant can be obtained by plotting $\log(F_0 - F)/F$ versus $\log(1/([Q_t] - (F_0 - F)[P_t]/F_0))$.

Utilizing K_b, the free energy change (ΔG^0) value can be estimated from the following equation [28]:

$$\Delta G^0 = -RT \ln K_b \quad (3)$$

The negative sing of ΔG^0 value confirms the spontaneity of binding.

The binding constants (K_b), binding sites (n), and free energy changes (ΔG^0) of all catechin–HSA systems have been determined according to the Eqs. (2) and (3), respectively. The obtained values are presented in Table 1 and the logarithmic plots for determination of binding parameters are displayed in Fig. 6. The binding affinity was the strongest for epicatechin gallate and decreased in the order ECg ⩾ Cg > EGCg ⩾ GCg ≫ EC ⩾ C > GC ⩾ EGC. The non-galloylated catechins possessed significantly lower binding constants. The value of the number of binding sites (n) ranged from 0.87 to 1.10. Negative values of free energy changes (ΔG^0) for all studied interactions indicate that the binding between HSA and individual catechins proceeds spontaneously.

3.6. The distances between the catechins and HSA

Fluorescence resonance energy transfer (FRET) is a distance-dependent interaction in which is excitation energy transferred non-radiatively from the donor molecule (protein) to the acceptor molecule (drug). The efficiency of energy transfer can be used to evaluate the distance between the ligand and the tryptophan residues in the protein. According to Förster's non-radiative energy transfer theory [8,29], the efficiency of the energy transfer depends on: (a) the extent of overlap between the emission spectrum of the donor and the absorption spectrum of the acceptor, (b) the orientation of the transition dipole of the donor and the acceptor, and (c) the distance between the donor and the acceptor. The efficiency of energy transfer (E) between the donor and the acceptor is given by:

$$E = 1 - (F/F_0) = R_0^6/(R_0^6 + r_0^6) \quad (4)$$

where F_0 and F are the fluorescence intensities of HSA in the absence and presence of catechin, r_0 is the distance between donor and acceptor, and R_0 is the critical distance when the transfer efficiency is 50%. The value of R_0^6 can be calculated using the equation:

$$R_0^6 = 8.8 \times 10^{-25} k^2 N^{-4} \Phi J \quad (5)$$

where k^2 is the spatial orientation factor describing the relative orientation in space of the transition dipoles of the donor and the acceptor, N is the refractive index for the medium, Φ is the fluorescence quantum yield of the donor in the absence of the acceptor, and J is the overlap integral of the emission spectrum of the donor and acceptor absorption spectrum ($cm^3\,l\,mol^{-1}$). J is given by:

Table 1
The bimolecular quenching rate constants (K_q), binding constants (K_b), number of binding sites (n) and free energy change (ΔG^0) of tested catechin–HSA systems (pH 7.4, 37 °C).

Tested compound	K_q [$\times 10^{12}$ $M^{-1}\,s^{-1}$]	K_b [$\times 10^4$ $l\,mol^{-1}$]	n	ΔG^0 [kJ mol^{-1}]
Catechin	2.15^c	1.10^b	1.00	-23.99^b
Epicatechin	2.44^c	1.12^b	0.91	-24.03^b
Gallocatechin	1.10^b	0.43^a	0.87	-21.54^a
Epigallocatechin	0.84^a	0.34^a	0.89	-20.93^a
Catechin gallate	16.25^{de}	9.21^{de}	1.01	-29.46^{de}
Epicatechin gallate	19.26^e	10.57^e	0.97	-29.82^e
Gallocatechin gallate	13.33^d	6.75^c	1.10	-28.66^c
Epigallocatechin gallate	14.65^d	7.79^d	1.03	-29.03^d

$K_q = K_{SV}/\tau_0$; $\tau_0 = 5 \times 10^{-9}$ s [8]. Correlation coefficients (R) were higher than 0.990. Standard deviations (mean value of three independent experiments) were lower than 10%. Data were analyzed by Student's t-test and groups with different letters are significantly different ($p < 0.01$). Differences in the number of binding sites were not statistically significant.

$$J = \Sigma F(\lambda)\varepsilon(\lambda)\lambda^4\Delta\lambda / \Sigma F(\lambda)\Delta\lambda \quad (6)$$

where $F(\lambda)$ is the fluorescence intensity of the donor at wavelength λ, $\varepsilon(\lambda)$ is the molar absorption coefficient of the acceptor at wavelength λ to $\lambda + \Delta\lambda$ (cm^{-1} mol^{-1} l).

The overlaps of the UV–Vis absorption spectra of individual catechins with the fluorescence spectrum of HSA occurred for all tested systems. There was noticed significant effect of the galloyl moiety on the extent of spectral overlapping. The galloylated catechins (Cg, ECg, GCg, and EGCg) caused much greater overlap integral than the non-galloylated catechins (C, EC, GC, and EGC) (Fig. 7). In the present case, $k^2 = 2/3$, $N = 1.336$, $\Phi = 0.118$ [20], the values of J, E, R_0, and r_0 for the tested systems have been determined according to the Eqs. (4)–(6). The obtained results are stated in Table 2. All binding distances (r_0) were much lower than 8 nm, and fulfilled the following condition $0.5R_0 < r_0 < 1.5R_0$, which indicates that non-radiation energy transfer from HSA to catechins occurred with high probability [27].

3.7. Effect of catechins on molecular charge of HSA

Native PAGE was used to investigate the changes in the molecular charge of HSA due to interactions with the catechins (Fig. 8). The results were expressed as increment in electrophoretic mobility of individual samples compared to the native protein (control). The changes in the HSA molecule were exerted as broadening of protein band as well as increased sample mobility towards anode, which indicated that the molecule of HSA became more anionic due to the interaction with catechin gallates (Cg, ECg, GCg, and EGCg). On the other hand, the non-galloylated catechins (C, EC, GC, and EGC) caused no significant changes in electrophoretic mobility of HSA. The loss of positive charges in HSA molecule was in a good agreement with a number of hydroxyl groups and molecular weight of the galloylated catechins. Moreover, catechin gallates with the pyrogallol group on the B-ring (GCg and EGCg) showed more pronounced effect on mobility than catechin gallates with the catechol moiety (Cg and ECg). The electrophoretic mobility of tested systems decreased in the following order: EGCg (6.25%) > GCg (5.05%) > ECg (3.61%) > Cg (3.37%) ≈ EC (3.13%) > C (1.53%) ≥ GC (0.51%) ≈ EGC (0.24%).

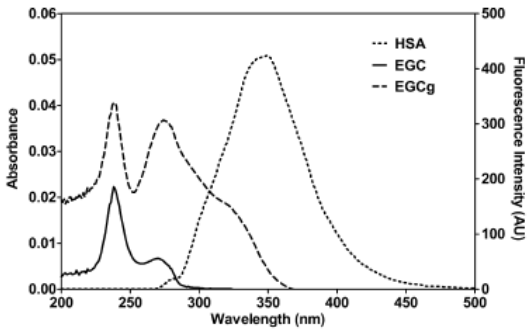

Fig. 7. Spectral overlaps between the fluorescence emission spectrum of HSA and the absorption spectra of selected catechins (pH 7.4, 37 °C). [HSA] = [EGC] = [EGCg] = 4×10^{-6} M, λ_{ex} = 295 nm and λ_{em} = 348 nm.

Table 2
The overlap integral (J), efficiency of energy transfer (E), critical distance (R_0), and distance between donor (HSA) and acceptor (catechin) (r_0) (pH 7.4, 37 °C).

Tested compound	J [$\times 10^{-16}$ cm^3 l mol^{-1}]	E	R_0 [nm]	r_0 [nm]
Catechin	0.40^{c}	0.18^{b}	0.98^{bc}	1.26^{a}
Epicatechin	0.44^{bc}	0.20^{c}	0.99^{c}	1.25^{a}
Gallocatechin	0.16^{ab}	0.11^{a}	0.84^{ab}	1.19^{a}
Epigallocatechin	0.12^{a}	0.08^{a}	0.80^{a}	1.20^{a}
Catechin gallate	26.04^{de}	0.61^{de}	1.96^{d}	1.82^{b}
Epicatechin gallate	28.15^{e}	0.66^{e}	1.98^{d}	1.78^{b}
Gallocatechin gallate	25.80^{de}	0.57^{d}	1.96^{d}	1.85^{b}
Epigallocatechin gallate	22.00^{d}	0.60^{d}	1.91^{d}	1.78^{b}

Standard deviations (mean value of three independent experiments) were lower than 10%. Data were analyzed by Student's t-test and groups with different letters are significantly different ($p < 0.01$).

3.8. Protein cross-linking and aggregation

The ability of aggregation and cross-link formation of tested catechins was not proved by SDS–PAGE. No formation of high molecular weight protein adducts was observed.

4. Discussion

In the presented study, the relationships between the chemical structure of catechins and their binding affinities to HSA were studied in detail by spectroscopic and electrophoretic methods. The main attention was focused on the structural differences such as the presence and the absence of the galloyl moiety on the C-ring, the number of hydroxyl groups on the B-ring (pyrogallol- and catechol-type), and spatial arrangement (*cis*- and *trans*-structure). Flavonoids probably form reversible non-covalent complexes with the molecule of serum albumin mainly through hydrogen bonding of their hydroxyl groups with amino acid residues and hydrophobic interactions between their aromatic rings and amino acid residues in the protein chain [3,7]. The spatial orientation can also play an important role in protein–flavonoid association [3,17].

Obtained results confirmed importance of the galloyl moiety on the C-ring in the binding affinity of catechins to HSA due to a presence of additional aromatic ring with three hydroxyl groups. The effect of this structural feature was clearly underlined by all applied methods. Also data found in literature support these findings, e.g. Ishii et al. [17] who studied binding affinities of catechins to the serum albumin with respect to their structural features using high-performance affinity chromatography with immobilized albumin column.

Considerable changes in UV–Vis absorption spectra of HSA upon interaction with catechin gallates (Cg, ECg, GCg, and EGCg) supported the idea of the complex formation. Moreover, all these complexes were emissive at excitation wavelength which is equal to the wavelength of the newly appeared absorption maxima. Catechins lacking the galloyl moiety in their structure (C, EC, GC, and EGC) caused only negligible alterations in the protein molecule. Longer time of interaction between HSA and tested compounds in phosphate buffer (pH 7.4) than 30 min proved to be inadequate due to a non-stability of studied catechins which is consistent with literature [30–32]. On the other hand, catechins can cause protein carbonyl formation in HSA via their pro-oxidant action [14] and protection of (−)-epigallocatechin gallate by the thiol groups of HSA, which act as an antioxidant, against oxidation under aerobic conditions has been described [33]. The similar effect may be expected also for other flavonoids.

All catechin gallates caused more pronounced decrease in the tryptophan fluorescence than other catechins (Table 1). Furthermore, remarkable red shifts in their fluorescence quenching spectra were observed (Fig. 4B). Generally, red shift in the emission maximum of a tryptophan residue, which is located in a hydrophobic pocket, indicates changes in its microenvironment, i.e. a polypeptide strand of a protein molecule is more extended and the

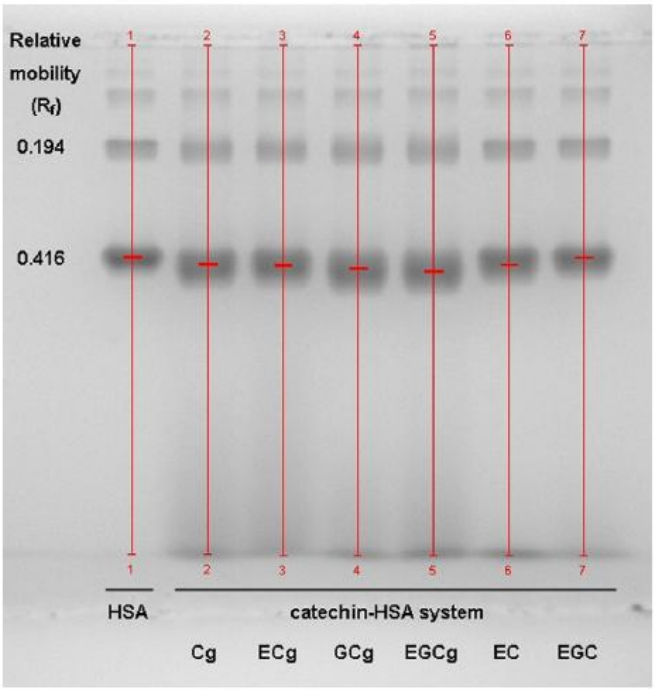

Fig. 8. Effect of selected catechins on a molecular charge of HSA. [HSA] = 15×10^{-6} M, [catechin] = 6×10^{-4} M. Samples were incubated for 30 min at 37 °C. Electrophoretic mobilities were expressed as a rise in percentage mobility compared to the native protein (control).

hydrophobicity around this tryptophan residue is decreased [34]. These data suggest that Trp-214, which is the only one tryptophan residue in the HSA molecule, has been brought to a more hydrophilic environment and the protein secondary structure has been changed. No shifts in the emission maximum of HSA were observed after gradual additions of the non-galloylated catechins. Maiti et al. [18] also reported the red shift in the fluorescence quenching spectra of (−)-epigallocatechin gallate–HSA system. By contrast, no shifts in the emission spectra of bovine serum albumin after titration with increasing amounts of (+)-catechin, (−)-epicatechin, and (−)-epicatechin gallate were noticed [2,24].

The bimolecular quenching constant (K_q) reflects an efficiency of quenching or an accessibility of the fluorophores to a quencher. One of the criterions for determination of a static quenching mechanism is that the value of K_q is higher than the value of a diffusion-limited rate constant of a biomolecule ($K_{diff} = 1.0 \times 10^{10}$ l mol^{-1} s^{-1}) [8]. Considering the values of K_q were higher than that of K_{diff} for all tested systems, the static quenching mechanism is likely the main reason of protein fluorescence quenching by catechins in the range of concentrations 0–2×10^{-5} M. The importance of the presence of the galloyl moiety on the C-ring was evident because quenching constants for all catechin gallates (Cg, ECg, GCg, and EGCg) were significantly higher than those of catechins lacking the galloyl group (C, EC, GC, and EGC). Catechin gallates with 2,3-*cis* structure (ECg and EGCg) possessed greater K_q values than catechin gallates with 2,3-*trans*-structure (Cg and GCg). Catechins with the catechol group on the B-ring (C, EC, ECg, and Cg) showed more pronounced quenching effect than their analogs with pyragollol group (GC, EGC, EGCg, and GCg).

In general, a binding constant K_b reflects the power of ligand–protein association and thus can be used for comparison of the binding affinities of structurally-related ligands to a protein molecule connected with the alterations in its secondary structure. Number of binding sites (n) and free energy change (ΔG^0) are other important parameters that contribute to better understanding of ligand–protein interactions [19].

The hydrophobicity, presence or absence of some functional group, steric hindrance, and spatial arrangement seem to be key factors in the affinity of natural polyphenols towards plasmatic proteins [3]. The galloylated catechins (Cg, ECg, GCg, and EGCg) showed significantly higher binding ability than the non-galloylated catechins (C, EC, GC, and EGC), which is in agreement with earlier reports [17]. It also emphasizes the significance of the galloyl group on the C-ring due to the presence of additional aromatic ring and three hydroxyl groups, which can establish hydrophobic interactions and hydrogen bonds, respectively. In addition, catechol-type catechins (ECg ≥ Cg > EC ≥ C) possessed stronger binding affinity than pyragollol-type catechins (EGCg > GCg > GC > EGC), which suggests that the insertion of an additional hydroxyl group at the 5-position on the B-ring does not contribute to their binding affinities as was described in literature [17]. The effect of the spatial arrangement of catechins (i.e. *cis*- and *trans*-structure) on binding to HSA was not explicit. Ishii et al. [17] observed that the *trans*-type catechins (C, GC, Cg, and GCg) had rather higher binding abilities than their epimers (EC, EGC, ECg, and EGCg). In this study, the opposite effect was observed in the case of the galloylated catechins. Diniz et al. [3] found out using capillary electrophoresis that (−)-epicatechin showed no affinity towards HSA whilst (+)-catechin had intermediate binding ability to HSA ($K_b = 2.2 \times 10^3$ M^{-1} and $n = 1$), which the authors attributed to the spatial arrangement of tested catechins. Ishii et al. [17] noticed negligible differences in binding affinities among (+)-catechin, (−)-catechin, and (−)-epicatechin obtained by affinity

HPLC on immobilized HSA column. The latter results well correspond with our data where insignificant difference between binding constants of (−)-catechin and (−)-epicatechin was observed. One of the most studied flavan-3-ols is (−)-epigallocatechin gallate and the results obtained by Maiti et al. [18] for the system EGCg-HSA are in good agreement with our data although the experimental conditions were slightly different. Binding of (−)-epigallocatechin gallate to serum albumins was studied in detail also by circular dichroism [25].

Further factor which could contribute to binding affinity of tested catechins to HSA is deprotonation of hydroxyl groups in their molecules. It is supposed that the catechins lacking the galloyl moiety (C, EC, GC, and EGC) are fully protonated at the tested pH (i.e. pH 7.4) because their first dissociation constants reach higher values (about pH 9) [35,36]. On the other hand, catechins with the galloyl moiety in C-ring (Cg, ECg, GCg, and EGCg) have the first dissociation constants near pH 7.4 [36], thus partial deprotonation can play role in increase of their binding affinity to HSA.

Number of binding sites determined for catechin–HSA systems ranged from 0.87 to 1.10 suggesting that one molecule of HSA associated with one molecule of catechin in the drug to protein ratio up to 5:1. The spontaneity of HSA–catechin interactions was confirmed by the negative values of ΔG^0. These findings are supported by the previous reports [18].

The efficiency of an energy transfer has been used to detect the distance between catechins and Trp-214 in the molecule of HSA. The galloyl moiety in the C-ring proved to have significant effect on the extent of spectral overlapping. The overlap integrals of catechin gallate–HSA systems were much greater than those of catechin–HSA systems (Table 2). The obtained binding distances for all tested systems confirmed that non-radiation energy transfer from HSA to catechins occurred with high probability [27,28].

Catechin gallates (Cg, ECg, GCg, and EGCg) caused an increase in the electrophoretic mobility of HSA on native PAGE gels, which was dependent on increasing molecular weight of given compound. These changes are connected with the change of HSA molecular charge which became more anionic upon the interaction with catechin gallates. Moreover, catechin gallates with *cis*-structure (ECg and EGCg) caused more pronounced changes in the molecule of HSA than those with *trans*-structure (Cg and GCg). Nevertheless, no changes in the molecular weight of HSA were observed for any catechin–HSA system on SDS–PAGE gels.

5. Conclusions

In this paper, the interactions between catechins and HSA were investigated by fluorescence spectroscopy, UV–Vis absorption spectroscopy, and electrophoretic methods (native PAGE and SDS–PAGE). All tested catechins quenched tryptophan fluorescence of HSA in the studied range of concentrations mainly by static quenching mechanism and thus the non-fluorescent catechin–HSA complexes were formed. The complex formation for the galloylated catechins and HSA was confirmed also by UV–Vis absorption spectroscopy. All catechins bound spontaneously to the molecule of HSA with different binding affinity. The most important structural features of the tested catechins contributing to HSA binding were the galloyl group on the C-ring, followed by the number of hydroxyl groups on the B-ring, and the spatial arrangement (*cis*- and *trans*-structure). The number of binding sites was roughly one for all systems suggesting that one molecule of HSA associated with one molecule of catechin. All catechin–HSA interactions were spontaneous processes based on the free energy changes. Non-radiation energy transfer from HSA to all tested catechins occurred. The galloylated catechins increased the electrophoretic mobility of HSA while the ability of aggregation and cross-linking of all tested catechins was not proved. The presented study contributes to the current knowledge in the area of protein–ligand binding, particularly catechin–HSA interactions.

Acknowledgements

The presented study was supported by the Grant SVV-2010-261-003, the Specific research 2009 of the University of Hradec Králové, and the Development program of Czech Ministry of Education No. 14/87/2009.

References

[1] J. Tian, J. Liu, X. Tian, Z. Hu, X. Chen, J. Mol. Struct. 691 (2004) 197.
[2] A. Papadopoulou, R.J. Green, R.A. Frazier, J. Agric. Food Chem. 53 (2005) 158.
[3] A. Diniz, L. Escuder-Gilabert, N.P. Lopes, R.M. Villanueva-Camañas, S. Sagrado, M.J. Medina-Hernández, Anal. Bioanal. Chem. 391 (2008) 625.
[4] X. Shi, X. Li, M. Gui, H. Zhou, R. Yang, H. Zhang, Y. Jin, J. Lumin. 130 (2010) 637.
[5] T. Peters, All About Albumin: Biochemistry, Genetics and Medical Applications, Academic Press, San Diego (CA), 1996 (Chapters 2 and 3).
[6] D.C. Carter, J.X. Ho, Adv. Protein Chem. 45 (1994) 153.
[7] M. Otagiri, Drug Metab. Pharmacokinet. 20 (5) (2005) 309.
[8] J.R. Lakowicz, Principles of Fluorescence Spectroscopy, Kluwer Academic/Plenum Press, New York, 1999 (Chapters 8 and 13).
[9] Z. Ďuráčková, S. Knasmüller, The Activity of Natural Compounds in Diseases Prevention and Therapy, Slovak Academic Press, Bratislava, 2007.
[10] P. Velayutham, A. Babu, D. Liu, Curr. Med. Chem. 15 (18) (2008) 1840.
[11] C. Cabrera, R. Artacho, R. Giménez, J. Am. Coll. Nutr. 25 (2) (2006) 79.
[12] M. Kaku, K. Nakagawa, J. Health Sci. 55 (3) (2009) 441.
[13] T.L. Weir, H.P. Bais, J.M. Vivanco, J. Chem. Ecol. 29 (11) (2003) 2397.
[14] T. Ishii, T. Mori, T. Ichikawa, M. Kaku, K. Kusaka, Y. Uekusa, M. Akagawa, Y. Aihara, T. Furuta, T. Wakimoto, T. Kan, T. Nakayama, Bioorg. Med. Chem. 18 (2010) 4892.
[15] C.A. Rice-Evans, N.J. Miller, G. Paganga, Trends Plant Sci. 2 (4) (1997) 152.
[16] P.-G. Pietta, J. Nat. Prod. 63 (7) (2000) 1035.
[17] T. Ishii, K. Minoda, M.-J. Bae, T. Mori, Y. Uekusa, T. Ichikawa, Y. Aihara, T. Furuta, T. Wakimoto, T. Kan, T. Nakayama, Mol. Nutr. Food Res. 54 (6) (2010) 816.
[18] T.K. Maiti, K.S. Ghosh, S. Dasgupta, Proteins 64 (2006) 355.
[19] S. Bi, L. Ding, Y. Tian, D. Song, X. Zhou, X. Liu, H. Zhang, J. Mol. Struct. 703 (2004) 37.
[20] W. He, Y. Li, C. Xue, Z. Hu, X. Chen, F. Sheng, Bioorg. Med. Chem. 13 (2005) 1837.
[21] J.-L. Yuan, Z. Iv, Z.-G. Liu, Z. Hu, G.-L. Zou, J. Photochem. Photobiol. A: Chem. 191 (2007) 104.
[22] J. Tian, J. Liu, Z. Hu, X. Chen, Bioorg. Med. Chem. 13 (2005) 4124.
[23] J. Xiao, M. Suzuki, X. Jiang, X. Chen, K. Yamamoto, F. Ren, M. Xu, J. Agric. Food Chem. 56 (2005) 2350.
[24] S. Soares, N. Mateus, V. de Freitas, J. Agric. Food Chem. 55 (2007) 6726.
[25] A. Nozaki, M. Hori, T. Kimura, H. Ito, T. Hatano, Chem. Pharm. Bull. 57 (2) (2009) 224.
[26] R.A. Frazier, A. Papadopoulou, R.J. Green, J. Pharm. Biomed. Anal. 41 (2006) 1602.
[27] X. Guo, L. Zhang, X. Sun, X. Han, C. Guo, P. Kang, J. Mol. Struct. 928 (2009) 114.
[28] H.M. Rawel, S.K. Frey, K. Meidtner, J. Kroll, F.J. Schweigert, Mol. Nutr. Food Res. 50 (2006) 705.
[29] T. Förster, O. Sinanoglu (Eds.), Modern Quantum Chemistry, vol. 3, Academic Press, New York, 1966, p. 93.
[30] M. Mochizuki, S. Yamazaki, K. Kano, T. Ikeda, Biochim. Biophys. Acta 1569 (2002) 35.
[31] S. Sang, M.-J. Lee, Z. Hou, C.-T. Ho, C.S. Yang, J. Agric. Food Chem. 53 (2005) 9478.
[32] V. Roginsky, A.E. Alegria, J. Agric. Food Chem. 53 (2005) 4529.
[33] M.-J. Bae, T. Ishii, K. Minoda, Y. Kawada, T. Ichikawa, T. Mori, M. Kamihira, T. Nakayama, Mol. Nutr. Food Res. 53 (2009) 709.
[34] M.-X. Xie, M. Long, Y. Liu, Ch. Qin, Y.-D. Wang, Biochim. Biophys. Acta 1760 (2006) 1184.
[35] J.M. Herrero-Martínez, M. Sanmartin, M. Rosés, E. Bosch, C. Ràfols, Electrophoresis 26 (2005) 1886.
[36] M. Muzolf, H. Szymusiak, A. Gliszczyńska-Świgło, I.M.C.M. Rietjens, B. Tyrakowska, J. Agric. Food Chem. 56 (2008) 816.

Mol Cell Biochem (2011) 357:323–330
DOI 10.1007/s11010-011-0903-5

Comparison of glycation of glutathione S-transferase by methylglyoxal, glucose or fructose

Iva Boušová · Zuzana Průchová · Lucie Trnková · Jaroslav Dršata

Received: 14 February 2011 / Accepted: 19 May 2011 / Published online: 29 May 2011

Abstract Glycation is a process closely related to the aging and pathogenesis of diabetic complications. In this process, reactive α-dicarbonyl compounds (e.g., methylglyoxal) cause protein modification accompanied with potential loss of their biological activity and persistence of damaged molecules in tissues. We suppose that glutathione S-transferases (GSTs), a group of cytosolic biotransformation enzymes, may be modified by glycation in vivo, which would provide a rationale of its use as a model protein for studying glycation reactions. Glycation of GST by methylglyoxal, fructose, and glucose in vitro was studied. The course of protein glycation was evaluated using the following criteria: enzyme activity, formation of advanced glycation end-products using fluorescence and western blotting, amine content, protein conformation, cross linking and aggregation, and changes in molecular charge of GST. The ongoing glycation by methylglyoxal 2 mM resulted in pronounced decrease in the GST activity. It also led to the loss of 14 primary amino groups, which was accompanied by changes in protein mobility during native polyacrylamide gel electrophoresis. Formation of cross links with molecular weight of 75 kDa was observed. Obtained results can contribute to understanding of changes, which proceed in metabolism of xenobiotics during diabetes mellitus and ageing.

Keywords Advanced glycation end-products · Glutathione S-transferase · Methylglyoxal · Protein glycation · Protein conformation

I. Boušová (✉) · Z. Průchová · L. Trnková · J. Dršata
Department of Biochemical Sciences, Faculty of Pharmacy, Charles University in Prague, Heyrovského 1203, 500 05 Hradec Kralove, Czech Republic
e-mail: Iva.Bousova@faf.cuni.cz

L. Trnková
Department of Chemistry, Faculty of Science, University of Hradec Králové, Rokitanského 62, 500 03 Hradec Kralove, Czech Republic

Introduction

Glutathione S-transferases (GST, EC 2.5.1.18) are a group of xenobiotic-metabolizing enzymes that play a crucial role in the phase II of detoxification. These enzymes catalyze conjugation of toxic compounds with endogenous tripeptide glutathione (GSH) to deactivate them and increase their hydrophilicity [1]. In humans, GSTs are extremely ubiquitous, e.g., constituting about 4% of total soluble protein in the liver [2]. They can be divided into three subfamilies according to the cellular localization: cytosolic, microsomal, and mitochondrial. Among them, cytosolic GSTs are numerous and well described. Seven classes of mammalian cytosolic GSTs, called alpha, kappa, mu, omega, pi, theta, and zeta, have been identified and categorized based on a sequence identity (at least 40% sequence identity within a class) [3–5]. The most widely distributed GST isoforms come from alpha, mu, and pi classes [3]. These enzymes exist as dimeric proteins, with an approximate molecular weight of 25 kDa for each subunit. Each of the subunits possesses a GSH binding site (G-site) as well as an adjacent relatively hydrophobic site (H-site) for the binding of the electrophilic substrate [2, 6].

Diabetes mellitus is a chronic metabolic disorder with high prevalence in human population. This disease, unless it is controlled therapeutically, is characterized by hyperglycemia and glycosuria. The hyperglycemia is not only a

hallmark but also the main cause of diabetic complications development [7]. Sugar binds in the process of glycation to free amino groups of extracellular as well as intracellular proteins, modifies their molecules, causes formation of cross-links between adjacent protein chains, and contributes to the formation of irreversible protein adducts known as advanced glycation end products (AGEs) [8, 9]. Intermediate products (Schiff bases and Amadori products) can be fragmented to α-dicarbonyl compounds, such as glyoxal, methylglyoxal (MGO), and 3-deoxyglucosone. These compounds are more reactive than the parent sugars and are mainly responsible for protein cross-linking and formation of AGEs [10]. MGO plays a key role in the formation of AGEs on intracellular proteins. MGO-modified proteins are important physiological ligands for scavenger receptors of monocytes and macrophages (MSR-AII and MSR-BI), the cells responsible for their endocytosis, and consequent lysosomal degradation [11, 12].

Raza et al. [13] suggested that glutathione metabolism and GST distribution in the tissues of diabetics may be crucial in the etiology, pathology, and prevention of diabetes. It was also reported that long-term hyperglycemia resulted in decreased activities of GST as well as of other enzymes in diabetic animals [14–16]. These findings indicate that ongoing diabetes may modify the detoxification metabolism. The present study examined the effect of MGO, fructose, and glucose on structural and catalytic properties of cytosolic mu-class GST.

Materials and methods

Chemicals

GST, a recombinant enzyme from *Schistosoma japonicum*, was purchased from GenScript, New Jersey, USA. MGO, aminoguanidine, D-fructose, 2,4,6,-trinitrobenzenesulfonic acid, 1-chloro-2,4-dinitrobenzene, reduced glutathione, β-alanine, Bradford reagent, and chemicals used for realization of electrophoresis were the products of Sigma-Aldrich Co., St. Louis, USA. PVDF membrane (0.2 μm), Precision Plus molecular weight standards, and non-fat dry milk were obtained from Bio-Rad Laboratories, Hercules, USA. D-Glucose, sodium bicarbonate, and sodium azide were purchased from Lachema, Brno, Czech Republic. Rabbit polyclonal antibody to AGE (primary antibody) and goat polyclonal anti-rabbit IgG antibody conjugated with alkaline phosphatase (secondary antibody) were obtained from Acris GmbH, Hiddenhausen, Germany. Mouse monoclonal antibody [3C] to MGO-derived AGEs and rabbit polyclonal anti-mouse IgG antibody conjugated with alkaline phosphatase were products of Abcam plc, Cambridge, UK. Chemiluminescent/fluorescent substrate for alkaline phosphatase DuoLux was ordered from Vector Laboratories, Burlingame, USA. X-ray films CL-XPosure were obtained from Thermo Fisher Scientific, Rockford, USA. Fixing and developing bath were products of Foma Bohemia, Hradec Králové, Czech Republic. All chemicals used were of analytical grade.

Sample preparation and incubation

GST (0.5 mg/ml) was incubated in the presence or absence of glycating agents (MGO 0.5 mM, MGO 1 mM, MGO 2 mM, fructose 50 mM, or glucose 50 mM) at 37°C for up to 28 days in 100 mM phosphate-buffered saline (pH 7.4, 0.05% sodium azide). The low-molecular compounds were removed using Microcon centrifugal filtration device with 10 mM phosphate-buffered saline (pH 7.4), protein content was measured using Bradford assay, and adjusted to the concentration 0.5 mg/ml. Aliquots were stored frozen at −20°C until analysis. All the samples were assessed in triplicates, and experiments were repeated twice if not stated otherwise.

Enzyme assay

GST (0.025 mg/ml) was incubated in the presence or absence of glycating agents for 180 min at 37°C. Sample aliquots were taken away at 0, 60, 120, and 180 min, diluted and their activity was assessed by colorimetric method based on the GST-catalyzed reaction between GSH and GST substrate 1-chloro-2,4-dinitrobenzene at pH 6.5. Product of this reaction, S-(2,4-dinitrophenyl)glutathione, can be detected spectrophotometrically at 340 nm [17].

Determination of amino groups

Amine content, which is a measure of protein glycation, was estimated spectrophotometrically with trinitrobenzenesulfonic acid [18] using β-alanine as the standard. Sample containing 50 μg of GST was incubated with 0.1% trinitrobenzenesulfonic acid in alkaline conditions for 2 h at 37°C. The reaction was stopped by acidification (1 M HCl) and addition of 10% SDS. The absorbance of trinitrophenyl-amino acid complex was measured at 340 nm. The standard curve was linear in the range 5–100 nmol of NH_2.

Fluorescence measurements

Formation of fluorescent AGEs and changes in tryptophan (intrinsic) fluorescence were determined using multimode reader Tecan Infinite M200. Fluorescence was measured at excitation and emission wavelengths of 370/440 nm (fluorescent AGEs) and 295/386 nm (tryptophan

fluorescence), respectively, in 96-well plate using 100 µg of GST per well. Emission wavelength for tryptophan fluorescence determination was found experimentally.

Effect of glycation on molecular charge of GST

Native PAGE was used to investigate the change in the molecular charge of GST due to glycation. Electrophoresis was performed in Ornstein–Davies discontinuous system with 4% stacking gel and 10% separating non-denaturating gel [19, 20]. All lanes were loaded with 10 µg of protein. Electrophoresis was performed at 30 mA for about 3 h using Mini Protean III apparatus. The gel was then stained by colloidal Coomassie Blue G250, scanned, and relative migration distances were calculated from R_f using Quantity One software (BioRad). Electrophoretic mobilities were expressed as a rise in percentage mobility compared with the native enzyme (control).

Western blotting

Formation of AGEs, protein cross-linking, and fragmentation were assessed using western blotting with corresponding antibodies. Proteins were first separated by SDS-PAGE on Mini Protean III apparatus (BioRad). SDS-PAGE was performed using discontinuous system with 4% stacking gel and 12.5% separating gel according to the method of Laemmli [21]. Lanes were loaded with 4 µg of protein. Proteins were then transferred to PVDF membrane [22] at a constant voltage 100 V for 90 min (Mini Trans-Blot Electrophoretic Transfer Cell, Bio-Rad).

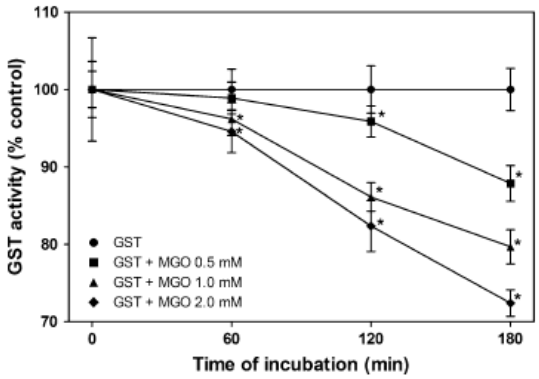

Fig. 1 Effect of glycation by MGO on GST activity. GST (0.025 mg/ml) was incubated in 0.1 M sodium phosphate buffer (pH 7.4) containing 0 mM (*circle*), 0.5 mM (*square*), 1.0 mM (*triangle*), and 2.0 mM (*diamond*) MGO for 180 min at 37°C. Catalytic activity of GST was expressed as percentage of control sample activity at all time intervals, which was 100% ± SD(%). Every point represents an average of two independent experiments, in which assays were performed in hexaplicates (*$P < 0.05$, Student's *t*-test)

After blotting, membranes were blocked in 8% non-fat dry milk in Tris buffered saline-Tween-20 buffer overnight at 4°C. After washing in Tris buffered saline-Tween-20 buffer, the membranes were reacted with either primary rabbit anti-AGE antibody (dilution 1:1000) or primary mouse anti-MGO [3C] antibody (1:1000) for 45 min at room temperature. Subsequently, membranes were washed six times with Tris buffered saline-Tween-20 buffer and incubated with corresponding secondary antibody for 45 min (dilution 1:2000 for anti-rabbit IgG and 1:1000 for anti-mouse IgG). The blots were extensively washed in 0.1 M Tris buffer containing 5 mM $MgCl_2.6H_2O$ (pH 9.5), covered with chemiluminescent substrate DuoLux and incubated for 5 min. Protein bands were then detected by both chemiluminescent detection and staining with Ponceau S. Membranes, and X-ray films (CL-XPosure film, Thermo Fisher Scientific) were scanned on GelDoc XR system and quantified by Quantity One software (BioRad).

Statistical analysis

Values of catalytic activity are given as means ± SD and mostly expressed in % of the time 0 of individual samples ± relative SD. Values of fluorescence (RFU) and amine content are given as mean ± SD. Statistical significance was determined using Student's *t*-test, and differences were regarded as significant when $P < 0.01$.

Results

Enzyme assay

Activity of control sample (GST alone) was stable throughout the experiment. MGO caused an irreversible decrease in enzymatic activity of GST (Fig. 1). When GST was incubated with MGO (0.5, 1.0, and 2.0 mM), activity decreased by 12.1, 20.3, and 27.6% after 180 min at 37°C, respectively. The rate of enzyme inactivation increased with increasing concentrations of MGO. Only slight changes (decrease up to 6%) in the enzymatic activity of GST incubated with fructose 50 mM or glucose 50 mM were observed (data not shown).

Determination of amine content

Protein glycation, the chemical modification of primary amines (ε-amino group of lysine residues and α-amino group of N-terminal amino acids), leads to the decrease in amine content. Incubation of GST with MGO, fructose or glucose led to the reduction in amine content, which differed according to the nature and concentration of glycating agent used (Table 1). Incubation of GST with MGO

Table 1 Primary amine content

Sample	Amine content (mol NH_2/mol GST) (days)		Number of primary amino groups (days)	
	7	28	7	28
GST	52.76 ± 1.17^{a}	52.59 ± 1.23^{a}	44	44
GST + MGO 0.5 mM	46.19 ± 2.68^{cd}	–[g]	39	–[g]
GST + MGO 1 mM	40.70 ± 1.22^{e}	–[g]	34	–[g]
GST + MGO 2 mM	36.44 ± 1.42^{f}	–[g]	30	–[g]
GST + Frc 50 mM	48.82 ± 1.82^{bc}	44.16 ± 1.26^{d}	41	37
GST + Glc 50 mM	52.01 ± 1.92^{ab}	46.80 ± 0.72^{cd}	43	39

[a,b,c,d,e,f] Groups with different letters vary significantly ($P < 0.01$, Student's t-test)

[g] Amine content was not determined

2.0 mM and fructose 50 mM for 7 days caused 31 and 8% decrease in amine content due to chemical modification of primary amines, respectively. GST in its native dimeric form contains 44 primary amino groups, suggesting that about 14 and 3 amino groups were modified during its incubation with MGO 2.0 mM and Frc 50 mM, respectively. By contrast, no changes in amine content were observed in the case of glucose 50 mM after 7 days of incubation. Therefore, the samples containing fructose 50 mM and glucose 50 mM were incubated as long as for 28 days, and then, these glycating agents caused 16 and 11% decrease in amine content, respectively.

Fluorescence measurements

Incubation of GST with glycating agents led to the increase in fluorescence intensity due to the formation of AGEs with fluorescent properties (Fig. 2a) and the decrease in tryptophan fluorescence (Fig. 2b). The 7-day incubation of GST with MGO (0.5, 1.0, and 2.0 mM) at 37°C caused an increase in AGEs formation by 32.0, 55.1, and 85.3% and a decrease in tryptophan fluorescence by 11.3, 16.6, and 27.7% compared with the control sample (GST alone), respectively. Fructose and glucose showed much lower effect both on formation of AGEs and tryptophan fluorescence in this time interval. Their effect was more pronounced after 28 days of incubation at 37°C, when fructose 50 mM caused 51.3% increase in AGEs formation and 10.6% decrease in tryptophan fluorescence.

To determine whether the changes in tryptophan fluorescence observed in the samples containing various

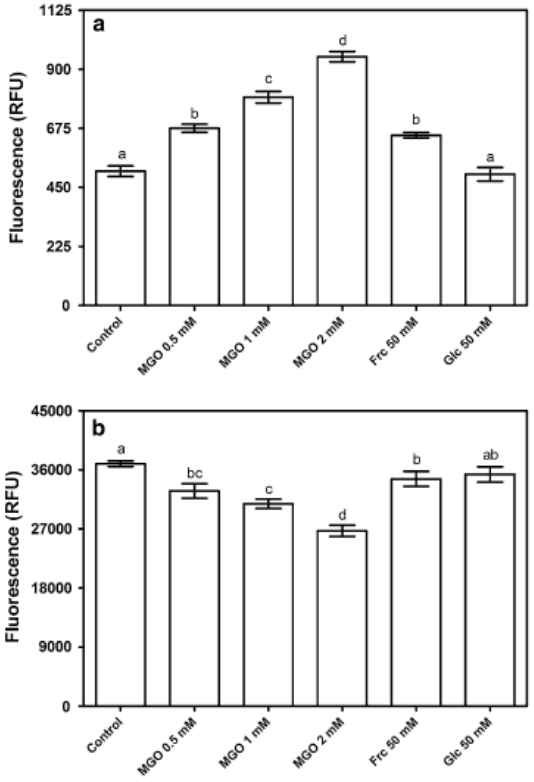

Fig. 2 Effect of glycating agents on the formation of fluorescent AGEs (**a**) and tryptophan fluorescence (**b**). GST (0.5 mg/ml) was incubated with or without MGO (0.5–2.0 mM), fructose (Frc 50 mM) and glucose (Glc 50 mM) in 0.1 M sodium phosphate buffer (pH 7.4) at 37°C for 7 days. Glycating agents were then removed by centrifugal filtration. Fluorescence of samples containing 100 μg of GST was measured at specific excitation and emission wavelengths ($\lambda_{ex}/\lambda_{em}$) corresponding to AGEs (370/440 nm) and tryptophan (295/386 nm). Data of fluorescence were expressed in relative fluorescence units ± SD. Every point represents an average of two independent experiments (six samples). Groups with different letters are significantly different ($P < 0.01$, Student's t-test)

concentrations of MGO (0–2.0 mM) correlated with the loss of primary amino groups in these samples, the fluorescence intensity was plotted as a function of amine content. The decrease in fluorescence emission ($\lambda_{ex}/\lambda_{em} = 295/386$ nm) varied directly with the loss of primary amino groups ($r = 0.987$, $P < 0.013$; Fig. 3a). Changes in tryptophan fluorescence also correlated well with the formation of fluorescent AGEs ($r = 0.997$, $P < 0.003$; Fig. 3b). In addition, the amine content was plotted as a function of AGEs fluorescence (Fig. 3c), indicating that MGO-induced formation of AGEs was directly proportional to an irreversible loss of primary amino groups in GST molecule ($r = 0.995$, $P < 0.005$).

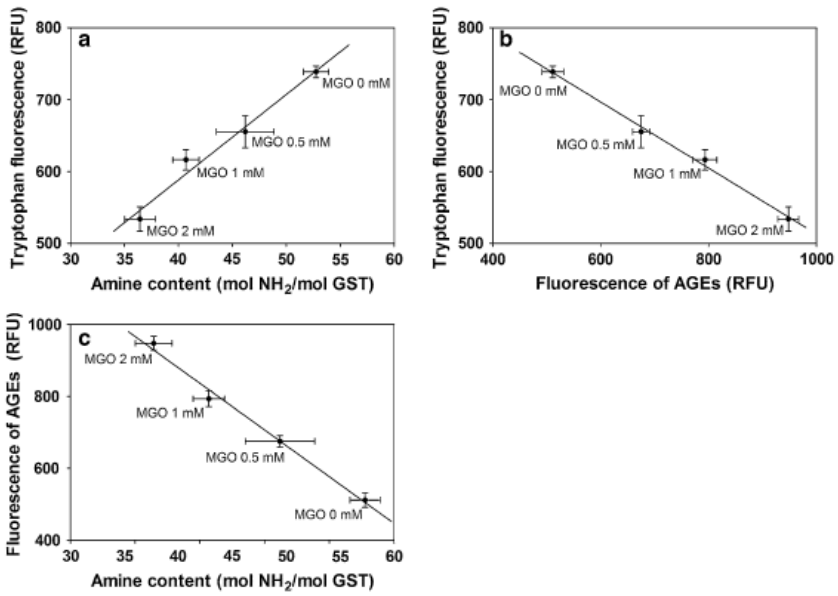

Fig. 3 Correlations between amine content, tryptophan fluorescence, and formation of fluorescent AGEs in the samples containing GST and various concentrations of MGO (0–2 mM). MGO-induced decrease in tryptophan fluorescence intensity correlated with the loss of primary amino groups (**a**) ($r = 0.987$, $P < 0.013$). Correlation between the decrease in tryptophan fluorescence and formation of AGEs (**b**) ($r = 0.997$, $P < 0.003$). Plot of an increase in AGEs formation as a function of amine content (**c**) ($r = 0.995$, $P < 0.005$)

Table 2 Effect of glycation on molecular charge of GST

Sample	Relative mobility (%)[a,b]				
	day 0	day 1	day 3	day 7	day 14
GST	100.0	100.0	100.0	100.0	100.0
GST + MGO 0.5 mM	99.8	106.1	113.9	116.2	117.4
GST + MGO 1 mM	99.5	109.1	115.5	118.9	121.7
GST + MGO 2 mM	99.3	111.6	116.8	121.9	122.6
GST + Frc 50 mM	–[c]	–[c]	100.0	101.2	105.4
GST + Glc 50 mM	–[c]	–[c]	99.9	100.4	101.4

[a] Standard deviations (mean value of three independent experiments) were lower than 4.1%

[b] Relative mobilities of all the samples were compared with the relative migration of the main protein band ($R_f = 0.517$)

[c] Native PAGE was not performed

Effect of glycation on molecular charge of GST

Native PAGE was run several times, and the average values of protein relative mobility are presented in Table 2. Incubation of GST with MGO in all the tested concentrations caused significantly increased mobility of the sample toward the positive electrode. This phenomenon was noticeable since the day 1 of incubation, when migration of the sample containing GST + MGO 2.0 mM rose by 11.6% compared with GST alone. On the other hand, changes in the mobility of sample containing fructose 50 mM and glucose 50 mM were less pronounced (5.4 and 1.4%), and they were apparent since the days 7 and 14, respectively. Typical native PAGE gel is presented in Fig. 4.

Western blotting

Immunoblotting with specific antibody against advanced glycation end products and against AGEs derived from MGO (anti-MGO [3C]) was employed to confirm the formation of protein aggregates as a result of glycating agent's activity. The presence of high-molecular protein cross-links in samples containing GST + MGO and GST + fructose was observed using both the antibodies (Fig. 5a). These protein aggregates had molecular weight about 50 and 75 kDa corresponding to GST dimer and trimer, respectively. Also cleavage to shorter peptides (~ 14 kDa) occurred in immunoblotts that were incubated with anti-MGO primary antibody. Membranes were then stained with Ponceau S and changes in the migration of the main GST band (26 kDa) toward higher molecular weight and loss of its intensity were observed in all the samples containing MGO (Fig. 5b). These results suggest that glycation by MGO was accompanied mainly by cross-linking, formation of high-molecular protein aggregates containing AGEs, and as well as protein fragmentation.

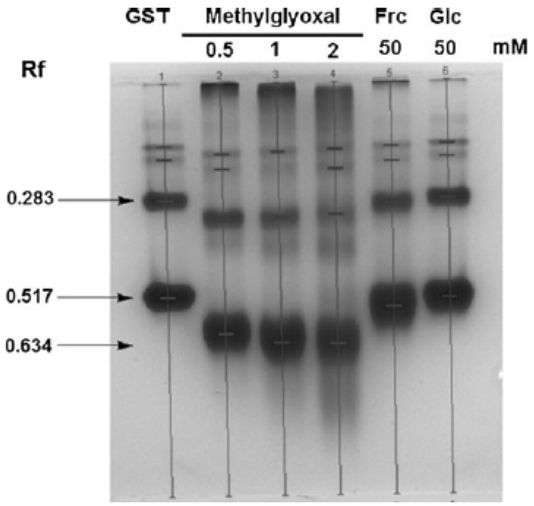

Fig. 4 Effect of glycation on molecular charge of GST. GST (0.5 mg/ml) was incubated with or without MGO (0–2 mM), fructose (Frc 50 mM), and glucose (Glc 50 mM) in 0.1 M sodium phosphate buffer (pH 7.4) at 37°C for 7 days and then subjected to native PAGE. Proteins were visualized by Coomassie Blue G250

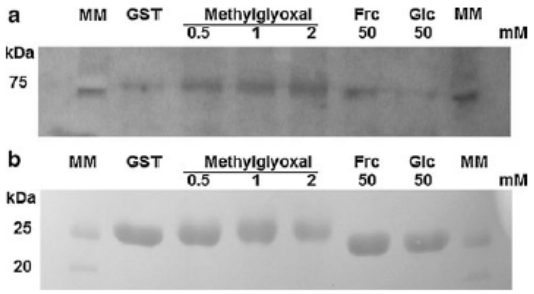

Fig. 5 Immunoblots of GST samples treated with MGO, fructose, and glucose. GST (0.5 mg/ml) was incubated with or without MGO (0–2 mM), fructose (Frc 50 mM), and glucose (Glc 50 mM) in 0.1 M sodium phosphate buffer (pH 7.4) at 37°C for 11 days and then subjected to SDS-PAGE with subsequent western blotting. Blot was reacted with rabbit anti-AGE primary antibody. Molecular weight standard (first and last lane) and protein bands were marked by goat anti-rabbit IgG using a chemiluminescent detection with an alkaline phosphatase substrate (a). Membrane was further stained with Ponceau S (b)

Discussion

In this study, the effect of MGO, fructose, and glucose on structural and catalytic properties of recombinant cytosolic GST from *S. japonicum* was investigated. This enzyme shares striking sequence homology, the characteristics of the amino acid residues in the G-site, and a common GSH-binding mode with mammalian mu-class GSTs [23, 24]. Glutathione metabolism and GST distribution in the tissues of diabetics may be crucial in the etiology, pathology, and prevention of diabetes [13]. Furthermore, the long-term hyperglycemia results in the decrease of GST enzymatic activity in tissues of diabetic animals [14–16, 25]. Administration of MGO to Swiss albino mice reduced GSH content and inhibited catalytic activity of several enzymes including GST, superoxide dismutase, glyoxalase I and II, and catalase [26]. All these findings indicate that ongoing diabetes may modify the detoxification metabolism. They also suggest that GST may be modified by non-enzymatic glycation in vivo, and hence, provide a rationale of this enzyme use for studying glycation reactions.

Reactive α-dicarbonyls (e.g., MGO) are important precursors in the formation of AGEs in vivo. These compounds are far more reactive than the parent sugars (e.g., glucose) concerning their abilities to form inter- and intra-molecular protein cross-links [11, 27]. MGO is mainly generated not only by the fragmentation of triosephosphates, but also by the catabolism of ketone bodies and threonine and the degradation of glucose-modified proteins in vivo. MGO has been identified as an intermediate in non-enzymatic glycation, and increased levels of MGO have been reported in patients suffering from diabetes mellitus [28].

MGO, glucose, and fructose chemically modified GST by a process with the generally accepted features of glycation as evidenced by a decrease in amine content. Lysine and arginine residues are target sites for reducing sugars as well as MGO modification via the Maillard reaction [29]. Typical arising products of MGO-mediated glycation of lysine and arginine residues are N_ε-(1-carboxyethyl)lysine, 1,3-di(N_ε-lysino)-4-methyl-imidazolium, argpyrimidine, and three structural isomers of hydroimidazolone. Glucose causes generation of fluorescent AGE product pentosidine [9]. All of the aforementioned compounds were described and quantified in vivo [30]. The GST dimer contains 44 Lys and 20 Arg residues with four Lys–Lys and two Lys–Arg sequence pairs, which are possible targets for glycating agents. Approximately 10, 3, and 1 Lys residues per GST molecule were irreversibly modified during 7-day incubation with MGO 1.0 mM, fructose 50 mM, and glucose 50 mM, respectively (Table 1).

Furthermore, the incubation of GST with MGO led to the inhibition of its catalytic activity (Fig. 1). This effect of MGO was concentration dependent. The glycation-induced conformational changes in protein topography and modification of lysine residues, which may play a role in the enzyme catalysis (e.g., Lys 44 is involved in the formation of G-site), probably contributes to enzyme inhibition. Also the formation of intra-molecular cross-links induced by AGEs (Fig. 5a) may be accompanied by progressive

localized compaction of protein molecule that may result in its dysfunction (e.g., creation of surface to interior channels, impairment of conformational transition, and inhibition of domain movement during catalysis). Moreover, introducing AGEs, which are hydrophobic, would also promote a local condensation of substructures [9, 31].

MGO-induced chemical modifications led to a change in molecular charge of GST, which became more anionic as revealed by native PAGE. The effects of fructose and glucose on GST electrophoretic mobility were less pronounced (Fig. 4; Table 2). These results indicate the progressive loss of the positive charge in the glycation-modified GST molecule, which is caused by the irreversible modification of Arg and Lys residues [27, 32] as was confirmed by determination of amine content (Table 1). MGO proved to be potent and fast-acting glycating agent because it progressively modified molecular charge of GST within the first 3 days of incubation, while the effect of fructose and glucose became apparent since the day 14 of incubation.

The SDS-PAGE and subsequent western blotting clearly showed formation of protein cross-links with higher molecular weight (75 kDa) than native enzyme in the samples containing MGO or fructose (Fig. 5a, b). Also, the migration of the main protein band toward higher molecular weight was observed in all the samples containing MGO after 11 days of incubation (Fig. 5b). These results suggest that glycation by MGO and fructose was accompanied by cross-linking and formation of high-molecular protein aggregates containing AGEs. Such glycation-modified sites on proteins act as trapping agents that bind transition metals and proteins, which may provide a nucleation center for extracellular plaque or intracellular inclusion body formation [31]. Protein aggregation takes part in the development and progress of various diseases including cataract [33, 34] and Alzheimer's disease [35].

It can be concluded that the ability of the glycating agents to irreversibly modify GST increased in the order D-glucose < D-fructose < MGO, which is in agreement with published results of other studies concerning glycation reactions of various glycating agents [10, 33, 36]. MGO proved to be the most potent glycating agent among studied compounds. It caused concentration-dependent inhibition of GST catalytic activity, generation of AGEs, decrease in amine content and tryptophan fluorescence, cross-link formation, as well as changes in molecular charge of the studied enzyme.

Acknowledgment This study was supported by the Czech Science Foundation (grant number 524/09/P121) and by the Charles University in Prague (Project SVV 263 004).

Conflict of interest statement None declared.

References

1. Uetrecht JP, Trager W (2007) Drug metabolism: chemical and enzymatic aspects. Informa Healthcare, New York
2. van Bladeren PJ (2000) Glutathione conjugation as a bioactivation reaction. Chem Biol Interact 129:61–76
3. Dourado DF, Fernandes PA, Ramos MJ (2008) Mammalian cytosolic glutathione transferases. Curr Protein Pept Sci 9:325–337
4. Nebert DW, Vasiliou V (2004) Analysis of the glutathione S-transferase (GST) gene family. Hum Genomics 1:460–464
5. Sheehan D, Meade G, Foley VM, Dowd CA (2001) Structure, function and evolution of glutathione transferases: implications for classification of non-mammalian members of an ancient enzyme superfamily. Biochem J 360:1–16
6. Mannervik B, Danielson UH (1988) Glutathione transferases—structure and catalytic activity. Crit Rev Biochem 23:283–337
7. Halliwell B, Gutteridge JMC (2007) Free radicals in biology and medicine. Oxford University Press, New York
8. Hunt JV, Dean RT, Wolff SP (1988) Hydroxyl radical production and autooxidative glycosylation. Glucose autoxidation as the cause of protein damage in the experimental glycation model of diabetes mellitus and ageing. Biochem J 256:205–212
9. Ulrich P, Cerami A (2001) Protein glycation, diabetes, and aging. Recent Prog Horm Res 56:1–22
10. Schalkwijk CG, Stehouwer CD, van Hinsbergh VW (2004) Fructose-mediated non-enzymatic glycation: sweet coupling or bad modification. Diabetes Metab Res Rev 20:369–382
11. Matsumoto K, Sano H, Nagai R, Suzuki H, Kodama T, Yoshida M, Ueda S, Smedsrød B, Horiuchi S (2000) Endocytic uptake of advanced glycation end products by mouse liver sinusoidal endothelial cells is mediated by a scavenger receptor distinct from the macrophage scavenger receptor class A. Biochem J 352:233–240
12. Ohgami N, Nagai R, Miyazaki A, Ikemoto M, Arai H, Horiuchi S, Nakayama H (2001) Scavenger receptor class B type I-mediated reverse cholesterol transport is inhibited by advanced glycation end products. J Biol Chem 276:13348–13355
13. Raza H, Ahmed I, John A (2004) Tissue specific expression and immunohistochemical localization of glutathione S-transferase in streptozocin induced diabetic rats: modulation by *Momordica charantia* (karela) extract. Life Sci 74:1503–1511
14. Lapshina EA, Sudnikovich EJ, Maksimchik JZ, Zabrodskaya SV, Zavodnik LB, Kubyshin VL, Nocun M, Kazmierczak P, Dobaczewski M, Watala C, Zavodnik IB (2006) Antioxidative enzyme and glutathione S-transferase activities in diabetic rats exposed to long-term ASA treatment. Life Sci 79:1804–1811
15. Thomas H, Schladt L, Knehr M, Oesch F (1989) Effect of diabetes and starvation on the activity of rat liver epoxide hydrolases, glutathione S-transferases and peroxisomal β-oxidation. Biochem Pharmacol 38:4291–4297
16. Saito-Yamanaka N, Yamanaka H, Nagasawa S (1993) Glutathione-related detoxication functions in streptozocin-induced diabetic rats. J Vet Med Sci 55:991–994
17. Habig WH, Pabst MJ, Jakoby WB (1974) Glutathione S-transferases: the first enzymatic step in mercapturic acid formation. J Biol Chem 249:7130–7139
18. Steinbrecher UP (1987) Oxidation of human low density lipoprotein results in derivatization of lysine residues of apolipoprotein B by lipid peroxide decomposition products. J Biol Chem 262:3603–3608
19. Ornstein L (1964) Disc electrophoresis. I. Background and theory. Ann NY Acad Sci 121:321–349
20. Davies BJ (1964) Disc electrophoresis. II. Method and application to human serum proteins. Ann NY Acad Sci 121:404–427

21. Laemmli UK (1970) Cleavage of structural proteins during the assembly of the head of bacteriophage T4. Nature 227:680–685
22. Towbin H, Stachlin T, Gordon J (1979) Electrophoretic transfer of proteins from polyacrylamide gels to nitrocellulose sheets: procedure and some applications. Proc Natl Acad Sci USA 76:4350–4354
23. Lim K, Ho JX, Keeling K, Gilliland GL, Ji X, Rüker F, Carter DC (1994) Three-dimensional structure of *Schistosoma japonicum* glutathione S-transferase fused with a six-amino acid conserved neutralizing epitope of gp41 from HIV. Protein Sci 3:2233–2244
24. Ji X, Tordova M, O'Donnell R, Parsons JF, Hayden JB, Gilliland GL, Zimniak P (1997) Structure and function of the xenobiotic substrate-binding site and location of a potential non-substrate-binding site in a class pi glutathione S-transferase. Biochemistry 36:9690–9702
25. Petlevski R, Hadzija M, Slijepcević M, Juretić D, Petrik J (2003) Glutathione S-transferases and malondialdehyde in the liver of NOD mice on short-term treatment with plant mixture extract P-9801091. Phytother Res 17:311–314
26. Choudhary D, Chandra D, Kale RK (1997) Influence of methylglyoxal on antioxidant enzymes and oxidative damage. Toxicol Lett 93:141–152
27. Kang JH (2006) Oxidative modification of human ceruloplasmin by methylglyoxal: an in vitro study. J Biochem Mol Biol 39:335–338
28. West IC (2000) Radicals and oxidative stress in diabetes. Diabet Med 17:171–180
29. Seidler NW, Kowalewski C (2003) Methylglyoxal-induced glycation affects protein topography. Arch Biochem Biophys 410:149–154
30. Thornalley PJ (1996) Pharmacology of methylglyoxal: formation, modification of proteins and nucleic acids, and enzymatic detoxification—a role in pathogenesis and antiproliferative chemotherapy. Gen Pharmacol 27:565–573
31. Seidler NW (2005) Carbonyl-induced enzyme inhibition: mechanism and new perspectives. Curr Enzyme Inhib 1:21–27
32. Nagai R, Matsumoto K, Ling X, Suzuki H, Araki T, Horiuchi S (2000) Glycolaldehyde, a reactive intermediate for advanced glycation end products, plays an important role in the generation of an active ligand for the macrophage scavenger receptor. Diabetes 49:1714–1723
33. Argirova M, Breipohl W (2002) Comparison between modifications of lens proteins resulted from glycation with methylglyoxal, glyoxal, ascorbic acid, and fructose. J Biochem Mol Toxicol 16:140–145
34. Harding JJ (2007) Protein glycation and cataract: a conformational disease. In: Uversky VN, Fink AL (eds) Protein misfolding, aggregation, and conformational diseases. Part B: molecular mechanisms of conformational diseases, 1st edn. Springer Science, New York, pp 499–514
35. Apostolova LG, Cummings JL (2007) The pathogenesis of Alzheimer's disease: general overview. In: Uversky VN, Fink AL (eds) Protein misfolding, aggregation, and conformational diseases. Part B: molecular mechanisms of conformational diseases, 1st edn. Springer Science, New York, pp 3–29
36. Beránek M, Držata J, Palička V (2001) Inhibitory effect of glycation on catalytic activity of alanine aminotransferase. Mol Cell Biochem 218:35–39

Abstracts of presentations and posters

Trnková, L., Boušová, I., Kubíček, V., Dršata, J. (8.-12.6.2008): Spectroscopic studies on stability of hydroxycinnamic acids and their interaction with molecule of serum albumin. 19th International Symposium on Pharmaceutical and Biomedical Analysis, Gdańsk, Poland. Book of abstracts, p. 308. ISBN 978-83-927125-0-3.

Trnková L., Boušová I., Ortová I., Dršata J. (23.-25.10.2008): Antioxidants and environmental stress: Spectroscopic studies on interaction of natural compounds with protein in an *in vitro* model. 17th Central European Conference ECOpole´08, Piechowice, Poland. Proceedings of ECOpole3(1): 27-34. ISSN 1898-617X.

Trnková, L., Boušová, I., Ortová, I., Dršata, J. (9.-11.7.2009): Study of interaction between catechins and human serum albumin by tryptophan fluorescence quenching method. 12th Meeting of the International Society for Tryptophan Research, Florence, Italy. Book of abstracts, p. 70.

Boušová, I., **Trnková L.**, Dršata, J. (9.-19.7.2009): May uptake of flavonoids during pregnancy influence fetal development? International Academic Summer School: Determinism and outcomes in the framework of environment – nutrition (CEEPUS). Brasov, Romania. Book of abstracts, p. 58-59. ISBN 978-973-598-536-3.

Trnková, L., Boušová, I., Ortová, I., Dršata, J. (31.8.-2.9.2009): Evaluation of effects of naturally occurring catechins on methylglyoxal-mediated protein glycoxidation. 9th International conference Vitamins, nutrition, diagnostics, Brno, Czech Republic. Book of abstracts, p. 132-133. ISBN 978-80-7318-809-2.

Trnková L., Boušová I., Ortová I., Dršata J. (14.-17.10.2009): Damage to proteins caused by free radicals from environment: effect of natural antioxidants. 18th Central European Conference ECOpole´09, Piechowice, Poland. CD of abstracts, p. 71.

Dršata J., **Trnková L.**, Boušová I. (26.-28.10.2009): Effect of catechin derivatives on serum albumin conformation and its glycation by reactive alpha-dicarbonyl

compounds. 3rd BBBB-Bosphorus International conference on Pharmaceutical Sciences, Antalya, Turkey. Eur. J. Pharm. Sci. 38(1 Suppl.): 153-154. ISSN 0928-0987.

Boušová I., **Trnková L.**, Srbová L., Průchová Z., Dršata J. (26.6.-1.7.2010): Glycation-induced changes in the molecule of glutathione S-transferase. 35th FEBS Congress, Molecules of Life, 2010, Göteborg, Švédsko, FEBS J. 277(Suppl. 1):63. ISSN 1742-464X.

Boušová I., Průchová Z., **Trnková L.**, Dršata J. (8.-12.9.2010): Inhibitory effect of natural flavonoids on equine liver glutatione S-transferase, XXII. Biochemický Zjazd, Martin, Slovensko, Book of abstracts. p. 226. ISBN 978-80-88866-83-1.

Trnková L., Boušová I., Altieri F., Dršata J. (13.-15.10.2011): Interaction of proteins with low-molecular substances occurring in environment: Structure-activity relationships. 20th Central European Conference ECOpole´11, Zakopane, Poland. File of abstracts, p. 70.